Tuning flavor-active components

Saffarionpour, Shima

DOI
10.4233/uuid:ecb7ff22-bfce-4378-8784-6738aa99d545

Publication date
2018

Document Version
Final published version

Citation (APA)
Saffarionpour, S. (2018). *Tuning flavor-active components*. [Dissertation (TU Delft), Delft University of Technology]. https://doi.org/10.4233/uuid:ecb7ff22-bfce-4378-8784-6738aa99d545

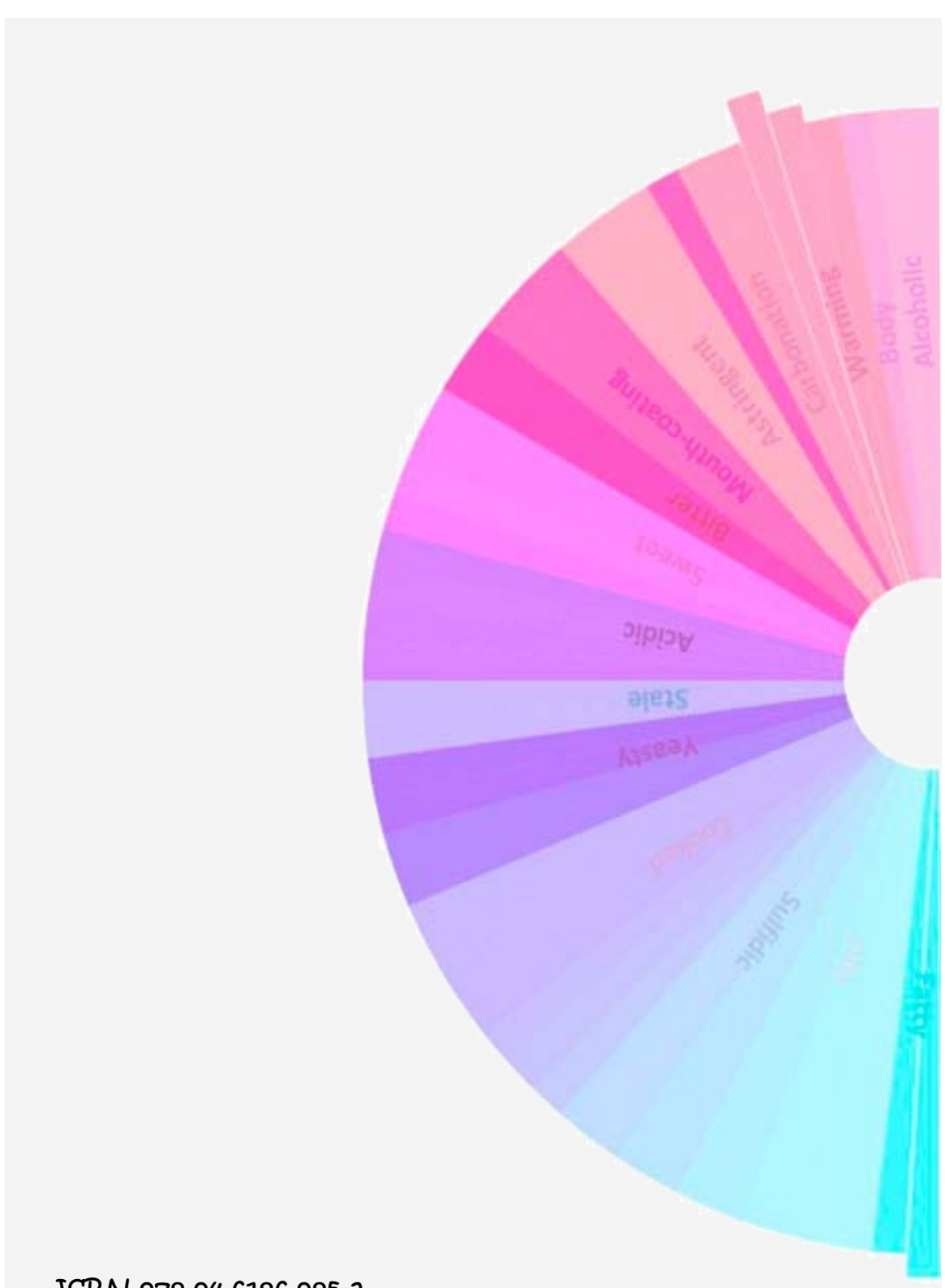

Tuning flavor-active components

Shima Saffarionpour

Tuning flavor-active components

Shima Saffarionpour

ISBN 978-94-6186-985-2

Tuning flavor-active components

Proefschrift

ter verkrijging van de graad van doctor
aan de Technische Universiteit Delft,
op gezag van de Rector Magnificus Prof. dr. ir. T. H. J. J. Van der Hagen
voorzitter van het College voor Promoties,
in het openbaar te verdedingen op
maandag 26 november 2018 om 12:30 uur

door

Shima SAFFARIONPOUR

Professional Doctorate in Engineering in Process and Product Design,
Eindhoven University of technology, The Netherlands

geboren te Tehran, Iran

Dit proefschrift is goedgekeurd door de promotoren.

Samenstelling promotiecommissie bestaat uit:

Rector magnificus,	voorzitter
Dr.ir. M. Ottens	Technische Universiteit Delft, promotor
Prof.dr.ir. L.A.M. Van der Wielen	Technische Universiteit Delft, promotor
Onafhankelijke leden:	
Prof. dr. A.J.van der Goot	Universiteit Wageningen
Prof. dr. ir. M.T. Kreutzer	Technische Universiteit Delft
Prof. dr. M. H. M. Eppink	Universiteit Wageningen/Synthon
Prof. dr. H. J. Noorman	Technische Universiteit Delft
Andere leden:	
Dr. E. Brouwer	Heineken Supply Chain

The research work presented in this thesis was performed at Bioprocess Engineering group, Department of Biotechnology, Delft University of Technology, Delft, The Netherlands. This research was financially supported by ISPT (Institute of Sustainable Process Technology) under the grant number FO 10-05.

Printed by IPSKAMP printing in The Netherlands

ISBN: 978-94-6186-985-2

Contents

Chapter 1. Introduction

1.1 History of beer brewing (Past and present trends) 1

1.2 Beer processing 3

1.3 Project FO-10-05 Selective removal of volatiles 5

1.4 Scope and outline of the thesis 8

References 10

Chapter 2. Techniques for flavor recovery in liquid food processing

ABSTRACT 15

2.1 Volatile flavor-active components 16

2.2 Alternative techniques for flavor recovery 18

2.2.1 Aroma recovery through distillation 19

2.2.2 Pervaporation membrane separation technique 21

2.2.3 Aroma recovery through Supercritical fluid extraction 24

2.2.4 Regeneration and recovery of aromas via adsorption 26

2.3 Conclusions 27

References 35

Chapter 3. Method development for selective removal of flavor-active components

ABSTRACT 41

3.1 Fine-tuning and control of flavor-active components 42

3.2 High Throughput Experimentation technique 43

3.3 Selective adsorption of flavor-active components 44

3.4 Materials 44
3.4.1 Chemicals 44
3.4.2 Adsorbents 44
3.5 Methods 47
3.5.1 Analysis 47
3.5.2 Isotherm models 47
3.5.3 Batch uptake method 50
3.5.4 Calculation of liquid holdup volume 51
3.5.5 Breakthrough analysis 52
3.5.6. Experimental procedure 53
3.5.7 Resin selection procedure 54
3.5.8 Error calculations 55
3.6. Experimental results 56
3.6.1 Single-component adsorption isotherms 56
3.6.2 Isotherms retrieved from column breakthrough analysis 58
3.6.3 Multi-component adsorption isotherms 59
3.7. Discussions 62
3.8. Resin selection 64
3.9. Conclusions 65
References 67

Chapter 4. Influence of ethanol and temperature on adsorption of flavor-active esters on hydrophobic resins

ABSTRACT 71
4.1 Introduction 72
4.2 Materials 73
4.2.1 Chemicals 73
4.2.2 Adsorbents 73
4.3 Methods 73
4.3.1 Gas Chromatographic Analysis 73

4.3.2 Thermodynamic analysis 74
4.3.3. Batch uptake method 79
4.3.4 Experimental procedure 80
4.4 Results and Discussions 80
4.4.1 Influence of temperature on single-component adsorption 80
4.4.2 Influence of temperature and ethanol concentration on multicomponent adsorption 92
4.5 Conclusions 101
Nomenclature 103
References 104

Chapter 5. Evaluating the application of Adsorbed Solution Theory for predicting competitive adsorption behavior of flavor-active esters on hydrophobic resins

ABSTRACT 107
5.1 Introduction 108
5.2 Theory 109
5.2.1 Adsorbed Solution Theory 109
5.3 Experimental 112
5.3.1 Batch uptake experimentation tests 113
5.4 Results and discussions 113
5.4.1 Single component adsorption isotherms 113
5.4.2 Determination of multicomponent isotherms (IAST approach) 114
5.5 Conclusions 117
Nomenclature 119
References 119

Chapter 6. Column chromatography for separation and fractionation of flavor-active esters on hydrophobic resins and simulation of breakthrough behavior

ABSTRACT 121
6.1 Introduction 122

6.2 Materials and methods 124
6.2.1 Materials 124
6.2.2. Methods 125
6.3. Experimental 136
6.3.1 Chromatographic system 136
6.3.2 Setup 136
6.3.3 Procedures 137
6.4. Results and Discussions 138
6.4.1 Estimated parameters 138
6.4.2 Single-component breakthrough simulation 140
6.4.3 Multi-component breakthrough simulation 144
6.4.4 Cyclic operation for adsorption/elution in a fixed-bed column 149
6.5. Conclusions 161
Nomenclature 163
References 165

Chapter 7. Concluding remarks and outlook

7.1 Challenges in method development for selective removal of flavor components 169
7.2 Selection and development of adsorbent material 171
7.3 Thermodynamic properties and isotherm models 172
7.4 Column chromatography for separation of esters 173

Appendix A. Determination of partition coefficients for three-phase equilibrium and headspace analysis

A.1 Introduction 175
A.2 Classical Phase Ratio Variation Method (PRV) 176
A.2.1 Modified Phase Ratio Variation Method (M-PRV) 177
A.3 Methods for determination of three phase partition coefficients 178

A.3.1 Liquid Phase Ratio Variation method (LPRV) 178
A.3.2 Solid Phase Ratio Variation Method (SPRV) 181
A.4 Experimental procedure 182
A.4.1 Measurements based on LPRV method 182
A.4.2 Measurements based on SPRV method 184
References 188

Summary 189
Samenvatting 191
List of Publications 195
About the Author 199
Acknowledgement 201

Introduction 1

1.1 History of beer brewing (Past and present trends)

Drinks and beverages, besides food, have an important role in human nutrition. Specifically by discovery of fermentation alcoholic drinks have been consumed and are popular among various cultures. Consuming alcohol as a beverage dates back to prehistoric times, when ethyl alcohol was discovered [1]. By the discovery of alcoholic drinks, production and consumption of alcoholic beverages, mainly beer and wine have played an important role in developing complex and organized societies. The first evidence of beer brewing was observed in 5000 BC, in Egypt and Mesopotamia [1-3]. Sumeria is reported as the oldest region, where cereal domestication was observed. First evidence of Sumerian beer has been obtained from a site at Godin Tepe, Zagros mountains, in present-day Iran [1-4]. The evidence of production and use of beer in Egypt goes back to (5500-3100 BC). It is recorded in the literature that beer was very important and well-established in the culture of that period, used also as a compensation for labour [4]. Beer drinking was also popular in Mesopotamia, like in Egypt, during all eras and among different social classes of the community, including women. Beer drinking was popular among the community and they believed that its consumption brings happiness and civilized life. It was common to drink beer through straws, to prevent gross sediment [1]. Evidences have been found, as reported in the literature, showing individuals drinking through straws (usually made of reeds, copper, silver or gold) from a communal vessel, which shows that drinking beer was a social activity [1, 5-10]. About the flavorings used in old world beer, several plant species has been used to flavor the product, including lupin, skirret, rue, safflower, mandrake fruit, grape pips, date, fig, etc.[6, 11-14].

The archaeological evidences show the emergence of beer brewing in other countries like Israel, Palestine dating back to the late 4th millennium, and in Cilicia, a region in south Anatolia [1, 10, 14]. The history of beer brewing in Holland dates back to AD 900 onwards [1]. Unger describes the history of brewing in Holland using a chronological approach. He explains the transformation in beer production, by using hops, during the year 1300, which was a transformation to a more professional beer brewing together with producing beer products with better taste [15, 16]. He explains the increase in beer production, between years 1450 up to 1650, what he calls the golden age of brewing. As there was a competition between beer and other drinks such as wine, coffee, or tea, and there was also a rise in the cost of raw materials, there was a decline in growth of brewing industry after 1650 [15, 16]. Through adaptation and application of technical innovations in the production process, such as steam engines and refrigeration systems (originated from England and Bavaria), there was a growth in beer production from 1860s onwards, and Dutch beer producers like Heineken and Amstel had great contributions to the growth of beer industry [15, 16]. The years between 1860 and 1880, are considered as zenith of British brewing industry, and there was an evolution to a more scientific beer brewing [1, 17]. By the end of 18th century, the technology of beer brewing in great Britain was more developed compared to that in Germany, Holland, Austria and America [1]. There was little attempt on advancing knowledge through research laboratories, in the early 20th century and during years 1950-1970, the second golden age, there was more research with involvement of research foundations and universities [17]. The top three leading brewing countries, Germany, the United Kingdom, and the United States contributed to 68.5% of beer production [18] and by the year 1906, the beer production increased in the United States more than that in the United Kingdom and Germany, with increased production until 1910 [18]. China showed a potential market for international companies, who were looking for new markets in the last quarter of 20th century and by the end of twentieth century, when output reached 200 million hl., China could overtake the United States with the highest beer output [18]. Because of the increase of beer production in China, the overall beer production increased by 2.5% to an estimated 1400 million hl in the year 2002 [17]. During the year 2014, the global beer production was led by China, United States, and Brazil, increased to 1.93 billion liters in comparison to 1.3 billion in 1998

[19]. The increase in world beer production from year 1998 to 2015 is illustrated in **Figure 1.1** [20].

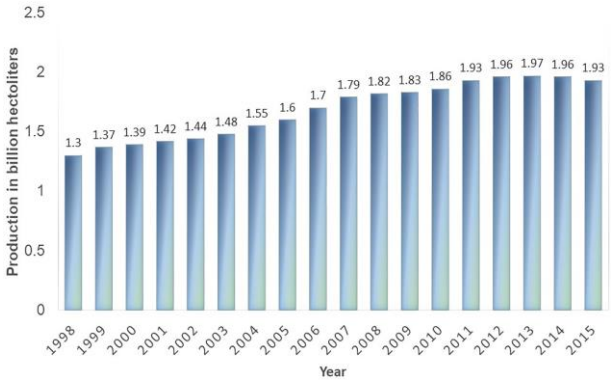

Figure 1.1. World beer production per hectoliter (Years 1998-2015) [20]

The top ten leading countries in worldwide beer production are shown in **Figure 1.2** during the year 2015 [21].

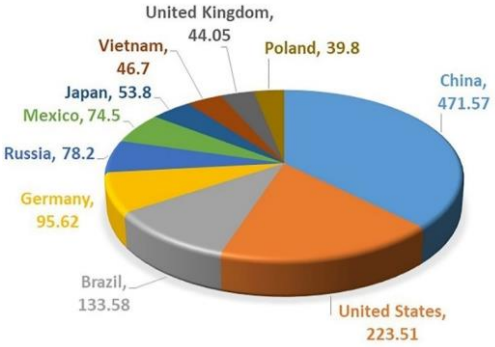

Figure 1.2. Top 10 leading countries in beer production (in million hectoliters) [21]

1.2 Beer processing

Various beer types were produced from a combination of different ingredients, processing conditions, packaging, and culture.

The main ingredients used for beer production were a) water, b) fermentable carbohydrates such as malt, barley, rice, starch, and sugar adjuncts (e.g. maize as a fermentable sugar source), c) hops, and d) yeast [17, 18, 22-25]. Different combinations of the ingredients helped to define various styles of beer products. During the processing step, however there were some factors, which had influence on the perceived aroma and mouthfeel, e.g. a) Configuration and design of the equipment, b) Milling of grains, c) Mashing step, d) Lautering step, e) Type and length of boiling (type of equipment and conditions used) [18, 26] f) Temperature selected for fermentation, g) Time considered for maturation, and h) The filtration step [3, 6, 17, 27].

The first step starts with malting the grains and steeping them into water, laying them out in a dark and cool place to germinate [28, 29]. After the growth of the roots, the malt is dried in a kiln or in the sun and crushed and mixed with hot water in the next step in a mash tun to extract the wort [28, 30]. During the Lautering process, liquid is drained from the mash, and hot water is trickled in the next step to collect large quantity of liquid, which is known as sparging [31, 32]. The wort is then boiled with herbs and hops before fermentation through addition of yeast from previous brew [28]. The beer brewing process with the explained stages in processing is depicted in **Figure 1.3**.

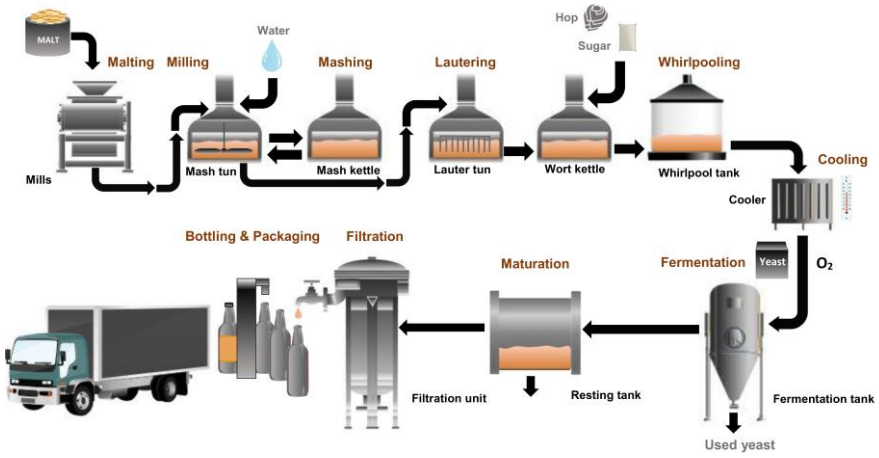

Figure 1.3. Beer brewing process scheme [27, 33, 34]

With development of beer brewing processes, there was a need to develop a method to judge the quality of the beer by human senses.

As some of the variables which helped to distinguish various beer styles, appearance (which is related to quality of foam, color, and clarity of beer) [6, 17, 18, 35-38], *aroma* (if it is malt or hop-related, and changes in aromas during handling and maturation) [6, 18, 39] , *flavor* (related to malt fermentation, packaging and handling, and balance of flavors) can be mentioned [6, 17, 40]. Besides these factors, mouthfeel, could also distinguish various types of beer products [6, 41-43]. In the initial list of flavors developed by Clapperton, he included some factors related to mouthfeel such as CO_2 tingle, harsh, viscous, watery, light, heavy, warming, metallic, mouth coating, mouth puckering, dry, and smooth (creamy) [43, 44]. In later studies, Langstaff et al. identified nine sensory attributes, which were found to be more important in describing thirty commercial beers and related to the mouthfeel of beer, classified them into three groups, which described carbonation (sting, volume of the foam, size of the bubbles, and total CO_2), fullness (density and viscosity), and after-feel, which is related to attributes such as astringency, stickiness and oily mouthcoat [43, 44]. The change that could occur in the flavor profile of beer in different stages of processing, could result in loss of important key aroma components which could affect the final quality of the product, therefore improvements in different stages of processing was always a concern in beverage industry to control the level of key aroma and flavor components that can lead to producing a final product with enhanced stability which is acceptable by the consumer [45-47].

In this thesis, the aim was to investigate alternative techniques, with the focus on adsorption for selective removal and recovery of these flavor-active components, which are critical in producing a high quality final product according to consumers' needs.

1.3 Project FO-10-05 Selective removal of volatiles

The project FO-10-05 defined and granted by ISPT (Institute of Sustainable Process Technology) in the food sector, was focused on selective removal and recovery of volatiles from aqueous food streams (beer) and is in close collaboration with industry, Heineken Supply Chain B.V. in Zoeterwoude, in the Netherlands, University of Wageningen and Delft University of Technology. The aim of this project is to come up with tailored composition beer profiles, which are no longer limited by yeast capabilities and non-alcoholic beer products that match the flavor profile of a normal beer. In order

to accomplish this aim, there are several boundary conditions for applying different technologies within Heineken, e.g. all the materials which are going to be used during processing need to be food-grade and the developed technology should fit within the ball-park of normal brewing operations (e.g. the existing adsorption technologies). Flavor-active components are present at various levels in different process streams, as is illustrated in **Figure 1.4**. The final aim is to achieve high selectivity for separation of flavors over ethanol. During the studies, opportunities for flavor separation and fractionation are investigated, if various products with combination of tuned flavor-active components (e.g. esters) can be produced or different scenarios in adsorption/elution steps can be considered for their enhanced recovery and separation.

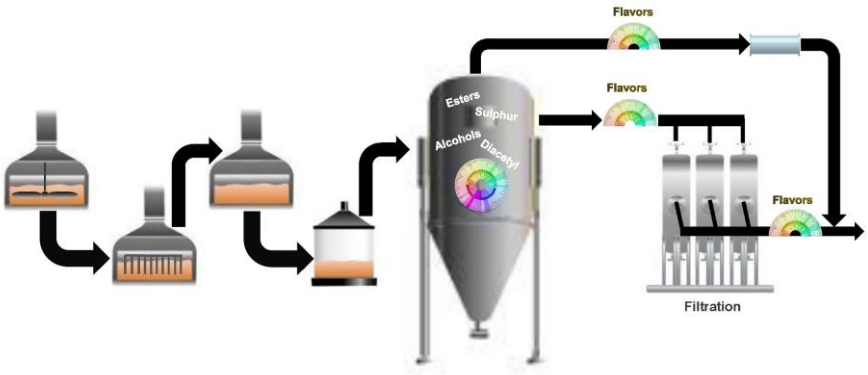

Figure 1.4. Flavor fractionation and balancing, Separation of flavor-active components after fermentation and filtration steps from various process streams [27, 33, 34, 48, 49]

The main aim is to investigate the possibility of separation and selective recovery of esters (mainly ethyl acetate and isoamyl acetate), higher alcohols (mainly isoamyl alcohol), Diketones (mainly diacetyl), and investigate their selective recovery over ethanol. The main target components and typical constituents of beer are summarized in **Table 1.1**.

In previous studies, stripping with selective condensation showed promising results while it's a simple and robust technology, with low CAPEX in large-scale, and achieving significant opportunity of selective recovery over ethanol [68-73].

Table 1.1. Main flavor-active compounds in beer with their concentration range

Flavor-active component	Concentration level in beer (ppm)	References
Diketones		
Diacetyl	0.002- 1	[49-59]
Esters		
Ethyl acetate	8-48	[57-62]
Isoamyl acetate	0.6-7	[59, 60]
Other esters	0.01-1	[56, 59, 60, 62]
Aldehydes		
Acetaldehyde	1.2-24.4	[56, 59, 60, 62-64]
Acetone	1	[59, 62, 65]
Iso-butyraldehyde	0-0.024	[59, 62]
Higher alcohols		
Ethyl alcohol	40,000	[59]
Isobutyl alcohol	2-46	[59, 66]
Isoamyl alcohol	50-60	[59, 66, 67]
Active amyl alcohols	11-25	[59, 67]
Sulphur compounds		
Dimethyl sulphide (DMS)	0.01-1	[59, 66]

Adsorption also shows potential for recovery of aldehydes, diketones and other flavor-active compounds [73-76], therefore further investigation is worthwhile to study different possibilities of selective recovery of volatiles by means of these two techniques (stripping and adsorption), as combined or stand-alone techniques. A simple process scheme for combination of these two techniques is depicted in **Figure 1.5**.

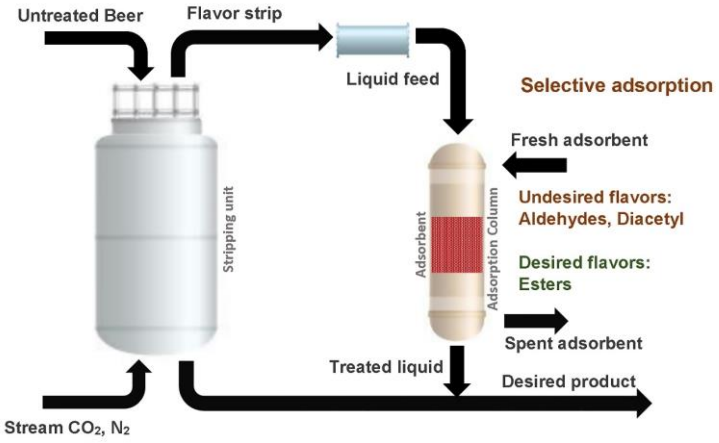

Figure 1.5. Example of process scheme

1.4 Scope and outline of the thesis

The scope of the project, described in this thesis, is on investigating the possibility of selective removal and recovery of flavor-active components and volatile aroma compounds through adsorption. In order to investigate the selective adsorption of flavor-active components, which are present in the beer matrix at low concentration range, and are similar in structure, high throughput experimentation techniques are applied, in combination with thermodynamic and mechanistic modeling. The experimental analysis is performed faster through parallel rather than sequential experiments. Based on the experimental and thermodynamic studies performed in lab-scale, further design is performed for designing an industrial adsorber for flavor separation and fractionation that can be combined and integrated in the whole process with distillation/ stripping unit in different process scenarios or can be applied as an alternative technique for flavor separation and recovery. The ultimate integrated process combines capabilities of high selectivity towards target components and manageability of large volume process streams.

In this thesis selective removal and recovery of volatile flavor-active components is presented using an adsorption process and in seven chapters. **Chapter one** (This chapter) gives an overview of past and future trends on beer brewing, explains the beer processing stages and steps and discusses the outline of the thesis**. Chapter two** highlights the recent advances in available techniques, which are applied for flavor recovery in liquid food processing. Advantages and drawbacks of each technique are discussed for flavor recovery from liquid foods with the aim of minimizing their loss during processing and enhancing the quality of the final product. Adsorption is identified as one of the available techniques for flavor recovery with high potential to be used in combination with thermal processing. The application of this technique is demonstrated for selective removal of flavor-active components in **Chapter three,** through applying high throughput experimentation techniques. The high throughput experimentation technique, which is widely used for separation of proteins, is adapted for separation of flavor components, which are volatile. This chapter discusses the developed methods based on batch uptake experimentation, which are validated with column breakthrough analysis. The improved batch uptake method is applied for investigating the selective

removal of flavor-active components (mainly esters, higher alcohols, diketones, and ethanol). Based on the performed experiments on resin screening, thermodynamic and isotherm studies, and calculated selectivity, optimum resin is proposed which can be applied for designing an adsorption column in an industrial scale.

The tested flavor-active components are present in low concentrations in different process streams with ethanol which is present in high concentration in comparison to flavor-active components, therefore in order to investigate the competitive adsorption of flavors in presence of huge amounts of ethanol, which is present in the matrix and study the possibility of esters' fractionation in an adsorption column, the effect of ethanol concentration is investigated on selective removal and recovery of the flavor-active esters. In order to design the adsorption column for recovery of flavor-active esters in non-isothermal condition, the influence of temperature on maximum equilibrium binding capacities and physical properties like enthalpy of adsorption should be studied and investigated**. Chapter four** presents the results of studies on the influence of ethanol concentration on selective removal of flavor-active esters and influence of temperature on maximum resin uptake and physical properties such as energy and enthalpy of adsorption. In order to investigate the effect of temperature on selective recovery of esters, temperature dependent thermodynamic isotherm models are applied and discussed. The obtained results of selective adsorption of flavor-active esters are used to design the adsorption column for separation and fractionation of flavor-active esters. **Chapter five** discusses the application of predictive models developed based on Adsorbed Solution Theory for predicting the multicomponent adsorption isotherm behavior for flavor-active esters from single-component adsorption isotherms, when experimental information is not available. The application of the obtained experimental information, discussed in chapter four for designing the adsorption column is discussed in **Chapter six,** where the possibility of separation of major esters in beer is investigated in an adsorption column packed with the optimal resin identified in chapter three. The results of the predicted breakthrough curves and the validation with the fractionation results are reported and discussed. Outlooks and recommendations on application of the designed adsorption unit for flavor separation and fractionation and integration of the adsorption column with other

techniques is discussed in **Chapter seven** where the main conclusions of each chapter are given.

References

1. Hornsey, I.S., *A history of beer and brewing*. 2003, Cambridge, UK: The Royal Society of Chemistry.
2. Cardello, A.V., et al., *Cognitive and emotional differentiators for beer: An exploratory study focusing on "uniquness"*. Food Qual. Prefer., 2016. **54**: p. 23-38.
3. Serna-Saldivar, S.O., *Creal Grains, Laboratory reference and procedure manual*. 2012, United States: CRC Press, Taylor & Francis Group L.L.C.
4. Renneberg, R., V. Berkling, and V. Loroch, *Beer, Bread, and Cheese, The tasty side of Biotechnology*, in *Biotechnology for beginners*, R. Renneberg, V. Berkling, and V. Loroch, Editors. 2017, Elsevier Inc.
5. Nelson, M., *The Barbarian's Beverage :A history of beer in ancient europe*. 2005, London & New York: Routledge, Taylor & Francis Group.
6. Oliver, G., *The oxford companion to beer*. 2012, New York: Oxford University Press Inc.
7. Hames, G., *Alcohol in world history*. 2012, London & New York: Routledge.
8. Gately, I., *Drink:A cultural history of alcohol*. 2008, New York: GOTHAM Books, Penguin Group (USA) Inc.
9. Meussdoerffer, F.G., *A comprehensive history of beer brewing*, in *Handbook of brewing: Processes, Technology, Markets*, H.M. Eßlinger, Editor. 2009, Wiley-VCH Verlag GmbH & Co.: Weinheim.
10. Hornsey, I.S., *Alcohol and its role in the evolution of human society*. 2012, Cambridge, UK: Royal Society of Chemistry (RSC).
11. Forbes, R.J., *Studies in Ancient Technology, Volume III*. 1955, Leiden: E.J. Brill.
12. Lutz, H.F., *Viticulture and brewing in the ancient orient*. 1922, Bedford, MA.: Applewood Books.
13. Nelson, M., *Beer in Greco-Roman Antiquity*, in *Department of Classical, Near-Eastern, and Religious Studies*. 2001, The University of British Columbia: Vancouver, Canada.
14. Deming, D., *Science and technology in world history, Volume 4 The origin of chemistry, the principle of progress, the enlightenment and the industrial revolution*. 1954, Jefferson, North Carolina: Mc Farland & Company Inc.
15. Unger, R.W., *A history of brewing in Holland, 900-1900: Economic, Technology, and the State*. 2001: Brill.
16. Poelwijk, A., *Review, A history of brewing in holland, 900-1900: Economy, Technology, and the State by Richard W. Unger.* J. Econ. Hist., 2003. **63**(3).
17. Anderson, R.G., *The pattern of brewing research : A personal view of the history of brewing chemistry in the British Isles.* J. Inst. Brew., 1992. **98**: p. 85-109.
18. Stewart, G.G., I. Russel, and A. Anstruther, *Handbook of brewing*. third ed.: CRC Press, Taylor & Francis Group.
19. Albanese, L., et al., *Beer-brewing powered by controlled hydrodynamic cavitation: Theory and real-scale experiments.* J. Clean. Prod., 2017. **142**: p. 1457-1470.

20. *Beer production worldwide from 1998 to 2016 (in billion hectoliters)*. [cited 2018 24 February]; Available from: https://www.statista.com/statistics/270275/worldwide-beer-production/.
21. *Leading 10 countries in worldwide beer production in 2016 (in million hectoliters)*. [cited 2017 20 October]; Available from: https://www.statista.com/statistics/270269/leading-10-countries-in-worldwide-beer-production/.
22. Davies, N., *Malts*, in *Brewing materials and processes; A practical approach to beer excellence*, C.M. Bamforth, Editor. 2016, Elsevier Inc.: London, UK.
23. Robert, T.R., *Hops*, in *Brewing materials and processes; A practical approach to beer excellence*, B.C. M., Editor. 2016, Elsevier Inc.: London, UK.
24. Russell, I., *Yeast*, in *Brewing materials and processes; A practical approach to beer excellence*, C.M. Bamforth, Editor. 2016, Elsevier Inc.: London, UK.
25. Mayer, H., et al., *Development of an all rice malt beer: A gluten free alternative.* LWT-Food Sci. Technol., 2016. **67**: p. 67-73.
26. Hegarty, P.K., *Beer Foam*, in *Foams: Physics, Chemistry and Structure*, A.J. Wilson, Editor. 1989, Springer-Verlag Berlin Heidelberg GmbH: New York.
27. Preedy, V.R., *Beer in health and disease prevention*. 2009, New York: Oxford University Press.
28. Bescherer Metheney, K. and M.C. Beaudry, *Archeology of food: An Encyclopedia*. 2015, London, UK: Rowman & Littlefield.
29. Linko, M., et al., *Recent advances in malting and brewing industry.* J. Biotechnol., 1998. **65**(2-3): p. 85-98.
30. Briggs, D.E., et al., *The science of Mashing*, in *Brewing:Science and Practice*. 2004, Woodhead Publishing Limited & CRC Press LLC: Boca Raton, US.
31. Boulton, C., *Encyclopedia of brewing*. 2013: John Wiley & Sons.
32. Rabin, D., C. Forget, and G. Smith, *The dictionary of beer and brewing*. 1998, Chicago, US; London, UK: FITZROY DEARBORN PUBLISHERS.
33. Kottenhaler, M., W. Back, and M. Zambow, *Wort production*, in *Handbook of brewing: Processes, Technology, Markets*, H.M. Eßlinger, Editor. 2009, John Wiley & Sons.
34. De Winde, J.H., *Functional genetics of industrial yeasts*. 2003, Berlin: Springer.
35. Hill, A.E., *Brewing Microbiology, Managing microbes, ensuring quality and valorising waste*. 2015, UK: Woodhead Publishing.
36. Lusk, L.T., *Controlling beer foam and gushing*, in *Brewing materials and processes, A practical approach to beer excellence*, C.M. Bamforth, Editor. 2016, Elsevier Inc.: London, UK.
37. Bamforth, C.W., *Beer: TAp into the art and science of brewing*. second ed. 2003, New York: Oxford University Press.
38. Evans, D.E. and C.W. Bamforth, *Beer foam: achieving a suitable head*, in *Handbook of alcoholic beverages series, Beer : A quality perspective*, C.W. bamforth, Editor. 2009, Elsevier Inc.: USA.
39. Carpenter, D., *Lager: The definitive guide to tasting and brewing the world's most popular beer styles*. 2017, China: Quarto Publishing USA Inc.
40. Li, Q., J. Wang, and C. Liu, *Beers*, in *Current developments in biotechnology and bioengineering : Foods and Beverages Industry*, A. Pandey, et al., Editors. 2017, Elsevier B.V.: Amsterdam, The Netherlands.
41. Schultz, S., *Beer, Food and Flavor: A guide to tasting, pairing and the culture of craft beer*. 2015: Skyhorse Publishing Inc.
42. Bamforth, C.W., *Beer and Cider*, in *Physico-Chemical aspects of food processing*, S.T. Beckett, Editor. 1995, Chapman & Hall: Galsgow, NZ.
43. Baxter, E.D. and P.S. Hughes, *Beer: Quality, safety and nutritional aspects*. 2001, Manchester, UK: Royal Society of Chemistry.

44. langstaff, S.A. and M.J. Lewis, *The mouthfeel of beer-A review*. J. Inst. Brew., 1993. **99**: p. 31-37.
45. Stewart, G.G., *Beer: Raw materials and wort production*, in *Encyclopedia of Food and Health*, B. Caballero, P.M. Finglas, and F. Toldra, Editors. 2016, Elsevier Ltd.: UK.
46. Bamforth, C.W., *Practicalities of achieving quality*, in *Handbook of alcoholic bevergaes series, Beer: A quality perspective*, C.W. Bamforth, Editor. 2009, Elsevier Inc.: USA.
47. Hughes, P.S., *THe Stability and Stabilization of beer*, in *Post-fermentation and - Distillation technology: Stabilization, Aging, and Spoilage*, M. Bordiga, Editor. 2018, CRC Press, Taylor & Francis Group: Boca Raton, FL.
48. Meilgaard, M.C., *Beer flavor terminology*. J. Inst. Brew., 1979. **85**: p. 38-42.
49. Krogerus, K. and B.R. Gibson, *125th Anniversary review: Diacetyl and its control during brewery fermentation.* J. Inst. Brew., 2013. **119**: p. 86-97.
50. Martineay, B., T. Acree, and T. Henick-Kling, *A simple and accurate GC/MS method for quantitative analysis of diactyl in beer and wine.* Biotechnol.Tech., 1994. **8**(1): p. 7-12.
51. Harrison, G.A.F., W.J. Byrne, and E. Collins, *The determinationm of diactyl and 2,3-Pentanedione in beer headspace by gas chromatography.* J.Inst. Brew., 1964. **71**: p. 336-341.
52. Portno, A.D. and B. M.I., *Some factors affecting the concentration of diacetyl in beer.* J. Inst. Brew., 1966. **72**: p. 193-196.
53. Wainwright, T., *Diacetyl- A Review, Part I- Analytical and biochemical considerations: Part II- Brewing experience.* J. Inst. Brew., 1973. **79**: p. 451-470.
54. Godtfredsen, S.E. and M. Ottesen, *Maturation of beer with α-acetolactate decarboxylase.* Carlsberg Res. Commun., 1982. **47**: p. 93-102.
55. Bradee, I.H. and D.H. Wastermann, *Beer and brewing*, in *Encyclopedia of Chemical Procesiing and Design*, J.J. Mc Ketta and A. Cunningham, Editors. 1977, Marcel Dekker Inc.: New York, US.
56. Meilgaard, M.C., *Flavor chemistry of beer: part II: flavour and treshold of 239 aroma volatiles.* Tech. Quart. MBAA, 1975. **12**: p. 151-168.
57. Boulton, C. and D. Quain, *Brewing yeast and fermentation*. 2013: John Wiley & Sons.
58. Meilgaard, M.C., *Prediction of flavor diferences between beers from their chemical composition.* J. Agric. Food Chem., 1982. **30**: p. 1009-1017.
59. Harrison, G.A.F., *The flavour of beer- A review.* J. Inst. Brew., 1970. **76**: p. 486-495.
60. Yonezawa, T. and T. Fushiki, *Testing for taste and flavor of beer*, in *Analysis of taste and aroma*, J.F. Jackson and H.F. Linksens, Editors. 2002, Springer: Heidelberg, Germany.
61. Hornsey, I.S., *Brewing*. 1999, UK: Royal Society of Chemistry.
62. Berry, D.R. and D.C. Watson, *Production of organoleptic compounds*, in *Yeast Biotechnology*, D.R. Berry, I. Russell, and G.G. Stewart, Editors. 1987, Allem & Unwin Inc.
63. Otter, G.E. and L. Taylor, *Estimation and occurrence of acedtaldehyde in beer.* J. Inst. Brew., 1971. **77**: p. 467-472.
64. *Physical and chemical properties of beer*, in *Brewing: Science and practice*, D.E. Briggs, et al., Editors. 2004, Woodhead Publishing Limited & CRC Press LLC: Boca Raton.
65. *Aliphatic acrbonyl compounds*, in *Aroma of beer, wine, and distilled alcoholic beverages*, L. Nykanen and H. Suomalainen, Editors. 1983, Reidel Publishing Company: Dordrecht, The Netherlands.
66. Engan, S., *Organoleptic threshold values of some alcohols and esters in beer.* J. Inst. Brew., 1972. **78**: p. 33-36.
67. Reed, G. and T.W. GNagodawithana, *Yeast technology*. 1991, New York: Van Nostrand Reinhold.
68. Catarino, M. and A. Mendez *Non-alcoholic beer-A new industrial process.* Sep. Purif. Technol., 2011. **79**: p. 342-351.

69. Blanco, C.A., C. Andres-Iglesias, and O. Montero, *Low-alcohol beers: Flavor compounds, defects, and improvement strategies.* Crit. Rev. Food Sci., 2016. **56**(8): p. 1379-1388.
70. Del Olmo, Á., et al., *Pervaporation methodology for improving alcohol-free beer quality through aroma recovery.* J. Food. Eng., 2014. **133**: p. 1-8.
71. Catarino, M., A. Ferreira, and A. Mendes, *Study and optimization of aroma recovery from beer by pervaporation.* J. Membrane. Sci., 2009. **341**(1-2): p. 51-59.
72. Purwasasmita, M., et al., *Beer dealcoholization using non-porous membrane distillation.* Food Bioprod. Process., 2015. **94**: p. 180-186.
73. Branyik, T., et al., *A review of methods of low alcohol and alcohol-free beer production.* J. Food Eng., 2012. **108**(4): p. 493-506.
74. Kaneda, H., et al., *Adsorption to or desorption of beer components from a lipid membrane related to sensory evaluation.* J. Biosci. Bioeng., 2001. **92**(3): p. 221-226.
75. Ottens, M., S. Saffarionpour, and T.R. Noordman, *Method of producing beer having a tailored flavour profile.*, Application date: 26 July 2017, Application number EP3193632A1.
76. Saison, D., et al., *Optimization of a complete method for theanalysis of volatiles invloved in the flavour stability of beer by solid phase microextraction in combination with gas chromatography and mass spectrometry.* J. Chromatogr. A, 2008. **1190**: p. 342-349.

Techniques for flavor recovery in Liquid food processing

2

ABSTRACT

Recovery of volatile flavor-active aroma compounds which are key components of processed liquid food streams is of utmost concern to food industry, as these compounds contribute to the quality of the final product. This review paper highlights the recently published research on different techniques that can be applied for recovery of the key flavor components which all aim for minimizing the loss of volatile aromas and (re-) using them in process streams, in order to enhance the flavor profile of the liquid food product. Among the available techniques for flavor recovery in food industry, distillation or stripping, pervaporation, supercritical fluid extraction, and adsorption, showed potential for selective recovery of the flavor components from liquid food streams. These techniques can be combined in different stages of the process or applied as an alternative to the other techniques for aroma recovery. Less attention has been paid to supercritical fluid extraction among the available techniques, especially for recovery of aroma components from alcoholic beverages. Since this technology demonstrated high selectivity for flavor recovery in fruit juices and can take profit from applying natural solvents like CO_2, further research on the application of this technology combined with counter-current flow in a multi-stage contactor is recommended to optimize the recovery process. Adsorption also shows potential for flavor recovery that can be combined with thermal processing or applied as an alternative stand-alone technique.

This chapter is adapted from:

S. Saffarionpour, M. Ottens, Recent advances in techniques for flavor recovery in liquid food processing, Food Eng. Rev., 2018. 10:81-94 https://doi.org/10.1007/s12393-017-9172-8

2.1 Volatile flavor-active components

Flavor perception is the sensory impression of food or any other chemical substance, determined by chemical senses of taste and smell [3]. Flavors are a mixture of volatile aroma compounds, which are classified to Natural, Natural identical, and Artificial flavorings [1, 4-6]. Different chemical substances contribute to particular flavor perceptions [6, 7] as is depicted in **Figure 2.1.** Flavor-active compounds, which are normally present in beverages and liquid foods, are various organic compounds, typically present at low concentrations (ppm levels). Different classes of these organic compounds, which can be regarded as aromas, for instance, are *aldehydes* [7-9], *esters* [10-12], *carboxylic acids* [13, 14], *phenols* [15-18], *hydrocarbons* [19], *ketones* [20], and *terpenes* [21, 22]. These flavor-active components are widely used in beverage industry with the largest market in North America, followed by Asia-pacific and Europe [23]. These markets are highly mature and emerging in Latin America and Eastern countries. Approximately a growth rate of 5% is projected to food flavor market since 2015 and continuous growth is expected till 2020 [24].

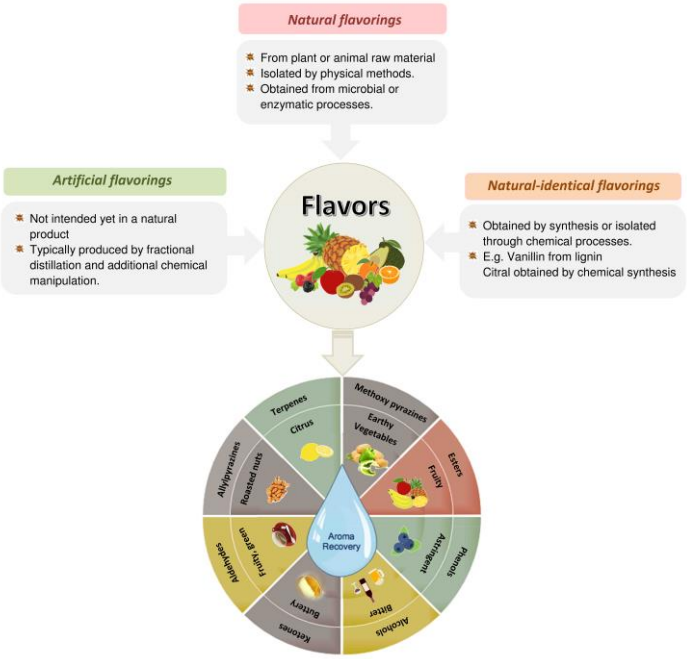

Figure 2.1. Classifications of flavors in food and beverages and contribution of chemical compounds to various flavors [4, 5]

The value of food flavor market is projected to reach USD 15.1 Billion by 2020 [27, 28]. Several alcoholic drinks such as wine, beer, cider, and spirits are available in the market, in which global top players account for share above 60%. Flavored alcoholic beverages (FABs) share an important market segment based on different age groups and beer, cider, and FABs dominated the global market in 2014 [29]. Considering the growing demand for flavor-active components' consumption in food and beverage industry, it is of extreme importance to quantify and control the level of these compounds accurately. The main flavor-active compounds present in liquid foods and beverages together with their physical properties (hydrophobicity and solubility) are presented in **Figure 2.2.** The functional groups (groups responsible for chemical reactions) for each molecule are illustrated in red color. The higher value of partition coefficient, indicates more hydrophobicity of the flavor compound and less solubility in water can be achieved [30].

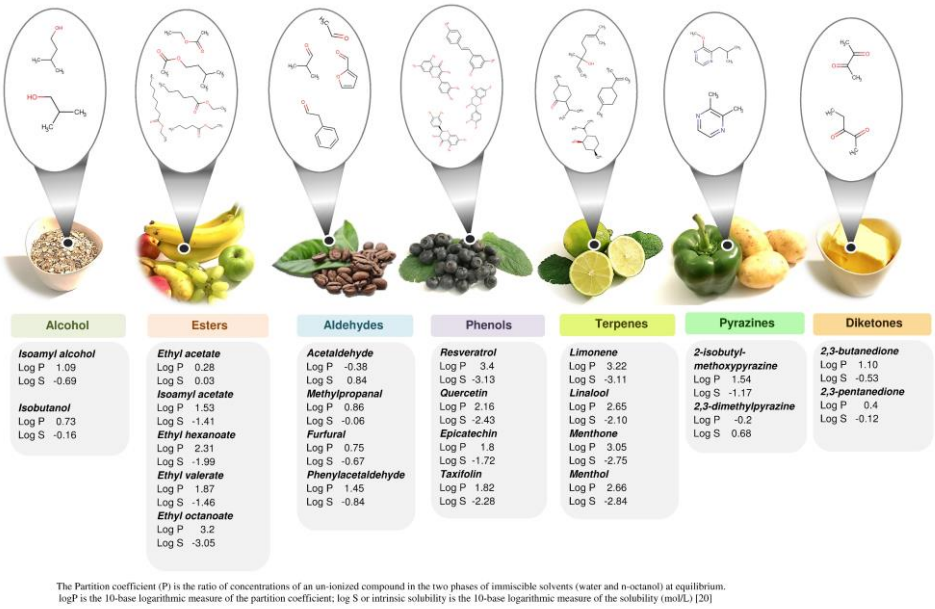

Figure 2.2. Main flavor-active components in liquid foods and their physical properties (Hydrophobicity and solubility) [31]

During processing, the flavor composition of the beverage might alter to a great extent, due to chemical and physical changes of the aroma complex [32]. Chemical changes might occur due to oxidations or Maillard reactions [33], during heat treatment that can result in losses of the flavor compounds or formation of new flavor compounds from original flavors. Physical changes in the flavor composition can also occur during concentration and removal of the excess water, while some amounts of the volatile flavor compounds like esters might be lost due to evaporation. These changes in flavor composition are considered as undesired, and in order to prevent or reduce the unwanted changes in composition of flavors, different techniques can be implemented, which take advantage of the physical properties of flavor-active components like solubility, relative volatility, and hydrophobicity for their separation (as explained in **Figures 2.3, 2.4, 2.5, and 2.6**). To reduce the unwanted changes and losses of flavors during processing, volatile aroma compounds, found in different side-streams of the process, can be selectively recovered or removed from the raw material prior to processing, or improvements in the design can be implemented to achieve the desired recovery. In the latter approach, achieving the desired process option is not always possible and many factors should be taken into account in order to design the appropriate process, which is also feasible in terms of costs in comparison to traditional process. Alternative techniques can be applied and have been proposed by researchers to enhance the aroma recovery, which all aim for minimizing the aroma loss, by producing an aroma concentrate, which can be put back to the final product and consequently improves its sensory quality. This paper serves as a summary, with the aim of giving an overview on the research and developments in techniques that are being applied for aroma recovery in liquid food process industry over the recent years.

2.2 Alternative techniques for flavor recovery

Recovery of the volatile aroma components is practiced in processing of fruit juices, alcoholic beverages, and other liquid food streams and is usually connected with evaporation [34-36]. It is mainly performed by stripping or distillation processes (based on differences in components' relative volatility) and also other alternatives like pervaporation (using vapor and liquid phase and a membrane), supercritical fluid extraction (using liquid/ solid and a supercritical fluid), and adsorption (using solid as

auxiliary phase and liquid). An overview of current research advances in each technology is provided in the next sections.

2.2.1 Aroma recovery through distillation

The principle of the classical distillation system is stripping the aqueous food stream containing the most volatile compounds and concentrate them by fractional distillation to a solution about 100-200 times the original concentration [37]. It usually combines stripping with rectifying and enrichment of the volatile aroma compounds [38] (represented in **Figure 2.3**), in which the former depends on the relative volatility of the aroma components.

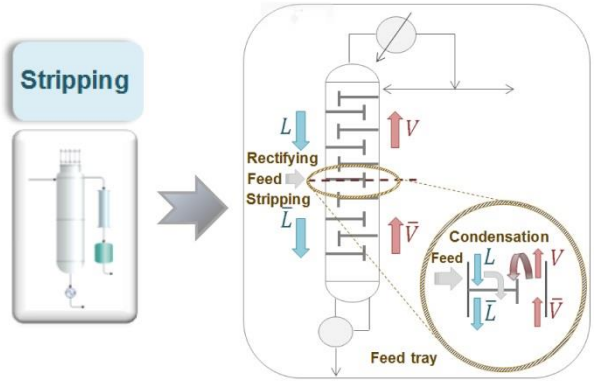

Figure 2.3 Distillation/Stripping technology based on vapor/liquid equilibrium

An impressive number of research works contributes to our understanding of the application of this technology for flavor recovery from liquid food and beverages [39-52]. Few recent research works unequivocally demonstrated the application of Membrane Distillation (MD) and Vacuum Membrane Distillation (VMD) for flavor recovery during the last four years [41, 47, 53, 54]. Performance of MD is investigated during beer dealcoholization process and the effect of feed and vacuum pressure are investigated on flux and selectivity of a thin film composite polyamide membrane. The increase of feed and vacuum pressure could improve the membrane flux, but decreased the membrane selectivity [54] and no major change in composition of the flavor components, maltose and glycerol was observed, only slight loss of maltose in dealcoholized beer was related to the adsorption phenomena on the membrane surface for which membrane flushing for

recovery of the flavor compound was proposed. In comparison to MD configurations, VMD is believed to be an attractive and cost-competitive technology, besides being characterized by a lower operating temperature and hydrostatic pressure. It permits higher partial pressure gradients, therefore higher permeate flux can be achieved [43, 46, 53].

The application of this technology is investigated recently for fractionation and separation of hydrocarbon terpenes of green mandarin from alcohols, ketones and aldehydes [42]. The influence of column pressure on boiling point of essential oil and the composition of compounds in distillate is studied. According to this study, efficient separation of terpenes could not be achieved unless higher number of stages are used and no major degradation of distillate and bottom streams was observed, with no effect on the quality of the final product [42]. In the other studies, different operating strategies like variable reflux rate, are explored to increase the level of terpenic compounds in specific wine distillate fractions to emphasize on floral aroma [40]. A drastic reduction of internal reflux could enhance the recovery of terpenic compounds, while producing a distillate, which is reach in floral aromas, and reduction in cooling flow could increase the presence of higher alcohols and esters. The application of MD is compared with VMD, for comparison of volatile composition of wine fractions by two different dealcoholization techniques, i.e. using a Membrane contactor (MC) and Distillation under vacuum (D). The main difference observed between the two techniques, was the concentration grade reached by the dealcoholized fractions which was 5 to 6 times higher when applying VMD, due to associated loss of water [39]. The result obtained was in agreement with previous observations reported in other research works [44]. Recent study, conducted by Schmitz Ongaratto et al. [45], is concerned with foaming, the main problem associated with stripping which might occur due to formation of gas bubbles in the liquid and their stabilization through adsorption of active surface agents at their interface. They have studied the application of this technology for fruit juice processing, with the focus on studying the feasibility of air stripping implementation, using a bubble column for recovery of the flavor components.

2.2.1.1 Aroma recovery through centrifugal distillation

Distillation can be performed in a Spinning Cone Column (SCC), a technology developed by Conetech [3], for recovery of aromas and removing undesirable volatile

components from fruit juices and other food liquid streams (see **Figure 2.4**). This technology has the advantage that it operates at low temperatures, short residence times, with effective vapor/liquid mixing. Counter-current contacting the vapor and the liquid in alternating and rotating truncated cones which act as contacting stages, increases the mass transfer rates and has the advantage over conventional plate columns, operating at atmospheric pressure, since separation efficiency about 20NTU/m, can be achieved in SCC in comparison to 6NTU/m in packed columns [37].

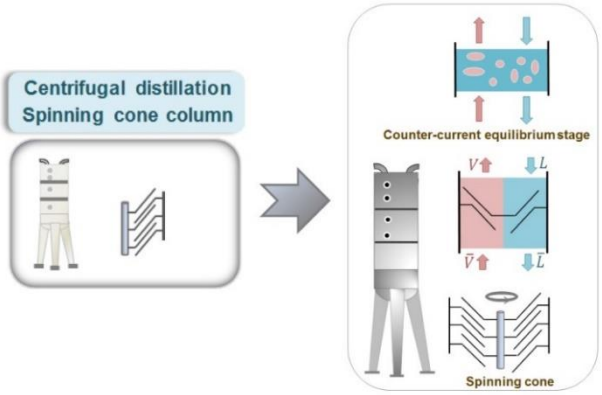

Figure 2.4 Centrifugal distillation technique based on vapor / liquid equilibrium[2, 3]

It has been successfully applied for recovery of volatile aroma compounds in wine and beer industry, for removing delicate aromas, removal of sulphur dioxide from grape juice, production of grape concentrates and alcohol reduction in wines [2, 55, 56]. A number of comparative studies are available on the application of this technology for aroma recovery for liquid foods. **Table 2.1** highlights the most recent research conducted on the application of this technology.

2.2.2 Pervaporation membrane separation technique

Pervaporation is an attractive technology for processing thermal sensitive aroma compounds. This membrane process is based on a selective transport of a liquid mixture through a selective ceramic or polymeric membrane [57] (As illustrated in **Figure 2.5**). This technique can be an alternative to conventional separation processes such as steam distillation, liquid solvent extraction, and vacuum distillation and has been successfully

applied during the last years, for recovery of aroma compounds from fruits and fruit juices [58-63] and subsequent addition to the same juice after concentration by evaporation [64-66]. Pervaporation technique has also been applied for ethanol removal over the last few years [67-69] and aroma recovery from alcoholic beverages [56, 70-72]. The most recent studies for the application of this technique, conducted by different researchers in food industry are summarized in **Table 2.1**.

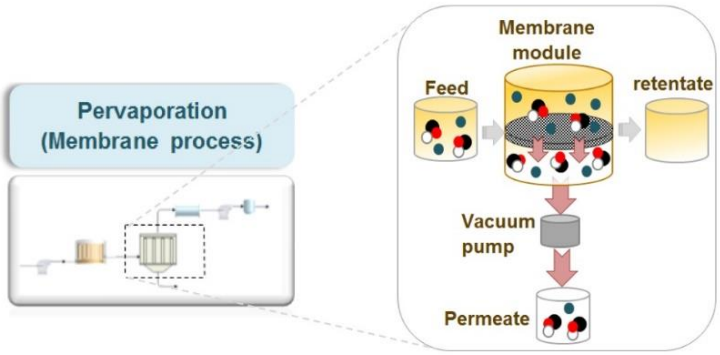

Figure 2.5 Pervaporation membrane technique based on vapor/liquid equilibrium

In the recent studies conducted on aroma recovery from beer and wine, [69, 72] the effect of operating conditions such as feed velocity and temperature and permeate pressure are studied on process performance, considering the responses of permeate flux and aromas/ethanol selectivities, ethanol concentration and ratio between higher alcohols and esters in the permeate. They proposed the optimum operating conditions and the range of selectivities for higher alcohols and esters; four alcohols (ethanol, propanol, isobutanol, and isoamyl alcohol), two esters (ethyl acetate and isoamyl acetate) and an aldehyde (acetaldehyde). According to their studies on lab scale, selectivity of higher alcohols was positively affected by the temperature and to a minor extent by the feed velocity, while permeate pressure affects negatively their selectivity due to their low saturated vapour pressures (low volatilities) [72, 73]). This trend was not observed on industrial plant scale. On the other hand, selectivity of esters decreased with temperature and increased with permeate pressure and velocity. As a result, the ratio of higher alcohols/esters increased with the temperature and decreased with feed velocity and

permeate pressure. A new industrial process was proposed in further studies for producing non-alcoholic beer [69, 72]. The aroma compounds are obtained by pervaporation of the original beer using the same composite membrane, which they had tested in order to investigate the effect of operating conditions in their previous studies. High permeation temperature and low feed flowrate were the most effective for maximizing the permeation flux and the equilibrium of the flavor profile. For production of dealcoholized wine, they could also successfully combine pervaporation with Nano-filtration (NF) for recovery of aroma compounds before the dealcoholisation step and adding the recovered aromas back again to the dealcoholized product, which increased the flavor sensation. The application of pervaporation with NF is investigated for recovery of aromas from low-alcohol white wines [72, 74]. They have investigated the performance of the combined units in pilot scale for recovery of aroma components. A two-stage NF process was tested for sugar reduction of must, followed by pervaporation to recover aroma precursors from grape must (i.e. higher alcohols and esters) and restitution of the flavor precursors. They could achieve the best results for obtaining an optimal aroma profile close to original must, by combining pervaporation with a two stage NF. To achieve more desirable results, they proposed the enhancement of mass transfer during pervaporation through increasing the pervaporation time, a higher feed tangential flow or feed pressure, which improves the aroma transfer, taking into account the limit for maximum pressure drop. In the other studies [75], the final quality of the alcohol-free beer was improved through pervaporation to recover the aromas and flavor constituents of beer, such as isobutyl alcohol, ethyl acetate and isoamyl acetate. The application of pervaporation concentrating volatile aroma compounds in industrial soluble coffee is studied in the research work conducted by Weschenfelder et al. [76]. They have investigated the effect of feed flow rate, temperature, and permeate pressure on the pervaporation performance of selected compounds in the group of ketones (i.e. 2,3-butanedione, and 2,3-pentanedione), aldehydes (i.e. benzaldehyde, and acetaldehyde and furfural and 5-methyl-furfural) and alcohols (i.e. 3-methyl-butanal) and 2,5-dimethylpirazene. For all the tested compounds, permeation flux increased with temperature and results indicated that aroma compound fluxes decreased with partial pressure except for 5-methyl-furfural, and 2,3-butanedione and 2,5-dimethyl pirazene presented the highest enrichment factors in the experimental conditions evaluated in their work. They proposed an optimization step for industrial

purposes in order to concentrate the aroma profile for soluble coffee. More information on current state of research on application of this technology for flavor recovery is given in **Table 2.1**.

2.2.3 Aroma recovery through Supercritical fluid extraction

Supercritical fluid extraction (SFE) is a process, which uses gases at pressure and temperature above the critical point, as illustrated in **Figure 2.6** as solvents to extract valuable materials [77-79].

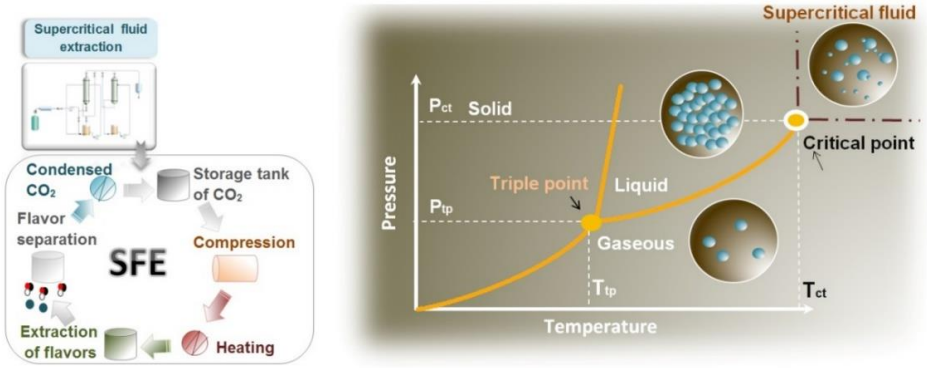

Figure 2.6 Supercritical fluid extraction based on liquid/solid and supercritical fluid

Supercritical extraction with CO_2 has been widely adopted for isolation of volatile aroma compounds in plants and fruits [78, 80, 81] and vegetable oils from preprocessed seeds [82, 83]. There are some research works concerned with aroma recovery from alcoholic beverages [84] combined with dealcoholization process [85-87]. Supercritical CO_2 can be applied for batch extraction of solids, for multi-stage counter-current separation and fractionation of liquids, and for adsorptive and chromatographic separations [85, 88]. This technique is mainly carried out at different modes of operation, which is mainly concerned with extraction from solids, carried out in batch or single-stage mode. Single-stage extraction consists of two process steps, extraction and separation of the extract from the solvent. This simple mode of operation enables contacting the feed until a certain mean residual concentration in the solid raffinate is

achieved, however during the extraction process many factors like extraction kinetics might change due to depletion of the solid substrate from solid that might change the optimum process conditions. In addition, loading the solvents can be enhanced by increasing the number of stages and operating in a counter-current mode. This alteration reduces the amount of solvent required and makes continuous production of extract achievable [85]. Application of counter-current supercritical extraction is studied for apple aroma recovery [78]; the effect of temperature, pressure, and solvent to feed ratio on fractionation and concentration characteristics of six apple aromas is investigated. They could achieve high separation of individual aromas over water, extraction yield of aromas higher than 86%; however, polarity difference between the tested compounds was the drawback of application of this technique for separation of some tested alcohols from aldehydes. The other recent research work, is concerned with extraction of catechins and caffeine from green tea, using different co-solvents, (i.e. ethyl lactate, ethyl acetate, and ethanol) and supercritical CO_2 (SC-CO_2) [89]. Two approaches of static and dynamic were tested in pilot-scale. The highest caffeine extraction yield was obtained with ethyl acetate using both approaches (13 and 14.2 $mg.g^{-1}$ of tea), followed by ethanol (10.8, and 8.8 $mg.g^{-1}$). Lowest extraction yield was achieved using ethyl acetate as co-solvent (lower than 7 $mg.g^{-1}$). Application of ethanol as a co-solvent in extraction of flavors, using SC-CO_2 is also investigated for extraction of fatty acid esters, phenols, coumarin and terpene derivatives from citrus [81]. The most enriched and concentrated extracts of coumarin (osthole) was obtained (approximately 47%) at 170 bar. Furthermore, SCE is successfully applied for flavor recovery and ethanol removal from alcoholic beverages [80, 84, 87, 90]. In the studies conducted by Ruiz Rodrigues et al. [87], this technique is implemented for aroma recovery and ethanol removal from aqueous solutions. They have developed a two-step process for production of low-alcohol beverage from wine by recovering the aromas in a counter-current packed column using low CO_2/wine ratios. The developed two-step process proved to have similar antioxidant activities and aroma profile to the original wine. Recovery of volatile alcohols, and esters is investigated on pilot-scale using counter-current supercritical fluid extraction (CC-SFE) from grape-spirits [90]. The effect of different solvent-to-feed ratios is examined on recovery of volatiles. As they concluded in their survey, in order to achieve the highest ethanol and volatiles' extraction yield, lowest solvent-to-feed-ratio should be used.

SC-CO_2 extraction is employed for extraction of aroma compounds from sugar cane in the work of Gracia et al. [80], for rum production. According to their studies, the extraction yield increased with increasing the temperature and pressure. Optimization of counter-current supercritical fluidic extraction (CC-SFE) conditions is explored by Senorans et al. [84] for obtaining high quality brandy aromas. As is demonstrated in their work, increasing the flow-rate increased the presence of aroma compounds in the separator. When increasing the extraction pressure, a higher sample flow-rate have to be used to achieve the maximum extraction.

Supercritical CO_2 technology is adopted widely and its economic feasibility and advantages over conventional techniques should be proven for each applied technology. Despite initial high capital costs, operating costs would be lower, as it is operated as a continuous process [87, 88, 91], and overall feasibility can be proven at certain scales of operation. This technology enables the possibility of combining an extraction operation with column fractionation under supercritical conditions to concentrate the bioactive flavor components [88]. In comparison to other techniques for aroma recovery, less attention has been paid to application of this technology for recovery of aroma compounds from liquid food streams. Further studies on application of this technique for aroma recovery is recommended, especially for production of alcoholic beverages, which is of high economic interest [29].

2.2.4 Regeneration and recovery of aromas via adsorption

Among the available techniques for aroma recovery, adsorption is a technique, which shows potential for selective recovery of the flavor compounds and can be applied as an alternative to thermal processes or can be combined with distillation/stripping in an integrated process [92-94]. It can be applied as a technique for selective recovery of the compounds based on their affinity towards a ligand (Affinity Chromatography), based on charge (ion-exchange chromatography), hydrophobicity (Hydrophobic Interaction Chromatography (HIC)), and based on polarity, or size of the molecules (Size Exclusion Chromatography (SEC)) [95-97]. The mechanism of different modes of separation in adsorption technique are depicted in **Figure 2.7**. During the last two years this technique has been successfully applied to recover mainly phenolic compounds besides other volatile aroma components from liquid streams in food-processing industry using

adsorbents such as activated carbon, chitosan, minerals (zeolites) and synthetic resins [34, 98-104]. In the recent studies, application of this technique is investigated for recovery of coffee aroma compound benzaldehyde on granular activated carbon derived from coconut husk [98]. The effect of fixed-bed operating parameters like inlet concentration, and inner diameter of the bed are investigated on adsorption and recovery of the aroma component. They could use the obtained results from column performance to perform a scale-up study with error of less than 12%.

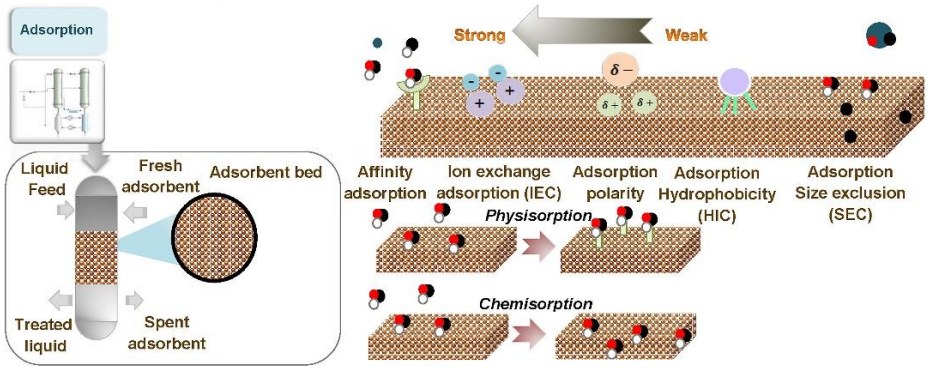

Figure 2.7 Adsorption technique for flavor recovery based on solid / liquid equilibrium[1]

The current research focus is on development of this technique to synthesize new adsorbent materials which have more affinity to adsorb aroma components [103]. The application of synthesized Chitosan, functionalized with Fe_3O_4 magnetic microspheres coated with polyaniline, is studied for adsorption of phenolic components in juice samples. According to the obtained results, synthetic microspheres showed high permeability and acceptable recovery of the phenolic components (between 85 to 107%) [103]. Considering the high potential of this technique for aroma recovery, in combination with other separation techniques or as an alternative, further research is worthwhile to investigate new synthesized and functionalized adsorbent materials, which are also applicable in food industry for recovery of volatile aroma components. **Table 2.1** highlights the recent research and developments on each of the discussed techniques.

2.3 Conclusions

Various techniques are proposed and tested according to studies reported in literature for recovery of aroma components, which all aim for minimizing the loss of aroma

compounds and recovering the key components, which are valuable in producing a high quality final product. The technologies that can be applied for aroma recovery in food industry according to former investigations are stripping or distillation, which can be performed as membrane vacuum distillation or centrifugal distillation, pervaporation, supercritical extraction, and adsorption. Among these available techniques, stripping and distillation are widely applied for aroma recovery in processing alcoholic beverages and juices. Pervaporation as an alternative technique could show promising achievements for recovery of the aroma compounds from aqueous food streams. The current research focus on the application of this technique on aroma recovery is focused on the optimization of conditions to enhance the selectivity over specific aroma components in the process. In comparison to the other alternatives, less attention has been paid to supercritical extraction of aromas, specifically for aroma recovery from alcoholic beverages. The great selectivity of supercritical extraction has been proved by several investigators, which are demonstrative, since they fully take profit of applying supercritical fluid carbon dioxide as a non-toxic, and natural GRAS (Generally Recognized As Safe) solvent with high selectivity at relatively low temperature, which prevents alteration of thermolabile products. Applying this technology, selectivity and capacity can be tuned by changing operating pressure and temperature. Meanwhile combining this technique with counter-current flow and reflux in a multistage contactor can lead to an optimized process conditions. Further research is recommended to study the application of this technique for recovery of aroma compounds, especially in alcoholic beverage industry which is of high economical interest, and where alcoholic beverage fractionation is a challenge, since ethanol is present at significant concentration in comparison to aroma components which are often present at trace levels, and modifies the carbon dioxide solvent power in reducing its selectivity over water and other aroma products. Among the reviewed techniques, adsorption can be applied as a promising technique for selective recovery of aroma components and adding back the recovered key components to process streams, in order to produce a high quality final product. Additional research is required to study the possibilities of applying this technique for flavor recovery as an alternative or combined with thermal processing. This thesis is going to focus on the application of this technique for selective recovery of volatile flavor-active components present in beer in combination with thermal processing or as an alternative technique.

Table 2.1. Recent research on alternative techniques for recovery of food flavors

		Flavor type	Mediator	Matrix	Application	Reference
Techniques based on vapor/ liquid equilibrium	**Distillation / Stripping**	Organic acids, polyphenols, anthocyanins	polypropylene hollow fibers	Rose wine, Pelaverga, and Barbera red wine	MC & VMD for dealcoholization, Influence of treatment on dealcoholized fractions	[39]
		Alcohols, esters, acetaldehyde	Membranes, heat processing	Beer and alcoholic drinks	Ethanol removal and flavor recovery through membrane-based and thermal methods.	[41]
		Terpenes (limonene, linalool, α-terpineol, β-citronellol, geraniol. nerol)	Water vapor/ thermal processing	Wine	Variable reflux rate operating strategies to increase the levels of terpenic compounds in specific distillate fractions to emphasize its floral aroma.	[40]
		Terpenes (methyl-Nmethyl anthranilate, alpha sinensal)	Water vapor	Green mandarin	Vacuum fractional distillation for removal of terpenes	[42]
		Ethyl butyrate, hexanal, ethyl acetate, linalool	air	Fruit juice	Effect of air bubbling on the physicochemical properties of flavors during the extraction of their volatile aroma compounds using a bubble column operated with antifoam.	[45]
		Maltose, glycerol	non-porous membrane, TW30-1812-75 (polyamide)	Beer	MD for dealcoholization of beer. Studying effect of vacuum pressure and membrane flux on flavor recovery	[54]
		Ethyl acetate, ethanol, butanol, acetaldehyde	membrane	Fruit juice	Osmotic distillation (OD) and Vacuum membrane distillation (VMD) for aroma	[48]

					recovery. Studying effect of hydrodynamic conditions and vacuum pressure.	
		Ethyl butanoate, isoamyl acetate, linalool, β-damascenone, furfural, diacetyl, 1,8 cineol, 3-methyl-1butanol, benzaldehyde, cis-hexen-1-ol, 4-terpinenol, eugenol	Sweeping gas, polytetrafluoroethylene (K150) membrane	Berry fruit juice	Sweeping gas membrane distillation (SGMD) for aroma recovery. Studying the influence of temperature, feed and sweeping gas flow-rate on recovery.	[49]
		ethyl 2,4-decadienoate	polypropylene (PP) microporous membranes	Fruits (Pear)	Pear aroma recovery by VMD	[51]
		Ethyl butanoate, isoamyl acetate, linalool, β-damascenone, furfural, diacetyl, 1,8 cineol, 3-methyl-1butanol, benzaldehyde, cis-hexen-1-ol, 4-terpinenol, eugenol	Membrane, water	Black currant juice	Studying VMD for recovery of 12 characteristic aroma compounds.	[52]
	Centrifugal distillation (Spinning cone column SCC)	Ethanol, propanol, isobutanol, amyl alcohol, ethyl acetate, isoamyl acetate, acetaldehyde	Water vapor	Beer	Stripping ethanol and volatile aroma compounds from water vapor stream	[56]
		Resveratrol, flavonols (rutin, quercetin, myricetin), flavan-3-ols, Anthocyanins, non-flavonoids	Water vapor	Wine	Dealcoholization of wine, studying antioxidant activity & phenolic compound composition of red, rose, and white wine	[105]
		Ethanol, glycerol, acetate, succinate, acetoin, 2,3 butanediol, acetaldehyde	Membranes, water vapor	Wine	Recovery of aromas in a two-stage process for aroma recovery (28°C) and for ethanol removal (38°C)	[2]

		Alcohols, aldehydes	Membranes, water vapor	Wine	Comparison of SCC technology for aroma recovery and dealcoholization of wine with other technologies.	[55]
	Pervaporation (PV) membrane separation	Hexal, i-AmOL, 1-HexOL, BezAL, BezOL, 2-PhetOL	Polydimethylsiloxane (PDMS)membrane	Wine	PV combined with Nano-filtration (NF) for aroma recovery	[74]
		isobutanol, ethyl acetate, and isoamyl alcohol	polymethyloctylsiloxane–polyetherimide (POMS/PEI) membranes	Beer	Membrane selectivity used in PV from solubility	[75]
		crustaceans	membranes	Seafood Juices	Aroma concentration of fish and shellfish and issues related to technical and economic feasibility of industrial processes	[106]
		2,3-Butanedione, 2,3-Pentanedione, 3-Methylbutanal, Benzaldehyde, Acetaldehyde, Furfural, 2,5-Dimethylpirazine, 5-Methyl furfural	PDMS membrane	Coffee	Membrane in plate and frame module was used to concentrate key aromas of coffee. The effect of feed flow rate, temperature, permeate pressure was investigated.	[76]
		acetaldehyde, propanol, isobutanol, amyl alcohols (2-methylbutanol plus 3-methylbutanol), ethyl acetate and isoamyl acetate	(POMS/PEI) membrane	Wine	PV combined with Nano-filtration (NF) production of dealcoholized wine	[69]
		Higher alcohols and esters	(POMS/PEI) membrane	Beer	studying the effect of operating conditions	[72]
		isopentyl acetate, 3-methyl-butanal, n-hexanol, and α-ionone	POMS/PDMS membranes	Pomegranate Juice	Recovery of aromas	[63]

		Ethyl Acetate, Ethyl Butyrate, Hexanal, Limonene, Linalool, α-Terpineol	PDMS-PVDF-PP composite membrane with a functional layer of PDMS	Orange juice	Recovery of volatile aroma compounds and studying effect of feed flow rate, temperature and permeate pressure.	[107]
Techniques based on liquid / solid and supercritical fluid equilibrium	**Supercritical fluid extraction (SFE)**	esters	dense CO_2	Alcoholic beverages	Countercurrent supercritical fractionation (CC-SFF) of flavors in packed columns, membrane contactors and mixer-settler systems.	[108]
		(E)-2-hexenal and hexanal	Supercritical CO_2	Apple	CC-SFF of six key apple aromas using dense CO_2 , studying the effect of temperature, pressure and solvent-to-feed ratio on extraction of aromas	[78]
		Epicatechin, Epigallocatechin, Epicatechin gallate, Epigallocatechin gallate, caffeine	Supercritical CO_2	Green tea	Using different solvents (ethyl acetate, ethyl lactate, and ethanol) with SC-CO_2 for extraction in static and dynamic mode in pilot-scale	[89]
		Fatty acid esters, phenols, cumarin and terpene derivatives	Supercritical CO_2	Citrus	Extraction of flavors using ethanol as co-solvent to optimize extraction yield	[81]
		triolein stearic, oleic, linoleic, linolenic	Supercritical CO_2	Vegetable oil	Extraction of vegetable oil from preprocessed seeds, studying the key important parameters for scale-up.	[82]
		Esters (e.g. ethyl acetate, isoamyl acetate, etc.), alcohols (e.g. 2-Methyl-1-propanol, n-Butanol , etc.) acids (Caprylic acid, Isovaleric acid, etc.)	Supercritical CO_2	Wine	Aroma recovery from white and red wine using Supercritical CO_2, Studying different ratios of CO_2/Wine. Recovery of aromas from rose wine in a two-step process.	[87]

		Alcohols (e.g. ethanol, methanol, etc.), esters (e.g. ethyl acetate, isoamyl acetate, etc.)	Supercritical CO_2	Grape-spirit	Recovery of volatiles using CC-SFE, effect of different solvent-to-feed-ratios on extraction yield.	[90]
		Higher alcohols, phenols, fatty acids, esters, ketones,	Supercritical CO_2	Sugar cane spirits	Extraction of intermediate aromas. Effect of temperature and pressure on extraction yield.	[80]
		Esters, aldehydes, ketones, terpenes, lactones	Supercritical CO_2	Brandy	CC-SFE is applied in pilot scale for extraction of aromas and influence of temperature and pressure on extraction yield are investigated.	[84]
Techniques based on solid / liquid equilibrium	**Adsorption**	Esters, higher alcohols, diketones, ethanol	Synthetic hydrophobic resins (XAD series and DIAION resins)	Beer	Adsorption of flavor compounds present in beer. Isotherm studies and resin selectivity. optimum resin proposed for industrial scale.	[99]
		phenols	Ion-exchange resins (Amberlyst A26, Amberlite IRA-67)	Olive	Recovery of flavors from olive mill wastewater. The effect of pH on recovery	[101, 102]
		Fatty acids (e.g. Acetic acid, Propionic acid, Valeric acid, etc.)	Ion exchange resins (Sepra NH2, Amberlyst A21,Sepra SAX, Sepra ZT-SAX	Grape	Recovery of volatile flavors, studying effect of pH on adsorption	[109]
		Carboxylic acids	Amberlite IRA-67, and activated carbon	Fermentation broth	Adsorption from broth under different pH conditions	[110]
		phenols	chitosan (CHI) functionalized Fe3O4 magnetic microspheres coated with polyaniline	Juices	Recovery of flavors	[103]
		catechins	Macroporous polymeric	Tea	Decaffeination of flavors, isotherm	[104]

			resins (XAD resins, DIAION resins)		studies and resin selection	
		benzaldehyde	Activated carbon	Coffee	Fixed-bed adsorption column for recovery of flavors. The effect of feed concentration, flow-rate, column diameter and bed length	[98]

References

1. Ottens, M. and S. Chilamkurthi, *Advances in process chromatography and applications in the food, beverage and neutraceutical industries*, in *Separation, extraction and concentration processes in the food, beverage and neutraceutical industries*, S. Rizvi, Editor. 2010, Woodhead publishing series. p. 109-147.
2. Schmidtke, L.M., J.W. Blackman, and S.O. Agboola, *Production technologies for reduced alcoholic wines.* J Food Sci, 2012. **71**(1).
3. *Conetech 2016*. [cited 23 November 2016]; Available from: http://www.conetech.com/.
4. Branen, A.L., et al., *Food Additives*. Second ed. 2002, Basel, Switzerland: Dekker,M. Inc.
5. *Food additives, Ameliorating the flavors, Enriching the food*. [cited 9 Aug, 2017]; Available from: http://www.foodadditivesworld.com/flavorings.html.
6. Reineccius, G., *Flavor chemistry and technology*. Second ed. 2005: Taylor & Francis Group, LLC.
7. Suriyaphan, O., et al., *Characteristic aroma components of British farmhouse cheddar cheese.* J Agric Food Chem, 2001. **49**: p. 1382-1387.
8. Kiralan, M., *Volatile compounds of Black Cumin Seeds (Nigella savita L.) from microwave-heating and conventional roasting.* J Food Sci, 2012. **77**(4): p. 481-484.
9. Erten, E.S. and K.R. Cadwallader, *Identification of predominant aroma components of raw, dry roasted and oil roasted almonds.* Food Chem, 2017. **217**: p. 244-253.
10. Lee, L.W., et al., *Modulation of the volatile and non-volatile profiles of coffee fermented with Yarrowia lipolytica: I. Green coffee.* LWT-Food Sci Technol, 2017. **77**: p. 225-232.
11. Steen, I., et al., *Influence of serving temperature on flavour perception and release of Bourbon Caturra coffee.* Food Chem, 2017. **219**: p. 61-68.
12. Dulsat-Serra, N., B. Quintanilla-Casas, and S. Vichi, *Volatile thiols in coffee: A review on their formation, degradation, assessment and influence on coffee sensory quality.* Food Res Int, 2016. **89**: p. 982-988.
13. Liu, Q.-R., et al., *Preparation and stabilization behavior of octenyl succinic esters of soybean soluble polysaccharide in acidified milk beverages.* Food Hydrocolloids, 2017. **63**: p. 421-428.
14. Wang, J., et al., *Method development for the analysis of phthalate esters in tea bevergaes by ionic liquid hollow fibre liquid-phase microextraction and liquid chromatographic detection.* Food Control, 2016. **67**: p. 278-284.
15. Cinelli, G., et al., *Study of XAD-2 adsorbent for the enrichment of trace levels of phthalate esters in hydroalcoholic food beverages and analysis by gas chromatography coupled with flame ionization and ion-trap mass spectrometry detectors.* Food Chem, 2014. **146**: p. 181-187.
16. Tan, J., R. Li, and Z.-T. Jiang, *Discrimination of fresh fruit juices by a fluorescent sensor array for carboxylic acids based on molecularly imprinted titania.* Food Chem, 2014. **165**: p. 35-41.
17. Da Silva Padilha, C.V., et al., *Rapid determination of flavonoids and phenolic acids in grape juices and wines by RP-HPLC/DAD: Method validation and characterization of commercial products of the new Brazilian varieties of grape.* Food Chem, 2017. **228**: p. 106-115.
18. Zhou, Q., Y. Qian, and M.C. Qian, *Analysis of volatile phenols in alcoholic beverages by ethylene glycol-polydimethylsiloxane based stir bar sorptive extraction and gas chromatography-mass spectrmetery.* J Chromatogr A, 2015. **1390**: p. 22-27.
19. Da Silva, L.F., et al., *Solid cation exchange phase to remove interfering anthocyanins in the analysis of other bioactive phenols in red wine.* Food Chem, 2017. **227**: p. 158-165.

20. Kalayioglu, Z. and F.B. Erim, *Total phenolic contents, antioxidant activities, and bioactive ingredients of juices from pomegranate cultivars worldwide.* Food Chem, 2017. **221**: p. 496-507.
21. Shahidi, F. and P. Ambigaipalan, *Phenolics and polyphenolics in foods, beverages and spices: Antioxidant activity and health effects-A review.* J Funct Foods, 2015. **18**: p. 820-897.
22. Plaza-Bolanos, P., A.G. Frenich, and J.L. Martinez Vidal, *Polycyclic aromatic hydrocarbons in food and beverages. Analytical methods and trends.* J Chromatogr A, 2010. **1217**: p. 6303-6326.
23. Dongmo, S.N., et al., *Flavor of lactic acid fermented malt based beverages: Current status and perspectives.* Trends Food Sci Technol, 2016. **54**: p. 37-51.
24. Kupska, M., et al., *Comprehensive two-dimensional gas chromatography for determination of the terpenes profile of blue honeysuckle berries.* Food Chem, 2014. **152**: p. 88-93.
25. Dellacassa, E., et al., *Pineapple (Ananas comosus L. Merr.) wine production in Angola: Characterization of volatile aroma compounds and yeast native flora.* Int J Food Microbiol, 2017. **241**: p. 161-167.
26. Marketresearch.com, *Global natural colors and flavors market, By types, applications and Geography : Forecast up to 2017*. MarketsandMarkets.
27. Marketsandmarkets.com. *Food Flavors Market by Type (Chocolate, Vanilla, Fruits & Nuts, Others), Origin (Natural, Synthetic), Application (Beverages, Savory & Snacks, Bakery & Confectionery, Dairy & Frozen Products, Others), & by Region - Global Forecast to 2020*. 2015 [cited 16 February 2017]; Available from: www.marketsandmarkets.com/Market-Reports/food-flavors-market-93115891.html.
28. Barcelo, C. and M. Gassiot, *Determination of diacetyl in beer by gas chromatography with flame-ionization detection.* J Chromatogr, 1978. **147**: p. 463-469.
29. BeverageMarketTrends. *Global alcoholic drinks market size, share, development, growth and demand forecast to 2020- Industry insights by segment, by distribution channel and by geography*. 2015 [cited 17 February 2017]; Available from: http://www.reportlinker.com/p03605424-summary/Global-Alcoholic-Drinks-Market-Size-Share-Development-Growth-and-Demand-Forecast-to-Industry-Insights-by-Segment-Beer-Cider-FABs-by-Distribution-Channel-Supermarkets-Hypermarkets-Specialist-Retailers-On-premise-Others-and-by-Geograph.html.
30. Pires, E.J., et al., *Yeast: The soul of beer's aroma- a review of flavor-active esters and higher alcohols produced by the brewing yeast.* Appl Microbiol Biotechnol, 2014. **98**: p. 1937-1949.
31. *ChemAxon*. [cited 16 February 2017]; Available from: https://www.chemaxon.com/.
32. Karlsson, H.O.E. and G. Tragardh, *Aroma recovery during beverage processing.* J Food Eng, 1997. **34**: p. 159-178.
33. Mottram, D.S., *The Maillard reaction: Source of flavour in thermally processed foods*, in *Flavors and Fragrances, Chemistry, Bioprocessing and Sustainability*, R.G. Berger, Editor. 2007, Springer-Verlag Berlin Heidelberg: Germany.
34. Wylock, C., et al., *Review on the potential technologies for aroma recovery from food industry flue gas.* Trends Food Sci Tech, 2015. **46**: p. 68-74.
35. Valentas, K.J., E. Rotstein, and R.P. Singh, *Handbook of Food Engineering Practice*. 1997: CRC Press LLC.
36. Rao, M.A., et al., *Engineering Properties of Foods*. fourth ed. 2014: Taylor & Francis Group LLC.
37. Saravacos, G. and A.E. Kostaropoulos, *Handbook of Food Processing Equipment*, ed. G.V. Barbosa-Canovas. 2016: Springer International Publishing Switzerland.
38. Maroulis, Z.B. and G.D. Saravacos, *Food Process Design*. 2003, New York: Marcel Dekker Inc.

39. Motta, S., et al., *Comparison of the physichochemical and volatile composition of wine fractions obtained by two different dealcoholization techniques.* Food Chem, 2017. **221**: p. 1-10.
40. Matias-Guiu, P., et al., *Floral aroma improvement of Muscat spirits by packed column distillation with variable internal reflux.* Food Chem, 2016. **213**: p. 40-8.
41. Müller, M., et al., *Physikalische Verfahren zur Entalkoholisierung vershiedener Getränkematrizes und deren Einfluss auf qualitätsrelevante Merkmale.* Chem Ing Tech, 2016. **12**: p. 1911-1928.
42. Silvestre, W.P., et al., *Fractionation of green mandarin(Citrus deliciosa Tenore) essential oil by vacuum fractional distillation.* J Food Eng, 2016. **178**: p. 90-94.
43. Tang, N., et al., *High permeation flux polypropylene/ethylene vinyl acetate co-blending membranes via thermally induced phase separation for vacuum membrane distillation desalination.* Desalination, 2016. **394**: p. 44-55.
44. Ferrarini, R., et al., *Variation of oxygen isotopic ratio during wine dealcoholization by membrane contactors: Experiments and modelling.* J Membrane Sci, 2016. **498**: p. 385-394.
45. Schmitz Ongaratto, R., et al., *Extraction of aroma compounds of fruit juices by air stripping using a bubble column operating with antifoam and its effect on juice properties.* J Food Eng, 2015. **159**: p. 1-8.
46. Drioli, E., A. Ali, and F. Macedonio, *Membrane distillation:Recent developments and perspectives.* Desalination, 2015. **356**: p. 56-84.
47. Chen, G., et al., *Performance enhancement and scaling control with gas bubbling in direct contact membrane distillation.* Desalination, 2013. **308**: p. 47-55.
48. Hasanoğlu, A., et al., *Effect of the operating variables on the extraction and recovery of aroma compounds in an osmotic distillation process coupled to a vacuum membrane distillation system.* J Food Eng, 2012. **111**(4): p. 632-641.
49. Bagger-Jørgensen, R., et al., *Recovery of volatile fruit juice aroma compounds by membrane technology: Sweeping gas versus vacuum membrane distillation.* Innov Food Sci Emerg, 2011. **12**(3): p. 388-397.
50. Bagger-Jørgensen, R., et al., *Recovery of volatile aroma compounds from black currant juice by vacuum membrane distillation.* J Food Eng, 2004. **64**(1): p. 23-31.
51. Diban, N., et al., *Vacuum membrane distillation of the main pear aroma compound: Experimental study and mass transfer modeling.* J Membrane Sci, 2009. **326**(1): p. 64-75.
52. Soni, V., et al., *Modeling and analysis of vacuum membrane distillation for the recovery of volatile aroma compounds from black currant juice.* J Membrane Sci, 2008. **320**(1-2): p. 442-455.
53. Abd El-Rady Abu-Zeid, M., et al., *A comprehensive review of vacuum membrane distillation technique.* Desalination, 2015. **356**: p. 1-14.
54. Purwasasmita, M., et al., *Beer dealcoholization using non-porous membrane distillation.* Food Bioprod process, 2015. **94**: p. 180-186.
55. Margallo, M., et al., *Life cycle assessment of technologies for partial dealcoholisation of wines.* Sus Prod Consump, 2015. **2**: p. 29-39.
56. Catarino, M. and A. Mendez *Non-alcoholic beer-A new industrial process.* Sep Purif Technol, 2011. **79**: p. 342-351.
57. Araujo, W.A., M.E.T. Alvarez, and M.R. Wolf-Maciel, *Evaluation of pervaporation process for recoverying a key orange juice flavour compound: Modeling and simulation.* Comput Aided Chem Eng, 2008. **25**: p. 175-180.
58. Figoli, A., et al., *Evaluation of pervapoartion process for kiwifruit juice by SPME-GC/Ion Trap Mass Spectrometry.* Desalination, 2009. **250**: p. 1113-1117.
59. Pereira, C.C., et al., *Membrane for processing tropical fruit juice* Desalination, 2002. **148**(1-3): p. 57-60.

60. Isci, A., S. Sahin, and G. Sumnu, *Recovery of strawberry aroma compounds by pervaporation.* J Food Eng, 2006. **75**(1): p. 36-42.
61. Olsson, J. and G. Tragardh, *Influence of feed flow velocity on pervaporation aroma recovery from a model solution of apple juice aroma compounds.* J Food Eng, 1999. **39**: p. 107-115.
62. Borjesson, J., H.O.E. Karlsson, and G. Tragardh, *Pervaporation of a model apple juice aroma solution comparison of membrane performance.* J Membrane Sci, 1996. **119**: p. 229-239.
63. Raisi, A. and A. Aroujalian, *Aroma compound recovery by hydrophobic pervaporation: The effect of membrane thickness and coupling phenomena.* Sep Purif Technol, 2011. **82**: p. 53-62.
64. Garcia, V., et al., *Separation and concentration of bilberry impact aroma compound from dilute model solution by pervaporation.* J.Chem.Technol.Biotechnol., 2008. **83**(7): p. 973-982.
65. She, M. and S.T. Hwang, *Recovery of key aroma components from real flavour concentrates by pervaporation.* J.Membrane Sci., 2006. **279**(1-2): p. 86-93.
66. Karlsoon, H.O.E. and G. Tragardh, *Applications of pervapoartion in food processing.* Trends Food Sci.Technol., 1996. **7**(3): p. 78-83.
67. Verhoef, A., et al., *Performance of a nanofiltration membrane for removal of ethanol from aqueous solutions by pervaporation.* Sep. Purif.Technol., 2008. **60**(1): p. 54-63.
68. Takacs, L., G. Vatai, and K. Korany, *Production of alcohol free wine by pervapoartion.* J.Food Eng., 2007. **78**(1): p. 118-125.
69. Catarino, M. and A. Mendes, *Dealcoholizing wine by membrane separation processes.* Innov Food Sci Emerg, 2011. **12**(3): p. 330-337.
70. Brazinha, C. and J.G. Crespo, *Aroma recovery from hydro alcoholic solutions by organophilicpervaporation:modeling of fractionation by condensation.* J.Membrane Sci., 2009. **341**(1-2): p. 109-121.
71. Karlsoon, H.O.E., S. Loureiro, and G. Tragardh, *Aroma compound recovery with pervaporation-temperature effects during pervaporation of a muscat wine.* J.Food Eng., 1995. **26**(2): p. 177-191.
72. Catarino, M., A. Ferreira, and A. Mendes, *Study and optimization of aroma recovery from beer by pervaporation.* J Membrane Sci, 2009. **341**(1-2): p. 51-59.
73. Lipzinki, F., J. Olsson, and G. Tragardh, *Scale-up of pervaporation for the recovery of natural aroma compounds in the food industry. Part1.Simulation and performance.* J.Food.Eng., 2002. **54**(3): p. 183-195.
74. Salgado, C.M., et al., *Application of pervaporation and nanofiltration membrane processes for the elaboration of full flavored low alcohol white wines.* Food Bioprod Process, 2017. **101**: p. 11-21.
75. Del Olmo, Á., et al., *Pervaporation methodology for improving alcohol-free beer quality through aroma recovery.* J Food Eng, 2014. **133**: p. 1-8.
76. Weschenfelder, T.A., et al., *Concentration of aroma compounds from an industrial solution of soluble coffee by pervaporation process.* J Food Eng, 2015. **159**: p. 57-65.
77. Da Silva, R.P.F.F., T.A.P. Rocha-Santos, and A.C. Duarte, *Supercritical fluid extraction of bioactive compounds.* Trends Anal Chem, 2016. **76**: p. 40-51.
78. Bejarano, A. and J.M. del Valle, *Countercurrent fractionation of aqueous apple aroma constituents using supercritical carbon dioxide.* J Supercrit Fluid, 2017. **120**: p. 266-274.
79. Sanchez-Carmago, A.P., et al., *Supercritical Fluid Extraction.* References Module in Chemistry, Mol Sci Chem Eng, 2014.
80. Gracia, I., et al., *Isolation of aroma compounds from sugar cane spirits by supercritical CO2.* J Supercrit Fluids, 2007. **43**: p. 37-42.
81. Trabelsi, D., et al., *Supercritical extraction from Citrus aurantium amara peels using CO2with ethanol as co-solvent.* J Supercrit Fluid, 2016. **117**: p. 33-39.

82. Del Valle, J.M., *Extration of natural compounds using supercritical CO2:Going from the laboratory to the industrial application.* J Supercrit Fluid, 2015. **96**: p. 180-199.
83. Nunez Montoya, G.A., *Development of a simulation tool for the economic optimization of an extraction plant for vegetable substrates using supercritical CO2*, in *ESCUELA DE INGENIERIA*. 2013, PONTIFICIA UNIVERSIDAD CATOLICA DE CHILE: Santiago de Chile.
84. Senorans, F.J., et al., *Isolation of brandy aroma by countercurrent supercritical fluid extraction.* J Supercrit Fluids, 2003. **26**: p. 129-135.
85. Brunner, G., *Supercritical fluids:technology and application to food processing.* J Food Eng, 2005. **67**: p. 21-33.
86. Medina, I. and J.L. Martinez, *Dealcoholisation of Cider by Supercritical Extraction with Carbon Dioxide.* J Chem Tech Biotechnol, 1997. **68**: p. 14-18.
87. Ruiz-Rodriguez, A., et al., *Supercritical CO2 extraction applied toward the production of a functional beverage from wine.* J Supercrit Fluid, 2012. **61**: p. 92-100.
88. Martinez, J.L., *Supercritical fluid extraction of nutraceuticals and bioactive compounds*. 2008: Taylor & Francis Group.
89. Villanueva Bermejo, D., et al., *Effect of cosolvents (ethyl lactate, ethyl acetate and ethanol) on thesupercritical CO2extraction of caffeine from green tea.* J Supercrit Fluid, 2016. **107**: p. 507-512.
90. Da Porto, C. and D. Decorti, *Countercurrent supercritical fluid extraction of grape-spirit.* J Supercrit Fluid, 2010, **55**: p. 128-131.
91. Perrut, M. and M. Nunes Da Ponte, *The extraction of aromas from fermented and distilled beverages.* Proceedings of the 4th International Symposium on Supercritical fluids,ISBN 4-925085-02-6, 1997. **C.**: p. 845.
92. Ottens, M., S. Saffarionpour, and T.R. Noordman, *Method of producing beer having a tailored flavour profile.*, Application date: 26 July 2017, Application number EP3193632A1.
93. Cheng, P.-S., *Method of Producing an aromatised food or beverage product*, S.A. Nestech, Editor. 2016.
94. Heijman, G., W.J. De Bruin, and M.J. Verhoeven, *Process for the production of a liquid coffee concentrate*. 2014, Koninklijke Douwe Egberts B.V.
95. Hage, D.S. and J. Cazes, *Handbook of Affinity Chromatography*. 2005, Taylor and Francis.
96. Schmidt-Traub, H., M. Schulte, and A. Seidel-Morgenstern, *Preparative Chromatography*. second ed. 2012: John Wiley & Sons.
97. Guiochon, G., et al., *Fundamentals of preparative and nonlinear chromatography*. Second ed. 2006, San Diego: Elsevier Academic Press.
98. Dias Canteli, A.M., et al., *Fixed-bed column adsorption of the coffee aroma compound benzaldehyde from aqueous solution onto granular activated carbon from coconut husk.* LWT-Food Sci Technol, 2014. **59**: p. 1025-1032.
99. Saffarionpour, S., et al., *Selective adsorption of flavor-active components on hydrophobic resins.* J Chromatogr A, 2016. **1476**: p. 25-34.
100. Carpine, D., et al., *Adsorption of volatile aroma compound 2-phenyl ethanol from synthetic solution onto granular activated carbon in batch and continuous modes.* J Food Eng, 2013. **117**: p. 370-377.
101. Victor-Ortega, M.D., J.M. Ochando-Pulido, and A. Martinez-Ferez, *Phenols removal from industrial effluents through novel polymeric resins: Kinetics and equilibrium studies.* Sep Purif Technol, 2016. **160**: p. 136-144.
102. Victor-Ortega, M.D., J.M. Ochando-Pulido, and A. Martnez-Ferez, *Performance and modeling of continuous ion exchnage processes for phenols recovery from olive mill wastewater.* Process Saf Environ, 2016. **100**: p. 242-251.

103. Jiang, X., et al., *Polyaniline-coated chitosan-functionalized magnetic nanoparticles: Preparation for the extraction and analysis of endocrine-disrupting phenols in environmental water and juice samples.* Talanta, 2015. **141**: p. 239-246.
104. Mendez Sevillano, D., et al., *Resin selection for the separation of caffeine from green tea catechins.* Food Bioprod process, 2014. **92**: p. 192-198.
105. Belisario-Sanchez, Y.Y., et al., *Dealcoholized wines by spinning cone column distillation:Phenolic compounds and antioxidant activity measured by the 1,1 Diphenyl-2-picrylhydrazyl method.* J Agric Food Chem, 2009. **57**: p. 6770-6778.
106. Bourseau, P., et al., *Recovery of aroma compounds from seafood cooking juices by membrane processes.* J Food Eng, 2014. **128**: p. 157-166.
107. Aroujalian, A. and A. Raisi, *Recovery of volatile aroma components from orange juice by pervaporation.* J Membrane Sci, 2007. **303**: p. 154-161.
108. Bejarano, A., P.C. Simoes, and J.M. Del Valle, *Fractionation technologies for liquid mixtures using dense carbon dioxide.* J Supercrit Fluid, 2016. **107**: p. 321-348.
109. Rebecchi, S., et al., *Volatile fatty acids recovery from the effluent of an acidogenic digestion process fed with grape pomace by adsorption on ion exchange resins.* Chem Eng J, 2016. **306**: p. 629-639.
110. Yousuf, A., et al., *Recovery of carboxylic acids produced during dark fermentation of food waste by adsorption on Amberlite IRA-67 and activated carbon.* Bioresource Technol, 2016. **217**: p. 137-140.

Method development for selective removal of flavor-active components

3

ABSTRACT

This chapter aims to propose an optimum resin that can be used in industrial adsorption process for tuning flavor-active components or removal of ethanol for producing an alcohol-free beer. A procedure is reported for selective adsorption of volatile aroma components from water/ethanol mixture on synthetic hydrophobic resins. High throughput 96-well microtiter-plates batch uptake experimentation is applied for screening resins for adsorption of esters (i.e. isopentyl acetate, and ethyl acetate), higher alcohols (i.e. isoamyl alcohol and isobutyl alcohol), a diketone (diacetyl) and ethanol. The miniaturized batch uptake method is adapted for adsorption of volatile components, and validated with column breakthrough analysis. The results of single-component adsorption tests on Sepabeads SP20-SS are expressed with single-component Langmuir, Freundlich, and Sips isotherm models and multi-component versions of Langmuir and Sips models are applied for expressing multi-component adsorption results obtained on several tested resins. The adsorption parameters are regressed and the selectivity over ethanol is calculated for each tested component and tested resin. Resin scores for four different scenarios of selective adsorption of esters, higher alcohols, diacetyl, and ethanol are obtained. The optimal resin for adsorption of esters is Sepabeads SP20-SS with resin score of 87% and for selective removal of higher alcohols, XAD16N, and XAD4 from Amberlite resin series are proposed with scores of 80 and 74% respectively. For adsorption of diacetyl, XAD16N and XAD 4 resins with score of 86% are the optimum choice and Sepabeads SP2MGS and XAD761 resins showed the highest affinity towards ethanol.

This chapter is partly published as:

S. Saffarionpour, D. Mendez Sevillano, L. A. M. Van der Wielen, T.R. Noordman, E. Brouwer, M. Ottens, Selective adsorption of flavor-active components on hydrophobic resins , J Chromatogr A, 1476 (2016) 25-34, https://doi.org/10.1016/j.chroma.2016.10.053

3.1 Fine-tuning and control of flavor-active components

The quality of a food product is often judged based on its flavor, which is one of the parameters influencing consumer acceptance, hence flavor profile is an important attribute of the final product. Flavor-active components, which may result in the changes in the perceived food flavor, are present in a wide range of concentrations in a food matrix, being in a delicate balance [1-4]. These components are considered as flavor defects or off-flavor when present above certain concentration levels in the food matrix [5]. Producing a product that is consistent in flavor is a major challenge for brewers and off-flavors are foremost concern to the food industry. As key and important contributors to beer flavor and aroma which characterize the quality and palatability of beer, esters, higher alcohols, sulphur components, organic acids, diketones and carbonyl components can be mentioned [6, 7]. Volatile esters are aroma trace components which are generally characterized by fruity-flowery aroma [6], important for flavor profile of fermented beer. The most important flavor-active esters in beer are ethyl acetate (solvent-like aroma) [8, 9], isopentyl acetate (fruity, banana aroma) [8-10], ethyl caproate (sour apple) [8, 9], and ethyl pentanoate (ethyl valerate), (apple, peach, apricot) [11]. Presence of different esters can have a synergistic effect on the individual flavors, besides, esters can affect beer flavor below their threshold concentration level [8, 12] and minor changes in their concentration may have dramatic effects on beer flavor [8, 13].

Higher alcohols contribute to beer flavor by intensifying alcoholic perception and imparting warm mouth-feel [6]. Alcohols contributing most to beer flavor are isoamyl alcohol, phenethyl alcohol, active amyl alcohols and isobutyl alcohol [14, 15]. For beer production, a low concentration of these components can already be large enough to render the flavor of the product unpleasant; this is especially true of isopentyl acetate which is produced in the largest amount [15]. Main vicinal diketones (VDKs) present in beer are diacetyl (2,3-butanedione) [16] and pentane-2,3-dione. Controlling concentrations of these components is of importance in beer industry since they have pronounced butter like aroma's, where especially diacetyl can become unpleasant even at low concentration levels [6, 17-19].

All these flavor-active components must be controlled within specific limits and their relative concentration can confer beneficial or undesirable flavor traits since a shift in their concentration might result in a different flavor for the beer [6, 20]. To produce a high quality beer, one should ensure that the concentrations of negative flavor constituents are below their threshold value, meanwhile one should also ensure that the well-adjusted amount of higher alcohols, esters, and diketones imparts a positive contribution to the end product [6, 21].

3.2 High Throughput Experimentation technique

Different techniques are used for controlling off-flavors, which mostly take advantage of solubility, adsorption or the volatility of aroma components for removing them from the food matrix. High throughput resin screening technique (HTS) has become an important tool in adsorption downstream process development, which saves time and leads to less sample consumption through miniaturization [22]. Applying this technique, the experimental analysis is performed not only faster through parallel rather than sequential experiments, but also done smarter by using experimental design algorithms to obtain “best compromise” with few experiments as possible [23]. Models for large-scale adsorption processes can be developed, relying on adsorption parameters, which are derived from small-scale experimentation. There are some approaches on the application of HTS methods for adsorption. Hermann et al. proposed a device for equally sized resin particles distributed in a 96-well format for measuring the adsorption isotherms and kinetics in protein chromatography [24]. Also a novel technique for measuring protein uptake kinetics based on batch uptake measurements is demonstrated by Traylor et al.[25]. While an impressive literature contributes to our understanding of the application of high throughput experimentation technique for protein separation, less information is reported about this technique as an established method for adsorption of volatile aroma components. The underlying work in this chapter discusses a procedure for adopting the high throughput experimentation technique for adsorption of volatile flavor-active components, where evaporation of the samples from 96-well plate is the main concern.

3.3 Selective adsorption of flavor-active components

Selective adsorption of esters, higher alcohols, diketones, and ethanol from model solutions of the flavor-active components prepared in a co-solvent mixture of ethanol/water is investigated on porous hydrophobic resins, which showed potential for separation of these components according to previous studies reported in the literature [26-30], and batch uptake experimentation is selected and improved in order to study the single and multi-component adsorption of the flavor-active components with high volatility, followed by expressing the experimental results with different thermodynamic models (i.e. Langmuir, Freundlich, and Sips models). Single-component tests are validated for adsorption of ethyl acetate with column breakthrough analysis. Additionally, multi-component adsorption of the flavor-active components is investigated on selected commercially available food-grade resins and the results are expressed with multi-component Langmuir and Sips models. Using regressed interaction parameters, an optimum resin is selected for selective removal of the flavor-active components defined for several scenarios.

3.4 Materials

3.4.1 Chemicals

Ethyl acetate ($purity \geq 99.5\%$), isopentyl acetate (98%), isoamyl alcohol ($\geq 98\%$), and diacetyl (2, 3-butanedione 97%) purchased from Sigma-Aldrich, and isobutyl alcohol (99%) is purchased from SAFC. MilliQ grade water is used and ethanol 96%, is purchased from Merck. Methanol 99.9% for HPLC is purchased from Sigma-Aldrich used in column testing for elution steps. Acetone $\geq$ 99.5% is purchased from Sigma-Aldrich, used for measuring the dead volume of the system in column tests. Sodium chloride is purchased from J.T. Baker for liquid holdup measurements.

3.4.2 Adsorbents

Eight food-grade resins were selected for the adsorption tests. From the Amberlite XAD hydrophobic resin series, 16N (20-60) mesh, 7HP, and 761 are tested, purchased from Sigma-Aldrich and XAD4 is purchased from Fluka. The aromatic type HP resin series, Sepabeads SP20SS, is purchased from Sigma-Aldrich. The brominated modified type, Sepabeads SP207 and Sepabeads SP207SS (smaller particle size version

of SP207), methacrylic type, Sepabeads SP2MGS (smaller particle size version of HP2MG) are purchased from Mitsubishi Chemical Corporation, Resindion, Biokal Labsystems. The selected adsorbents with their physical properties are presented in **Table 3.1**.

Table 3.1 Selected synthetic adsorbents and their physical properties [31, 32]

Resin	Chemical nature	Particle size (µm)	Dry density (Vs. wet) (g/ml)	Surface area (m2/g)	Mean pore size (A°)	Pore volume (ml/g)
Amberlite XAD resin series						
XAD16N	Styrene-DVB	(20-60 mesh) 560-710µm	1.08(1.02)	800	200	0.55
XAD4	Styrene-DVB	(20-60 mesh)	1.08(1.02)	900	100	0.55
XAD7HP	Acrylic ester	(20-60 mesh) 560-710µm	1.24(1.05)	450	90	0.50
XAD761	Formophenolic matrix	(16-50 mesh)	1.24(1.11)	200	600	0.43
DIAION synthetic adsorbents						
Aromatic type HP series						
Sepabeads SP20-SS	Styrene-DVB	50-100µm	(1.3)	500	260	1.01
Aromatic chemically modified						
Sepabeads SP207	Brominated-SDVB	>250µm	(1.18)	600	105	1.1
Sepabeads SP207SS	Brominated-SDVB	63-150µm	----	600		0.9
Methacrylic type						
Sepabeads SP2MGS	Methacrylic	120-160µm	----	500	500	1.3

3.4.2.1 Synthetic adsorbents DIAION series

The selected adsorbents from DIAION resin series are water insoluble three-dimensional cross-linked polymers, which have no ion-exchangeable functional group and have large surface area for adsorbing various organic compounds by means of van der Waals force. These adsorbents are classified based on chemical composition in two types of *aromatic* and *DVB-Styrene copolymers* and the *acrylic type* (methacrylic type). The former aromatic type is

classified to unsubstituted type, which has no functional group (HP series) and chemically modified SP series with high hydrophobic adsorbing property. Each classification has its own properties in accordance with pore distributions (radius). The classification of DIAION synthetic adsorbents is illustrated in **Figure 3.1** [32].

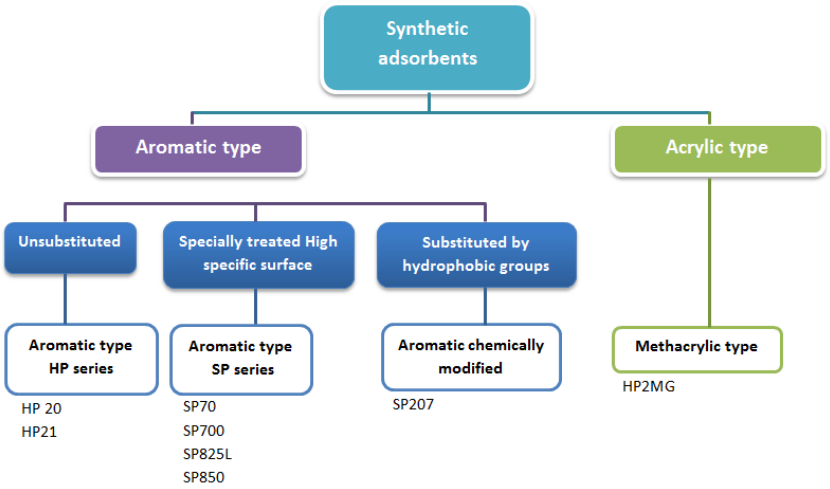

Figure 3.1 Classification of synthetic adsorbents from DIAION resin series [32]

The selected adsorbent Sepabeads SP20SS, which is selected from group of aromatic chemically modified resins, is the smaller particle size version of HP20 with particle size of 63-150 µm. Higher surface area per volume for this resin makes it an efficient packing material for chromatographic separations. The selected resin Sepabeads SP207 functionalized with bromine groups in its aromatic ring has strong hydrophobic property, which makes it possible to be used in batch operations. Sepabeads SPMGS, is the finer particle size version of HP2MG, a methacrylic adsorbent which is an efficient packing material for chromatographic separations [32].

The selected and tested adsorbents from both Amberlite XAD resin series and DIAION synthetic adsorbents are shown in **Figure 3.2.**

Figure 3.2 Tested synthetic adsorbents from Amberlite XAD resins and DIAION Sepabeads

3.5 Methods

3.5.1 Analysis

The tested components are analyzed using Gas chromatography (Focus GC, Thermo Inter-Science, Rodano, Milan, Italy) coupled with FID in a Zebron ZB-WAX Plus $20m\times 0.18\,mm\ ID \times 0.18\mu m\ df$ column. As carrier gas, helium was used in the system. The retention time of tested components is measured during 15 minutes. The obtained chromatogram for the measured components showed the retention time (minutes) of 2.9, 2.6, 2.4, 4.7, 4.5, and 6.4 for diacetyl, ethanol, ethyl acetate, isopentyl acetate, isobutyl alcohol, and isoamyl alcohol respectively. Column breakthrough analysis tests are performed on the Äkta Explorer system 100, purchased from General Electric Life Sciences, Uppsala, Sweden.

3.5.2 Isotherm models

In order to design large-scale adsorption processes, it is necessary to understand how adsorption is influenced by process variables and equilibrium conditions [33-35].

The main experimental challenge is to measure adsorption equilibria accurately, since the tested components, especially esters are highly volatile.

A considerable number of adsorption isotherm models have been suggested in the literature depending on the nature of adsorbent and adsorbate. These models can be divided in different categories for homogeneous and heterogeneous surfaces and whether the adsorbate-adsorbate interaction is significant or negligible [36]. The Langmuir model is an important model that can be used to describe the adsorption behavior of single components. It is a two parameter isotherm model, which refers to monolayer adsorption, and is characterized by an adsorption plateau and saturation point, frequently used to quantify and contrast the performance of different sorbents [37]. However, actual adsorbent surfaces are heterogeneous and adsorption data on real adsorbents are usually expressed with bi-Langmuir, multi-Langmuir, Toth and Freundlich isotherm models. In this work well-known relationships, Langmuir and Freundlich, are selected and compared for single component adsorption tests. Difficulties can arise in accurate description of the adsorbed amount with the Freundlich model at high concentrations, due to the increase of concentration with power 1/n, and it is expected that this model is unable to predict the maximum load at high concentrations, therefore the Sips isotherm, a combined form of Langmuir and Freundlich expressions, circumventing the limitation of the rising adsorbate concentration associated with the Freundlich isotherm [38] is also selected and compared with the tested Langmuir and Freundlich models. In order to describe the competitive adsorption behavior of the tested components in a mixture, multi-component models for the Langmuir adsorption isotherm and Sips adsorption isotherm are used and subsequently compared [39, 40]. The multi-component Freundlich model is not considered, as for single-component adsorption tests, this model showed a lower accuracy in predicting the maximum capacities and a lower value of R^2 was obtained in comparison to the Langmuir and Sips models.

3.5.2.1 Langmuir isotherm

The Langmuir isotherm is a two-parameter model, widely used to describe physical and chemical adsorption [33]. This model is expressed as:

$$q_e = \frac{kq_{max}C_{eq}}{1+kC_{eq}} \tag{3.1}$$

Where q_e is the adsorbed quantity (mg of the adsorbed component/g of the dry resin). C_{eq} is the equilibrium concentration of the liquid in the bulk phase (mg/L), the two parameters k and q_{max} are Langmuir constant (L/mg) and saturation capacity (mg adsorbate /g-dry resin) respectively.

3.5.2.2 Freundlich isotherm

This isotherm is an empirical expression, which describes the adsorption capacity as a function of adsorbate concentration, with a logarithmic scale. The Freundlich expression is presented as [33, 41, 42]:

$$q_e = K_f {C_{eq}}^{1/n} \tag{3.2}$$

Where K_f is the maximum capacity (mg/g-resin)(mg/l) $^{(-1/n)}$ and 1/n is the adsorption intensity(-).

3.5.2.3 Sips isotherm

The Sips isotherm is a combined form of Langmuir and Freundlich expressions, which circumvents the limitation of the rising adsorbate concentration associated with Freundlich isotherm. This model reduces to Freundlich isotherm at low concentrations, while at high concentrations it predicts a mono-layer adsorption capacity characteristic of the Langmuir isotherm model. The equation parameters in this model are governed mainly by the operating conditions such as the alteration of temperature and concentration [38, 43]. It is described in equation (3.3).

$$q_e = \frac{q_{max} k_s {C_e}^{1/n}}{1 + k_s {C_e}^{1/n}} \tag{3.3}$$

Where k_s is the Sips constant related with the affinity constant (mg/L) $^{-1/n}$ and q_{max} is the Sips maximum capacity (mg/g-resin).

3.5.2.4 Multi-component Langmuir isotherm

The non-modified multi-component Langmuir model, is an extension of the Langmuir model, which describes the competition of component i with nc components in the mixture, see equation (3.4) [44, 45].

$$q_{e,i} = \frac{q_{max,i}\, k_i C_{eq,i}}{1+\sum_{j=1}^{nc} k_j C_{eq,j}} \quad (3.4)$$

Where $C_{eq,i}$ represents the concentration in the bulk liquid of species i at equilibrium condition (mg/L), $q_{e,i}$ is the load of species i (concentration of adsorbate on solid) (mg/g-resin), q_{max} represents the maximum load (mg/g-resin), and k_i is the equilibrium constant (L/mg), which shows the affinity of component towards the tested resins.

3.5.2.5 Multi-component Sips isotherm

The multi-component Sips isotherm can be written as explained in equation (3.5) [46].

$$q_{e,i} = \frac{q_{max}\ k_{s,i} C_{e,i}\ (\sum_{j=1}^{nc} k_{s,j} C_{e,j})^{1/n-1}}{1+(\sum_{j=1}^{nc} k_{s,j} C_{e,j})^{1/n}} \quad (3.5)$$

Where $k_{s,i}$ (mg/L) $^{-1/n}$ is the Sips constant for each measured component. q_{max} is the Sips maximum capacity (mg/g-resin).

Both Langmuir and Freundlich isotherms can be viewed as the weighted integral shown in equation (3.6) [47, 48].

$$q_e = \int_{-\infty}^{\infty} g(K_a) \frac{K_a C_{eq}}{1+K_a C_{eq}}\, dK_a \quad (3.6)$$

Where density function *g(K$_a$)*, represents the individual density values of elementary isotherms with its affinity constant *K$_a$* .The distribution of *g(K$_a$)* reduces to Dirac's delta function for Langmuir isotherm and has a normal distribution for Freundlich isotherm [48]. The Sips isotherm allows varying the density function for heterogeneous systems using the index of n (-) for heterogeneity, which varies between zero and one. For a homogeneous material this value is equal to one and is less for a heterogeneous material [49].

3.5.3 Batch uptake method

High throughput experimentation is used for screening the selected synthetic resins. Experiments are performed in 96-well microtiter-plates (Millipore USA), which were filled with the selected resins with the aid of a Titan 96 well Resin Loader (Radleys, UK) and resins are prepared through washing steps with methanol, followed by an

equilibration step with water. Afterwards microtiter-plates are loaded with different concentrations of the solution and covered to prevent evaporation. The schematic view of the 96-well microtiter-plates is depicted in **Figure 3.3.**

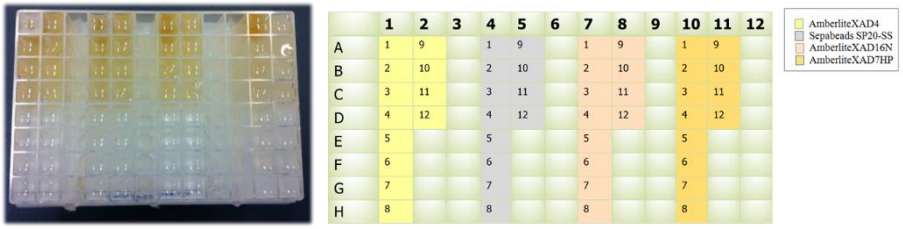

Figure 3.3 Schematic view of a 96-well plate filled with resin and samples

Filter plates are stirred at 300 rpm for 30 minutes equilibration time on a thermo-mixer comfort Eppendorf, Hamburg, Germany with keeping the temperature at (4°C) to reduce the evaporation. The microtiter-plates are then centrifuged on to a deep-well plate (VWR, International, USA) and the remaining bulk liquid after adsorption, and the blank samples are collected in vials for subsequent GC analysis.

The amount of solute i adsorbed per unit mass on adsorbate (q_i) is calculated using the mass balance (equation (3.7)) [40, 50].

$$q_i = \frac{M_{init} - M_{bulk} - M_{lost,evap}}{m_{resin}} \tag{3.7}$$

Where M_{init} is the initial mass of the tested analyte (mg), M_{bulk} is the mass of the analyte remaining after adsorption (mg), which is equal to $C_{bulk} \times (V_{bulk} + V_H)$; C_{bulk} is the bulk concentration of analyte (mg/L), V_{bulk} and V_H are the volume of the collected bulk sample and the hold-up volume of the tested resin(L), m_{resin} is the mass of the tested resin in contact with the bulk (g), $M_{lost,evap}$ is the amount of analyte which is lost due to evaporation (mg), which is calculated by subtracting the mass of the blank samples from the initial mass of the analyte.

3.5.4 Calculation of liquid holdup volume

The resin after centrifugation is never dry and carries some amount of liquid. In order to correctly calculate the amount of adsorbed target component, the volume of

liquid holdup should be considered in the calculations. Liquid holdup determination by salt solution is widely used because of its practical simplicity [51, 52]. For determination of holdup volume, first the resin is prepared according to the procedure explained in section 3.3. Afterwards a known concentration of salt solution is added to the resin, equilibrated for 10 minutes without agitation at 20°C, followed by centrifugation of the plate at 2900g at 20°C for 5 minutes. The permeate is collected and the conductivity of salt is measured. This procedure is repeated until the conductivity of the collected permeate equals the conductivity of the initial salt solution. As the final step, one washing step with water is performed to elute the salt and calculate the hold-up volume from the remaining salt concentration, see equation (3.8).

$$V_H = \frac{C_{salt,f}\, V_W}{C_{salt,initial} - C_{salt,f}} \tag{3.8}$$

$C_{salt,f}$ is the final concentration of salt measured after washing step with water ($g.L^{-1}$), and $C_{salt,initial}$ is the initial concentration of the prepared salt stock solution($g.L^{-1}$) and V_W is the volume of water added to the resin in the final step (L).

3.5.5 Breakthrough analysis

Adsorption isotherms can be retrieved from column tests via breakthrough analysis. In the breakthrough experiment, the limitation of effluent concentration is the influent concentration, which corresponds to achieve adsorption capacity in equilibrium with the influent concentration [53]. The equilibrium capacity can then be calculated from equation (3.9) by calculating the equilibrium binding capacity from the breakthrough curve.

$$q_e = \frac{q_{EBC}}{m_{resin}} \tag{3.9}$$

Where q_{EBC} is the calculated equilibrium binding capacity (mg), m_{resin} is the mass of the resin packed in a column (g). The equilibrium binding capacity is obtained by integrating the area above the breakthrough curve considering also the area corresponding to the dead volume inside the column. The integration for calculating the equilibrium binding capacity is shown in equation (3.10).

$$q_{EBC} = \int_0^v (C_F - C_{out})dv \tag{3.10}$$

Where C_F is the effluent concentration (mg/ml), and C_{out} is the concentration in the outlet stream (mg/ml), v is the column volume (ml).

3.5.6. Experimental procedure

3.5.6.1 Single-component adsorption

Preliminary batch uptake experiments are performed in order to investigate the adsorption of the flavor-active components on Sepabeads SP20-SS. Approximately 2 g/L of the flavor-active components, isoamyl alcohol, isobutyl alcohol, isopentyl acetate, and diacetyl are prepared in 4%w/v co-solvent mixture of ethanol/water. Batch uptake method, as is explained in section 3.3, is applied to investigate the single-component adsorption of the aforementioned components.

3.5.6.2 Column breakthrough tests

In order to validate the results obtained from single-component adsorption tests in batch-uptake mode, breakthrough curves on chromatography column are measured. Approximately 500ml of 2 g/L ethyl acetate solution is prepared in 4%w/v co-solvent mixture of ethanol/water and ethanol/water 4%w/v is used for the dilution steps. Prepared samples are sonicated for 15 minutes, using a Bransonic ultrasonic cleaner 3510, Danbury, CT, USA, to de-gas the prepared solutions. Approximately 2.4 cm^3 resin, Sepabeads SP20-SS, is packed after preparation, (washing steps with water and methanol solution 1%v/v volume in water) by gravity settling. Pure methanol is used for elution and regeneration of the column. Acetone injection is performed to calculate the dead volume of the system and column. The breakthrough curves are retrieved for 10, 20, 30, and 40% concentration of the initially prepared ethyl acetate solution. Experiments are repeated in two sets. The Equilibrium Binding Capacity (EBC) (mg) is calculated by integrating the area above the breakthrough curves, considering also the dead volumes of the system. Equilibrium capacities are calculated according to equation (3.7), and isotherm data are generated in duplicate. Results are compared with the experimental data obtained from single-component adsorption of approximately 2g/L of ethyl acetate on Sepabeads SP20-SS resin, via the Batch uptake method, according to the procedure explained in section 3.3. The experimental results are expressed and compared with Single-component Langmuir model.

3.5.6.3 Multi-component adsorption

The competitive adsorption behavior of the tested flavor-active components is measured via the validated Batch uptake method. Approximately 2 g/L model solution, mixture of the components, i.e. ethyl acetate, diacetyl, isobutyl alcohol, isopentyl acetate, and isoamyl alcohol is prepared in 4%w/v co-solvent mixture of ethanol/water. The experimental data are analyzed via multi-component Langmuir, and Sips isotherm models.

3.5.7 Resin selection procedure

The selectivity is calculated over ethanol for each tested component and for each tested resin, according to equation (3.11).

$$S_i = \frac{K_i}{K_{Ethanol}} \tag{3.11}$$

S_i is the selectivity of the resin towards component i(-). K_i is the affinity calculated for component i (L/g-resin). From the calculated selectivity and the (q_{max}) calculated for monolayer adsorption of each component on each tested resin, optimum resin is selected thereafter. The monolayer adsorption capacity is considered for resin selection and it is assumed that adsorbed molecules occupy the largest possible projected area, with the availability of the whole resin surface for adsorption. The value of q_{max} is calculated according to equation (3.12) [40].

$$q_{max,i} = \frac{S_A M_{w,i}}{A_{m,i}} \tag{3.12}$$

S_A represents the resin surface area (m^2/g-resin), $M_{w,i}$ is the molecular weight of component i (g/mol), and $A_{m,i}$ is the molecular projected area of component i (m^2/mol), obtained from chemAxon [54].

Four different scenarios are considered for the resin selection. The first scenario is if selective adsorption of esters over other components is desired. In this case, selectivity of esters group over ethanol, higher alcohols, and diacetyl and the capacity of resins for esters is considered to score the resins. In the second scenario, separation of higher alcohols is aimed for. In this situation, the selectivity and capacity of higher alcohols over ethanol, esters, and diacetyl are considered. The same procedure is followed for the third

scenario, if we are interested to separate diacetyl, and for the fourth scenario, if we are aimed for removing ethanol from the mixture. Comparison of the selectivity and capacities of the resins will be calculated according to equations (3.13) to (3.18).

$$\theta_{Ester.EtOH} = \frac{\prod_{Ester} \sqrt[2]{K_i}}{K_{Ethanol}} \tag{3.13}$$

$$\theta_{HigherAlcohol.EtOH} = \frac{\prod_{Higher\ alcohol} \sqrt[2]{K_i}}{K_{Ethanol}} \tag{3.14}$$

$$\theta_{Diacetyl.Ethanol} = \frac{K_{DC}}{K_{Ethanol}} \tag{3.15}$$

$$Cap_{Ester} = \frac{\sum_{Ester} Q_{m,i}}{N_{Ester}} \tag{3.16}$$

$$Cap_{HigherAlcohol} = \frac{\sum_{HigherAlcohol} Q_{m,i}}{N_{Higheralcohol}} \tag{3.17}$$

$$Cap_{Diketones} = Q_{m,Diacetyl} \tag{3.18}$$

Π represents the product and Σ the sum and N is the total number of tested components. In order to score the resins, the maximum capacities calculated for monolayer adsorption are considered and weighting factor for three selectivities in each criteria and capacity are considered as 0.2 and 0.4 respectively. Normalization of equations (3.13) to (3.18) is performed by using equation (3.19).

$$Resin\ score = \sum weight \times \frac{Criteria}{Maximum\ value\ of\ the\ criterion} \tag{3.19}$$

3.5.8 Error calculations

The accuracy of the model fitted to the experimental data is considered taking into account experimental errors.

3.5.8.1 Error in measurements

In order to calculate the error propagation in the measurements, equation (3.20) has been used [40, 55].

$$\delta q = \sqrt{((\frac{\partial q}{\partial x_1})^2\ \delta x_1^2 + (\frac{\partial q}{\partial x_2})^2\ \delta x_2^2 + \cdots + (\frac{\partial q}{\partial x_n})^2\ \delta x_n^2)} \tag{3.20}$$

Where δq represents the error propagation in the calculated q. q is the calculated capacity and x_1, …, x_n are the parameters measured experimentally. δx represents the deviation (uncertainty) in each experimentally measured value.

3.5.8.2 Error in regressed parameters

The average relative error function (ARE) is used to calculate the functional error through the entire concentration range which is defined as equation (3.21) [56] and the errors of regressed parameters are taken from the covariance matrix calculated from the Jacobian given by the fitting function [40, 57].

$$ARE(\%) = \frac{100}{n}\sum_{i=1}^{n}\left|\frac{q_{e,i,calc}-q_{e,i,meas}}{q_{e,i,meas}}\right| \quad (3.21)$$

3.5.8.3 Error in calculated resin scores

Different combinations of weighing factors are considered for calculated selectivity in each criteria and also the capacity, and resins are scored based on five different tested combinations of weighing factors. Weighing factor of 0.4 for capacity and 0.6 for selectivity (0.2 for each category) is selected and deviation in calculated resin scores for different combinations of weighing factors are shown in **Fig 3.9** with error bars for each defined scenario and tested resin.

3.6. Experimental results

3.6.1 Single-component adsorption isotherms

The experimental single-component adsorption isotherms for isoamyl alcohol, isobutyl alcohol, isopentyl acetate, and diacetyl, are shown in **Fig 3.4**, together with single-component Langmuir, Freundlich, and Sips isotherm models. The regressed parameters from each model are presented in **Table 3.2**, and the accuracy of the tested models in prediction of the parameters is given.

As the regressed parameters reveal, higher accuracy in prediction is achieved by both Langmuir and Sips models in comparison to Freundlich model (lower value of R^2 is calculated for isopentyl acetate for Freundlich model).

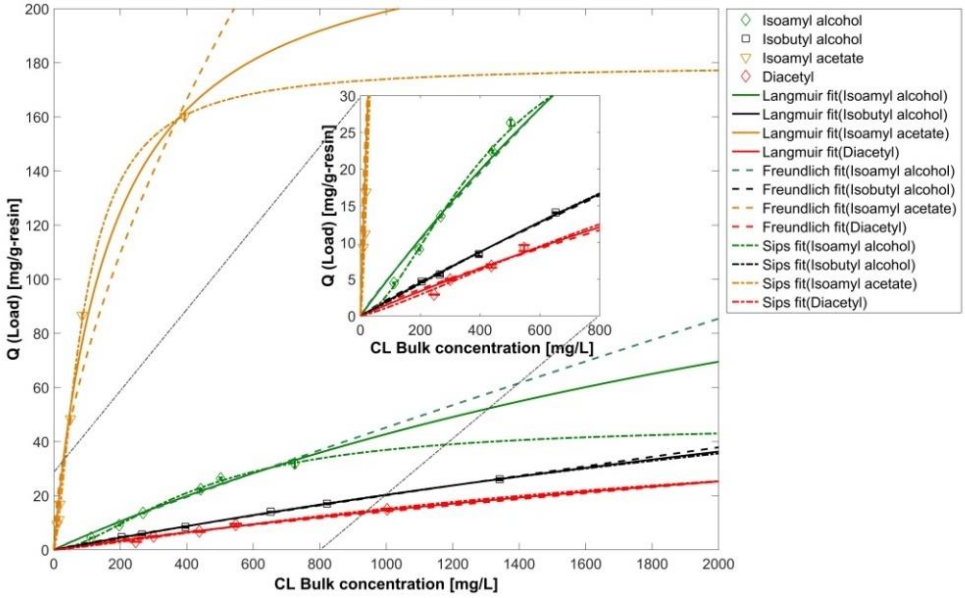

Figure 3.4 Single-component adsorption isotherms, adsorption on Sepabeads SP20SS resin

Table 3.2 Regressed parameters for Langmuir, Freundlich, and Sips isotherm models

Components	**Isoamyl alcohol**	**Isobutyl alcohol**	**Isopentyl acetate**	**Diacetyl**
Langmuir isotherm				
$q_{max}(mg/g)$	185.63±80.82	173.01±110.84	233.67±2.99	92.25±25.90
$(k \times 10^3)(L/mg)$	0.30±0.20	0.13±0.09	5.70±0.20	0.20±0.10
R^2	0.982	0.999	0.987	0.989
Freundlich isotherm				
$k_f\ (mg/g)(mg/L)^{-1/n}$	0.08±0.02	0.04±0.01	4.48±0.15	0.04±0.01
n(-)	1.09±0.06	1.09±0.07	1.66±0.02	1.19±0.07
R^2	0.977	0.998	0.956	0.991
Sips isotherm				
$q_{max}(mg/g)$	46.43±7.92	116.43±181.98	178.98±2.26	51.24±22.29
$(k_s \times 10^3)(mg/L)^{-1/n}$	0.03±0.04	0.14±0.07	1.20±0.17	0.09±0.11
n(-)	0.59±0.09	0.95±0.24	0.67±0.02	0.82±0.17
R^2	0.998	0.999	0.998	0.997

3.6.2 Isotherms retrieved from column breakthrough analysis

A sample of the breakthrough curve derived for initial tested concentration 200 mg/L, is illustrated in **Fig 3.5**.

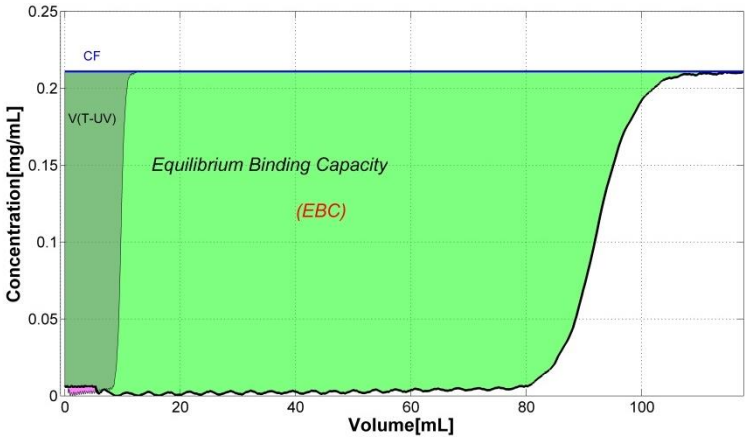

Figure 3.5 Schematic view of a breakthrough curve for concentration 200 mg/L and the integrated area for calculating EBC (Adsorption of ethyl acetate on Sepabeads SP20SS)

Obtained isotherm data for two sets of column experiments and four tested concentrations are demonstrated in **Fig 3.6**, and compared with the isotherm data retrieved from batch uptake experimeı

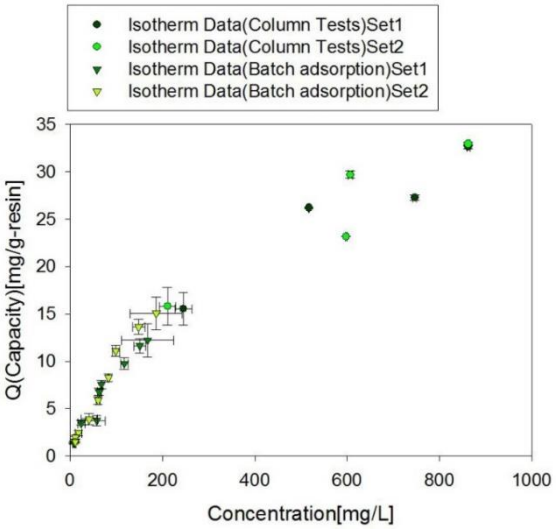

Figure 3.6 Isotherm data for two sets of batch uptake experiments and column breakthrough analysis (Adsorption of ethyl acetate on Sepabeads SP20SS)

The experimental data are expressed with single-component Langmuir model and the parameters are regressed for each experimental set and all the experimental data together. The regressed parameters are assembled in **Table 3.3**.

Table 3.3 Regressed parameters from Batch uptake experiments and column breakthrough analysis, adsorption of ethyl acetate on Sepabeads SP20SS

Test	qmax (mg/g-resin)	(ki× 10^3) (L/mg)	Ki (L/g)
Column test (Set1)	51.02±10.65	1.80±0.80	0.092±0.008
Column test (Set2)	50.26±17.28	2.00±1.50	0.100±0.026
Batch adsorption test(Set 1)	28.50±8.91	4.50±2.10	0.129±0.009
Batch adsorption test (Set2)	44.12±11.24	2.90±1.00	0.128±0.011
All dataset	45.77±2.49	2.50±0.30	0.114±0.001

As the regressed parameters from both methods reveal, the maximum capacity that can be achieved by single-component adsorption of ethyl acetate on Sepabeads SP20-SS resin, is between 30 to 50 (mg/g-resin) and the calculated affinity parameter from both methods, shows similar value considering the standard error in the regressed parameters.

3.6.3 Multi-component adsorption isotherms

The experimental results obtained from multi-component adsorption tests, are expressed with multi-component Langmuir and Sips models. The predicted loads (q modelled) based on Multi-component Langmuir model, are shown for the calculated capacities versus the (q experimental), in a parity plot, depicted in **Figure 3.7** for the tested resin Sepabeads SP20SS, which showed high affinity towards the tested esters, and XAD16N which showed the highest selectivity towards higher alcohols and diacetyl.

The accuracy in fitting with the applied isotherm models is checked with the normal probability plot and histogram of residuals. It is checked if the distribution of residuals are clustered evenly near zero and if the distribution of residuals is normal. The skewness of the distribution is checked if the residuals are positively distributed. The normal probability plot and the histogram of residuals are illustrated in **Figure 3.8** for tested resin Sepabeads SP20SS as an example.

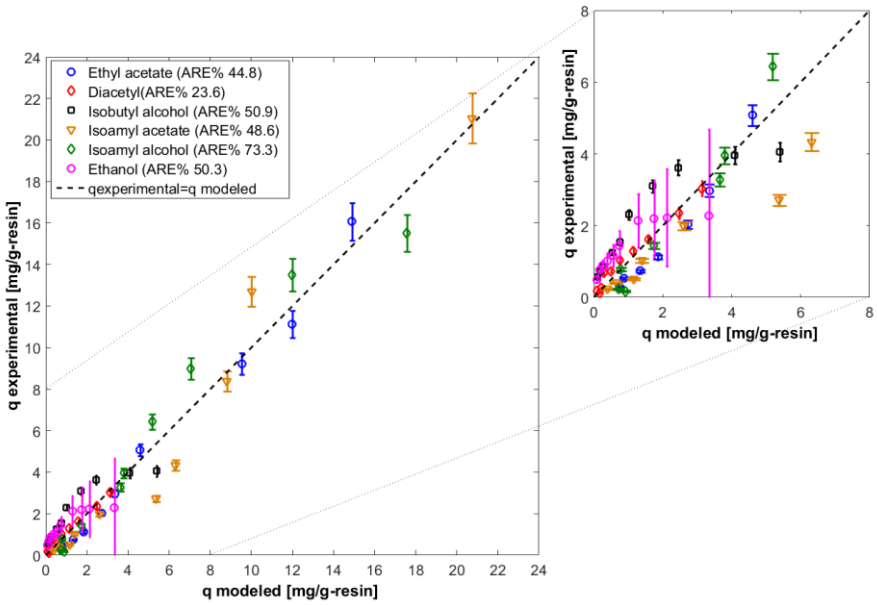

a)

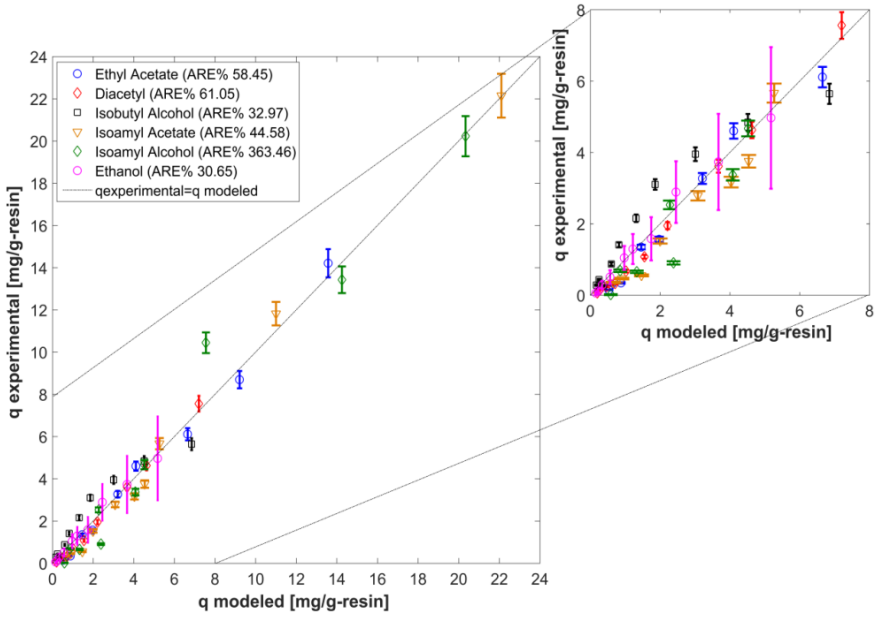

b)

Figure 3.7 Parity plot q experimental vs. q modeled
a) Adsorption on Sepabeads SP20SS b) Adsorption on XAD16N

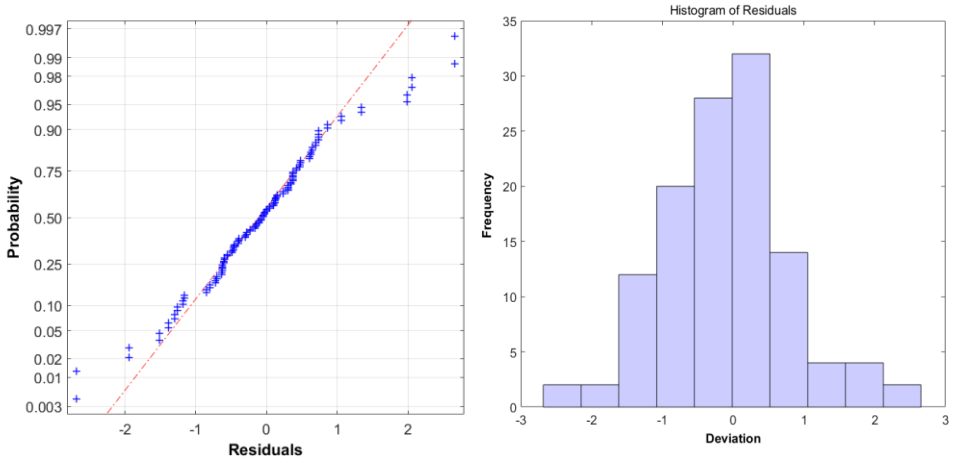

a) b)

Figure 3.8 Distribution of residual values (Multicomponent Langmuir fit), Adsorption on Sepabeads SP20SS a) Normal probability plot b) Histogram of residuals

As can be detected from the normal probability plot, the residuals are distributed close to the line and from the histogram it can be detected that the residual values are normally distributed with the positive skewness.

The regressed parameters from multi-component Langmuir and Sips models, are summarized in **Tables 3.4** and **3.5** respectively and compared.

Table 3.4 Regressed parameters from multi-component Langmuir model

	Tested components						
	Ethyl acetate	**Diacetyl**	**Isobutyl alcohol**	**Isoamyl acetate**	**Isoamyl alcohol**	**Ethanol**	
Resin	**(ki× 10^2) (L/g)**						**Qmax (g/g-resin)**
Amberlite Resin series							
XAD4	33.90±4.10	7.30±0.90	14.70±1.70	240.00±27.90	17.90±2.10	0.40±0.10	0.06±0.01
XAD16N	3.60±1.20	0.70±0.20	0.80±0.30	23.20±7.90	4.20±1.40	0.03±0.01	0.67±0.21
XAD7HP	3.40±1.20	0.80±0.30	1.50±0.50	20.20±7.40	1.90±0.70	0.03±0.01	0.24±0.08
XAD761	1.60±0.70	0.30±0.10	0.40±0.20	5.40±2.20	0.40±0.20	0.04±0.02	0.55±0.21
Sepabeads DIAION resin series							
SP20-SS	37.00±7.60	1.10±0.30	1.80±0.40	3050.00±640.00	7.60±1.60	0.06±0.01	0.23±0.04
SP207	8.90±2.70	1.30 ±0.30	3.00±0.80	48.50±11.90	3.40±0.90	0.05±0.01	0.13±0.02
SP207SS	20.00±2.5	5.90±0.90	12.30±1.60	770.00±90.70	37.10±4.50	0.28±0.04	0.13±0.01
SP2MGS	5.40±0.05	2.10±0.30	4.90±0.40	85.40±6.90	10.40±0.80	0.39±0.03	0.08±0.01

Table 3.5 Regressed parameters from multi-component Sips model

	Tested components							
	Ethyl acetate	**Diacetyl**	**Isobutyl alcohol**	**Isoamyl acetate**	**Isoamyl alcohol**	**Ethanol**		
Resin				**(ki× 10^2) (g/L) $^{(-1/n)}$**			**Qmax (g/g-resin)**	**n(-)**
Amberlite XAD resin series								
4	82.6±9.7	20.8±2.6	39.2±4.4	910.0±100.0	55.9±6.2	0.9±0.1	0.04±0.01	0.69±0.06
16N	25.2±6.8	5.9±1.6	6.1±1.7	250.0±68.1	38.5±10.4	0.2±0.1	0.18±0.03	0.81±0.05
7HP	38.3±4.2	10.6±1.3	18.7±2.0	360.0±39.5	26.9±2.9	0.5±.0.1	0.05±0.01	0.59±0.04
761	9.7±3.6	1.9±0.7	2.6±0.1	51.4±19.0	3.7±1.4	1.3±0.1	0.14±0.04	0.89±0.05
Sepabeads (SP) DIAION resin series								
20-SS	170.0±27.7	6.2±1.3	9.5±1.7	22720.0±3700.0	48.3±7.8	0.30±0.10	0.09±0.01	0.69±0.05
207	2.1±4.9	0.6±1.4	0.9±2.3	27.9±66.7	1.4±3.5	0.02±0.04	0.71±1.22	1.07±0.15
207SS	3.4±6.3	1.0±2.1	2.1±3.9	133.7±240.0	6.4±1.1	0.05±0.09	0.10±0.01	0.81±0.07
2MGS	6.0±1.4	2.3±0.6	5.5±1.3	95.6±22.2	11.7±2.7	0.44±0.10	0.08±0.01	0.97±0.05

3.7. Discussions

The results of single component tests and comparison of different isotherm models (i.e. Langmuir, Freundlich, and Sips models) fitted with the experimental data, reveals a better description with both the Langmuir and Sips models in comparison to the Freundlich model (i.e. lower calculated R^2 for Freundlich model in comparison to the other models). The difference in the fitted isotherm models can be most clearly observed for isopentyl acetate, which has a lower solubility in comparison to the other tested components and shows a more linear trend in the range of measured concentrations. A lower accuracy in the fitting is obtained with the Freundlich model since the experimental data are measured at a low concentration range and according to the definition of Freundlich model, the solid phase concentration increases with the power (1/n) and at higher concentrations it is expected that this model is unable to predict the maximum load. The Sips model, on the other hand, is able to explain the experimental isotherm data, with higher accuracy, as it predicts Freundlich behavior at low concentrations and a more accurate maximum capacity close to monolayer adsorption at higher concentrations, therefore the Langmuir and Sips models, which both showed high accuracy in prediction of single-component adsorption, are further used in expressing the multicomponent adsorption results, and Freundlich model is not considered to describe the multi-component studies, since it showed a lower accuracy in prediction in comparison to other tested models for single-component adsorption tests.

The multicomponent adsorption tests and the regressed values for the affinity constants, show relatively strong adsorption on the tested resins Sepabeads SP20-SS and Sepabeads SP207SS, from the DIAION resin series and the two tested resins XAD16N and XAD 4 from Amberlite resin series. The tested resin, Sepabeads SP20-SS shows more affinity towards more hydrophobic components in the mixture, i.e. the tested esters, mainly isopentyl acetate in comparison to ethyl acetate, therefore, less resin capacity remains for the other flavor-active components with lower hydrophobicity, i.e. higher alcohols and diacetyl. The relatively strong adsorption, which is achieved on this resin is due to the hydrophobic nature and small particle size of this resin (50-100µm) in comparison to the conventional HP20 resins (250-850µm). In the situation where high selective removal of esters is demanded, this resin can be an optimum choice. The aromatically modified resin Sepabeads SP207SS shows also high affinity towards esters, which is also due to its increased hydrophobic nature and because of the presence of bromine groups and the smaller uniform particle size (63-150µm) of this resin in comparison to the larger particle size version, Sepabeads SP207 (250µm), thereby enhancing adsorption. For adsorption of highly hydrophobic components, this resin can be applied, but while it has good adsorption properties, it is difficult to elute the strongly bounded components from this resin. Considering ease of elution of the flavor-active components, resins in the HP-MG series (Sepabeads SP2MGS) can be applied as well as resins from Amberlite XAD series, 4 and 16N, which have high surface areas and higher capacity in comparison to the other tested resins in this group, i.e. XAD7HP and 761, and also showed high affinity constants towards the tested components. The lowest affinity parameters were regressed with both models for diacetyl and ethanol respectively on all tested resins, in line with the fact that these components are more polar and hydrophilic in comparison to the other tested flavor-active components. The resins XAD761 from the Amberlite resin series and Sepabeads SP2MGS from the DIAION resin series, show a higher tendency to adsorb these more polar compounds. The heterogeneity index calculated from Sips model is between 0.6 to 1.1 for all the tested resins. The tested resins in the DIAION resin series, i.e. Sepabeads SP207 and Sepabeads SP2MGS showed heterogeneity index close to one, which shows the more homogeneous structure of these resins in comparison to the tested resins in Amberlite group.

3.8. Resin selection

Resins are scored in the four defined scenarios, according to the procedure explained in section 3.5.7 and a suitable resin in each defined scenario is selected by comparing the calculated resin scores for all of the tested resins for each scenario. The resin scores are depicted in **Fig 3.9** and the calculated maximum capacities for monolayer adsorption are assembled in **Table 3.6**.

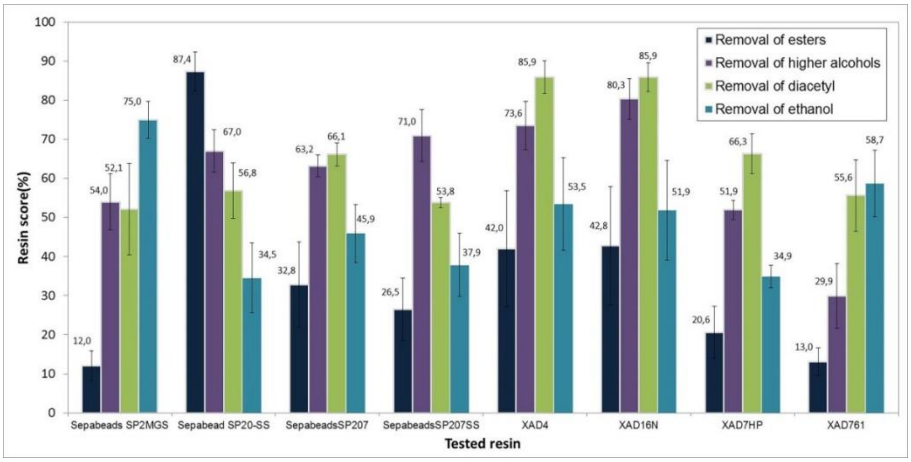

Figure 3.9 Calculated resin scores for all the tested resins

Table 3.6 Calculated maximum loads for monolayer adsorption of the flavor-active components

Component	Qmax (monolayer adsorption) (mg/g-resin)							
	Amberlite resin series				DIAION Sepabeads resin series			
					HP series		chemically modified	
	XAD 4	***XAD 16N***	***XAD 7HP***	***XAD 761***	***SP 20-SS***	***SP 207***	***SP 207SS***	***SP 2MGS***
Ethyl acetate	457.2	465.2	213.2	123.0	318.2	344.8	318.2	265.2
Diacetyl	513.5	522.5	239.5	138.2	357.4	387.2	357.4	297.9
Isobutyl alcohol	392.2	399.1	182.9	105.6	273.0	295.8	273.0	227.5
Isopentyl acetate	435.4	442.9	203.0	117.2	303.0	328.3	303.0	252.5
Isoamyl alcohol	391.5	398.3	182.6	105.4	272.5	295.2	272.5	227.1
Ethanol	385.9	392.6	179.9	103.9	268.6	290.9	268.6	223.8

For selective removal of esters, Sepabeads SP20-SS resin showed highest potential with the score of 87% in comparison to the other tested resins. For recovery of higher alcohols, XAD16N, XAD4, and Sepabeads SP207SS are the best options. Recovery of diacetyl is best achieved on XAD16N and XAD4, which have high capacity

and surface area. Sepabeads SP2MGS has a higher tendency to adsorb intermediate polar components in comparison to other hydrophobic resins, but since the maximum capacity for monolayer adsorption of this resin is lower in comparison to other tested resins in Amberlite resin series (i.e. XAD16N, and XAD4), lower resin score is calculated for this resin in case of diacetyl removal. Sepabeads SP2MGS and XAD761 are the resins with high potential to remove ethanol in comparison to the other tested resins. Based on the optimum selected resin, a process can be developed for fractionation, recovery or removal of the flavor-active components, either in a Batch mode chromatography, Fixed-bed [39, 58], or counter-current mode, in a Simulated Moving Bed, which is a cost-efficient separation technique that offers high productivity and low solvent consumption [59]. Detailed economic evaluation and design to evaluate the large-scale process falls beyond the scope of the present paper and is material for future work.

3.9. Conclusions

This study provides a procedure for developing an appropriate method for selective removal of flavor-active components, i.e. esters, higher alcohols, a diketone (diacetyl), and ethanol, from a mixture of ethanol/water, based on their competitive adsorption behavior. Batch uptake experimentation has been used successfully to investigate multi-component adsorption of the components, after validation of the results of single-component adsorption of tested components on one selected resin, with column dynamic testing and breakthrough analysis. Isotherms are obtained, and compared based on the different thermodynamic isotherm models, Langmuir, Freundlich, and Sips.

A higher accuracy in prediction was achieved through expressing the experimental results with Langmuir and Sips isotherm models in comparison to Freundlich model and the calculated values for R-squared neatly demonstrate this higher accuracy in prediction of adsorption behavior for all the tested components with these two models. Isotherm parameters, affinity constants, capacities, and heterogeneity indexes are regressed from the tested models (multi-component Sips and multi-component Langmuir) and results are compared for different screened resins and tested components. From the calculated selectivity and capacities, resins are scored in four different scenarios for selective removal of esters, higher alcohols, and diacetyl. As the

calculated resin scores reveal, Sepabeads SP20-SS is the optimum resin for selective removal of esters with highest rank of 87%. Maximum adsorption of higher alcohols can be achieved on XAD16N, and XAD 4, and Sepabeads SP207SS with score of 80, 74, and 71% respectively. Sepabeads SP2MGS and XAD761 are the best selection for removal of ethanol with high resin scores of 75 and 59%. For selective removal of diacetyl, XAD16N and XAD 4 resins in the Amberlite resin series, which have high surface area and capacity are proposed. The recommended resins in each scenario can be applied in the next step in process design of the adsorption unit for fractionation of the flavor-active components and production of alcohol-free product. Considering both the high selectivity of the resin towards the tested components and economic feasibility for implementing the resins in the process, tested resins in the Amberlite XAD resin series, i.e. XAD16N and XAD 4 are the two optimum selected resins, which have high surface area and high capacity for adsorption. Although Sepabeads SP20-SS resin is more expensive in comparison to the tested XAD resins, the higher calculated selectivities of this resin towards esters indicates that this resin shows comparable efficiency in esters' adsorption and can be applied in the process for esters' fractionation.

References

1. Verhagen, L.C., *Beer Flavor*, in *Natural flavors*, J.R. Piggot and A. Paterson, Editors. 1994, Springer-Science+Business Media, B.V.: Dordrecht. p. 967-997.
2. Aumatell, M.R., et al., *Assessment of the aroma profiles of low-alcohol beers using HS-SPME-GC-MS.* Food Res Int, 2014. **57**: p. 196-202.
3. Da Silva, G.A., F. Augusto, and R.J. Poppi, *Exploratory analysis of the volatile profile of beers by HS-SPME-GC.* Food Chem, 2008. **111**: p. 1057-1063.
4. Aquilani, B., et al., *Beer choice and consumption detrminants when craft beers are tasted: An exploratory study of consumer preferences.* Food Qual Prefer, 2015. **41**: p. 214-224.
5. Charalambous, G., *The Analysis and Control of Less-desireable Flavors in Foods and Beverages*. 1980: Academic Press.
6. He, Y., et al., *Wort composition and its impact on the flavour-active higher alcohol and ester formation of beer-a review.* J Inst Brew., 2014. **120**: p. 157-163.
7. Siqueira, P.H., H.M.A. Bolini, and G.A. Macedo, *Beer production and its effects on the presence of polyphenols.* Braz J Food Nutrition, 2008. **19**(4): p. 491-498.
8. Verstrepen, K.J., et al., *Flavor-active Esters: Adding Fruitiness to beer.* J Biosci Bioeng, 2003. **96**(2): p. 110-118.
9. Kobayashi, M., H. Shimizu, and S. Shioya, *Review,Beer Volatile Compounds and their application to low-malt beer fermentation.* J Biosci Bioeng, 2008. **106**(4): p. 317-323.
10. Da Silva, G.C., et al., *Method development by GC-ECD and HS-SPME-GC-MS for beer volatile.* Food Chem, 2015. **167**: p. 71-77.
11. Winter, R., *A Consumers' Dictionary of Food additives*. 7 ed. 2009, New York: Crown Publishing group.
12. Meilgaard, M.C., *Flavor chemistry of beer. Flavor interaction between principal volatiles.* MBAA Tech.Quart., 1975. **12**(3): p. 107-117.
13. Haammond, J.R.M., *Brewing yeast.In the Yeasts*, ed. A.H. Rose and J.S. Harrison. Vol. 5. 1993, London: Academic Press.
14. Harrison, G.A.F., *The Flavour of beer- A Review.* J Inst Brew, 1970. **76**: p. 486-495.
15. Rous, C.V. and R. Snow, *Reduction of higher alcohols by fermentation with a Leucine-Auxotrophic mutant of wine yeast.* J Inst Brew., 1983. **89**: p. 274-278.
16. Zandi, M., et al., *Evaluation of diacetyl encapsulated alginate-whey protein microspheres release kinetics and mechanism at simulated mouth conditions.* Food Res Int, 2014. **56**: p. 211-217.
17. Pacheco, J.G., et al., *Development of a membraneless extraction module for the extraction of volatile compounds: Application in the chromatographic analysis of vicinal diketones in beer.* Talanta, 2010. **81**: p. 372-376.
18. Mathis, C., M.N. Pons, and J.M. Engasser, *Development of an online method for the monitoring of vicinal diketones and their precursors in beer fermentation.* Anal Chimica Acta, 1993. **279**: p. 59-66.
19. Barcelo, C. and M. Gassiot, *Determination of diacetyl in beer by gas chromatography with flame-ionization detection.* J Chromatogr, 1978. **147**: p. 463-469.
20. Renger, R.S., S.H. Van Hateren, and K.C.A.M. Luyben, *The formation of esters and higher alcohols during brewery fermentation:The effect of carbon dioxide pressure.* J Inst Brew., 1992. **98**: p. 509-513.
21. Pires, E.J., et al., *Yeast: The soul of beer's aroma- a review of flavor-active esters and higher alcohols produced by the brewing yeast.* Appl Microbiol Biotechnol, 2014. **98**: p. 1937-1949.

22. Kittelman, J., M. Ottens, and J. Hubbuch, *Robust high-throughput batch screening method in 384-well format with optical in-line resin quantification.* J Chromatogr B, 2015. **988**: p. 98-105.
23. Fletcher, S.R., *High throughput approaches to designer products-myth or reality.* Colloids and Surfaces A: Physichochemical & Engineering Aspects, 2006. **288**(1-3): p. 21-25.
24. Herrmann, T., M. Schroder, and J. Hubbuch, *Generation of equally sized particle plaques using solid-liquid suspensions.* Biotechnol Prog, 2006. **22**: p. 914-918.
25. Traylor, S.J., et al., *Adaptation of the pore diffusion model to describe multi-addition batch uiptake high-throughput screening experiments.* J Chromatogr A, 2014. **1368**: p. 100-106.
26. Pandey, A., c.R. Soccol, and C. Larroche, *Current Developments in Solid-State Fermentation*. 2008, New Delhi: Springer, ASIATECH PUBLISHER, INC.
27. Maier, H.G. and R.U. Hartmann, *The adsorption of Volatile Aroma Constituents by Foods VIII.Adsorption of Volatile Carbonyl Compounds by Amino Acids.* Zeitschrift fuer Lebensmittel-Untersuchung und-Forschung, 1977. **163**: p. 251-254.
28. Medeiros, A.B.P., et al., *Production and recovery of aroma compiunds produced by solid-state fermentation using different adsorbents.* Food Technol Biotechnol, 2006. **44**(1): p. 47-51.
29. Edwards, C.G. and R.B. Beelman, *Extraction and analysis of volatile compounds in white wines using Amberlite XAD-2 resin and capillary gas chromatography.* J Agric Food Chem, 1990. **38**(1): p. 216-220.
30. Cinelli, G., et al., *Study of XAD-2 adsorbent for the enrichment of trace levels of Phthalate esters in hydroalcoholic food beverages and analysis by gas chromatography coupled with flame ionization and ion-trap mass spectrometry detectors.* Food Chem, 2014. **146**: p. 181-187.
31. *Amberlite Resin series*. 2016 [cited 2016 29January]; Available from: http://www.sigmaaldrich.com/catalog/search?term=Amberlite&interface=All&N=0&mode=match%20partialmax&lang=en&region=NL&focus=product.
32. *DIAION1, Manual of ion exchange resins and synthetic adsorbent*. 2008, Mitsubishi Chemical Corporation, BIOKAL Labsystems.
33. Lucas, S., et al., *Adsorption isotherms for Ethyl Acetate on activated acrbon from suprcritical CO2.* Fluid Phase equilibr, 2004. **219**: p. 171-179.
34. Harikrishnan, R., M.P. Srinivasan, and C.B. Ching, *Adsorption of ethyl benzene on activated carbon from supercritical CO2.* AICHE J, 1998. **44**(12): p. 2620-2627.
35. Aranovich, G.L. and M.D. Donohue, *Adsorption isotherms for microporous adsorbents.* Carbon, 1995. **33**(10): p. 1369-1375.
36. Guiochon, G., et al., *Fundamentals of preparative and nonlinear chromatography*. Second ed. 2006, San Diego: Elsevier Academic Press.
37. Da Silva, A.H. and E.V. Miranda, *Adsorption/desorption of organic acids on to different adsorbents for their recovery from fermentation broth.* J Chem Eng Data, 2013. **58**: p. 1454-1463.
38. Foo, K.Y. and B.H. Hameed, *Insights in to modeling of adsorption isotherm systems.* Chem Eng J, 2010. **156**: p. 2-10.
39. Tefera, D.T., et al., *Modeling Competitive adsorption of mixtures of volatile organic compounds in a fixed0bed of baeded activated carbon.* Environ Sci Technol, 2014. **48**: p. 5108-5117.
40. Mendez Sevillano, D., et al., *Resin selection for the separation of caffeine from green tea catechins.* Food Bioprod process, 2014. **92**: p. 192-198.
41. Prashant, K., et al., *Kafirin adsorption on ion-exchange resins:Isotherm and kinetic studies.* J Chromatogr A, 2014. **1356**: p. 105-116.

42. Chung, H.-K., et al., *Application of Langmuir and Freundlich isotherms to predict adsorbate removal efficiency or required amount of adsorbent.* J Ind Eng Chem, 2015. **28**: p. 241-246.
43. Kumar, P.S., et al., *Adsorption of dye from aqueous solution by cashew nut shell: studies on equilibrium isotherm, kinetics and thermodynamics of interactions.* Desalination, 2010. **261**: p. 52-60.
44. Do Carmo Ramos, S.N., et al., *Modeling mono-and multi-component adsorption of cobalt(II), Copper(II), and nickel(II) metal ions fro aqueous solution on to a new carboxylated sugarcane bagasse. PartI: batch adsorption study.* Ind Crop Prod, 2015. **74**: p. 357-371.
45. Yanxu, L., C. Jiangyo, and S. Yinghuang, *Adsorption of multicomponent volatile organic compounds on semi-coke.* Carbon 2008. **46**: p. 858-863.
46. De Faria dos Santos, J.C.G., *Study of New Adsorbents and Operation Cycles for Medical PSA Units*, in *Departamento de Engenharia Quimica Faculdade de Engenharia da Universidade do Porto*. 2005, Universidade do Porto.
47. Jeppu, G.P. and T.P. Clement, *A modified Langmuir-Freundlich isotherm model for simulating pH-dependent adsorption effects.* J Contam Hydrol, 2012. **129-130**: p. 46-53.
48. Limousin, G., et al., *Sorption isotherms: A review on physical bases, modeling and measurement.* Appl Geochem, 2007. **22**: p. 249-275.
49. Turiel, E., C. Perez-Conde, and A. Martin-Esteban, *Assesment of the cross-reactivity and binding sites characterization of a propazine-imprinted polymer using the Langmuir-Freundlich isotherm.* The Analyst, 2003. **128**(2): p. 137-141.
50. Abburi, K., *Adsorption of phenol and p-chlorophenol from their single and bisolute aqueous solutions an Amberlite XAD-16 resin.* J Hazard Mater B, 2003. **105**: p. 143-156.
51. Coffman, J.L., J.F. Kramarczyk, and B.D. Kelley, *High-throughput screening of chromatographic separations:I.Method development and column modeling.* Biotechnol Bioeng, 2008. **100**(4): p. 605-618.
52. Chilamkurthi, S., et al., *High-throughput determination of adsorption equilibria for chromatographic oligosaccharide separation.* J Chromatogr A, 2012. **1239**: p. 22-34.
53. Lu, Y., et al., *Relationship between breakthrough curve and adsorption isotherm of Ca(II) imprinted chitosan microsphere for metal adsorption.* Chinese J Chem Eng, 2015. **24**(2): p. 323-329.
54. [cited 2016 12 May]; Available from: http://www.chemicalize.org/.
55. Worthing, A.G. and J. Geffner, *Treatment of experimental data*. 1943, London,Chapman & Hall, limited: John Wiley & Sons, INC.
56. Chan, L.S., et al., *Error analysis of adsorption isotherm models for acid dyes on to bamboo derived carbon.* Chinese J Chem Eng, 2012. **20**(3): p. 535-542.
57. Press, w., H., *Computational statistics with application to bioinformatics Unit7:Fitting Models to data and estimating errors in model-derived quantities*. 2008: The University of Texas at Austin, William H. Press.
58. Zhou, J., et al., *Modeling of breakthrough curves of single and quaternary mixtures of ethanol, glucose, glycerol, and acetic acid adsorption on to a microporous hyper-cross-linked resin.* Bioresource technol, 2013. **143**: p. 360-368.
59. Grossmann, C., et al., *Optimizing control of simulated moving bed separations of mixtures subject to the generalized Langmuir isotherm.* Adsorption, 2008. **14**: p. 423-432.

4 Influence of ethanol and temperature on adsorption of flavor-active esters on hydrophobic resins

ABSTRACT

Flavor-active esters, produced during fermentation, are vital components and important contributors to the aroma of beer. In order to separate trace amounts of esters, their adsorption behavior in the presence of high concentrations of ethanol and their thermodynamic behavior under the influence of temperature needs to be understood. This chapter discusses the influence of temperature on single component adsorption isotherms of four esters (i.e. ethyl acetate, isopentyl acetate, ethyl 4-methylpentanoate, and ethyl hexanoate) on two hydrophobic resins (i.e. Amberlite XAD16N, and Sepabeads SP20SS) and the estimation of heat, entropy, and Gibbs energy of adsorption. Higher heat and entropy of adsorption are obtained for ethyl hexanoate and ethyl 4-methylpentanoate in comparison, due to their higher hydrophobicity, stronger binding, and the exothermic nature of their adsorption. A higher concentration of ethanol (tested from 1 to 30% (v/v)), lowers the activity coefficient of esters in the aqueous phase, and subsequently lowers adsorption and Langmuir affinity parameters. Increase of temperature from 284.15 to 325.15 K shows a reverse influence on maximum adsorption capacity and Langmuir affinity parameters. Langmuir affinity parameters are obtained at various ethanol concentrations and temperatures. The reported parameters and thermodynamic properties are essential for designing an industrial scale adsorption step for separation of flavor-active esters under non-isothermal conditions.

This chapter is partly published as:

S. Saffarionpour, S-Y S. Tam, L. A. M. Van der Wielen, E. Brouwer, M. Ottens, Influence of ethanol and temperature on adsorption of flavor-active esters on hydrophobic resins, Sep. purif. Technol., 210 (2019) 219-230, https://doi.org/10.1016/j.seppur.2018.05.026

4.1 Introduction

Esters are volatile trace compounds which are present in fermented beverages like beer and are extremely important for the flavor profile of the final product [1-4]. Although esters are produced in trace amounts in comparison to other yeast metabolites, like higher alcohols, they are important aroma elements due to their low odour threshold in beverages [5-7]. They are responsible for the sweet and fruity flavors of beer [8, 9] and if they are overproduced, they will negatively affect the final beer. Therefore, it is of importance to maintain optimum conditions to obtain a balanced ester profile in the final beer product [5, 10]. These compounds are primarily formed during fermentation by enzymatic chemical condensation of organic acids and alcohols and are divided into two major groups of acetate esters and medium chain fatty acid ethyl esters [5, 9-11]. While several esters are present in beer, the major ester components are considered to be ethyl acetate (solvent-aroma) [5, 9, 10] , isopentyl acetate (banana aroma) [9, 10, 12], isobutyl acetate (fruity aroma) [5], phenyl ethyl acetate (rose and honey aroma) [9, 10, 13], ethyl hexanoate (sweet apple aroma)[9], ethyl-4methylpentanoate (apple or pear aroma), and ethyl octanoate (sour apple aroma) [9]. During processing, however the level of esters and their relative concentrations might alter due to chemical and physical changes. In order to prevent the unwanted changes, esters can be selectively recovered and fractionated by means of adsorption and by tuning the level of esters present in different process streams, various beer products with fruity flavors can be produced. Fractionation of esters in beer beverages can be challenging since they are present in the matrix at trace levels in comparison to ethanol, which is present at significant concentration. In order to design the adsorption process for selective recovery of esters, several process parameters, like the effect of ethanol on adsorption of esters and heat of adsorption for each specific compound in the mixture need to be understood. Therefore, this chapter aims to provide improved knowledge on adsorption mechanism of flavor-active esters under the influence of temperature and various ethanol concentrations. Four major esters which contribute to beer flavor, i.e. ethyl acetate, isopentyl acetate, ethyl hexanoate and ethyl 4-methylpentanoate are selected and the adsorption of aforementioned esters is investigated on the synthetic hydrophobic resins, Sepabeads SP20SS and Amberlite XAD16N, which showed high affinity towards esters according to our previous investigations, both for

single and multi-compound mixtures [14]. The uptake on each resin is examined at different concentrations of ethanol and the influence of temperature on adsorption of single and multi-compound mixture of esters is explored. Based on the acquired results, the thermodynamic properties such as the heat, entropy, and Gibbs energy of adsorption for each specific ester present in the mixture are calculated and affinity of each resin towards the tested esters at various ethanol concentrations and temperatures is obtained. The estimated thermodynamic properties and the obtained affinity parameters have application in designing the adsorption column for selective recovery of flavor-active esters.

4.2 Materials

4.2.1 Chemicals

Ethyl acetate (purity≥ 99.5%), isopentyl acetate (98%), ethyl hexanoate, and ethyl 4-methylpentanoate are purchased from Sigma-Aldrich, The Netherlands. MilliQ water is used for dilutions and ethanol 96%, is purchased from Merck.

4.2.2 Adsorbents

Food grade resin XAD16N from Amberlite resin series and the aromatic type Sepabeads SP20SS from HP resin series are purchased from Sigma-Aldrich, The Netherlands, and used for adsorption tests. Detailed specifications and physical properties of the tested resins are reported in our previous work [14].

4.3 Methods

4.3.1 Gas Chromatographic Analysis

The esters of interest were analyzed by Static-Headspace-Gas-Chromatography (HS-GC) method using the GC (Trace 1300, Thermofischer Scientific, Switzerland) coupled with Triplus RSH Autosampler (Thermofischer Scientific, Switzerland) and FID in a RESTEK Rxi 624Sil MS column ($20mm \times 0.18mmID \times 1\mu m\ df$), (Restek Co., US). Helium was used as the carrier gas in the system. The incubation temperature of the GC agitator was set to 40°C and samples were measured with incubation time of 20 minutes. Syringe temperature was set to 60°C and detector temperature to 250°C. Instead of direct injection of the vapor to the GC column, injection is performed through a GC

splitting inlet, which aids obtaining sharper peaks and reduces the amount of sample reaching the GC column. Split ratio of 30 was used for the measurements. Ramped oven temperature was considered for the GC settings, 60°C with holding time of 1 minute, increase to 75°C with the increasing rate of 10°C/min, and the second increase to 175°C with the speed of 30°C/min with the holding time of 1 minute. The retention time of tested components is measured during 7 minutes analysis time. The chromatograms obtained from the measurements show the retention time (minutes) of 1.5, 2.4, 4.9, 5.5, and 5.7 for ethanol, ethyl acetate, isopentyl acetate, ethyl 4-methylpentanoate, and ethyl hexanoate respectively.

4.3.2 Thermodynamic analysis

4.3.2.1 Selected isotherm models

An extensive study on various isotherm models is discussed in detail in chapter three. Among the tested isotherms proposed in the literature, Langmuir, Freundlich, and Sips models were selected as appropriate models for prediction of adsorption behavior and equilibrium data. Results of the tests revealed high accuracy in prediction with Langmuir and Sips models, therefore the previously tested models are selected to explain the adsorption behavior of flavor-active esters for this study and Langmuir and Sips models, which were able to predict the experimental adsorption equilibrium data with higher accuracy are further investigated for determination of isosteric enthalpy of adsorption in the next step. Expression of various tested models, i.e. Langmuir, Freundlich, and Sips, are discussed in sections 3.5.2.1, 3.5.2.2, and 3.5.2.3 in chapter three.

4.3.2.2 Determination of adsorption isosteric enthalpy

Isosteric enthalpy, which is the basic quantity in adsorption study, is explained as the ratio of the infinitesimal change in the adsorbate enthalpy to the infinitesimal change in the amount adsorbed. When heat is released due to adsorption, part of the released energy is adsorbed by the solid adsorbent and it is partly dissipated into the surrounding. The heat adsorbed by the solid particle, increases the particle temperature which leads to slowed down adsorption kinetics, therefore it is of importance to understand and quantify the amount of the Isosteric enthalpy for further studies. The

amount of this heat can be calculated based on Van't Hoff relation, as explained in equation (4.1) [15-19].

$$-\left(\frac{\partial lnC}{\partial T}\right)_q = \frac{\Delta H_s}{R\,T^2} \tag{4.1}$$

Where ΔH_s is the Isosteric enthalpy of adsorption, kJ/mol, R is the gas constant (8.314 J/mol.K), T is the temperature in K, and C is the equilibrium concentration (mmol/L) [20-22].

4.3.2.2.1 Langmuir approach

The simplest model, which describes the monolayer adsorption, is the Langmuir model. This model works under the assumption that the resin surface consists of several different regions and each region follows the Langmuir assumption that one molecule is adsorbed to one site, homogeneous surface and a localized adsorption [20, 21]. This model can be explained as is shown in equation (4.2).

$$\theta = \frac{q}{q_{max}} = \frac{k_{ads}C}{1+k_{ads}C} \tag{4.2}$$

Where θ is the fractional coverage (-), q and $\mathrm{q_{max}}$ are the adsorption capacity, and maximum load respectively (mmol/L), k_{ads} is the Langmuir constant (L/mmol), and C is the equilibrium concentration of the analyte (mmol/L).

This expression shows the monolayer adsorption since $(C \to \infty), (q \to q_{max})$, while at low concentrations of the analyte, Henry's approach will follow, which can be explained as equation (4.3) [21, 23].

$$\lim_{C\to 0}\left(\frac{q}{C}\right) = k_{ads}q_{max} = K \tag{4.3}$$

q_{max} represents fixed number of surface sites and is independent of temperature. However, the Langmuir constant is dependent on temperature as is explained by Arrhenius equation, presented in equation (4.4) [24, 25].

$$k_{ads} = k_{\infty}\exp\left(-\frac{\Delta H_s}{RT}\right) \tag{4.4}$$

k_∞ is the temperature-independent factor (L/mmol), ΔH_s is the isosteric enthalpy of adsorption (kJ/mol) which in this case is assumed to be equal to heat of adsorption [20], *R* is the gas constant (J/mol K) and *T* is the temperature (K). The magnitude of the heat of adsorption indicates the dominant type of adsorption (physical or chemical). The heat of adsorption for physisorption process is between 5-40 kJ/mol while higher heat of adsorption can be achieved in chemisorption (40-800 kJ/mol) [25, 26]. If the adsorption process is exothermic and q_{max} decreases with the temperature, the heat of adsorption will increase with the loading and if the Isosteric enthalpy has a finite value at high coverage, the saturation capacity is independent of temperature and heat of adsorption will be constant [20]. Then equation (4.1) can be rewritten as explained in equation (4.5) [21].

$$-\left(\frac{\partial lnC}{\partial T}\right)_q = \frac{\Delta H_S}{R\,T^2} = \frac{dln\,K}{R\,T^2} = \frac{\Delta H^0}{R\,T^2} \tag{4.5}$$

Where ΔH^0 is the heat of adsorption (kJ/mol).

4.3.2.2.2 Sips approach

Sips equation makes it possible to achieve an improved fit at high concentrations by combination of the Freundlich and Langmuir equations [14, 27, 28].This isotherm model can be written in the generalized form, shown in equation (4.6).

$$\theta = \frac{q}{q_{max}} = \frac{(k_{ads}C)^{1/n}}{1+(k_{ads}C)^{1/n}} \tag{4.6}$$

For the affinity constant k_{ads} and the exponent n, temperature dependency can be considered as explained in the next equations.

$$k_{ads} = k_\infty exp(\frac{-\Delta H_S}{RT}) = k_0 \exp[\frac{-\Delta H_S}{RT_0}\left(\frac{T_0}{T} - 1\right)] \tag{4.7}$$

$$\frac{1}{n} = \frac{1}{n_0} + \alpha(1 - \frac{T_0}{T}) \tag{4.8}$$

Where k_∞ is the adsorption affinity constant at infinite temperature, k_0 is that at reference temperature T_0, n_0 is the same parameter n at the same reference temperature and α is a constant parameter. Unlike ΔH_s in the Langmuir equation, where it is equal to the isosteric enthalpy, this parameter can only express the heat of adsorption in the Sips equation and the temperature dependency of exponent n needs to be considered. The maximum

saturation capacity can be considered as constant or it can be expressed as is shown in equation (4.9) , the choice of this temperature dependency is arbitrary [20].

$$q_{max} = q_{max,0} \exp[\chi \left(1 - \frac{T}{T_0}\right)] \quad (4.9)$$

$q_{max,\ 0}$ is the saturation capacity at the reference temperature T_0 and χ is a constant parameter. q_{max} can be considered as temperature dependent, or the term χ can be set to zero [20]. In order to obtain the Isosteric enthalpy for the temperature dependence form of the Sips equation from the Van't Hoff relation, and considering temperature dependence of k_{ads}, and $1/n$, the Isosteric enthalpy can be written as explained in equation (4.10) [20].

$$-\Delta H_s = Q - (\alpha R T_0)\, n^2 \ln(\frac{\theta}{1-\theta}) \quad (4.10)$$

With the assumption that temperature variation of q_{max} is negligible. It can be observed from equation (4.10) that the isosteric enthalpy decreases with loading. When the loading is equal to zero, it goes to infinity and when it reaches the saturation point, it approaches minus infinity.

Although this model is capable to predict the final maximum capacity with accuracy at high concentrations, for accurate estimation of heat of adsorption, it is only applicable for intermediate range of concentrations [20].

The physical meaning of parameter Q is explained in equation (4.10). At fractional coverage equal to one half, the isosteric enthalpy is equal to the value of Q (kJ/mol) [20].

$$Q = (-\Delta H_s)|_{\theta=1/2} \quad (4.11)$$

4.3.2.3 Determination of Gibbs energy (ΔG^0) from Langmuir constant

The Gibbs energy change indicates the degree of spontaneity of the adsorption process. The higher negative value indicates a more favorable adsorption. The amount of change in Gibbs energy can be calculated according to equation (4.12), from Langmuir constant K [19, 23, 29].

$$\Delta G^0 = -RT \ln K \quad (4.12)$$

Where K is the Langmuir equilibrium constant (q/C) and is dimensionless, T is the absolute temperature (K) and R is the gas constant (8.314 J/mol K).

4.3.2.4 Determination of heat (ΔH^0) and (ΔS^0) entropy of adsorption

The Gibbs free energy change is related to the heat *(ΔH^0)* and entropy change *(ΔS^0)* of adsorption which the relation can be expressed as equation (4.13) [19, 21, 30, 31].

$$\ln K = \frac{\Delta S^0}{R} - \frac{\Delta H^0}{RT} \tag{4.13}$$

Where *K* is the equilibrium dimensionless constant (-). The values of heat of adsorption (ΔH^0) and entropy change of adsorption (ΔS^0) can be calculated from the slope and intercept of the Van't Hoff plot, ln *K* versus the (*1/T*) [31-33].

4.3.2.5 Determination of competitive adsorption parameters

4.3.2.5.1 Multicomponent Langmuir approach

For designing an adsorption column at an industrial scale for separation and fractionation of flavor-active esters which are present in different process streams with large amounts of ethanol, the competitive adsorption behavior of these compounds present with various concentrations of ethanol and at different temperatures needs to be investigated. In order to study the adsorption behavior and obtain the required parameters for the design stage, a multi-component Langmuir model is used to express the experimental data collected from adsorption tests performed through batch uptake experimentation at different concentrations of ethanol and at various temperatures. The extension of the Langmuir model, which describes the competition of component i with nc components in the mixture, is used to express the experimental data (see equation (4.14)) [14, 34-37].

$$q_i = \frac{q_{max}\, k_{ads,i} C_i}{1+\sum_{j=1}^{nc} k_{ads,j}\, C_j} \tag{4.14}$$

Where C_i represents the concentration in the bulk liquid of species i at equilibrium condition (mmol/L), q_i is the load of species i (concentration of adsorbate on solid) (mmol/L) , q_{max} represents the maximum load (mmol/L), and $k_{ads,i}$ is the Langmuir constant (L/mmol).

4.3.3. Batch uptake method

Batch uptake experimentation is used for testing the adsorption behavior of selected esters on the two synthetic hydrophobic resins. Experiments are performed in 10 ml clear crimp top headspace vials (Thermofischer Scientific, Switzerland), which were filled with the selected resins after the resin preparation step. Since resins are rather hydrophobic, they are prepared through washing steps with methanol, followed by an equilibration step with water and addition of the resins to each vial. Afterwards, different concentrations of the solution are added to the vials and closed with Crimpcap Bi-metal septum 20 mm (Thermofischer Scientific, Switzerland) to prevent evaporation. Vials are stirred at 500 rpm for one hour equilibration time on a thermo-mixer (comfort Eppendorf, Hamburg, Germany) at different temperatures tested for the experiments. After equilibration, bulk liquid is filtered using the Millex-HV low binding syringe filter unit, 0.45 µm, PVDF, 33 mm (Merck Millipore, The Netherlands) through 5 ml syringe in the 10 ml headspace vial and closed with metal caps, prepared for the analysis.

The amount of solute i adsorbed per unit mass on adsorbate (q_i) is calculated using the mass balance (equation (4.15)) [38].

$$q_i = \frac{M_{init} - M_{bulk} - M_{lost,evap}}{m_{resin}} \quad (4.15)$$

Where M_{init} is the initial number of moles of the analyte in the solution (mmol), calculated from the initial molar concentration and initial sample volume C_0V_0 where C_0 is the initial molar concentration (mmol/L), and V_0 is the initial volume of the analyte (L). M_{bulk} is the number of moles of the bulk liquid remained after adsorption (mmol). In order to take into account the effect of evaporation, the amount of moles of the analyte which are lost due to evaporation are considered in the estimation of the equilibrium capacity which can be estimated from $(C_0V_0 - C_{blank}V_{blank})$, where V_{blank} is the volume of the blank samples after the equilibration time. The value of m_{resin} is the gram of the wet resin.

4.3.4 Experimental procedure

4.3.4.1 Single-component adsorption test

Batch uptake experiments are performed to investigate the adsorption of the flavor-active esters on two hydrophobic resins Sepabeads SP20SS and Amberlite XAD16N. Approximately 0.4 g/L of the flavor-active esters, i.e. ethyl acetate, isopentyl acetate, ethyl hexanoate, and ethyl-4methylpentanoate are prepared in 1% (v/v) co-solvent mixture of ethanol/water. Batch uptake experimentation, is applied as explained in section 4.3.3 to investigate the single-component adsorption of the aforementioned components. The adsorption experiments are performed at four different tested temperatures, i.e. 284.15, 297.15, 309.15, and 333.15 K).

4.3.4.2 Multi-component adsorption tests

Ester components are present in trace amounts in comparison to ethanol, which is present at higher concentration range. In order to investigate the competitive adsorption of esters, studying the influence of temperature and ethanol concentration on their binding capacity is required; therefore, the competitive adsorption of flavor-active esters is investigated through batch uptake experimentation according to the procedure explained in section 4.3.3. Approximately 0.4 g/L of each flavor-active ester is prepared in co-solvent mixture of ethanol/water. Experiments are performed over wide range of ethanol concentration (i.e. 1, 7.5, 15, 22.5, and 30 % (v/v)) and at three different temperatures (i.e. 284.15, 297.15, and 325.15 K).

4.4 Results and Discussions

4.4.1 Influence of temperature on single-component adsorption

4.4.1.1 Single-component adsorption isotherms

The results of the adsorption isotherms at four different tested temperatures are illustrated in **Figure 4.1** for adsorption of the flavor-active esters on Sepabeads SP20SS resin and for the four tested esters. The adsorption equilibrium data are explained with single-component Langmuir, Freundlich, and Sips models. As can be observed from **Figure 4.1**, the increase of temperature is not favourable for adsorption, due to exothermic nature of adsorption, as a decrease for maximum capacity at saturation point is observed. Comparing the results obtained for four tested esters, i.e. ethyl acetate,

isopentyl acetate, ethyl 4-methylpentanoate, and ethyl hexanoate, it can be concluded that the resin has higher affinity towards the tested components in the order of their hydrophobicity, ethyl hexanoate as the most hydrophobic compound, followed by ethyl 4-methylpentanoate, isopentyl acetate, and ethyl acetate. The degree of hydrophobicity can be explained by the value of log P (Partition coefficient in octanol/water solution), which has the value of 2.31, 2.16, 1.53, and 0.28 for ethyl hexanoate, ethyl 4-methylpentanoate, isopentyl acetate, and ethyl acetate respectively [39]. By comparing the four figures for the tested esters, it can be clearly observed that ethyl hexanoate has more tendency to bind to the resin material, and the least bulk concentration after adsorption is obtained for this compound. The value of equilibrium bulk concentration increases as the hydrophobicity of the molecule decreases and less analyte is adsorbed on the resin material.

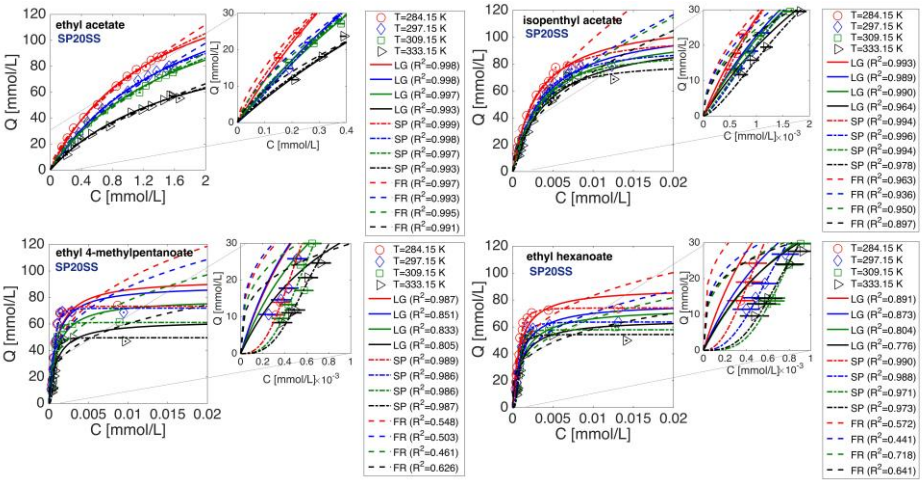

Figure 4.1. Adsorption isotherms for tested esters at four temperatures; Adsorption on Sepabeads SP20SS; Predictions based on Langmuir model (LG), Freundlich model (FR), and Sips model (SP)

Comparison of the Langmuir, Freundlich and Sips fit for the four tested esters presented in **Figure 4.1**, neatly demonstrate that high accuracy in prediction can be obtained for ethyl acetate by Langmuir, and Sips models (values of R^2 higher than 0.993). Prediction for adsorption behavior of isopentyl acetate, ethyl 4-methylpentanoate, and ethyl hexanoate obtained based on Langmuir model, is improved, specifically at the saturation point and lower concentration region through Sips model, as the higher values of R^2

demonstrate. This model combines the behavior of Freundlich and Langmuir model and is able to predict the maximum capacity for monolayer adsorption with higher accuracy, and circumvents the limitation of rising adsorbate concentration associated with the Langmuir model which is observed here [14, 40]. Freundlich model was not able to predict the adsorption behavior with high accuracy; lower values of R^2 obtained specially for ethyl 4-methylpentanoate and ethyl hexanoate. This model has the drawback that it cannot be applied with high accuracy for prediction of maximum saturation point due to increase in concentration with power 1/n. The results of single-component adsorption tests obtained in the similar condition for the four tested esters and on Amberlite XAD16N resin are presented in **Figure 4.2** More accurate prediction based on Langmuir model is obtained for the two components with the highest hydrophobicity (i.e. ethyl 4-methylpentanoate and ethyl hexanoate) in comparison to the predictions obtained for adsorption on SP20SS (higher values of R^2). The pore volume of XAD16N is smaller in comparison to SP 20SS, and the adsorption phenomena is less dominated by pore diffusion on this resin, therefore components with higher hydrophobicity, have less tendency to bind strongly to the resin in comparison to SP20SS and adsorption isotherms can be described more accurately by Langmuir model and monolayer adsorption. From the obtained results and isotherms, it can be concluded that Langmuir model is able to predict the adsorption behavior of flavor-active esters with accuracy. This prediction can be improved through Sips model, specifically for the components with high hydrophobicity, therefore these two models are selected to be studied for determination of heat of adsorption. Due to low accuracy in prediction with the Freundlich model, this model is not selected for further study.

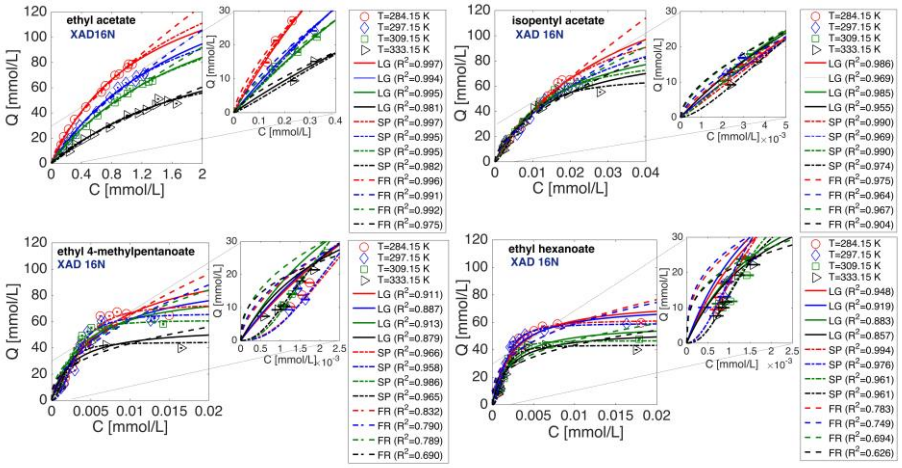

Figure 4.2. Adsorption isotherms for tested esters at four temperatures; Adsorption on Amberlite XAD16N; Predictions based on Langmuir model (LG), Freundlich model (FR), and Sips model (SP)

4.4.1.2 Heat of adsorption (ΔH^0)

4.4.1.2.1 Determination based on Langmuir model

Based on the obtained isotherms at four different temperatures, the values of maximum capacity (q_{max}), the temperature independent factor (k_∞), and heat of adsorption ΔH^0 are regressed using the nlinfit function in MATLAB, for the temperature dependent Langmuir model., explained in section 4.3.2.2.1.The values of 95% confidence intervals for the nonlinear least squares parameter estimates, are estimated based on coefficient covariance matrix and the toolbox nlparci [41, 42] in MATLAB. The calculated parameters, based on the temperature dependent Langmuir model, (Substituting equation (4.4) in equation (4.2)), are assembled in **Table 4.1** and **Table 4.2**, for adsorption on Sepabeads SP20SS and Amberlite XAD16N respectively.

The estimated heats of adsorption reveal that the adsorption is an exothermic phenomena and the increase of temperature is not favorable for adsorption. The regressed values for maximum capacities, for four tested esters show that, increase of temperature has a reverse influence on the value of maximum capacity, as the value for q_{max} decreases with temperature increase. The higher value for heat of adsorption is expected for higher

hydrophobic compounds, (i.e. ethyl hexanoate and ethyl 4-methylpentanoate) since they interact and compete more for binding to the resin material and there is a higher energy barrier that adsorbed molecules need to overcome to leave the adsorbed phase [20]. The estimated values for heat of adsorption, for ethyl acetate is below 20 kJ/mol and it indicates that the adsorption is mainly dominated by physisorption for this component, since the value of ΔH^0 for physical adsorption is the same order of magnitude as condensation (i.e. 2.1-20.9 kJ/mol) [43, 44] as extensively reported in the literature. If the value for heat of adsorption lies between 80-200 kJ/mol [43, 44].the adsorption phenomena is mainly dominated by chemisorption.

The calculated values for enthalpies of adsorption, for the other three hydrophobic components, are above 20 kJ/mol and below 80 kJ/mol, and they imply that simultaneous physical and chemical adsorption occur for esters with higher hydrophobicity as they bind stronger to the adsorbent.

Table 4.1. Regressed parameters for adsorption on Sepabeads SP20SS, based on temperature dependent Langmuir model

	Temperature (K)			
	284.15 K	**297.15 K**	**309.15 K**	**333.15 K**
Ethyl acetate				
q_{max} *(mmol.L^{-1})*	172.5	176.6	161.1	117.8
(95%confidence bound)	(157.6, 187.4)	(159.7, 193.4)	(141.9,180.3)	(99.1,136.5)
k_∞ *(L.mmol^{-1})*	0.0023	0.0021	0.0025	0.0045
(95%confidence bound)	(0.0019,0.0026)	(0.0018,0.0025)	(0.0020,0.0030)	(0.0032,0.0057)
(-ΔH^0) (KJ/mol)	-13.614	-13.657	-13.851	-13.441
(95%confidence bound)	(-13.612,-13.615)	(-13.655,-13.658)	(-13.850,-13.852)	(-13.440,-13.442)
Isopentyl acetate				
q_{max} *(mmol.L^{-1})*	115.6	112.0	105.9	102.8
(95%confidence bound)	(105.5, 125.8)	(100.7,123.3)	(95.5,116.4)	(82.5,123.1)
k_∞ *(L.mmol^{-1})*	0.0104	0.0110	0.0158	0.0188
(95%confidence bound)	(0.0082, 0.0125)	(0.0084,0.0137)	(0.0122,0.0195)	(0.0104,0.0272)
(-ΔH^0) (KJ/mol)	-24.375	-24.794	-24.925	-26.104
(95%confidence bound)	(-24.373,-24.375)	(-24.793,-24.795)	(-24.924,-24.925)	(-26.103,-26.104)
Ethyl 4-methylpentanoate				
Q_{max} *(mmol.L^{-1})*	94.1	89.3	78.9	62.7
(95%confidence bound)	(68.0,120.2)	(64.8,113.7)	(56.3,101.6)	(43.2,82.1)
k_∞ *(L.mmol^{-1})*	0.0099	0.0080	0.0239	0.0325
(95%confidence bound)	(0.0034,0.0164)	(0.0026,0.0135)	(0.0075,0.0402)	(0.0077,0.0573)
(-ΔH^0) (KJ/mol)	-27.253	-29.266	-27.315	-28.661
(95%confidence bound)	(-27.253,-27.253)	(-29.265, -29.266)	(-27.314,-27.315)	(-28.660,-28,661)
Ethyl hexanoate				
Q_{max} *(mmol.L^{-1})*	88.9	77.8	74.4	65.8
(95%confidence bound)	(71.8,106.1)	(60.4, 95.2)	(52.9, 95.8)	(45.9, 85.7)
k_∞ *(L.mmol^{-1})*	0.0038	0.0045	0.0053	0.0084
(95%confidence bound)	(0.0018.0.0058)	(0.0019, 0.0071)	(0.0016, 0.0090)	(0.0017, 0.0150)
(-ΔH^0) (KJ/mol)	-29.719	-30.129	-30.607	-32.196
(95%confidence bound)	(-29.719,-29.719)	(-30.128, -30.129)	(-30.606, -30.607)	(-32.195,-32.196)

Similar procedure is followed to obtain the parameters for adsorption on Amberlite XAD16N resin. The regressed values for this tested resin, are reported in **Table 4.2.**

Table 4.2. Regressed parameters for adsorption on Amberlite XAD16N, based on temperature dependent Langmuir model

	Temperature (K)			
	284.15 K	**297.15 K**	**309.15 K**	**333.15 K**
Ethyl acetate				
q_{max} *(mmol.L^{-1})*	191.9	199.9	182.6	131.9
(95%confidence bound)	(130.4,253.5)	(141.2,258.5)	(142.7,222.6)	(80.9,182.9)
k_{∞} *(L.mmol^{-1})*	0.0033	0.0030	0.0033	0.0037
(95%confidence bound)	(0.0016,0.0049)	(0.0017,0.0043)	((0.0023,0.0043)	(0.0016,0.0059)
(-ΔH^0) (KJ/mol)	-12.567	-12.368	-12.508	-12.825
(95%confidence bound)	(-12.566,-12.567)	(-12.368,-12,.368)	(-12.507,-12,508)	(-12,824,-12,825)
Isopentyl acetate				
q_{max} *(mmol.L^{-1})*	183.2	139.0	119.2	96.6
(95%confidence bound)	(123.8,242.6)	(101.5,176.5)	(91.3,147.2)	(68.3,124.9)
k_{∞} *(L.mmol^{-1})*	0.0053	0.0084	0.0180	0.0456
(95%confidence bound)	(0.0028, 0.0078)	(0.0047,0.0120)	(0.0106,0.0254)	(0.0198,0.0715)
(-ΔH^0) (KJ/mol)	-20.238	-20.761	-20.326	-20.134
(95%confidence bound)	(-20.236,-20.238)	(-20.760,-20.762)	(-20.325,-20.327)	(-20.133,-20.135)
Ethyl 4-methylpentanoate				
q_{max} *(mmol.L^{-1})*	114.6	98.2	85.9	56.3
(95%confidence bound)	(69.0,160.3)	(61.5,134.8)	(62.2,109.5)	(40.7,71.8)
k_{∞} *(L.mmol^{-1})*	0.0163	0.0337	0.0707	0.1966
(95%confidence bound)	(0.0041,0.0285)	(0.0082,0.0592)	(0.0279,0.1134)	(0.0626,0.3306)
(-ΔH^0) (KJ/mol)	-21.304	-21.058	-20.976	-20.955
(95%confidence bound)	(-21.302,-21.305)	(-21.057,-21.059)	(-20.975,-20.976)	(-20.953,-20.956)
Ethyl hexanoate				
q_{max} *(mmol.L^{-1})*	76.7	72.8	59.4	54.4
(95%confidence bound)	(63.8,89.6)	(58.4,87.3)	(45.6,73.2)	(39.81,68.9)
k_{∞} *(L.mmol^{-1})*	5.0788e-4	0.0010	0.0041	0.0086
(95%confidence bound)	(2.8327e-4,7.3250e-4)	(5.1270e-4,0.0015)	(0.0017,0.0064)	(0.0026,0.0145)
(-ΔH^0) (KJ/mol)	-32.001	-32.250	-29.899	-30.359
(95%confidence bound)	(-32.000,-32,001)	(-32.249,-32,250)	(-20.898,-20,899)	(-30.358,-30.359)

Lower value for heat of adsorption, is obtained for adsorption of three hydrophobic esters, i.e. isopentyl acetate, ethyl 4-methylpentanoate and ethyl hexanoate, on this resin in comparison to Sepabeads SP20SS. The observed trend can be explained by the nature of the adsorbent materials, since Sepabeads SP20SS has smaller particle size and larger pore volume in comparison, it has higher affinity towards the high hydrophobic esters and more heat is released after their adsorption.

Based on the regressed parameters, the value for k_{ads} is estimated from calculated heats of adsorption according to equation (4.4) and subsequently the equilibrium binding

capacity is calculated from equation (4.2), knowing the maximum binding capacity for each tested ester. The values of equilibrium binding capacity, predicted by the temperature dependent Langmuir model and obtained from experiments are compared in a parity plot for each ester and for adsorption on two tested hydrophobic resins, i.e. SP20SS, and XAD16N, presented in **Figures 4.3** and **4.4**.

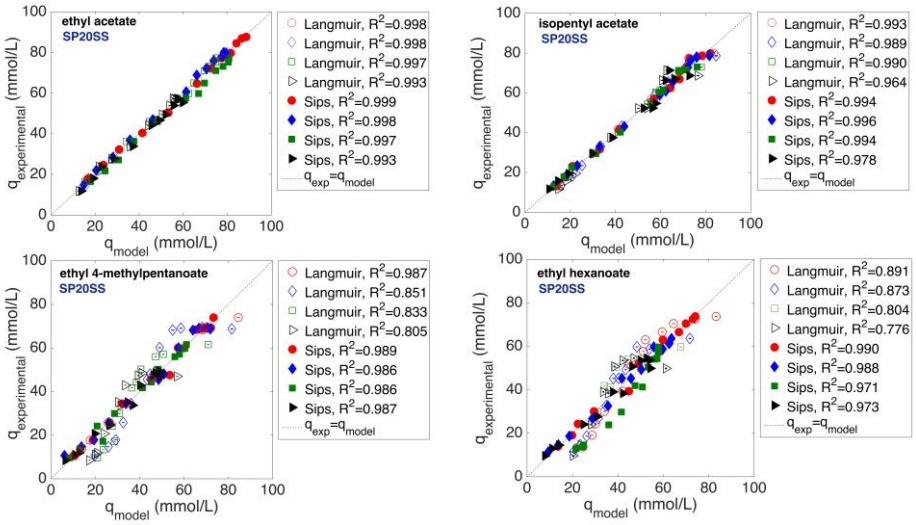

Figure 4.3. Parity plot q $_{model}$ (Predicted based on Langmuir and Sips) vs. q $_{experimental}$; Adsorption on Sepabeads SP20SS

The presented results in **Figures 4.3** and **4.4** show that, temperature dependent Langmuir model is able to predict the experimental isotherm with higher accuracy for ethyl acetate in comparison to other esters with higher hydrophobicity (higher value for R^2), for adsorption on two tested resins. Lower accuracy in prediction is observed mainly for ethyl 4-methylpentanoate and ethyl hexanoate, the two tested esters with higher hydrophobicity. As is also discussed in previous sections, the isotherms for these two esters cannot be completely explained by Langmuir model due to high slope of the isotherm and hydrophobic nature of the esters in comparison to ethyl acetate and lower accuracy in prediction can also be observed for these two tested esters.

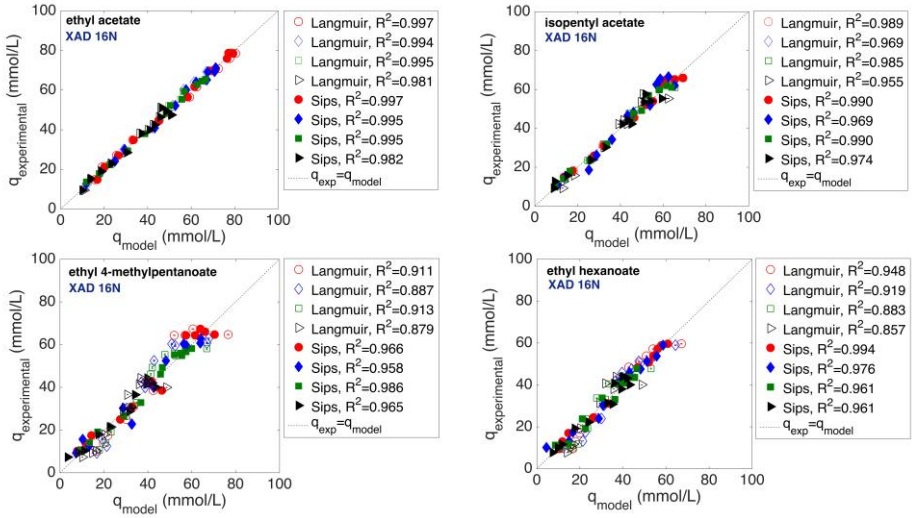

Figure 4.4. Parity plot q $_{model}$ (Predicted based on Langmuir and Sips) vs. q $_{experimental}$; Adsorption on Amberlite XAD16N

4.4.1.2.2 Determination based on Sips model

As it is shown in **Figures 4.1 to 4.4** and explained in section 4.3.2.2.2, although Sips model has advantages in predicting the maximum capacity for high hydrophobic compounds with higher accuracy, it is only applicable in intermediate range of concentrations, as discussed in section 4.3.2.2.2, and at low concentration range, and loading close to zero, it cannot predict the Isosteric enthalpy with high accuracy, therefore this model is only used for prediction of the isosteric enthalpy for ethyl acetate which is less hydrophobic and calculated values based on Sips prediction are compared with Langmuir model only for this ester component, and for the other three esters which are highly hydrophobic with equilibrium concentrations close to zero, Langmuir approach is used to predict the thermodynamic parameters. For the obtained isotherms at different four temperatures for ethyl acetate, as illustrated in **Figure 4.1,** the values of maximum capacity q_{max}, k_0, n_0, α, *and* Q, are regressed based on the equations presented in section 4.3.2.2.2 from the temperature dependent affinity and n parameters. The estimated values are assembled in **Table 4.3.** The standard error for each estimated parameter is obtained

from correlation matrix R, corresponding to covariance matrix C and values of standard deviation sigma are obtained for each regressed parameter, for both adsorption on Sepabeads SP20SS and Amberlite XAD16N.

Table 4.3. Regressed parameters for estimation of isosteric enthalpy of ethyl acetate based on Sips model

	Temperature (K)			
	284.15 K	**297.15 K**	**309.15 K**	**333.15 K**
Sepabeads Sp20SS				
$q_{max,0}$ *(mmol/L)*	266.215±0.004	146.756±0.008	210.172±0.007	140.39±0.011
k_0 $(\mathrm{mmol/L})^{-1/n}$	0.461±2.147	1.184±1.112	0.739±1.872	1.249±1.285
Q (KJ/mol)	13.299±0.074	13.278±0.122	13.280±0.1042	13.284±0.121
n_0*(-)*	1.231±0.803	0.959±1.188	1.271±1.088	1.286±1.248
α (-)	0.8209±1.205	0.733±1.419	0.986±1.402	0.825±1.946
$(-\Delta H_s\|_{\theta=1/2})$ ***(KJ/mol)***	**13.3**			
Amberlite XAD16N				
$q_{max,0}$ *(mmol/L)*	240.454±0.006	147.761±0.012	157.248±0.009	92.077±0.0235
k_0 $(\mathrm{mmol/L})^{-1/n}$	0.578±2.339	0.464±3.699	0.278±5.169	0.240±9.008
Q (KJ/mol)	13.063±0.103	13.063±0.131	13.060±0.110	13.067±0.166
n_0*(-)*	1.166±1.159	0.953±1.799	1.068±1.344	0.964±2.247
α (-)	0.946±1.428	0.879±1.949	0.915±1.569	0.801±2.702
$(-\Delta H_s\|_{\theta=1/2})$ ***(KJ/mol)***	**13.1**			

Based on the estimated values, reported in **Table 4.3,** fractional coverage (θ) is plotted versus enthalpy of adsorption as explained in equation (4.10), for four tested temperatures and for the two tested resins, shown in **Figure 4.5**. As can be observed from enthalpy curves at different temperatures, the value of enthalpy is higher at lower temperatures, where the maximum achieved adsorption capacity is higher, due to higher energy barrier that adsorbed molecules need to overcome, and the value of enthalpy decreases with increase in temperature.

At fractional coverage equal to 0.5, the value of isosteric enthalpy of adsorption will be equal for the four tested temperatures and this value is reported as the heat of adsorption, highlighted in **Table 4.3**. For adsorption on Sepabeads SP20SS, the value of isosteric enthalpy is obtained as -13.3 kJ/mol, while it has a lower value -13.1 kJ/mol on Amberlite XAD16N. The isosteric enthalpy predicted based on Langmuir model is -13.6 kJ/mol which considering the range of standard error, falls in the same range as is predicted by

Sips model, and the value predicted based on Langmuir model for adsorption on XAD16N, is -12.6 kJ/mol which is less than the value predicted by the Sips model.

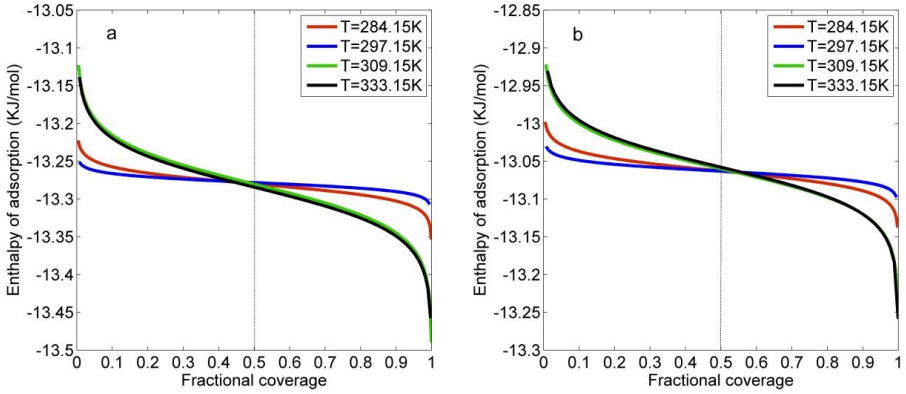

Figure 4.5. Estimated values for isosteric enthalpy of ethyl acetate adsorption versus fractional coverage; a) Adsorption on Sepabeads SP20SS b) Adsorption on Amberlite XAD16N

The difference in prediction is caused by the more accurate estimation of the maximum capacity, applying the Sips model, as is also illustrated in **Figure 4.1.** Although this model gives a more accurate prediction of maximum capacity at higher concentrations, it has application only in low concentration range, as explained in previous sections, therefore Langmuir model is used for calculation of thermodynamic parameters, Gibbs energy and entropy of adsorption.

4.4.1.3 Calculated Gibbs energy (ΔG^0) and Entropy (ΔS^0) of adsorption

The maximum capacity is dependent on temperature, as can be observed from the obtained isotherms shown in **Figure 4.1.** If the q_{max} decreases with temperature, the isosteric enthalpy increases with the loading, and it will reach a finite value when $\theta \rightarrow 1$ The Langmuir expression explained in section 4.3.2.2.1 and the estimated heats of adsorption are used to predict the values of Gibbs energy and entropy of adsorption, based on equations (4.12), and (4.13). The estimated values are reported in **Table 4.4** for adsorption on Sepabeads SP20SS and Amberlite XAD16N, respectively.

The values for heat of adsorption, increase with the hydrophobicity of the ester component, and greater value for higher hydrophobic components such as ethyl hexanoate in comparison to ethyl acetate, implies that this compound interacts more with the resin material and higher energy is required that this component leaves the adsorbed phase after adsorption. Higher negative value for entropy of adsorption for this compound indicates that after adsorption this component is more stabilized on the adsorbent surface and it is more difficult to elute this component from the resin due to stronger binding in comparison to ethyl acetate, and the other less hydrophobic tested esters and molecules are more ordered on the adsorbent surface after adsorption. Comparing the values for Gibbs energy of adsorption, a decrease is observed in the estimated values with increase in temperature. The Gibbs energy of adsorption, as explained in section 4.3.2.3 shows the degree of spontaneity of the adsorption and if the adsorption is favorable, The higher negative value indicates a more favorable adsorption and as it can be observed from the estimated values, the value of Gibbs energy of adsorption decreases with increase in temperature, which also justifies the fact that temperature increase is not favorable for adsorption due to the exothermic nature of the adsorption phenomena. For physical adsorption to occur, the Gibbs energy of adsorption is between (-20-0 kJ/mol) [44], while it lies between (-80 - -400 kJ/mol) [44] if chemisorption is dominant. The estimated value of ΔG^0 for ethyl acetate is approximately -10.5 kJ/mol, whereas it is above -20 kJ/mol for the other three hydrophobic compounds adsorbed on Sepabeads SP20SS. The presented values demonstrate that for ethyl acetate physisorption is dominant, and molecules bind to the surface of the adsorbent, and for the other three esters which has higher hydrophobicity and affinity towards the resin surface, adsorption is mainly chemical and molecules bind stronger to the adsorbent, and Gibbs energy of adsorption equal or higher than -20 kJ/mol is obtained for most of the tested temperatures for high hydrophobic components, i.e. ethyl 4-methylpentanoate and ethyl hexanoate. Comparing the calculated values of ΔH^0 and ΔG^0 for adsorption on Sepabeads Sp20SS, with the results obtained on XAD16N, it can be observed that lower value is calculated for adsorption on XAD16N, mainly for ethyl acetate, isopentyl acetate, and ethyl 4-methylpentanoate, and it is due to the higher affinity of the Sepabeads SP20SS resin towards the tested esters and more spontaneous reaction on the surface of this resin in comparison.

Table 4.4. Calculated values for heat, entropy and Gibbs energy of adsorption

		Ethyl acetate	Isopentyl acetate	Ethyl 4-methylvalerate	Ethyl hexanoate
Sepabeads SP20SS					
ΔH (KJ.mol^{-1})		-13.6	-25.0	-28.1	-30.7
ΔS (KJ. (mol.K)$^{-1}$		-0.001	-0.015	-0.008	-0.023
ΔG	284.15 K	-10.5	-21.2	-25.9	-22.5
(KJ.mol^{-1})	297.15 K	-10.3	-21.0	-25.8	-22.1
	309.15 K	-10.2	-20.8	-24.7	-21.7
	333.15 K	-9.9	-20.4	-25.5	-21.1
R^2		0.999	0.986	0.987	0.997
Amberlite XAD16N					
ΔH (KJ.mol^{-1})		-12.6	-20.3	-21.1	-31.1
ΔS (KJ. (mol.K)$^{-1}$		-0.009	-0.005	-0.175	-0.028
ΔG	284.15 K	-10.1	-18.8	-22.4	-23.1
(KJ.mol^{-1})	297.15 K	-9.9	-18.7	-20.1	-22.7
	309.15 K	-9.9	-18.7	-18.0	-22.4
	333.15 K	-9.7	-18.5	-13.8	-21.7
R^2		0.993	0.997	0.914	0.989

4.4.2 Influence of temperature and ethanol concentration on multicomponent adsorption

4.4.2.1 Effect of ethanol and temperature on K affinity

The influence of temperature and ethanol concentration is investigated on multicomponent adsorption of the four aforementioned flavor-active esters as explained in section 4.3.4.2. Multicomponent isotherms are obtained at the tested conditions for each flavor-active ester in the mixture, and for adsorption on the two tested resins. In order to compare the influence of tested conditions on equilibrium concentrations, and shape of the isotherms, the obtained isotherms for the tested conditions (temperatures 284.15, and 325.15 K), and ethanol concentrations (1 and 30% ethanol) are compared for each ester in the mixture and for each tested resin, depicted in **Figure 4.6**.

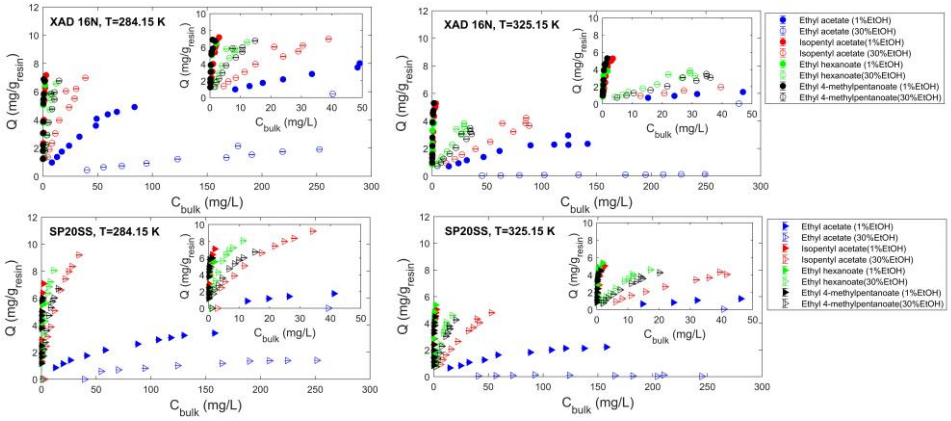

Figure 4.6. Multicomponent adsorption isotherms at ethanol concentrations (1 and 30% v/v) and temperatures(284.15 and 325.a5 K); Adsorption on XAD16N and SP20SS

Comparing the two figures at the top, it can be concluded that increase in temperature from 284.15 to 325.15 K, has higher influence on decrease of equilibrium binding capacity, at higher tested ethanol concentration, i.e. 30% ethanol. This influence is more significant for the decrease of equilibrium binding capacity for ethyl acetate, the more polar component in the mixture. Increase of both temperature and concentration of ethanol reveal a significant decrease in equilibrium binding capacity (approximately 93%), compared to 40% reduction at lower temperature (i.e. 284.15 K), and lower ethanol concentration (i.e. 1% v/v ethanol) for this ester. Similar behaviour is observed for adsorption on Sepabeads SP20SS, according to the results presented in figures at the bottom. Higher reduction in equilibrium binding capacity (approximately 92%) was observed for ethyl acetate at higher tested temperature compared to 30% reduction at lower temperature. The comparison of results obtained for adsorption in the same tested conditions for the two tested resins, reveal a higher affinity towards more hydrophobic components ethyl hexanoate, ethyl 4-methylpentanoate, and isopentyl acetate in comparison to ethyl acetate, for the tested resin Sepabeads SP20SS This resin has smaller particle size (between 50-100 µm) compared to XAD16N with particle size (between 560-710 µm), and has high surface area per volume. Moreover, larger pore volume for this resin as mentioned earlier, aids the diffusion and leads to stronger binding of highly hydrophobic esters. Subsequently lower adsorption of ethyl acetate was observed for adsorption on this resin and for all the tested conditions. Due to lower hydrophobic nature and more polarity, separation of this component will be easier from

the mixture in comparison to other tested components with higher hydrophobicity. The two components ethyl hexanoate and ethyl 4-methylpentanoate, with similar molecular structure and hydrophobicity, show similar adsorption behaviour and strong binding and separation of these two components from each other can be challenging.

The influence of temperature and ethanol concentration is investigated on multicomponent adsorption of the four aforementioned flavor-active esters as explained in section 4.3.4.2. The thermodynamic parameters q_{max} *and* $k_{ads,i}$, are regressed based on multicomponent Langmuir model. The value of affinity parameter $K_{affinity}$ (L/g_{resin}) is calculated by multiplication of the Langmuir constant $k_{ads,i}$ and the maximum capacity q_{max} for all the tested conditions, temperatures and concentrations of ethanol. The calculated values for $K_{affinity}$ are shown in **Figures 4.7** and **4.8** for adsorption on Sepabeads SP20SS and Amberlite XAD16N respectively. The error bars shown in the figures, are the standard errors calculated based on the diagonal of the covariance matrix estimated from the Jacobian given by the fitting function [14].

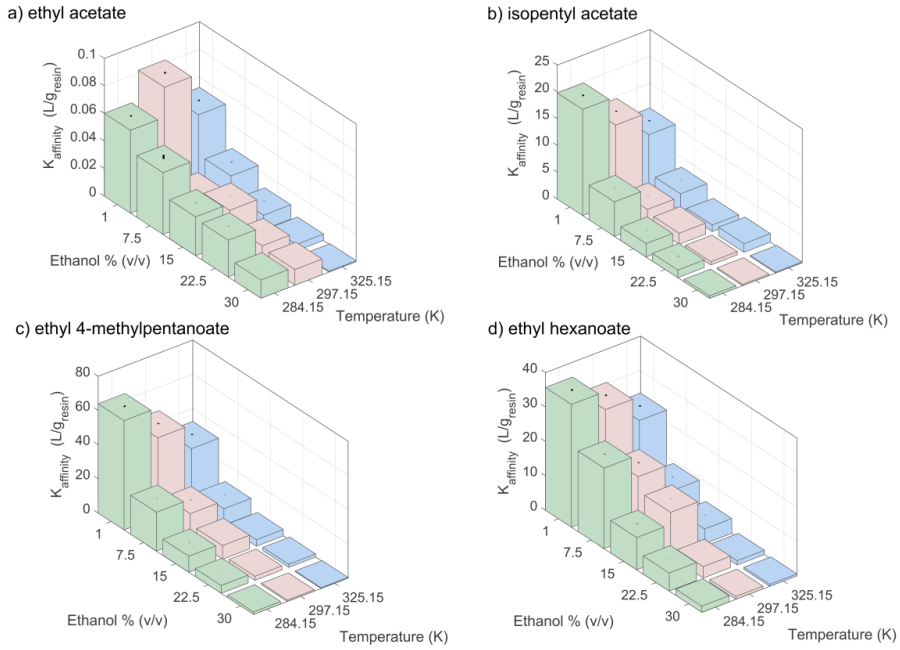

Figure 4.7. $K_{affinity}$ as function of temperature and ethanol concentration, adsorption on Sepabeads SP20SS; a) ethyl acetate b) isopentyl acetate c) ethyl 4-methylpentanoate d) ethyl hexanoate

It can be observed from **Figure 4.7,** that high affinity parameter is obtained for high hydrophobic components, i.e. ethyl hexanoate and ethyl 4-methylpentanoate. In comparison the affinity of both of the tested resins towards ethyl acetate, the less hydrophobic component is less. Higher affinity parameter obtained on Sepabeads SP20SS for the three hydrophobic esters, isopentyl acetate, ethyl 4-methylpentanoate, and ethyl hexanoate, and this increase in affinity in comparison to Amberlite XAD16N, is due to smaller particle size, larger pore volume, and high surface area per volume of the Sepabeads SP20SS resin , therefore an increase was observed in the slope of the isotherms for this three esters and the bulk concentration of the liquid remained after adsorption was lower in comparison to the concentrations measured for adsorption on Amberlite XAD16N.

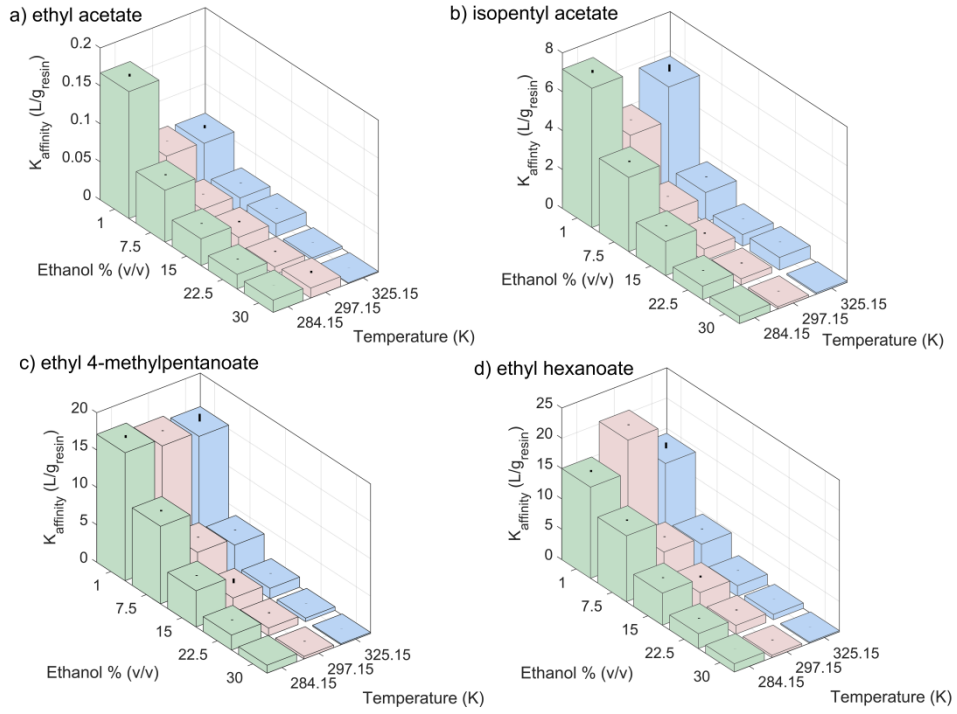

Figure 4.8. $K_{affinity}$ as function of temperature and ethanol concentration, adsorption on Amberlite XAD16N; a) ethyl acetate b) isopentyl acetate c) ethyl 4-methylpentanoate d) ethyl hexanoate

As it can be detected from **Figures 4.7** and **4.**8, increase in concentration of ethanol from 1 to 30% (v/v) has influence on the affinity parameter, as a considerable decrease in the value

of $K_{affinity}$ was observed for all of the tested esters present in the mixture. With the increase of the ethanol concentration, the activity coefficient of esters in the mixture will decrease, and esters will have less tendency to leave the aqueous solution, therefore according to equality of chemical potential for component i in adsorbed and liquid phase, the affinity parameter can be described as a function of activity coefficient in the liquid phase. As the activity coefficient for esters decreases with increase in ethanol concentration, lower value for affinity parameter and subsequently lower binding capacity is expected to be obtained

Increase of temperature from 284.15 K to 325.15 K, showed a slight decrease in maximum capacities, due to exothermic nature of the adsorption, and as a result, lower value of $K_{affinity}$ is obtained at higher temperatures.

4.4.2.2 Estimated parameters for $K_{affinity}$ as a function of Ethanol concentration and temperature

In order to obtain a relation between the calculated values of $K_{affinity,}$ as a function of ethanol concentration and also temperature, a polynomial fit is considered to describe the calculated values, as is explained in equation (4.16).

$$K_{affinity}\left(Temperature(K), Ethanol\%\left(\frac{v}{v}\right)\right) = p_{00} + p_{10} \times \left(Temperature(K)\right) + p_{01} \times \left(Ethanol\%\left(\frac{v}{v}\right)\right) + p_{11} \times (Temperature) \times \left(Ethanol\%\left(\frac{v}{v}\right)\right) + p_{02} \times \left(Ethanol\%\left(\frac{v}{v}\right)\right)^2 \quad (4.16)$$

The values of P_{00}, P_{10}, P_{01}, P_{11}, P_{02} coefficients are estimated based on the polynomial fit for each tested ester present in the mixture and for adsorption on the two tested resins. These values are reported in **Tables 4.5** and **4.6** with 95% confidence bounds, and the calculated R^2 values and accuracy of the fit.The obtained fits for each tested ester and for each tested resin are outlined in **Figures 4.9** and **4.10**.

As the calculated values of R^2 for the fits reveal, the polynomial fit can predict the value of $K_{affinity}$ as a function of temperature and ethanol concentration with higher accuracy for the two most hydrophobic compounds ethyl hexanoate and ethyl-4 methylpentanoate, R^2 value of 0.981 and 0.935 for adsorption on SP20SS and 0.919 and 0.946 for adsorption on

XAD16N respectively. The considered polynomial fit is able to explain the estimated $K_{affinity}$ parameters with higher accuracy for ethyl acetate and isopentyl acetate on SP20SS in comparison to XAD16N.

F-statistic test is also performed to check if the variance of estimated affinity parameters based on multicomponent Langmuir model and the values predicted by the polynomial fit are equal. If the null hypothesis (equality of variances) is true, the F distribution , the value of F will be close to 1, otherwise the null hypothesis is rejected [45]. A two-tailed test is performed and the value of α (0.05) is divided by 2 [46]. The area in the right tail of sampling distribution represents the p-value [45]. The p-value and $F_{critical}$ are calculated using *FDIST* function , which gives the F probability distribution, and the *FINV* function, which gives the probability of right-tailed F probability distribution. If the value of $F<F_{critical}$ and p-value>α we can conclude that there is no significant difference between the estimated values of affinity parameters from both methods with 95% confidence. The F Test is performed for each tested ester component and at three tested temperatures, for both tested resins.The calculated values are provided in **Table 4.7** for adsorption on Sepabeads SP20SS and Amberlite XAD16N respectively.

Table 4.5. Coefficients obtained from polynomial fit to the values of $K_{affinity;}$ Adsorption on Sepabeads SP20SS

	Sepabeads SP20SS			
Component	*Ethyl acetate*	*Isopentyl acetate*	*Ethyl hexanoate*	*Ethyl 4-methylpentanoate*
Coefficient (95% confidence bound)				
P00	0.179 (-0.015, 0.372)	64.120 (23.500, 104.700)	134.300 (100.300, 168.200)	225.300 (122.000, 328.500)
p10	-0.0004 (-0.0010, 0.0003)	-0.163 (-0.297, -0.029)	-0.341 (-0.453, -0.229)	-0.585 (-0.926, -0.244
p01	-0.004 (-0.015, 0.007)	-3.352 (-5.607, -1.097)	-5.264 (-7.150, -3.378)	-10.910 (-16.640, -5.178)
P11	-1.168e-6 (-3.598 e-5, 3.364 e-5)	0.007 (-6.525 e-4, 0.014)	0.0106 (0.004, 0.017)	0.022 (0.004, 0.0407)
P02	8.729e-05 (1.667e-05, 1.579 e-4)	0.029 (0.015, 0.044)	0.035 (0.023,0.048)	0.090 (0.052,0.128)
Goodness of fit				
R^2	0.848	0.896	0.981	0.935

Table 4.6. Coefficients obtained from polynomial fit to the values of $K_{affinity;}$ Adsorption on Amberlite XAD16N

	Sepabeads SP20SS			
Component	*Ethyl acetate*	*Isopentyl acetate*	*Ethyl hexanoate*	*Ethyl 4-methylpentanoate*
Coefficient (95% confidence bound)				
P00	0.619 (0.195, 1.043)	16.240 (-1.829, 34.320)	46.700 (8.372, 85.030)	43.910 (13.020, 74.790)
p10	-0.0017 (-0.0031, -0.0003)	-0.035 (-0.094, 0.025)	-0.097 (-0.224, 0.029)	-0.089 (-0.191, 0.012)
p01	-0.025 (-0.048, -0.001)	-0.782 (-1.785, 0.221)	-2.000 (-4.127, 0.128)	-1.982 (-3.697, -0.268)
P11	5.711e-05 (-1.910e-05, 1.333 e-4)	0.001 (-0.002, 0.004)	0.002 (-0.005, 0.009	0.002 (-0.004, 0.007)
P02	0.0002 (8.6070 e-6, 0.0003)	0.009 (0.003,0.016)	0.027 (0.013,0.041)	0.029 (0.018,0.040)
Goodness of fit				
R^2	0.778	0.855	0.919	0.946

Table 4.7. Estimated p and F values based on F statistic test; Adsorption on SP20SS and XAD16N

	Temperature (K)					
	T=284.15 K		**T=297.15 K**		**T=325.15 K**	
No. of observations	5	5	5	5	5	5
df	4	4	4	4	4	4
$F_{critical}$	9.604		9.604		9.604	
Alpha (α)	0.050		0.050		0.050	
Sepabeads Sp20SS						
Ethyl acetate						
p-value	0.743		0.478		0.939	
F	1.361		1.960		1.074	
Isopentyl acetate						
p-value	0.779		0.963		0.9092	
F	1.302		1.045		1.113	
Ethyl 4-methylpentanoate						
p-value	0.805		0.896		0.930	
F	1.261		1.130		1.085	
Ethyl hexanoate						
p-value	0.955		0.946		0.923	
F	1.054		1.066		1.095	
Amberlite XAD16N						
Ethyl acetate						
p-value	0.507		0.241		0.889	
F	1.875		3.094		1.140	
Isopentyl acetate						
p-value	0.721		0.475		0.710	
F	1.401		1.968		1.419	
Ethyl 4-methylpentanoate						
p-value	0.804		0.993		0.863	
F	1.264		1.008		1.176	
Ethyl hexanoate						
p-value	0.733		0.629		0.964	
F	1.379		1.576		1.043	

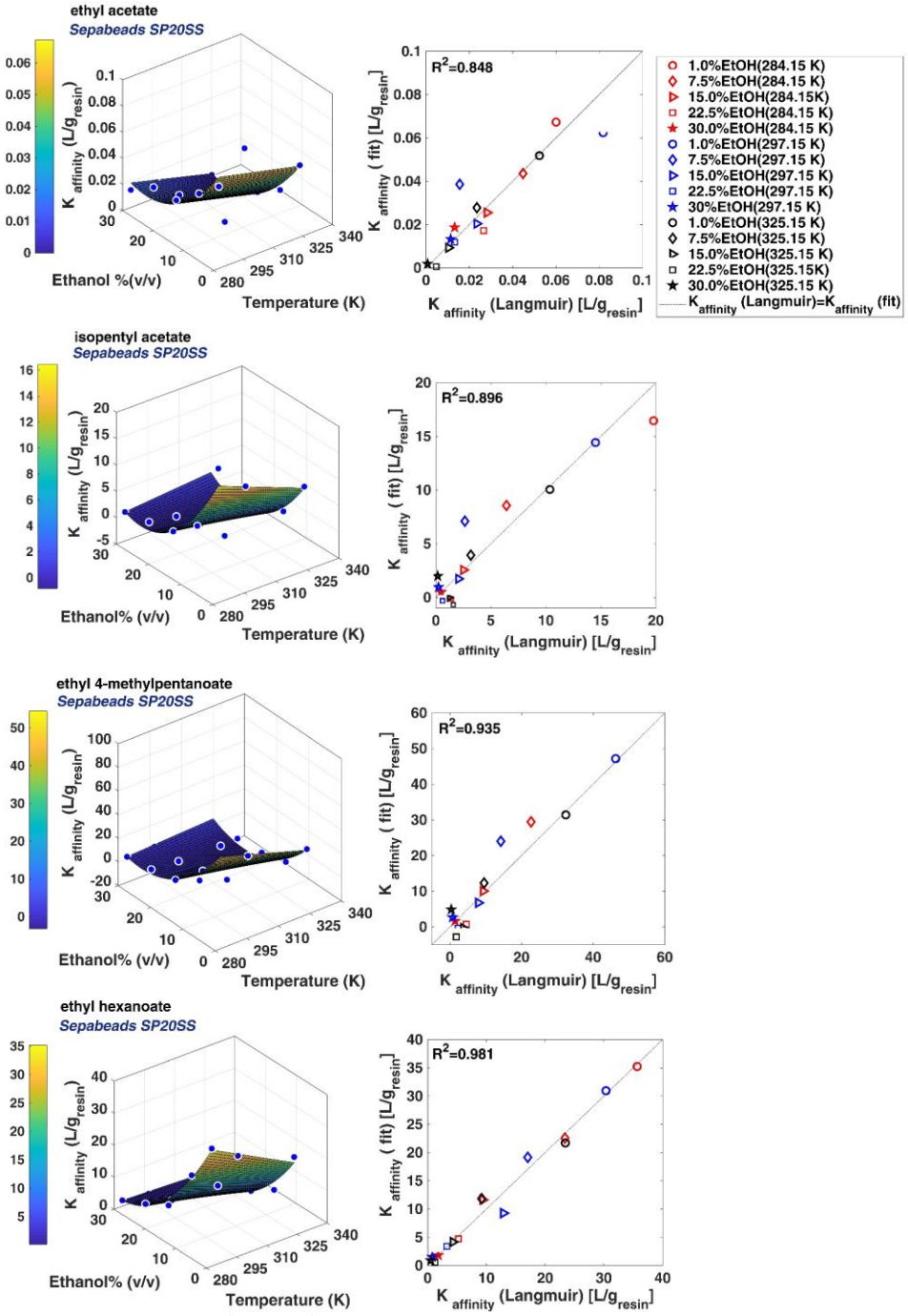

Figure 4.9. $K_{affinity}$ as function of temperature and ethanol% (v/v), adsorption on Sepabeads SP20SS

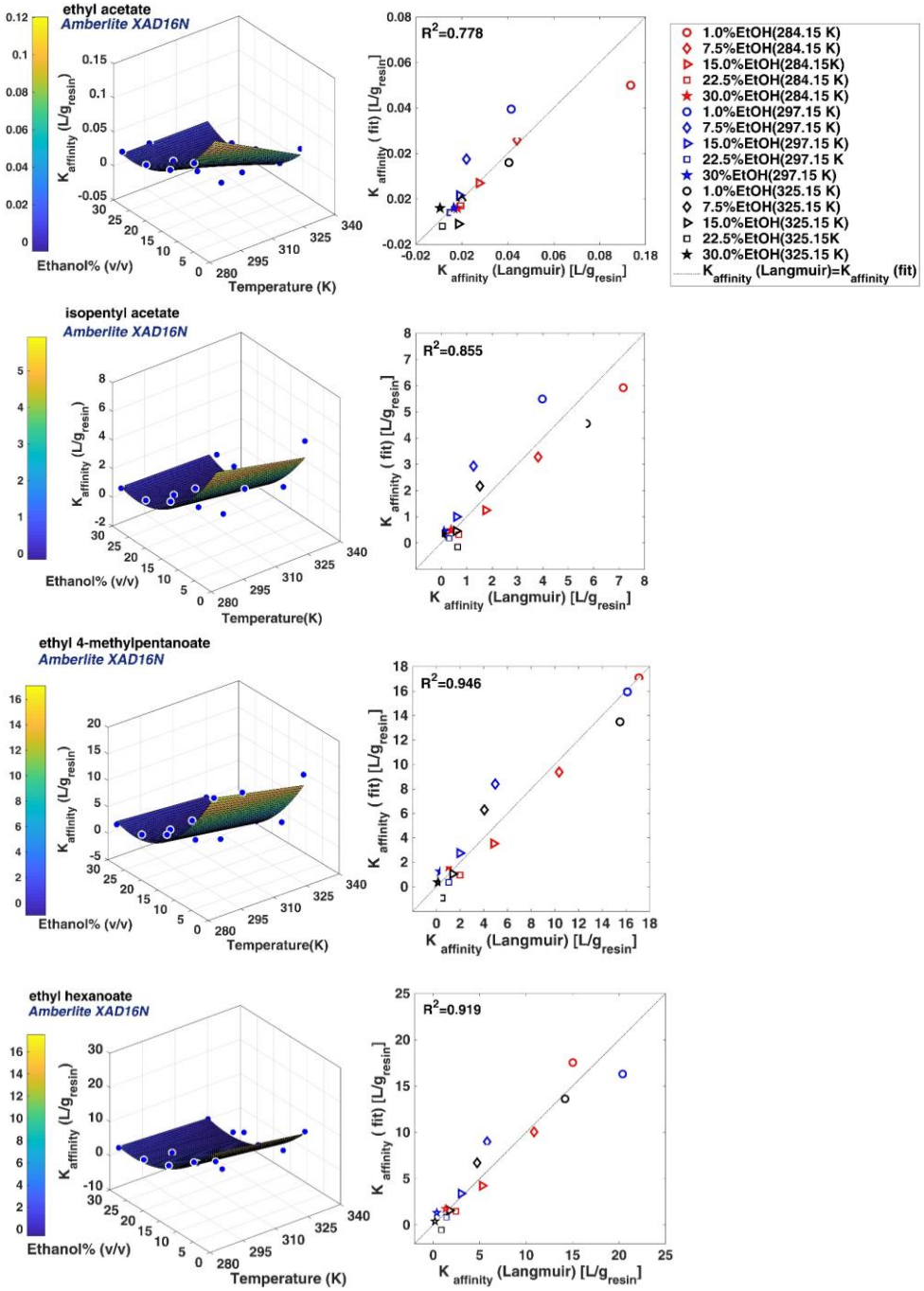

Figure 4.10. $K_{affinity}$ as function of temperature and ethanol % (v/v), adsorption on Amberlite XAD16N

The estimated F values are close to 1 (between 1 and 2) for most of the tested esters and p-value is greater than 0.05, as demonstrated in **Table 4.7**, which proves that there is no significant difference between the variances calculated for each set.
The obtained relation can be used for predicting the affinity for each tested ester in the mixture for adsorption on the investigated resins and when adsorption is going to be performed at other temperatures and ethanol concentrations.

4.5 Conclusions

This chapter focuses on studying the influence of temperature and ethanol on adsorption behavior of flavor-active esters using batch uptake experimentation and static headspace technique for analysis of equilibrium between two phases of gas and liquid. The application of static headspace technique for determination of partition coefficients and equilibrium between three phases is discussed in Appendix A., however this method requires a lot of sample preparation for performing the experiments based on variation of the phase ratio and considering the assumptions required for this method (concentration of analyte close to zero on the adsorbent or high degree of adsorption) it cannot be applied with high accuracy for determination of maximum capacity for a multi-compound mixture, therefore in order to investigate the influence of temperature on adsorption behaviour of flavor-active esters, batch uptake experimentation together with analysis of the samples and measuring the equilibrium between two phases of gas and liquid, is applied and isotherms are obtained for four major esters in beer, i.e. ethyl acetate, isopentyl acetate, ethyl 4-methylpentanoate, and ethyl hexanoate at four various temperatures (i.e. 284.15, 297.15, 309.15, and 333.15 K) on two hydrophobic resins (Sepabeads SP20SS, and Amberlite XAD16N). According to this study, lower adsorption capacity is obtained at higher temperature and due to the exothermic nature of adsorption, increase in temperature is not observed as favourable. Estimated thermodynamic properties like heat, entropy, and Gibbs energy of adsorption based on Van't Hoff relation, reveal that higher heat of adsorption is achieved by adsorption of esters with higher hydrophobicity, i.e. ethyl hexanoate, and ethyl 4-methylpentanoate in comparison to other flavor-active esters, value of ΔH^0 as -28.1 and -30.7 kJ/mol for adsorption of ethyl 4-methylpentanoate and ethyl hexanoate on Sepabeads SP20SS respectively, and -21.1, and -

31.1 kJ/mol for adsorption on Amberlite XAD16N. These two compounds bind stronger to the resin due to their high hydrophobicity and after adsorption they need to overcome a greater energy barrier to leave the solid phase. The calculated negative value for entropy of adsorption for these two compounds also justifies their strong binding to the resin material, since after strong binding of the esters to the resin, molecules are more ordered, stabilized, and confined between the pores, (value of ΔS^0 as -0.023 and -0.028 kJ/mol for adsorption of ethyl hexanoate on Sepabeads SP20SS and Amberlite XAD16N respectively). Higher value of Gibbs energy is obtained for adsorption on both resins at higher temperatures, which implies that adsorption phenomena is exothermic and increase in temperature is not favourable for adsorption. Comparing the two tested resins, greater heat of adsorption, obtained for adsorption on Sepabeads SP20SS, mainly for higher hydrophobic esters, i.e. isopentyl acetate, ethyl 4-methylpentanoate and ethyl hexanoate, can be explained by the structure of this resin. Sepabeads SP20SS has a small particle size (50-100 µm) in comparison to Amberlite XAD16N (560-710µm) and has high surface area per volume. Also the larger pore volume of this resin (1.01 mL/g) in comparison to Amberlite XAD16N (0.55 mL/g), aids the adsorption, as there is more free space available to confine the ester molecules.

From the results of the multicomponent adsorption tests at various ethanol concentrations and temperatures, it can be concluded that increase of ethanol concentration from 1 to 30%(v/v) has reverse influence on the calculated value of Langmuir affinity parameter, since increase in ethanol concentration, lowers the partition coefficient between vapour and liquid phase of the tested esters which is indicated by lower activity coefficients of esters in the aqueous phase, therefore lower affinity parameter is estimated at higher ethanol concentrations. Increase in temperature from 284.15 K to 325.15 K decreased the equilibrium binding capacity, and consequently the Langmuir affinity parameter, due to exothermic nature of adsorption. The obtained Langmuir affinity parameters at various tested temperatures and ethanol concentrations, the affinity parameters estimated based on second order polynomial fit, together with the estimated properties, i.e. heat, entropy, and Gibbs energy of adsorption, can be used in the next step for designing an adsorption column for separation of flavor-active esters and, to consider the non-isothermal condition for their separation.

Nomenclature

C	Equilibrium concentration (mmol/L)
ΔH_s	Isosteric enthalpy of adsorption (kJ/mol)
T	Temperature (K)
R	Gas constant (J/(mol.K))
q	Adsorption capacity (mmol/L)
q_{max}	Maximum load (mmol/L)
k_{ads}	Langmuir parameter (L/mmol)
K	Langmuir equilibrium constant (-)
k_∞	Langmuir temperature independent factor (L/mmol)
ΔH^0	Heat of adsorption (kJ/mol)
n	Sips parameter (-)
k_0	Adsorption affinity at reference temperature (L/mmol)
n_0	Sips parameter at reference temperature (-)
T_0	Reference temperature (K)
$q_{max,0}$	Saturation capacity at reference temperature (mmol/L)
Q	Isosteric enthalpy at $\theta = 1/2$ (kJ/mol)
ΔG^0	Gibbs energy of adsorption (kJ/mol)
ΔS^0	Entropy of adsorption (kJ/mol)
M_{init}	Moles of analyte in initial sample (mmol)
C_0	Initial molar concentration (mmol/L)
V_0	Initial volume of analyte (L)
M_{bulk}	Moles of analyte in bulk solution (mmol)
C_{blank}	Concentration blank (mmol/L)
V_{blank}	Volume blank (L)
m_{resin}	Mass of wet resin (g)
$K_{affinity}$	Langmuir affinity parameter (L/g)

Greek symbols

θ	Fractional coverage (-)
α	Sips constant parameter (-)
χ	Constant parameter for temperature dependent q_{max} (-)

References

1. Verstrepen, K.J., et al., *Flavor-active Esters: Adding Fruitiness to Beer.* J Biosci Bioeng, 2003. **96**(2): p. 110-118.
2. Meilgaard, M.C., *The flavor of beer.* MBAA Tech. Quart., 1991. **28**: p. 132-141.
3. Meilgaard, M.C., *Flavor chemistry of beer. Flavor interaction between principal volatiles.* MBAA Tech. Quart., 1975. **12**: p. 107-117.
4. Horak, T., et al., *Analysis of selected Esters in Beer Comparison of Solid-Phase MicroExtraction and Stir Bar Sorptive Extraction.* J Inst Brew, 2010. **116**(1): p. 81-85.
5. Pires, E.J., et al., *Yeast: the soul of beer's aroma--a review of flavour-active esters and higher alcohols produced by the brewing yeast.* Appl Microbiol Biotechnol, 2014. **98**(5): p. 1937-49.
6. Saison, D., et al., *Contribution of staling compounds to the aged flavour of lager beer by studying their flavour thresholds.* Food Chem, 2009. **114**: p. 1206-1215.
7. Hiralal, L., A.O. Olaniran, and B. Pillay, *Aroma-active ester profile of ale beer produced under different fermentation and nutritional conditions.* J Biosci Bioeng, 2014. **117**(1): p. 57-64.
8. Andrés-Iglesias, C., et al., *Simulation and flavor compound analysis of dealcoholized beer via one-step vacuum distillation.* Food Res Int, 2015. **76**: p. 751-760.
9. Branyik, T., et al., *A review of flavour formation in continuous beer fermentations.* J Inst Brew, 2008. **114**(1): p. 3-13.
10. Olaniran, A.O., Hiralal,L., M.P. Mokoena, and B. Pillay, *Flavour-active volatile compounds in beer: production, regulation and control.* J Inst Brew, 2017. **123**: p. 13-23.
11. Lea, A.G.H. and J.R. Piggott, *Fermented beverage production*. 2003: Kluwer academic/Plenum Publishers.
12. Torres, S., et al., *Enzymatic synthesis of banana flavour (isoamyl acetate) by bacillus licheniformis S-86 esterase.* Food Res Int, 2009. **42**: p. 454-460.
13. Harrison, G.A.F., *The Flavour of beer-A review.* J Inst Brew, 1970. **76**: p. 486-495.
14. Saffarionpour, S., et al., *Selective adsorption pf flavor-active components on hydrophobic resins.* J Chromatogr A, 2016. **1476**: p. 25-34.
15. Do, D.D., D. Nicholson, and H.D. Do, *On the Henry constant and isosteric enthalpy at zero loading in gas phase adsorption.* J Colloid Interf Sci, 2008. **324**: p. 15-24.
16. Ridha, F.N. and P.A. Webley, *Entropic effects and isosteric enthalpys of nitrogen and carbon dioxide adsorption on chabazite zeolites.* Micropor Mesopor Mat, 2010. **132**: p. 22-30.
17. Gritti, F. and G. Guiochon, *Isosteric enthalpy of adsorption in liquid–solid equilibria: Theoretical determination and measurement by liquid chromatography/mass spectrometry.* J Chromatogr A, 2009. **1216**: p. 4645-4751.
18. Prausnitz, J.M., *Moleculare Thermodynamics: opportunities and responsibilities.* Fluid Phase Equilibr, 1996. **116**: p. 12-26.
19. Seidel-Morgenstern, A. and G. Guiochon, *Thermodynamics of the adsorption of Troger's base enantiomers from ethanol on cellulose triacetate.* J Chromatogr 1993. **631**: p. 37-47.
20. Duong, D.D., *Adsorption analysis: Equilibria and kinetics*. 1998, London: Imperial College Press.
21. Ruthven, D.M., *Principles of adsorption and adsorption processes*. 1984, USA: John Wiley & Sons Inc.
22. Kim, H. and G. Guiochon, *Thermodynamic functions and intraparticle mass transfer kinetics of structural analogues of a template on molecularly imprinted polymers in liquid chromatography.* J Chromatogr A, 2005. **1097**: p. 84-97.
23. Überbacher, R., et al., *Hydrophobic interaction chromatography of proteins:thermodynamic analysis of conformational changes.* J Chromatogr A, 2010. **1217**(2): p. 184-190.

24. Barkat, M., et al., *Kinetics and thermodynamics studies of chromium(VI) ions adsorption onto activated carbon from aqueous solutions.* Chem Eng Process, 2009. **48**(1): p. 38-47.
25. Hameed, B.H., A.A. Ahmad, and N. Aziz, *Isotherms, kinetics and thermodynamics of acid dye adsorption on activated palm ash.* Chem Eng J, 2007. **133**(1-3): p. 195-203.
26. Nollet, H., et al., *Removal of PCBs from wastewater using fly ash.* Chemosphere, 2003. **53**: p. 655-665.
27. Sips, R., *On the structure of a catalyst surface.* J Phys Chem, 1948. **16**(5): p. 490-495.
28. Sing, K.S.W., F. Rouquerol, and J. Rouquerol, *Classical interpretation of physisorption isotherms at the gas-solid interface*, in *Adsorption by powders and porous solids, Principles, Methodology, and applications,* J. Rouquerol, et al., Editors. 2014, Elsevier Ltd.
29. Kulik, D.A., *Standard molar Gibbs energies and activity coefficients of surface complexes on mineral water interfaces (Thermodynamic insights)*, in *Interface Science and technology*, J. Lützenkirchen, Editor. 2006, Elsevier Ltd.
30. Tan, I.A.W., B.H. Hameed, and A.L. Ahmad, *Equilibrium and kinetic studies on basic dye adsorption by oil palm fibre activated carbon.* Chem Eng J, 2007. **127**(1-3): p. 111-119.
31. Gokmen, V. and A. Serpen, *Equilibrium and kinetic studies on the adsorption of dark colored compounds from apple juice using adsorbent resin.* J Food eng, 2002. **53**: p. 221-227.
32. Sarvinder Singh, T. and K.K. Pant, *Equilibrium, kinetics and thermodynamic studies for adsorption of As (III) on activated alumina.* Sep Purif Technol, 2004. **36**: p. 139-147.
33. Tan, I.A., A.L. Ahmad, and B.H. Hameed, *Adsorption isotherms, kinetics, thermodynamics and desorption studies of 2,4,6-trichlorophenol on oil palm empty fruit bunch-based activated carbon.* J Hazard Mater, 2009. **164**(2-3): p. 473-82.
34. Yanxu, L., C. Jiangyo, and S. Yinghuang, *Adsorption of multicomponent volatile organic compounds on semi-coke.* Carbon 2008. **46**: p. 858-863.
35. Storti, G., et al., *Optimal design of multicomponent countercurrent adsorption separation processes involving nonlinear equilibria.* Chem Eng Sci, 1989. **44**(6): p. 1329-1345.
36. Mazzotti, M., G. Storti, and M. Morbidelli, *Shock layer analysis in multicomponent chromatography and countercurrent adsorption.* Chem Eng Sci, 1994. **49**(9): p. 1337-1355.
37. Kaspereit, M. and A. Seidel-Morgenstern, *Process concepts in preparative chromatography*, in *Liquid Chromatography, Fundamentals and Instrumentation*, S. Fanali, et al., Editors. 2013, Elsevier Inc.
38. Abburi, K., *Adsorption of phenol and p-chlorophenol from their single and bisolute aqueous solutions an Amberlite XAD-16 resin.* J Hazard Mater B, 2003. **105**: p. 143-156.
39. https://www.chemaxon.com/. 28 June, 2017.
40. Foo, K.Y. and B.H. Hameed, *Insights into modeling of adsorption isotherm systems.* Chem Eng J, 2010. **156**: p. 2-10.
41. Xue, D. and Y. Chen, *Solving applied mathematical problems with MATLAB*. 2008: CRC Press, taylor & Francic Group I.I.C.
42. Zondervan, E., *A numerical primer for the chemical engineer*. 2015, CRC Press, Taylor & Francic Group.
43. Liu, Y. and Y.-J. Liu, *Biosorption isotherms, kinetics and thermodynamics.* Sep Purif Technol, 2008. **61**: p. 229-242.
44. Agarry, S.E., O.O. Oguneleye, and O.A. Ajani, *Biosorptive removal of Cadmium (II) ions from aqeous solution by chemically modified onion skin: Batch equilibrium, kinetic and thermodynamic studies.* Chem Eng Commun, 2015. **202**: p. 655-673.
45. Le Blanc, D., *Statistics, concepts and applications for science*. 2004, Mississauga, Canada: JONES AND BARTLETT PUBLISHERS.
46. Wang, G.C.S. and L.J. Chapman, *Regression analysis, Modeling & Forecasting*. 2003, New York, US: GRACEWAY PUBLISHING COMPANY.

5 Evaluating the application of Adsorbed Solution Theory for predicting competitive adsorption behavior of flavor-active esters on hydrophobic resins

ABSTRACT

Determination of thermodynamic equilibrium parameters for multicomponent adsorption of flavor-active esters based on isotherm studies is essential in order to be able to predict and simulate an adsorption step for their separation and recovery. This chapter aims to discuss the application of Adsorbed Solution Theory (AST) for prediction of multicomponent equilibrium adsorption isotherms from single-component adsorption equilibrium data, when information on competitive multi-compound behavior of flavor-active esters is not available. The approach developed based on this theory, for an ideal system (IAST approach), is evaluated for prediction of multicomponent adsorption of four major flavor-active esters in beer matrix, i.e. ethyl acetate, isopentyl acetate, ethyl 4-methylpentanoate, and ethyl hexanoate for adsorption on two hydrophobic resins, Sepabeads SP20SS, and Amberlite XAD16N. The developed predictive model based on IAST approach, was able to predict the multicomponent adsorption isotherms for ethyl acetate and ethyl hexanoate with higher accuracy (lower RMSE) for adsorption on XAD16N. The predictions for adsorption on SP20SS, show high accuracy for ethyl hexanoate and deviation between model prediction and experimental multicomponent isotherm data is observed at higher concentrations for the other three tested esters. The results obtained on developed predictive model (the IAST model) can be used as a tool for estimation of equilibrium binding capacities at low concentration region, when experimental data is not available. Although other approach, RAST (Real Adsorbed Solution Theory), can be applied for consideration of the non-ideality in the system, it requires multicomponent adsorption data for estimation of activity coefficients and cannot be considered as a predictive model as IAST approach.

5.1 Introduction

In order to design the adsorption process for selective recovery and fractionation of flavor-active esters, the equilibrium and isotherm data related to each ester present in the mixture is required. Different process parameters like temperature, and presence of other components in the mixture, like ethanol, can influence the competitive adsorption behavior of flavor-active esters [1, 2], nevertheless the experimental procedure for screening different adsorbent materials and testing the influence of all process parameters on competitive adsorption of flavor-active esters is time-consuming and requires a considerable experimental effort. Many predictive models have been developed for calculating the adsorption equilibrium for a multi-component mixture using only pure component data. Among these models, Adsorbed Solution Theory (AST) is a widely adopted approach for predicting equilibrium competitive adsorption, from single-component adsorption isotherms, when equilibrium data on multi-compound adsorption is not available. This approach is first developed by Myers and Prausnitz for a homogeneous adsorbed phase for mixed-gas adsorption [3] and further extended to liquid solutions by Radke and Prausnitz [4]. As one of the approaches developed based on this theory, is the Ideal Adsorbed Solution Theory (IAST), which has been extensively tested for ideal solutions and dilute systems [5-9]. This approach showed promising results in predicting multi-compound adsorption for low concentration levels, however at higher concentrations, when the system deviates from ideal behavior, this model did not give satisfactory results [6, 7, 10, 11]; in order to consider the non-ideality in the system another model, RAST (Real Adsorbed Solution Theory), can be considered through introduction of activity coefficients [3, 4, 12]. However, this approach cannot be considered as predictive as IAST, since for estimation of interaction parameters and activity coefficients, multicomponent experimental data is required [12-14].

The work discussed in this chapter, aims to evaluate the application of Ideal Adsorbed Solution Theory (IAST) for predicting the multicomponent adsorption of flavor-active esters on hydrophobic resins from single component adsorption isotherms. In order to develop the predictive models, single-component adsorption isotherms

obtained in our previous work [1] are used as input for the model. The results on model predictions are compared with experimental multicomponent adsorption isotherms obtained in the same tested condition. Based on the predictions obtained from the tested model, the application of Adsorbed Solution Theory for predicting the multicomponent adsorption of flavor-active esters on hydrophobic resins is evaluated.

5.2 Theory

5.2.1 Adsorbed Solution Theory

The Adsorbed Solution Theory (AST), which is first proposed by Myers and Prausnitz [3, 13] for gas mixtures, is based on the validity of thermodynamic equations for the adsorbed phase in physical adsorption. This theory is further extended for liquid systems by Radke and Prausnitz [4]. For writing the equations for the adsorbed phase, it is necessary to substitute the spreading pressure π for pressure P and substitute the area A for volume V [3]. The spreading pressure, an intensive thermodynamic variable for adsorption equilibria, is defined as the difference in surface tension between a clean surface and a surface covered with the adsorbate and has units of dynes per centimetre [3, 6, 15, 16]. Considering the above mentioned substitutions, the equations for internal and Gibbs energy of adsorption can be written as presented in equations (5.1) and (5.2) [3].

$$dU = TdS - \pi dA + \sum \mu_i dn_i \tag{5.1}$$

$$dG = -SdT + Ad\pi + \sum \mu_i dn_i \tag{5.2}$$

Gibbs free energy is expressed in terms of intensive variables, temperature, spreading pressure and composition and at constant pressure and temperature it can be summarized as equation (5.3), following the theory of Euler.

$$G = \sum n_i \mu_i \tag{5.3}$$

The term presenting the mechanical work (PdV) for a three-dimensional fluid, is presented as πdA in equation (5.1) [3]. For physical adsorption, π is positive, therefore during the adsorption process, system works on the surroundings.

5.2.1.1 Ideal Adsorbed Solution Theory (IAST)

One approach developed based on Adsorbed Solution theory is the Ideal Adsorbed Solution Theory (IAST), which works under assumption that the adsorbed mixture forms an ideal solution which is in equilibrium with the bulk liquid at a constant spreading pressure for each tested analyte [4]. For a mixture of solutes in equilibrium with an adsorbent, the chemical potential of solute i in the adsorbed phase is equal to that of liquid phase [4, 17].

The chemical potential for the adsorbed phase is dependent on temperature, spreading pressure and composition, as measured by mole fraction z_i. Equation (5.4) can be written, considering the ideality assumption [4].

$$\mu_i^a(T,\pi,z_i) = \mu_i^{a0}(T,\pi) + RTln\ z_i \tag{5.4}$$

For single-component adsorption, the concentration c_i^0 in the liquid phase, is fixed by variables T and π, hence μ_i^0 in equation (5.4) can be written as presented in equation (5.5) [4].

$$\mu_i^{a0} = \mu_i^{l0}\ [T, c_i^0(\pi)] = \mu_i^{l0}(T) + RTlnc_i^0(\pi) \tag{5.5}$$

When the liquid solution is dilute, no activity coefficient is required. The concentration $c_i^0(\pi)$ refers to solute i, which adsorbs from solution at the same temperature and spreading pressure. For dilute liquid mixture at constant temperature, μ_i^L is a function of c_i and the concentration of i in that mixture, therefore μ_i^l can be written as shown in equation (5.6) [4, 17] .

$$\mu_i(T,c_i) = \mu_i^{l0}(T) + RTlnc_i \tag{5.6}$$

When the system is restricted to dilute solutions, the presented equations above can be written as equation (5.7), which is the relation for Ideal Adsorbed Solution Theory [4].

$$c_i = c_i^0(T,\pi)z_i\ ,\quad i = 1,\dots,N \tag{5.7}$$

Where N is the number of components, c_i is the equilibrium liquid concentrations of solutes in a multicomponent system, c_i^0 is the single-solute liquid concentration in

equilibrium with q_i^0, the adsorption capacity for single-component mixture at the same temperature and spreading pressure of a multicomponent system, and z_i is the mole fraction of adsorbed species i.

The mole fraction of component i on the adsorbed phase (z_i), can be presented as:

$$z_i = \frac{q_i}{q_T} \qquad i = 1, \dots, N \tag{5.8}$$

$$q_T = \sum_{i=1}^{N} q_i \tag{5.9}$$

Where q_T, is the total surface loading (the sum of the adsorption capacities for solute i in the mixture (q_i) for a multi-compound system) [6]. Considering the assumptions for IAST model, the relation as presented in equation (5.10) can be written.

$$\frac{1}{q_T} = \sum_i \frac{z_i}{q_i^0} \quad i = 1, \dots, N \tag{5.10}$$

And sum of the mole fractions for all the species is equal to one for all the compounds present in the mixture.

$$\sum_{i=1}^{N} z_i = 1 \tag{5.11}$$

5.2.1.1.1 Determination of spreading pressure

In order to be able to use equations presented in previous section, spreading pressure needs to be estimated for each single compound in the mixture. From Gibbs adsorption isotherm, as presented in equation (5.12) [3, 4, 18].

$$\pi_i(c_i^0) = \frac{RT}{A} \int_0^{c_i^0} \frac{q_i^0(c_i^0)}{c_i^0}\, dc_i^0, \quad i = 1, \dots, N \quad (constant\ T) \tag{5.12}$$

The integrant in equation (5.12) is represented by the single-component adsorption isotherm. Where A is the specific adsorbent area, R is the universal gas constant, and T is the absolute temperature. Analytical solution of the integral in equation (5.12), can be expressed as presented in **Table 5.1**, for Langmuir and Sips (Langmuir-Freundlich) models [15, 19].

Where k_{ads}, q_i^{sat}, and n are Langmuir, and Sips parameters, which can be obtained from regression of the experimental data on single-component adsorption isotherms. According to IAST model, at equilibrium, the spreading pressure for each single compound is equal to the mixture, as is shown in equation (5. 13) [6].

Table 5.1. Analytical expressions of the spreading pressure for different isotherm models [15, 19]

	Isotherm	**Reduced spreading pressure**
Langmuir	$q_i^0 = \frac{q_i^{sat} k_{ads} C_i^0}{1 + k_{ads} C_i^0}$	$\frac{\pi_i A}{RT} = q_i^{sat} \ln(1 + k_{ads}\, C_i^0)$
Sips (Langmuir-Freundlich)	$q_i^0 = k_{ads}\, C_i^{0(\frac{1}{n})}$	$\frac{\pi_i A}{RT} = n\, q_i^{sat} \ln(1 + k_{ads}\, C_i^{0(\frac{1}{n})})$

$$\pi_1 = \pi_2 = \pi_3 = \cdots = \pi_i = \cdots = \pi_N \quad (5.13)$$

Multicomponent adsorption isotherms can be predicted using equations (5.7), (5.10), (5.11), and (5.12) by assigning C_i values and calculating the corresponding q_i values, starting from single-component adsorption isotherms [6]. For an ideal system, the IAST model does not consider the activity coefficients of the solutes in the mixture and they are considered equal to one in equation (5.7).

5.3 Experimental

This work evaluates the application of Adsorbed Solution Theory for prediction of multicomponent adsorption isotherms for flavor-active esters on hydrophobic resins, from single component adsorption isotherms. Detailed experimental procedure is followed in our previous works, explained in Chapter four, to understand the competitive adsorption behavior of flavor-active esters. In the condition that performing the extensive experiments is not possible, Adsorbed Solution Theory can be used as a tool to approximate the maximum adsorption capacity from single-component adsorption isotherms, and can reduce the need to perform time-consuming experiments. In this work, the application of this approach is evaluated for prediction of maximum capacities for multi-compound adsorption of four major flavor-active esters in beer, i.e. ethyl acetate, isopentyl acetate, ethyl 4-methylpentanoate, and ethyl hexanoate, from the available experimental data on their single component adsorption isotherms. The adsorption is investigated on two hydrophobic resins, Sepabeads SP20SS and Amberlite XAD16N, which showed high selectivity towards esters in our previous studies, explained in Chapter three.

5.3.1 Batch uptake experimentation tests

Batch uptake experimentation in headspace vials is used for determination of adsorption isotherms for both single and multi-compound mixtures, explained in Chapter four, sections 4.3.3 and 4.3.4.

The amount of solute i adsorbed per unit mass on adsorbate (q_i) is calculated using the mass balance (equation (4.15)).

5.3.1.1 Single component adsorption tests

Single component adsorption of 0.45 $g.L^{-1}$ of each tested flavor-active ester, prepared in 1% v/v co-solvent mixture of ethanol/water, is investigated on two synthetic hydrophobic resins Sepabeads SP20SS and Amberlite XAD16N at 284.15 K (Chapter four, section 4.3.4.1) The equilibrium concentrations in the bulk liquid and solid phase are obtained, and the adsorption behavior for each flavor-active ester is explained through Langmuir and Sips thermodynamic models. The single component adsorption isotherms and the parameters obtained based on model fits are used as input for IAST and RAST models to predict the maximum binding capacity for multi-compound adsorption.

5.3.1.2 Multi-compound adsorption tests

Multicomponent adsorption behavior of the tested flavor-active esters is investigated on the same resins and for the similar process conditions (i.e. ethanol concentration as background solution, and temperature) (Chapter four, section 4.3.4.2). The obtained equilibrium isotherm data for multi-component adsorption, is used for validating the model predictions for IAST approach.

5.4 Results and discussions

5.4.1 Single component adsorption isotherms

The results obtained on single component adsorption isotherms at temperature equal to 284.15 K, presented in chapter four, are expressed with the Langmuir and Sips model fits, shown in detail in chapter four together with accuracy in model predictions. The regressed thermodynamic parameters, derived based on each tested model, i.e. single-component Langmuir and Sips models, are assembled in **Table 5.2** for adsorption on Sepabeads SP20SS and Amberlite XAD16N.

Table 5.2. Regressed parameters for single component adsorption of esters (Langmuir and Sips models)

	Regressed parameters				
	Langmuir		**Sips**		
Component	k_{ads} (L/mg)	q_{sat} (mg/g-resin)	k_{ads} (L/mg)	q_{sat} (mg/g-resin)	n (-)
Sepabeads SP20SS					
Ethyl acetate	8.20 e-3 ±5.46 e-4	11.70±0.44	8.40 e-3±8.93 e-4	18.08±4.31	1.18±0.08
Isopentyl acetate	2.40±1.09	11.61±0.72	3.55±0.98	10.39±0.76	0.88±0.07
Ethyl 4-methylpentanoate	7.76±0.06	9.98±0.27	885.68±588.78	7.86±0.21	0.36±0.03
Ethyl hexanoate	5.30±1.66	10.35±0.45	142.69±1.08e3	8.35±0.39	0.42±0.06
Amberlite XAD16N					
Ethyl acetate	8.70e-3±7.73e-3	15.05±0.82	8.50e-3±1.40e-3	20.57±7.34	1.11±0.11
Isopentyl acetate	0.24±1.60e-6	18.52±1.81	3.55±0.98	10.39±0.76	0.88±0.07
Ethyl 4-methylpentanoate	9.48e-1±1.20e-3	16.14±2.29	885.68±588.78	8.35±0.39	0.36±0.3
Ethyl hexanoate	2.78±0.03	10.29±2.38	142.69±1.08e3	8.35±0.39	0.42±0.06

5.4.2 Determination of multicomponent isotherms (IAST approach)

In order to approximate the equilibrium binding capacity, for multi-compound adsorption of flavor-active esters, the experimental data on single component adsorption of flavor-active esters, presented in section 5.4.1 are used as input for the model. For the four tested esters, 2N+1 (9 equations) should be solved together to obtain the equilibrium binding capacity associated with each ester in a multi-compound mixture. Four equations are written for each ester, based on equation (5.7). Four other equations can be written based on the reduced form of the integrant and spreading pressure, explained in equation (5.12) and one equation for the summation of mole fraction of all the species in the

mixture, as presented in equation (5.11). The algorithm of the developed model based on IAST approach is presented in Figure 5.1.

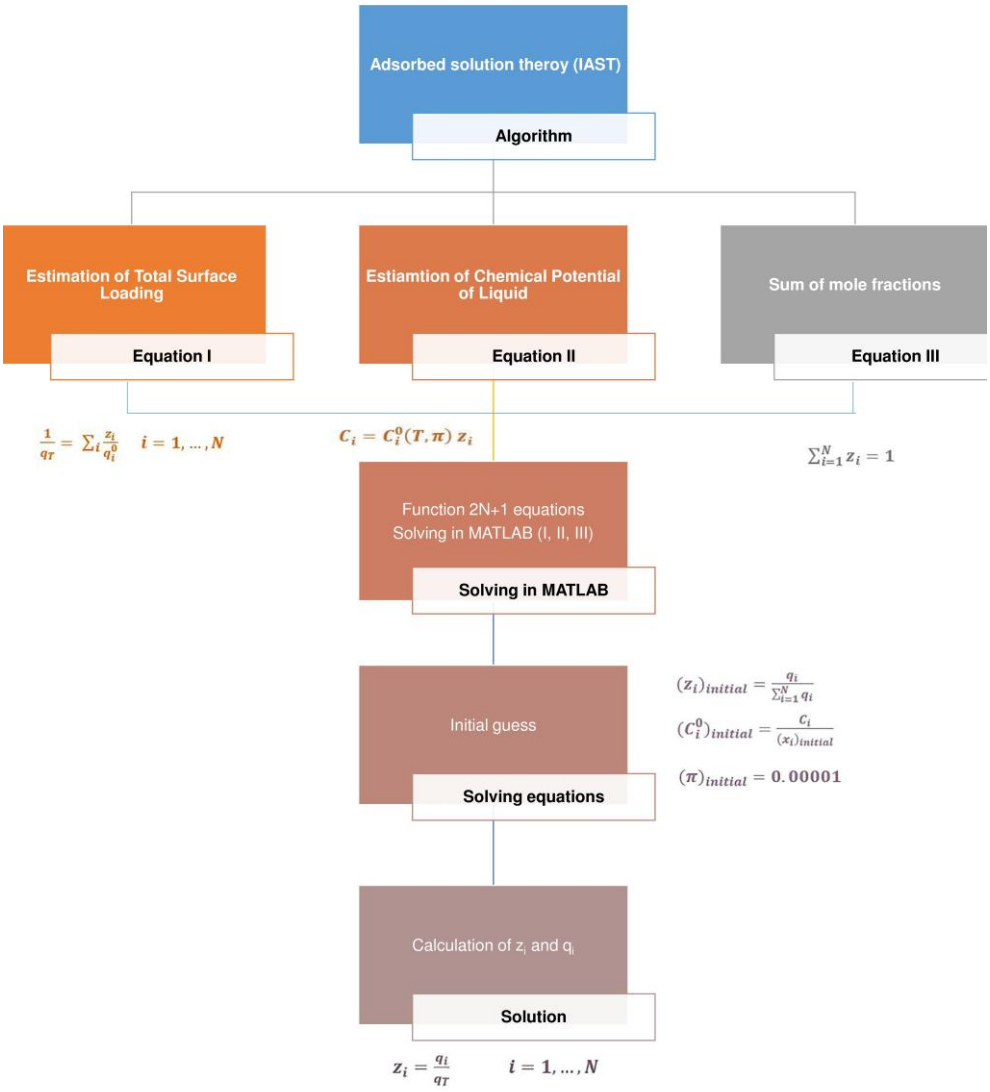

Figure 5.1. Algorithm of IAST approach

The regressed parameters based on Langmuir model, presented in **Table 5.2**, are used to express the reduced form of spreading pressure, and for estimation of the integrant presented in equation (5.13). The equations explained above are solved in Matlab software, version R 2015 b, using fsolve function. As the initial guess, for mass fractions and concentrations, following estimations are considered.

$$(z_i)_{initial} = \frac{q_i}{\sum_{i=1}^{N} q_i} \qquad (C_i^0)_{initial} = \frac{C_i}{(z_i)_{initial}}$$

$\pi_{initial}$ is considered as 0.00001 N/m. Considering the initial conditions explained as x_0, set of equations are solved in Matlab. After solving the equations, the equilibrium binding capacity, can be estimated for a multi-compound mixture, based on equations (5.8), and (5.10).

The comparison of single-component adsorption isotherms, the multi-compound adsorption isotherms predicted by the IAST model, and the experimental multi-compound adsorption isotherms is shown in **Figures 5.2** and **5.3**, for adsorption on Sepabeads SP20SS and Amberlite XAD16N respectively.

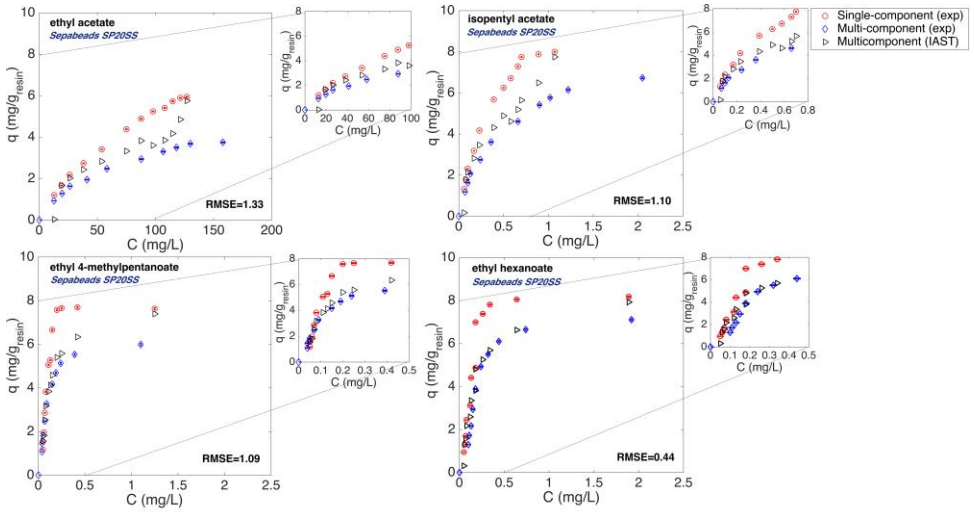

Figure 5.2. Comparison of experimental single-component adsorption isotherms with Experimental multi-component adsorption isotherms and IAST prediction; Adsorption on Sepabeads SP20SS at T=284.15 K

The results of the multicomponent adsorption isotherms, predicted by the IAST model, for adsorption on Sepabeads SP20SS, show a more accurate prediction for the two esters with higher hydrophobicity, i.e. ethyl 4-methylpentanoate and ethyl hexanoate (RMSE of 1.09 and 0.44 respectively). Comparing the experimental adsorption isotherms with the model predictions, it can be observed that at higher concentrations, the IAST model does not predict the maximum binding capacity with high accuracy and it is able to give a more accurate prediction at lower concentration range. For adsorption on Amberlite XAD16N, higher accuracy in prediction obtained for adsorption of ethyl acetate and ethyl hexanoate (RMSE of 1.37 and 1.18 respectively).

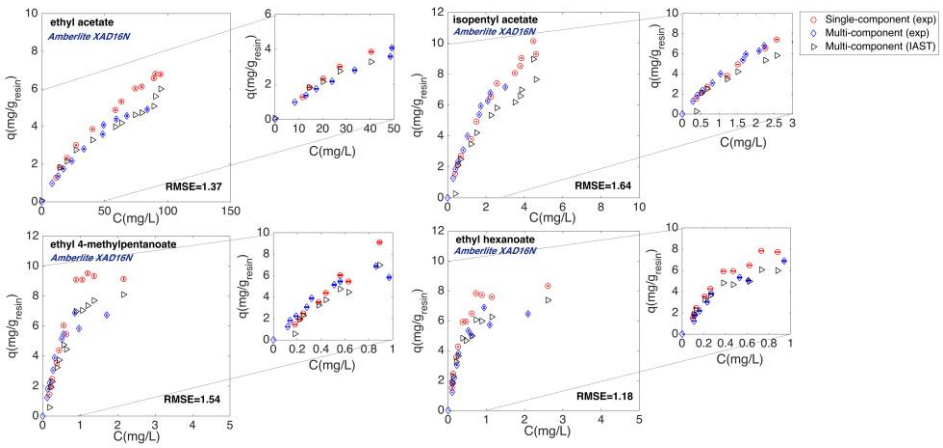

Figure 5.3. Comparison of experimental single-component adsorption isotherms with Experimental multi-component adsorption isotherms and IAST prediction; Adsorption on Amberlite XAD16N at T=284.15 K

5.5 Conclusions

The application of Adsorbed Solution Theory (AST) is dicussed and evaluated in this chapter for prediction of multicompound adsorption of flavor-active esters on hydrophobic resins Sepabeads SP20SS and Amberlite XAD16N, which showed high affinity towards tested esters in previous studies. An approach is developed based on Ideal Adsorbed Solution Theory (IAST) for prediction of multicompound adsorption behavior of flavor-active esters. While performing experiments based on Batch uptake experimentation or column breakthrough analysis proved to be time-consuming, in our

previous studies, this work evaluated the application of IAST approach for prediction of multi-compound adsorption behavior and if applying this approach the need for performing experiments, consuming also a lot of material can be reduced. The results of the predictive model, developed based on IAST approach, showed promissing results with high accuracy for predictions of multicompound adsorption of flavor-active esters on Amberlite XAD16N resin and Sepabeads SP20SS. For predictions obtained for adsorption on Sepabeads SP20SS, the model could not predict the multicompound adsorption isotherms for ethyl acetate and isopentyl acetate with high accuracy, specifically at high concentrations. In order to improve the model predictions at high concentrations, the non-ideality in the system can be considered through introduction of activity coefficients and estimation of binary interaction parameters for selected vapour-liquid equilibrium model applying RAST model. The drawback of this approach is the fact that one set of multicompound adsorption equilibrium data is required for the same components and for adsorption at the same temperature, in order to calculate the activity coefficients and this model cannot be considered as predictive, since corrections on predictive IAST model is performed based on multicompound adsorption equilibrium data. The results on model predictions based on IAST approach, reveal that this approach can successfully predict the multicomponent adsorption on Amberlite XAD16N from single-component adsorption isotherms, and shows promissing predictions for adsorption on Sepabeads SP20SS resin at low concentration region, which is of our interest.

Although RAST approach can improve the predictions obtained based on IAST approach, it cannot completely reduce the requirement of performing experiments, since multicompound adsorption data is required, therefore IAST approach is recommended to be applied for prediction of multicompound adsorption for flavor-active esters when multicompound adsorption data is not available and prediction of adsorption isotherms in a mixture is required to predict the thermodynamic parameters for flavor-active esters in the mixture for the design stage.

Nomenclature

z_i	Mole fraction of solute (-)
C_i	The equilibrium liquid concentrations of solutes in a multicomponent system (mol/m^3)
C_i^0	single-solute liquid concentration in equilibrium with q_i^0 (mol/m^3)
q_T	total surface loading (mol/g$_{resin}$)
q_i^0	Single solute equilibrium surface loading (mol/g$_{resin}$)
R	Gas constant (J/mol*K)
T	Temperature (K)
A	Specific adsorbent area (m^2/g)
G	Gibbs energy of the solution (J)

Greek symbols

π_i	Spreading pressure of component i (N/m)

References

1. Saffarionpour, S., et al., *The influence of ethanol concentration and temperature on adsorption of flavor-active esters on hydrophobic resins.* Sep Purif Technol, 2019. **210**: p 219-230
2. Saffarionpour, S., et al., *Selective adsorption of flavor-active components on hydrophobic resins.* J Chromatogr A, 2016. **1476**: p. 25-34.
3. Myers, A.L. and J.M. Prausnitz, *Thermodynamics of mixed-gas adsorption.* AICHE J, 1965. **11**(1): p. 121-127.
4. Radke, C.J. and J.M. Prausnitz, *Thermodynamics of Multi-solute adsorption from dilute liquid solutions.* AICHE J, 1972. **18**(4): p. 761-768.
5. Jadhav, A.J. and V.C. Srivastava, *Adsorbed solution theory based modeling of binary adsorption of nitrobenzene, aniline and phenol onto granulated activated carbon.* Chem Eng J, 2013. **229**: p. 450-459.
6. Erto, A., D. Lancia, and A. Musmarra, *A modeling analysis of PCE/TCE mixture adsorption based on Ideal Adsorbed Solution Theory.* Sep Purif Technol, 2011. **80**: p. 140-147.
7. Noroozi, B., et al., *Adsorption of binary mixtures of cationic dyes.* Dyes Pigments, 2008. **76**: p. 784-791.
8. Santori, G., M. Luberti, and H. Ahn, *Ideal adsorbed solution theory solved with direct search minimisation.* Comput Chem Eng, 2014. **71**: p. 235-240.

9. Costa, E., et al., *Adsorption of binary and ternary hydrocarbon-gas mixtures on activated carbon-experimental-determination and theoretical prediction of the ternary equilibrium data*. AICHE J, 1981. **27**: p. 5-12.
10. Yu, M., et al., *Adsorption of benzene mixtures on silicate-1 and NaX zeolites.* Micropor Mesopor Mat, 2006. **96**: p. 376-385.
11. Monneyron, P., et al., *Competitive adsorption of organic micropolutants in the aqueous phase onto activated carbon cloth: Comparison of the IAS model and Neural Networks in modeling data*. Langmuir, 2002. **18**: p. 5163-5169.
12. Erto, A., A. Lancia, and D. Musmarra, *A Real Adsorbed Solution Theory model for competitive multicomponent liquid adsorptio onto granular activated carbon.* Micropor Mesopor Mat, 2012. **154**: p. 45-50.
13. Gamba, G., et al., *Adsorbed Solution Theory Models for multicomponent adsorption equilibria.* AICHE J, 1989. **35**(6): p. 959-966.
14. Steffan, D.G. and A. Akgerman, *Thermodynamic modeling of binary and ternary adsorption on Silica Gel.* AICHE J, 2001. **47**(5): p. 1234-1246.
15. Brunchi, C.C., *Multicomponent adsorption of volatile organic compounds in the liquid phase, predictive engineering models, molecular simulations and experiments*. 2015, Technische Universiteit Delft: Delft.
16. Ruthven, D.M., *Principles of adsorption and adsorption process* 1984, New York: Wiley-Interscience.
17. Prausnitz, J.M., R.N. Lichtenthaler, and E.G. de Azevedo, *Molecular thermodynamics of fluid-phase equilibria*. 1999, New Jersey, USA: Prentice Hall PTR.
18. O'Brian, J.A. and A.L. Myers, *A comprehensive technique for equilibrium calculations in adsorbed mixtures: The generalized FastIAS method.* Ind.Eng.Chem.Res., 1988. **27**: p. 2085-2092.
19. Kangas, J., *Separation process modelling, highlighting the predictive capabilities of the models and the robustness of the solving strategies*, in *Faculty of Technology*. 2014, University of Oulu: Finland.

Column chromatography for separation and fractionation of flavor-active esters on hydrophobic resins and simulation of breakthrough behavior

6

ABSTRACT

For simulating an adsorption/elution step for separation and recovery of flavor-active esters in beer in the presence of ethanol at various temperatures, and validating the predicted breakthrough behavior, equilibrium data on concentration of each ester is required. This chapter discusses the application of frontal analysis method (FA) for prediction of breakthrough behavior for adsorption of ethyl acetate, and determination of equilibrium concentrations and binding capacity for competitive adsorption of four major flavor-active esters in beer (i.e. ethyl acetate, isopentyl acetate, ethyl 4-methylpentanoate, and ethyl hexanoate), together with improvement of the determined equilibrium concentrations obtained from competitive frontal analysis, through fraction collection and offline analysis on columns packed with hydrophobic resins, Amberlite XAD16N and Sepabeads SP20SS. Single-component adsorption of ethyl acetate reveal a shorter breakthrough time, and higher slope of breakthrough curve for adsorption on SP20SS, due to smaller particle size (50-100 µm), and enhanced mass transfer characteristics of this resin. Competitive frontal analysis tests, neatly demonstrate that increase in temperature is not favorable for adsorption but aids the elution step. Lower binding capacity of esters and shorter adsorption/elution cycle time is achieved at higher ethanol concentration and cyclic operation simulated under non-isothermal condition, exhibit higher accuracy between predicted and experimental breakthrough curves for XAD16N. A cyclic operation is simulated, for a larger scale column, for two scenarios, separation of ethyl acetate and complete separation of all flavor-active esters in the mixture. For more detailed prediction of breakthrough behavior, the influence of other components present in process streams needs to be investigated on competitive adsorption of esters.

This chapter is partly published as:

S. Saffarionpour, T.F. de Jong, L. A. M. Van der Wielen, E. Brouwer, M. Ottens, Column chromatography for separation of flavor-active esters on hydrophobic resins and simulation of breakthrough behavior, Sep. Purif. Technol., 210 (2019) 304-319
https://doi.org/10.1016/j.seppur.2018.05.008

6.1 Introduction

Liquid chromatography plays a key role in food industry nowadays which permits selective removal of wide variety of flavor and non-flavor active food ingredients through adsorption [1-3]. In order to be able to design a process for separation and recovery of these ingredients, detailed knowledge on process conditions and their influence on adsorption is required. This implies that the adsorption equilibrium concentrations of each component in liquid-solid phase needs to be measured and well-understood. Among these components and ingredients, flavor-active esters play a major role in beverage and brewing industry, and are important contributors to the aroma profile of the beer product [4-9]. During processing, the level of these compounds might alter due to chemical and physical changes of the aroma complex. Their separation and fractionation can be challenging, since they are present in trace levels (ppm) with relatively large amounts of ethanol, which is present in process streams at higher concentration in comparison. To produce a final product with balanced flavor profile, which is acceptable by the consumer, controlling and adjusting the level of esters is crucial [4, 10]. In order to design an adsorption process for selective recovery and fractionation of esters, multi-component thermodynamic adsorption equilibrium data and the influence of process conditions such as ethanol concentration and temperature on adsorption of flavor-active esters, is required. For determination of competitive equilibrium condition, several chromatographic methods can be applied, among which dynamic methods proved to be the fastest and most accurate methods [11-13]. The best-known and widely adopted method is frontal analysis (FA), which allows measuring the mass of the adsorbed component at equilibrium from the retention time of the breakthrough front. As one of the variants of this method, staircase frontal analysis is well-suited for measurement of the concentrations in intermediate sub-plateaus for a multi-compound mixture [14-16]. This work aims to investigate the application of frontal analysis method for measurement of the equilibrium adsorption for a multi-compound mixture of major esters present in beer matrix, i.e. ethyl acetate, isopentyl acetate, ethyl 4-methylpentanoate, and ethyl hexanoate and study the possibility of their separation in a fixed-bed column through simulation of breakthrough behavior. In order to investigate the possibility for separation of these flavor-active esters, and study the influence of

temperature and ethanol concentration on their competitive adsorption behavior, competitive frontal analysis method is applied in combination with fraction collection via the outlet stream and offline analysis to determine the concentration associated with each ester present in each intermediate sub-plateau. The equilibrium binding capacity is estimated for each ester present in the mixture from retention time and the breakthrough front, also from the breakthrough curves constructed through fraction collection. Possibility for separation of the aforementioned flavor-active esters, is investigated on columns packed with Amberlite XAD16N and Sepabeads SP20SS resins, which showed high selectivity towards esters in our previous studies [8, 17]. Additionally, breakthrough behavior is simulated and predicted in Aspen Adsorption V8.8, considering the equilibrium dispersive chromatographic model, for separation of the esters under the conditions tested at lab-scale and the results of the simulations are compared with experimental validation tests. The Influence of the flowrate and column length is investigated on shape and breakthrough retention time for adsorption on both resins for adsorption of ethyl acetate and the observed breakthrough behavior is explained based on properties for each tested adsorbent. The required parameters for simulation, i.e. single and multi-compound adsorption parameters for adsorption of esters based on the Langmuir isotherm model and heat of adsorption of the individual components, obtained through single-component isotherm studies at different temperatures and Van't Hoff relation, are acquired from previous work [8, 17], and used as input for simulation. Based on the lab-scale tests, a similar condition is simulated for a larger scale fixed-bed column for cyclic operation and separation of flavor-active esters. Two different scenarios are simulated, for separation of ethyl acetate as the major ester present in beer and separation of all of the flavor-active esters from feed stream. For the simulated scenarios, percentage of recovery for each tested ester and the productivity, the amount of feed processed during each batch cycle time, are calculated.

6.2 Materials and methods

6.2.1 Materials

6.2.1.1 Chemicals

Ethyl acetate (purity ≥ 99.5%), isopentyl acetate (98%), ethyl hexanoate, and ethyl-4-methylpentanoate are purchased from Sigma-Aldrich. MilliQ water is used for dilutions and ethanol 96%, is purchased from Merck. The tested flavor-active esters with their main physical properties are presented in **Table 6.1**.

Table 6.1.Physical properties of tested flavor-active esters [5, 18]

Component	Molecular structure	Molar mass ($g.mol^{-1}$)	Log P	Solubility ($mol.L^{-1}$)	Solvent accessible surface area ($Å)^2$	Flavor description
Ethyl acetate		88.106	0.28	0.03	287.33	Solvent-like, nail polish
Isopentyl acetate	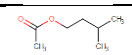	130.187	1.53	-1.41	375.79	Banana, Pear drop
Ethyl 4-methylpentanoate	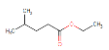	144.214	2.16	-1.92	412.57	apple
Ethyl hexanoate	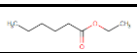	144.214	2.31	-1.99	438.56	apple

6.2.1.2 Adsorbents

Food grade resin XAD16N from Amberlite resin series and the aromatic type Sepabeads SP20SS from HP resin series are purchased from Sigma-Aldrich and used for adsorption tests. Detailed specifications and physical properties of the tested resins are reported in **Table 6.2**.

Table 6.2. Physical properties of the tested adsorbents [19]

Resin	Matrix	Particle size (µm)	Pore volume (ml/g)	Mean pore size (Å)	Surface area (m^2/g)	Dry density (vs. wet) (g/ml)
Sepabeads SP20SS	Styrene-divinylbenzene	50-100	1.01	260	500	(1.3)
Amberlite XAD16N	Styrene-divinylbenzene	560-710	0.55	200	800	1.08 (1.02)

6.2.2. Methods

6.2.2.1 Chromatographic model

6.2.2.1.1 Equilibrium dispersive model (EDM)

Equilibrium theory has proven to be capable in predicting overloaded elution, however, it works under assumption that the column possesses infinite number of plates which is not realistic [20]. In order to take into account the additional kinetic effects, the equilibrium dispersive model, proved to be successful in considering contributions leading to band broadening effects, such as axial dispersion and rate of mass transfer, which are lumped into an apparent term of dispersion coefficient D_{app}, therefore it relates the apparent axial dispersion and column HETP and is valid when the column efficiency is high for separation of small molecules with moderate polarity [21].

This model which is proposed by Lapidus and Amundson [22], consists of a set of two partial differential equations. The first equation related to mass balance can be written as equation (6.1) [11, 12, 22-26].

$$\frac{\partial C_i}{\partial t} + F\frac{\partial q_i}{\partial t} + \frac{\partial (u\, C_i)}{\partial z} = \widetilde{D}_{app,i}\frac{\partial^2 C_i}{\partial z^2} \tag{6.1}$$

Where C is the equilibrium concentration of analyte in bulk liquid (Kmol/m^3), t represents the time (s) and z the direction along column length (m), u is the linear velocity of mobile phase (m/s), F is the phase ratio ($F=V_s/V_m= (1-\varepsilon_T)/\varepsilon_T$), and ε_T is the total porosity of the resin material. Parameter $\widetilde{D}_{app,i}$ expresses the apparent dispersion coefficient including also the volume fractions and has relation with $D_{app,i}$ as is shown in equation (6.2) [26].

$$\widetilde{D}_{app,i} = \frac{u}{u_{int}} D_{app,i} \tag{6.2}$$

For equilibrium dispersive model, equation (6.3) represents the relation between apparent dispersion coefficient (D_{app}), axial dispersion coefficient (D_{ax}) and effective mass transfer coefficient (k_{eff}) [26].

$$D_{app} = D_{ax} + \left(\frac{\tilde{k}'}{1+\tilde{k}'}\right)^2 \frac{\varepsilon}{1-\varepsilon}\frac{r_p}{3}\frac{{u_{int}}^2}{k_{eff}} \tag{6.3}$$

Parameter D_{ax}, expresses the axial dispersion which sums the contribution of axial molecular diffusion and eddy diffusion [20, 27]. $\tilde{k}'$ is the modified retention factor, which has relation with the retention factor of the component of interest between the mobile and stationary phase (k') according to equation (6.4) [26]. The retention factor of the component of interest (k'), can be calculated from the difference between retention time of component i ($t_{R,i}$) and the dead time of the column for total liquid holdup (t_0), divided by t_0 [26]. ε is the void fraction, r_p is the particle radius, u_{int} is the interstitial velocity and k_{eff} is the effective mass transfer coefficient, which can be estimated from film mass transfer coefficient and pore diffusion [26].

$$\tilde{k}' = \frac{\varepsilon_T}{\varepsilon}(1 + k') - 1 \tag{6.4}$$

The second equation for equilibrium dispersive model, relates the two concentrations in equation (6.1), based on a linear kinetic model, presented as equation (6.5) [12, 25].

$$\frac{\partial q_i}{\partial t} = k_{ov}(q_i^* - q_i) \tag{6.5}$$

Where k_{ov}, is the overall mass transfer coefficient, and q_i^* is the concentration of the compound in the stationary phase, which is at equilibrium with the mobile phase.

By knowing the adsorption isotherms, elution profiles and breakthrough curves can be predicted. The extension of the Langmuir model, which describes the competition of component i with nc components in the mixture, is used, which is capable of offering best analytical solutions, considering appropriate transformations, explained as equation (6.6) [12, 17, 28-32].

$$q_i = \frac{q_{max}\, k_{ads,i} C_i}{1 + \sum_{j=1}^{nc} k_{ads,j}\, C_j} \tag{6.6}$$

Where C_i represents the concentration in the bulk liquid of species i at equilibrium condition (Kmol/m^3), q_i is the load of species i (concentration of adsorbate on solid) (Kmol/Kg_{resin}), q_{max} represents the maximum load (Kmol/Kg_{resin}), and $k_{ads,i}$ is the Langmuir constant (m^3/Kmol).

Column is simulated, considering two different constant states [20]. As initial condition:

$$c_i(t=0,x) = c_i^{Init}; i = 1, \dots, N \tag{6.7}$$

In addition, boundary condition:

$$c_i(t, x=0) = c_i^{Feed} \tag{6.8}$$

The contribution of axial dispersion and rates of mass transfer, which are described by the terms D_{ax} (m^2/s) and mass transfer coefficients k_{ov} (m^2/s) in the equilibrium dispersive model, can be estimated theoretically based on theoretical relations proposed in the literature, explained in the sections related to estimation of model parameters.

6.2.2.1.2 Non-isothermal adsorption system

In order to consider the heat of adsorption and deviation of the system from isothermal behavior, two differential energy balance equations are considered to complete the set of partial differential equations [12, 33], for the mobile and stationary phases. For the non-isothermal system, the differential energy balance for mobile phase can be written as equation (6.9).

$$-\lambda_L\, \varepsilon \frac{\partial^2 T_m}{\partial z^2} + C_{p,m}\, \rho_m u \frac{\partial T_m}{\partial z} + \varepsilon\, C_{p,m}\, \rho_m \frac{\partial T_m}{\partial t} + +S_v(1-\varepsilon) HTC(T_m - T_s) + \frac{4h_w}{d_c}(T_m - T_w) = 0 \tag{6.9}$$

Moreover, energy balance for stationary phase can be presented as:

$$-\lambda_s \frac{\partial^2 T_s}{\partial z^2} + \rho_p C_{p,s} \frac{\partial T_s}{\partial t} + \rho_p \frac{\partial T_s}{\partial t} \sum_{i=1}^{nc}(C_{p,m}\, q_i) + \rho_p \sum_{i=1}^{nc}(\Delta H_i \frac{\partial q_i}{\partial t}) - S_v\, HTC(T_m - T_s) = 0 \tag{6.10}$$

Where T_m, T_s, and T_w are the absolute temperatures of the mobile phase, the stationary phase, and the column wall, respectively. $C_{p,m}$, and $C_{p,s}$ are the heat capacities of the mobile and stationary phases. λ_L is the thermal conductivity of the mobile phase and λ_s is the thermal conductivity of the stationary phase. ΔH_i represents the heat of adsorption, h_w the heat transfer coefficient between fluid and column wall, *HTC* the overall heat transfer coefficient between stationary and mobile phases, d_c the column inner diameter, ρ_p is the density of the adsorbent material, and ρ_L the density of the mobile fluid. Here the system is considered as adiabatic with fluid and solid phase conduction.

6.2.2.2 Estimation of model parameters

6.2.2.2.1 Axial Dispersion coefficient

Axial Dispersion (D_{ax}) is considered in the material balance, which is estimated based on a dimensionless equation, proposed by Chung and Wen (1968) and Wen and Fan (1975). This equation shows dependency of the dispersion coefficient on the particle Reynolds number as presented in equation (6.11) [26].

$$D_{ax} = \frac{u_{int} d_p \varepsilon}{0.2+0.011(\varepsilon\, Re)^{0.48}} \qquad (10^{-3} \leq Re \leq 10^{3}) \tag{6.11}$$

Where ($u_{int}\, d_p/D_{ax}$) is known as the Peclet (Pe) number, and Re= ($u_{int}\, d_p/\, \nu$). d_p represents the adsorbent particle diameter (m), ν is the kinematic viscosity (m^2/s), and u_{int} is the interstitial velocity (m/s) which can be calculated based on equation (6.12).

$$u_{int} = \frac{Q_f}{\varepsilon\pi\frac{{d_c}^2}{4}} \tag{6.12}$$

Where Q_f is the volumetric flow-rate (m^3/s) and ε is the column void fraction (-). The column void fraction can be estimated from equation (6.13).

$$\varepsilon = \frac{V_{int}}{V_c} \tag{6.13}$$

Where interstitial volume (V_{int}) (ml) , can be estimated from subtracting the volume of adsorbent from column volume [26].

6.2.2.2.2 Pressure drop

A linear relation is normally considered between flow-rate and pressure drop explained based on Darcy's law, for (Re < 10) and steady state condition [4, 34] as is explained in equation (6.14).

$$Q_f = \frac{KA}{\mu L}\, \Delta P \tag{6.14}$$

Where A, is the cross sectional area normal to the flow direction, ΔP is the pressure drop across the bed, μ the fluid viscosity, L the length of the bed, and K is the permeability of the medium. Assuming that the granular bed is analogues to a group of capillaries, parallel

to the direction of flow, the permeability term can be written as presented in equation (6.15).

$$K = \frac{{\varepsilon_p}^3}{2\,{\tau_p}^2 S_v^2 (1-\varepsilon_p)^2} \tag{6.15}$$

Where ε_p is the average bulk porosity of the packed bed, S_v is the surface-face-to-volume ratio of the packing material and τ_p is the tortuosity of the bed. The value of τ_p is defined as the ratio of the actual tortuous length traveled by the fluid in the bed to the geometrical length of the bed. If the packing material is formed by mono-sized spheres, the term S_v can be simplified to $S_v=6/d_p$ and $\tau_p=1.58$; equation (6.14) can then be reduced to the Kozeny-Carman relation as expressed in equation (6.16) [13, 34-36].

$$K = \frac{{\varepsilon_p}^3 d_p^2}{180\,(1-\varepsilon_p)^2} \tag{6.16}$$

Where d_p is the diameter of the packing sphere and 180 is the Kozeny-Carman pre-factor [35]. If the packing material is non-spherical and shows a distribution in size, it should be taken into account and $d_p = \Phi\, d_{32}$, where Φ is the sphericity of the adsorbent material and d_{32} is the sauter mean diameter of the distribution. In case of having spherical packing material, the value of Φ will be equal to one. The Kozeny-Carman relation gives promising estimations for pressure drop along the column when the range of ε is between 0.36 to 0.92 [37], however if the void fraction is lower than the theoretical 0.36, this relation might estimate the pressure drop with error [38].

6.2.2.2.3 Overall mass transfer coefficient

The overall mass transfer coefficient is estimated based on equation (6.17), which can be described as [33, 36]:

$$k_{ov} = \left[\frac{d_p}{6k_f} + \frac{d_p^2}{60\varepsilon_p D_{eff}}\right]^{-1} \tag{6.17}$$

Where D_{eff} is the effective diffusivity, ε_p is the intraparticle porosity, which can be calculated by dividing the pore volume by volume of the adsorbent [26]. The external mass transfer coefficient k_f is estimated based on Wilson and Geankoplis correlation, as is described in equations (6.18) and (6.19) [39, 40].

$$Sh = \frac{1.09}{\varepsilon} Re^{1/3} Sc^{1/3} ; \qquad 0.0015 < Re < 55 \tag{6.18}$$

$$Sh = \frac{d_p k_f}{D_{AB}} ; \qquad Re = \frac{u_{int}\, d_p}{\nu} ; \quad Sc = \frac{\nu}{D_{AB}} \tag{6.19}$$

The free molecular diffusivity of moderate molecular weight compound, (D_{AB}) (molecular weight between 100 and 500) can be estimated as proposed by Wilke and Chang, described in equation (6.20) [12, 39, 41]. This relation is the most popular relation for the molecular diffusivities of low molecular weight compounds in conventional solvents.

$$D_{A,B} = 7.4 \times 10^{-8} \frac{\sqrt{\psi_B M_B}}{\eta_B V_A^{0.6}} T \tag{6.20}$$

Where V_A is the molar volume (cm^3/mol) of the liquid solute at its normal boiling point, M_B is the molecular weight of solvent (g), η_B its viscosity in (cP), and ψ_B is a constant, which counts for solute-solvent interactions. The value of ψ_B for all non- associated solvents is equal to 1 and recommended as 2.6 for water [12, 41]. The value for molar volume is estimated based on molecular radius (r_m) as described by equation (6.21) [42].

$$V = 4\pi r_m^3 N/3 \tag{6.21}$$

Where N is the Avogadro's constant. The value for molar radius is calculated based on solvent accessible surface area (SASA) [18], which considering a spherical surface area, it is then possible to calculate the molar radius from equation (6.22) [42].

$$r_m = \sqrt{\frac{SASA}{4\pi}} \tag{6.22}$$

The effective diffusivity considers corrections in free molecular diffusivity D_{AB}, by taking into account the effect of diffusional hindrance factor ψ_p, the intraparticle porosity (ε_p) and the tortuosity factor τ_p [43]. The tortuosity is essentially a geometric factor that is independent of either temperature or nature of the diffusing species, and for randomly oriented cylindrical pores, the value of τ_p may be considered equal to 3 [33]. The relation for effective diffusivity can be presented as shown in equation (6.23) [27, 44].

$$D_{eff} = \frac{\varepsilon_p D_{AB}}{\tau_p}\, \psi_p \tag{6.23}$$

In order to estimate the diffusional hindrance factor ψ_p, the ratio between the radius of the molecule (r_m) and radius of the adsorbent pore (r_{pore}), which is explained by λ_m needs to be determined, as can be described by equation (6.24).

$$\lambda_m = \frac{r_m}{r_{pore}} \tag{6.24}$$

For $\lambda_m < 2$ the diffusional hindrance factor can be calculated using equation (6.25) [43].

$$\psi_p = 1 + \frac{9}{8}\lambda_m \ln(\lambda_m) - 1.539\lambda_m \tag{6.25}$$

With the estimation of diffusivities and the overall mass transfer coefficients, the required parameters will be obtained for simulating the condition in Aspen Adsorption.

6.2.2.3 Simulation in Aspen Adsorption

Aspen Adsorption V8.8 is used as a simulation environment to design liquid adsorption step for flavor-active esters, knowing the thermodynamic parameters and physical properties of the tested components and the adsorbent materials. The information related to configuration of the adsorbent bed and the equations for each layer of adsorbent are adjusted in the configuration form, including discretization method for solving partial differential equations, material and momentum balance, selection of the kinetic and isotherm model, and energy balance equations [45, 46]. Mixed Differencing Scheme (MDS) with 29 nodes is used as the discretization method, among several options available for solving the partial differential equations, such as Upwind and Quadratic central differencing, which has the advantage of having precision and more stability in comparison to these methods and the required simulation time is less in comparison [45, 46]. As the assumption for material balance, convection with estimated dispersion is considered for the simulation and the dispersion coefficient is estimated as explained in section 6.2.2.2.1. Varying velocity is assumed inside the column and pressure drop is estimated based on Kozeny-Carman relation, discussed in detail in section 6.2.2.2.2. For the kinetic model assumption, linear lumped resistance is considered for the simulation and the driving force for mass transfer is assumed as a linear function of solid loading. As the isotherm model, multi-component Langmuir model, presented in equation (6.6), is considered to express the thermodynamic behavior for adsorption of flavor-active esters and the Langmuir parameters are obtained from batch uptake experimentation, based on previous work [8]. Energy balance is assumed as non-isothermal with conduction in fluid and solid phase. Heat of adsorption for each tested ester, acquired from our previous study [8] is used for the simulation of non-isothermal condition. Heat transfer to the environment is considered as adiabatic with no heat transfer between

adsorbent bed and the column wall and the last term in equation (6.9) is neglected. Cyclic operation is simulated with step control, using cycle organizer. Time driven steps are simulated for adsorption, elution, washing, and cooling steps and required cyclic operation time for each batch cycle is obtained for the two different simulated scenarios.

6.2.2.4 Competitive frontal analysis

Various chromatographic methods are available for determination of adsorption isotherms, and equilibrium concentrations among which Frontal Analysis (FA) is widely applied in liquid chromatography [11, 13, 20, 47, 48]. This method consists of step-wise replacement of the stream of the mobile phase percolating through the column with streams of solutions in the mobile phase, including the compound of interest with increasing concentration and recording the breakthrough curve at the column outlet [13]. From the recorded breakthrough curves, the concentration of the compound of interest in the stationary phase can be determined, which is the q in equilibrium with the initial feed concentration (C_0). This concept has application in determination of single-solute isotherms, through concentration dependency of the retention times in breakthrough fronts, however for determination of competitive multi-compound isotherms, the composition of the intermediate plateaus needs to be measured [20]. A sample breakthrough front for a multi-compound mixture, consisting of three components is illustrated in **Figure 6.1**.

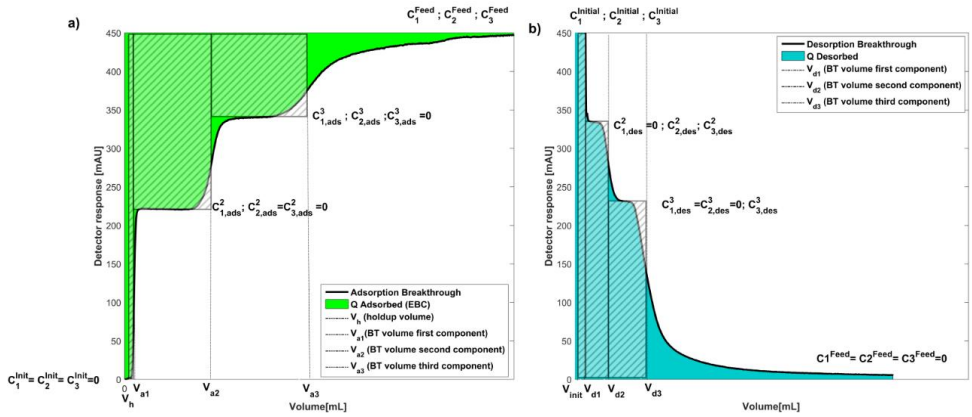

Figure 6.1. Stepwise breakthrough fronts for adsorption and desorption of a ternary mixture; a) Adsorption breakthrough front b) Desorption breakthrough front

In the left figure, breakthrough front for adsorption is depicted with three sub-plateaus corresponding to first, second, and third components. In the first breakthrough curve, the least binding compound will be detected with the breakthrough (BT) volume of V_{a1} (ml). The second component with stronger hydrophobicity will be detected in the second sub-plateau, followed by the third compound with the highest hydrophobicity, which will be present in the third breakthrough front, until the concentration in the outlet reaches the feed concentration. The adsorbed amount for each component can be calculated based on equations (6.26) to (6.28) for the first, second, and the third compound [47, 49, 50].

a. For adsorption of the first component

$$q_{1,ads} = \frac{(V_{a3}-V_h)C_1^{Feed}-(V_{a3}-V_{a2})C_{1.ads}^{3}-(V_{a2}-V_{a1})C_{1,ads}^{2}}{m_{resin}} \quad (6.26)$$

b. For adsorption of the second component

$$q_{2,ads} = \frac{(V_{a3}-V_h)C_2^{Feed}-(V_{a3}-V_{a2})C_{2,ads}^{3}}{m_{resin}} \quad (6.27)$$

c. For adsorption of the third component

$$q_{3,ads} = \frac{(V_{a3}-V_h)C_3^{Feed}}{m_{resin}} \quad (6.28)$$

Where V_{a1}, V_{a2}, and V_{a3} (ml) are breakthrough volumes for adsorption of the first, second, and the third components respectively. $C_{1,ads}{}^{3}$ and $C_{2,ads}{}^{3}$ (mg/ml) are the concentrations corresponding to the first and second components in the second plateau and $C_{1,ads}{}^{2}$ is the concentration of the first component in the first breakthrough front. m_{resin} is the mass of the packed column (g), and $q_{1,ads}$, $q_{2,ads}$, and $q_{3,ads}$ are equilibrium binding capacities for the first, second, and the third component (mg/g $_{resin}$). The same can be applied in order to estimate the amount desorbed from the column, considering the initial start volume for desorption as (V_{init}). The mass of each component desorbed from the resin can be estimated according to equations (6.29) to (6.31), assuming symmetrical frontal sub-plateaus as is depicted in **Figure 6.1**, ***part b***, from desorption breakthrough frontal curve.

d. For desorption of the first component

$$q_{1,des} = \frac{(V_{d1}-V_{init})C_1^{init}}{m_{resin}} \quad (6.29)$$

e. For desorption of the second component

$$q_{2,des} = \frac{(V_{d1}-V_{init})C_2^{init}+(V_{d2}-V_{d1})C_{2,des}^2}{m_{resin}} \quad (6.30)$$

f. For desorption of the third component

$$q_{3,des} = \frac{(V_{d1}-V_{init})C_3^{init}+(V_{d2}-V_{d1})C_{3,des}^2+(V_{d3}-V_{d2})C_{3,des}^3}{m_{resin}} \quad (6.31)$$

Where V_{d1}, V_{d2}, and V_{d3} (ml) are breakthrough volumes for desorption of the first, second, and the third components respectively. $C_{3,des}^2$ and $C_{2,des}^2$ (mg/ml) are the concentrations corresponding to the third and second components in the second plateau and $C_{3,des}^3$ is the concentration of the third component in the last sub-plateau of the breakthrough front. $q_{1,des}$, $q_{2,des}$, and $q_{3,des}$ are masses for the first, second, and the third component (mg/g $_{resin}$) eluted from the column.

This method can be applied for calculation of the binding capacity for a multi-compound mixture and determination of adsorption isotherms, when clear breakthrough fronts can be detected for each component in the mixture. However, in case of having compounds present in the mixture with the same physical properties and retention times, it might occur that one sub-plateau in the breakthrough front corresponds to more than one component in the mixture, therefore, this method will not be able to estimate the maximum capacity with high accuracy.

In this condition, various samples can be collected at different time steps through column outlet and fraction collection and the composition and concentration related to each component can be measured in the mixture through offline analysis. Through these measurements, the change in concentration profile of each compound during the breakthrough time can be measured and breakthrough curves can be constructed during the sampling time and at the tested column volume. The concentration of the compound of interest in the stationary phase q, can then be determined through integration of the constructed breakthrough curves, which is known as the Equilibrium Binding Capacity (q_{EBC}) (mg), and can be obtained by integrating the area above the breakthrough curves, considering the dead volume for the system [17, 48, 51], according to equation (6.32).

$$q_{EBC,i} = \int_0^{V_c}(C_{0,i} - C_{out,i})dV_c \qquad \text{i=1,…, N} \quad (6.32)$$

Where C_0 is the effluent concentration (mg/ml), and C_{out} is the concentration in the outlet stream (mg/ml), V_c is the column volume (ml). The equilibrium binding capacity for each

component can then be calculated from equation (6.33), through estimated q_{EBC} for each component in the mixture.

$$q_{e,i} = \frac{q_{EBC,i}}{m_{resin}} \tag{6.33}$$

With the use of the discussed approaches, the possibility for separation of four major flavor-active esters in beer, which are hydrophobic and have similar molecular structure, is tested in a packed column and the application of competitive frontal analysis is evaluated for isotherm determination and calculation of equilibrium concentrations and binding capacity. Since the molecular structure and physical properties of the two tested esters with the highest hydrophobicity is similar, they are detected in one sub-plateau and this method could not be successfully applied for isotherm determination and for more accurate measurement of the composition corresponding to each ester, fractions are collected and analyzed through offline analysis to construct the breakthrough curves. The influence of various ethanol concentrations and temperatures is investigated on breakthrough fronts, the constructed breakthrough curves through fraction collection, and subsequently the estimated binding capacity and for the prediction of breakthrough behavior, the adsorption parameters acquired from our previous studies [8] on batch uptake experimentation are used as input parameters for the simulation. The obtained breakthrough fronts and the constructed breakthrough curves derived from fraction collection, are used to validate the results of simulation.

6.2.2.5 Error estimation

The error between the predicted values of C/C_0 obtained from simulation and the experimental breakthrough curves constructed through fraction collection and offline analysis, are estimated with Marquardt's percent standard deviation (MPSD), as presented in equation (6.34) [52].

$$MPSD = 100\sqrt{\frac{1}{N-P}\sum_{i=1}^{n}\left[\frac{(C/C_0)_{exp}-(C/C_0)_{theo}}{(C/C_0)_{exp}}\right]_i^2} \tag{6.34}$$

Where N is the number of data points and P is the degrees of freedom. Also the percent deviation between the experimental and the breakthrough times derived from the simulation are calculated according to equation (6.35) [53].

$$E(t_b)\% = 100\left(\frac{t_{b,exp} - t_{b,cal}}{t_{b,exp}}\right) \quad (6.35)$$

6.3. Experimental

6.3.1 Chromatographic system

Frontal analysis is applied to obtain the breakthrough fronts and curves for determination of equilibrium concentrations. Experiments are carried out for single-solute mixture of 0.9 g/L of ethyl acetate prepared in 0.1% (v/v) co-solvent mixture of ethanol/water. The same background solution is used for elution steps. Tests are performed using columns packed with hydrophobic resins, Sepabeads SP20SS and Amberlite XAD16N, which showed high affinity towards esters in our previous studies [8, 17]. Resins are packed in an Omnifit glass chromatography column, *ID 15 mm*, *column length 150mm* (Thermofischer Scientific), suitable for experimental tests up to 40 bar. The experimental breakthrough data are processed using the UNICORN 5.1.1 data acquisition software. Multi-component breakthrough analysis is performed for a multi-component mixture of four major esters in beer (i.e. ethyl acetate, isopentyl acetate, ethyl 4-methylpentanoate and ethyl hexanoate), approximately 0.45 g/L of each component prepared in different concentrations of ethanol/water co-solvent mixture (i.e. 1 and 30% v/v) and at three different temperatures (i.e. 293.15, 313.15, and 333.15 K). Fractions are collected in Eppendorf conical tubes 15ml (purchased from Eppendorf Netherlands B.V.), using fraction collector FRAC 920, and column tests are performed on Äkta Explorer system 100, both purchased from General Electric Life Sciences, Uppsala, Sweden.

6.3.2 Setup

The Äkta explorer 100, FPLC chromatography system, is used for the breakthrough analysis tests. Samples are pumped through Äkta explorer pump P-900 (General electric Life Sciences, Uppsala, Sweden) to the system through an eight-port column selection valve [54]. The effluent from the analytical column, was monitored by a UV 900 detector (General electric Life Sciences, Uppsala, Sweden). For the tests performed at elevated temperatures, the column is heated using a heated tubing around the column, pumping water through a Lauda heating circulator circulating water bath MT/M3 (purchased from Lauda-Brinkmann, USA). The schematic view of the experimental setup is shown in **Figure 6.2.**

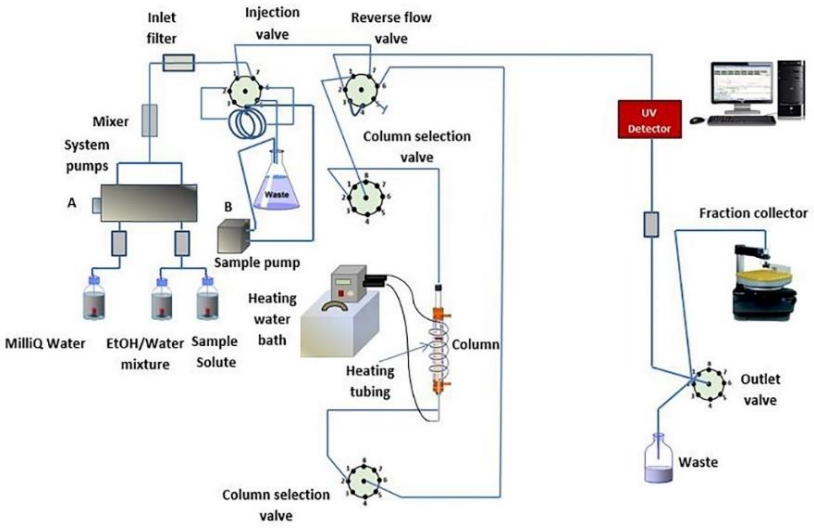

Figure 6.2. Schematic view of the experimental setup [54]

6.3.3 Procedures

Single-component tests are performed for ethyl acetate solution and breakthrough curves are obtained for various tested flow-rates, and column lengths, mentioned in the previous section, both for a column packed with Sepabeads SP20SS resin and Amberlite XAD16N. The shape of the breakthrough curves obtained on both resins and the retention times are compared for adsorption of this ester on both resins and the breakthrough curves are simulated under the same condition in Aspen Adsorption as explained in section 6.2.2.2, and compared with the experimental breakthrough curves. Next, the possibility of separation for the four major mentioned flavor-active esters is investigated in a multi-compound mixture at various ethanol concentrations and temperatures, explained in section 6.4.1. The column is preheated when tested at elevated temperatures. Stepwise breakthrough fronts are obtained for both adsorption and elution at various tested ethanol concentrations and temperatures. Elution is performed with the same background co-solvent mixture of ethanol/water used for preparation of the initial sample solution. To construct the breakthrough curves for each component present in the mixture, and measure the intermediate concentrations in the sub-plateaus, 5ml fractions are collected in 15 ml Eppendorf tubes from the outlet stream with the time interval of

2.5 minutes. Tubes are immediately closed after fraction collection and 5 ml of each selected fraction is added to 10 ml headspace vials and transferred to the GC for measurement. The collected fractions added to vials are subsequently analyzed using Static-Headspace-Gas-Chromatography (HS-GC) method with the GC (Trace 1300, Thermofischer Scientific, Switzerland) coupled with Triplus RSH Autosampler (Thermofischer Scientific, Switzerland) and FID in a RESTEK Rxi 624Sil MS column ($20mm \times 0.18mmID \times 1\mu m\ df$). Helium was selected as the carrier gas in the system. The agitator temperature was set to 40°C and samples are measured with incubation time of 20 minutes. Syringe temperature was set to 60 °C and detector temperature to 250 °C. Split ratio of 30 was used for the measurements. Ramped oven temperature was considered for the GC settings, 60°C with holding time of 1 minute, increase to 75°C with the speed of 10°C/min, and the second increase to 175°C with the speed of 30°C/min with the holding time of 1 minute. The retention time of tested components is measured during 7 minutes. The chromatograms obtained from the measurements show the retention time (minutes) of 1.5, 2.4, 4.9, 5.5, and 5.7 for ethanol, ethyl acetate, isopentyl acetate, ethyl 4-methylpentanoate, and ethyl hexanoate respectively. The breakthrough curves are constructed with the measured concentrations for each ester present in the mixture. The collected fractions and breakthrough curves are compared at various tested ethanol concentrations and temperatures.

6.4. Results and Discussions

6.4.1 Estimated parameters

The required model parameters, explained in section 6.2.2.3, are estimated for each tested condition (i.e. tested resin, flowrate, column length, and initial feed concentration). The main considered physical properties and column conditions are assembled in **Table 6.3**.

Table 6.3. Physical properties of the resins and the column condition considered for the experimental tests and simulation

	Resin	
Physical properties	**Amberlite XAD16N**	**Sepabeads SP20SS**
Resin particle diameter d_p (cm)	0.071	0.010
Resin density $\rho_{dry\ resin}$ (g/ml)	1.01	1.08
Resin density $\rho_{wet\ resin}$ (g/ml)	1.30	1.02
Column length L (cm)	1, 3, 5	1, 3, 5
Column diameter d_c (cm)	1.5	1.5
Feed flowrate Q_f (ml/min)	2, 5, 8	2, 5, 8, 10
Intraparticle porosity ε_p (-)	0.36	0.57
Total porosity ε_T (-)	0.55	0.79
Void fraction ε (-)	0.31	0.51
Adsorption temperature (K)	298.15, 333.15	298.15, 313.15, 333.15
Ethanol concentration %(v/v)	0.1, 1, 30	0.1, 1, 30
Initial feed concentration C_0 (g/L)	0.90, 0.45	0.90, 0.45

In order to simulate the breakthrough behavior, in Aspen Adsorption, the required Langmuir parameters for single and multi-component adsorption, presented in equation (6.6), derived from batch uptake experimentation at various ethanol concentrations and temperatures and the values for heats of adsorption for each tested ester, are obtained from our previous studies, to consider the deviation of the system from isothermal behavior [8]. The values for heats of adsorption for each tested ester, and for adsorption on each tested resin are assembled in **Table 6.4**.

Table 6.4. Heat of adsorption for flavor-active esters

	Heat of adsorption (ΔH) (KJ.mol^{-1})	
	Sepabeads SP20SS	Amberlite XAD16N
Ethyl acetate	-13.64	-12.57
Isopentyl acetate	-25.05	-20.26
Ethyl 4-methylpentanoate	-28.12	-21.07
Ethyl hexanoate	-30.66	-31.13

The value of volumetric heat capacity for the synthetic adsorbents with the structure of Styrene-divinylbenzene $C_{p,s}$ is considered as 1758.4 J/Kg/K [55]. Specific heat of the mixtures tested, considering the small molar fractions of the solutes in comparison to water is estimated as close to $C_{p,m}$ of water, estimated at various tested temperatures (e.g. $C_{p,m}$ at T=298.15 K is estimated as 4179.7 J/Kg/K [56], and thermal conductivity of the mixture is estimated as, 0.61 W/m/K [56]).

6.4.2 Single-component breakthrough simulation

Considering the assumptions, and required model parameters discussed in section 6.4.1, the breakthrough behavior is simulated in Aspen Adsorption for single-component adsorption of ethyl acetate at various flowrates and column lengths, in order to study the accuracy and agreement of the model predictions with the experimental data. For the experimental tests adsorption of ethyl acetate is investigated on a 3 cm column packed with resins, Sepabeads SP20SS, and Amberlite XAD16N and at various flow-rates (i.e. 2, 5, and 8 ml/min), and for a flow-rate of 10 ml/min for various column lengths for Sepabeads SP20SS resin (i.e. 1, 3, and 5 cm) column, and a flow-rate of 2 ml/min for the same column lengths of Amberlite XAD16N.

6.4.2.1 Influence of flow-rate

The results of the simulation are compared with the experimental breakthrough curves, obtained from column breakthrough analysis tests, depicted in **Figure 6.3** for adsorption on Sepabeads SP20SS and Amberlite XAD16N respectively. The breakthrough behavior of ethyl acetate on a column packed with Sepabeads SP20SS resin and Amberlite XAD16N, both for adsorption and elution steps is illustrated in **Figure 6.3.** As can be observed from **Figure 6.3**, one adsorption/elution cycle for Sepabeads SP20SS resin takes approximately half the time in comparison to Amberlite XAD16N (e.g. 150 minutes for flow-rate of 2 ml/min in comparison to approximately 300 minutes on Amberlite XAD16N), and the breakthrough curves observed on Sepabeads SP20SS resin, show steeper slope. The reason for being able to achieve earlier breakthrough time and steeper breakthrough curve for adsorption on Sepabeads SP20SS resin, can be explained by the resin structure. This resin has smaller particle size (50-100µm) in comparison to Amberlite XAD16N (250-710µm), therefore it is possible to pack the Sepabeads SP20SS

resin tighter in the column, which leads to less extra particle space (space between the particles), and less flow-through around the particles, since higher extra-particle space can cause the flow to follow the path with the least resistance [43] , which occurs here for Amberlite XAD16N with larger particle diameter. Moreover, a smaller particle size of Sepabeads SP20SS resin can lead to enhanced mass transfer, due to more effective pore diffusivity [57], which leads to shorter mass transfer zone and a steeper breakthrough curve.

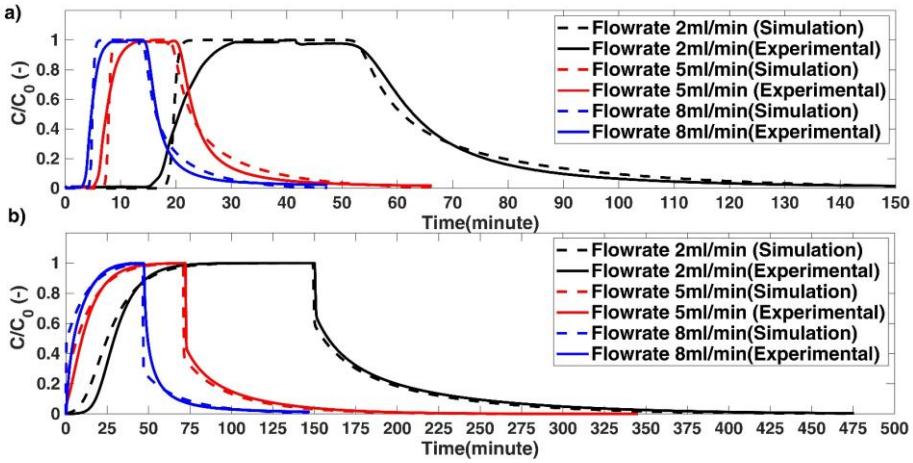

Figure 6.3. Influence of flow-rate on single-component adsorption of ethyl acetate on a 3 cm column; a) Sepabeads SP20SS b)Amberlite XAD16N

In contrast to breakthrough curves obtained for adsorption on Sepabeads SP20SS, the breakthrough curves for Amberlite XAD16N, demonstrate a different behavior, the breakthrough time is earlier and later exhaustion point is achieved on this resin, as the mass transfer zone is longer and more dispersed on this resin. Similar shape of the breakthrough curves obtained for adsorption on Sepabeads SP20SS indicates that even at higher flow-rates the residence time of ethyl acetate in the column was long enough for the mass transfer to occur. Different observed shape for the breakthrough curves for adsorption on XAD16N at higher flowrates in comparison to flowrate of 2ml/min implies that more residence time for enhanced mass transfer characteristics is required for adsorption on this resin.

6.4.2.2 Influence of column length

In order to investigate the influence of column length on breakthrough behavior of ethyl acetate and compare the results with predicted breakthrough curves obtained from simulation, various column lengths (i.e. 1, 3, and 5 cm) are tested for adsorption on Sepabeads SP20SS, with the sample flow-rate of 10 ml/min and for adsorption on Amberlite XAD16N, with the flow-rate of 2 ml/min. The obtained breakthrough curves are compared with Aspen simulations for various bed lengths and for adsorption on the two tested resins, presented in **Figure 6.4.** The breakthrough curves obtained for adsorption of ethyl acetate on Sepabeads SP20SS resin show a proportional increase in the breakthrough time and no change in the shape of the breakthrough curve was observed when the column length was increased. An increase in bed length increases the mass transfer zone; therefore, there will be a longer distance from column entrance to the exit point, which results in an extended breakthrough time. While the breakthrough time increases proportionally for adsorption on Sepabeads SP20SS, for various tested column lengths, different behavior is observed for adsorption on Amberlite XAD16N, **Figure 6.4, *part b*;** where the shape of the breakthrough curve observed as different when the tests are performed at longer column (i.e. 5 cm here).

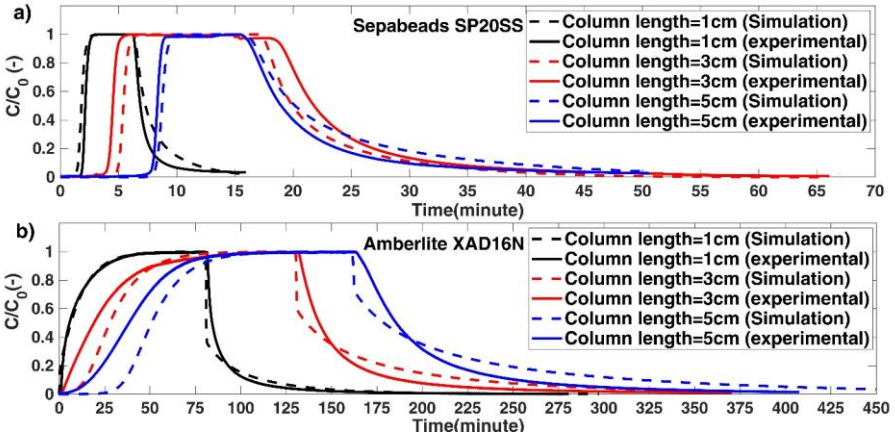

Figure 6.4. Influence of bed length on single-component adsorption of ethyl acetate on a 3 cm column; a) Sepabeads SP20SS (Flow-rate 10 ml/min) b) Amberlite XAD16N (Flow-rate 2 ml/min)

The observed phenomena can be explained by the shorter length of the used column, which has influence on pore diffusion. Due to the short column length used for Amberlite

XAD16N (1cm), pore diffusion is not sufficient which leads to earlier increase of effluent concentration and earlier breakthrough time.

The estimated errors for the breakthrough curves presented in **Figures 6.3** and **6.4** are estimated as explained in section 6.2.2.5**,** assembled in **Table 6.5**.

Table 6.5. Estimated errors for breakthrough times and percent standard deviation between simulated breakthrough curves and experimental frontal curves; Adsorption at 298.15 K and initial solution prepared in 1% v/v Ethanol

	Sepabeads SP20SS			**Amberlite XAD16N**		
	Flowrate (ml/min)			Flowrate (ml/min)		
	2(ml/min)	5(ml/min)	8(ml/min)	2(ml/min)	5(ml/min)	8(ml/min)
$E(t_b)$%	3.85	0.08	0.24	0.11	0	0.035
MPSD	55.69	23.50	90.12	26.48	35.05	33.23
	Column Length (cm)			Column length (cm)		
	1(cm)	3(cm)	5(cm)	1(cm)	3(cm)	5(cm)
$E(t_b)$%	0.23	0.56	0.61	0.02	0.02	0.26
MPSD	1776.38	58.56	73.52	51.84	73.65	114.89

As can be concluded from the presented values in **Table 6.5**, predictions at various flowrates show a more accurate estimation in comparison to different tested column lengths. For the tests performed on the two tested resins, at different flowrates, higher accuracy and lower standard error is calculated for adsorption on XAD16N in comparison to SP20SS. In comparison to the tests performed at various flowrates, the results of the tests at different column lengths show a higher percent standard error, specifically for the tests performed on a 1cm column packed with SP20SS, in which a larger deviation between simulation prediction and the experimental breakthrough front is observed in the elution step. For adsorption/elution on XAD16N, a higher standard deviation was obtained for adsorption on a 5 cm column in comparison to the other two tested lengths. The model predictions can be improved through experimental determination of intraparticle and effective diffusivities, which are calculated here based on the theoretical relations.

6.4.3 Multi-component breakthrough simulation

6.4.3.1 Influence of temperature

In order to investigate the influence of temperature on multi-component adsorption of flavor-active esters, competitive frontal breakthrough analysis is performed to test the multi-component separation of four major aforementioned flavor-active esters in beer. The influence of temperature is investigated both on the obtained breakthrough fronts and on the collected fractions. The comparison of the breakthrough curves with the collected fractions is depicted in **Figure 6.5** for each tested temperature.

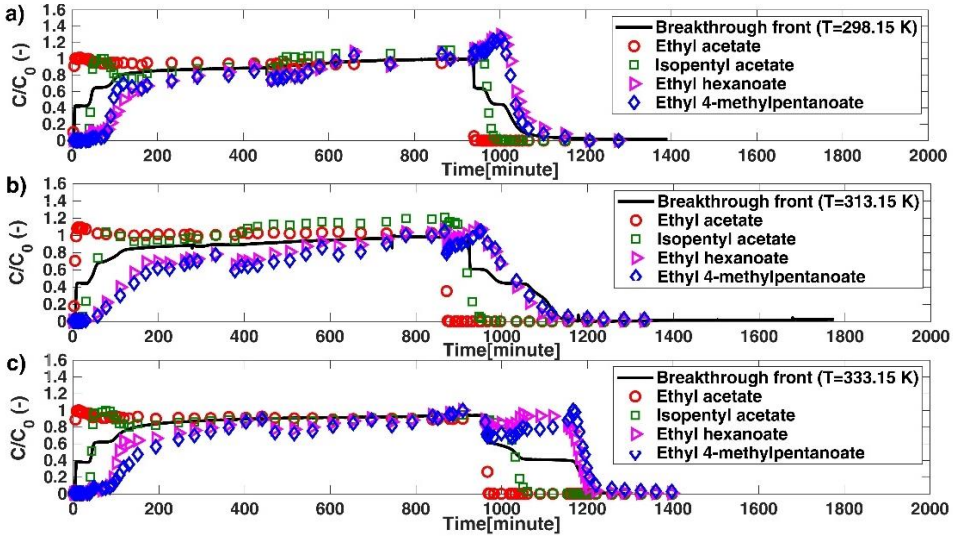

Figure 6.5. Comparison of competitive breakthrough fronts with collected fractions for adsorption/elution of multi-component mixture of esters on a 1cm Sepabeads SP20SS column prepared in 1% v/v ethanol; a) T=298.15 K b) T=313.15 K c) T=333.15 K

The amount of equilibrium binding capacity is estimated for each ester present in the mixture and for the three tested temperatures, according to the procedure explained in section 6.2.2.4 based on competitive frontal analysis and compared with the results obtained from integration of the breakthrough curves derived from fraction collection and offline analysis. The two components with higher hydrophobicity and similar molecular structure (i.e. ethyl 4-methylpentanoate and ethyl hexanoate) have the same physical properties and similar breakthrough time and show a similar breakthrough behavior and

both are detected in the third sub-plateau of the competitive frontal curve, therefore for estimation of equilibrium binding capacity, based on the competitive frontal analysis, both of them are considered as the third component, detected in the third sub-plateau and the corresponding concentrations are measured in each sub-plateau for each component and also from fraction collection and offline analysis. The comparison of equilibrium binding capacity based on competitive frontal analysis and integration of the breakthrough curves constructed through fraction collection and offline analysis are illustrated in **Figure 6.6,** ***part a,*** for adsorption on a 1 cm column packed with Sepabeads SP20SS resin and for the three tested temperatures.

The calculated values for binding capacity for each ester present in the multi-compound mixture reveal that, increase in temperature is not favorable for adsorption of the flavor-active esters since their adsorption is exothermic, which this phenomena was also observed in our previous studies on single and multi-component adsorption, using batch uptake experimentation [8].

It can be clearly observed from **Figure 6.6,** ***part a,*** that the more hydrophobic is the tested ester, the higher will be the value of Q (equilibrium binding capacity), as the component has more affinity for binding to the resin surface. The difference caused in estimations based on competitive frontal analysis and the integration is due to the constructed breakthrough curves, which are obtained from offline analysis and experimental measurements, which has influence on the shape of the breakthrough curves and integrated areas. The same procedure is applied for estimation of the amount eluted for each compound from the column. The results are presented in **Figure 6.6,** ***part b***, where the calculated values based on competitive frontal analysis and integration are compared for each ester present in the mixture.

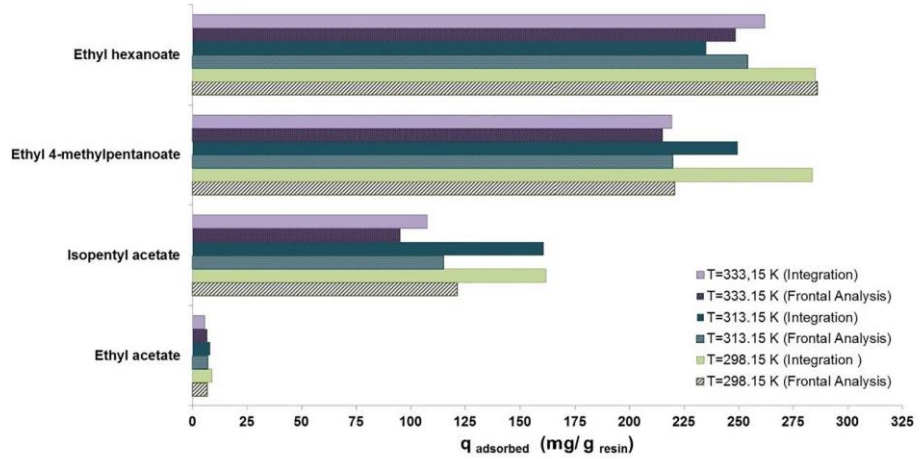

a)

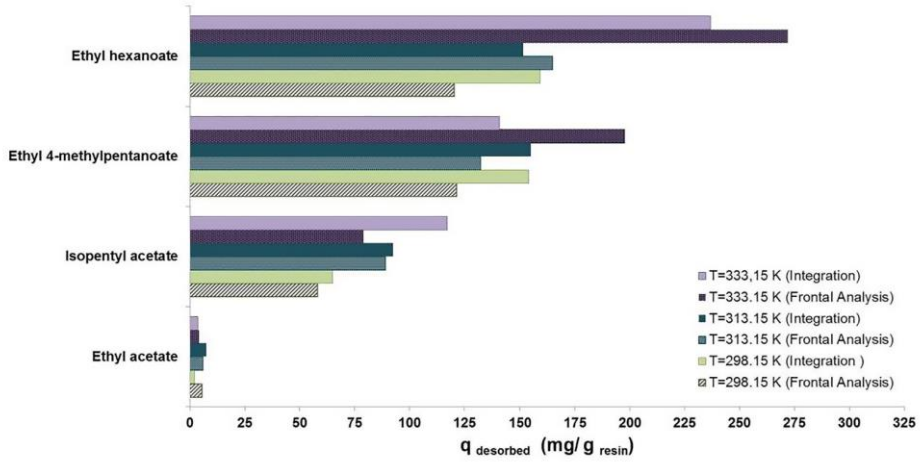

b)

Figure 6.6. Equilibrium binding capacity (adsorption) and mass eluted per gram of the packed resin from the column (elution) estimated at three tested temperatures and for the four esters, 1 cm Sepabeads SP20SS column, initial solution prepared in 1%v/v Ethanol; a) Adsorption b) Elution

Comparing the estimated values for the equilibrium binding capacity and the amount of mass, which is eluted from the resin, at various temperatures, we can conclude that, more compounds are released from the column and eluted at higher tested temperature, as almost between 63-100% of the adsorbed esters are recovered at 333.15 K. It is then followed by 313.15 K, in which 60-90% of the esters are eluted from the column. In comparison, lower recovery (40-80%) was achieved when elution was performed at lower temperature (298.15 K).

6.4.3.2 Influence of ethanol concentration

Influence of ethanol concentration on multi-component adsorption behavior of the major flavor-active esters of interest is investigated at temperature 333.15 K on a 1cm column packed with Sepabeads SP20SS, for initial samples prepared in 1, and 30% v/v co-solvent mixtures of ethanol/water. During the breakthrough analysis time, fractions are collected and analyzed with HS-GC. The comparison of the breakthrough fronts and the collected fractions is presented in **Figure 6.7**.

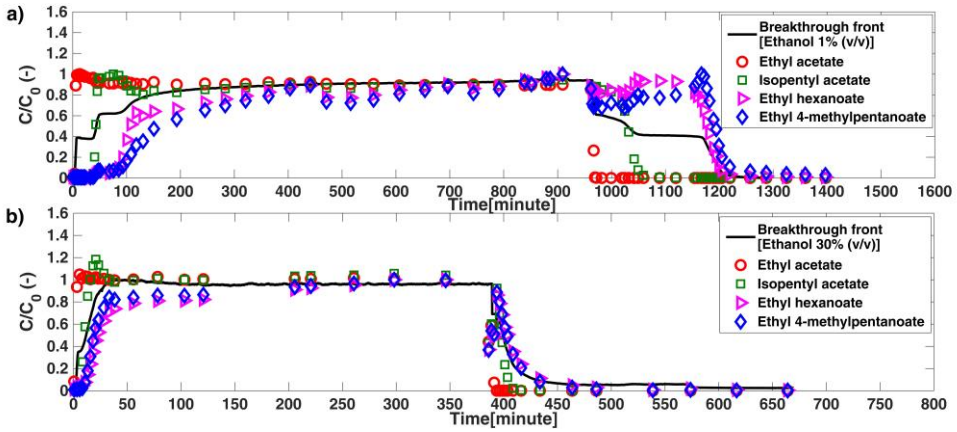

Figure 6.7. Comparison of competitive breakthrough fronts with collected fractions for adsorption/elution of multi-component mixture of esters on a 1cm Sepabeads SP20SS column at 333.15 K; a) Ethanol 1% v/v b) Ethanol 30%v/v

As the competitive breakthrough front illustrates, at higher percentage of ethanol (i.e. 30% v/v), separate sub-plateaus cannot be observed for each ester present in the mixture and the breakthrough time is reduced to a great extent in comparison to the tested case with 1% (v/v) ethanol, therefore it makes it difficult to estimate the equilibrium binding

capacity associated with each ester present in the mixture using the sub-plateaus as separate breakthrough curves are not detected. For this reason the amount of equilibrium binding capacity is estimated based on the breakthrough curves, constructed from fraction collection and off-line analysis and compared with previously estimated equilibrium binding capacity calculated for adsorption/elution at 1%v/v ethanol and T=333.15 K, presented also in **Figures 6.6** The comparison of the estimated equilibrium binding capacities is depicted in **Figure 6.8**.

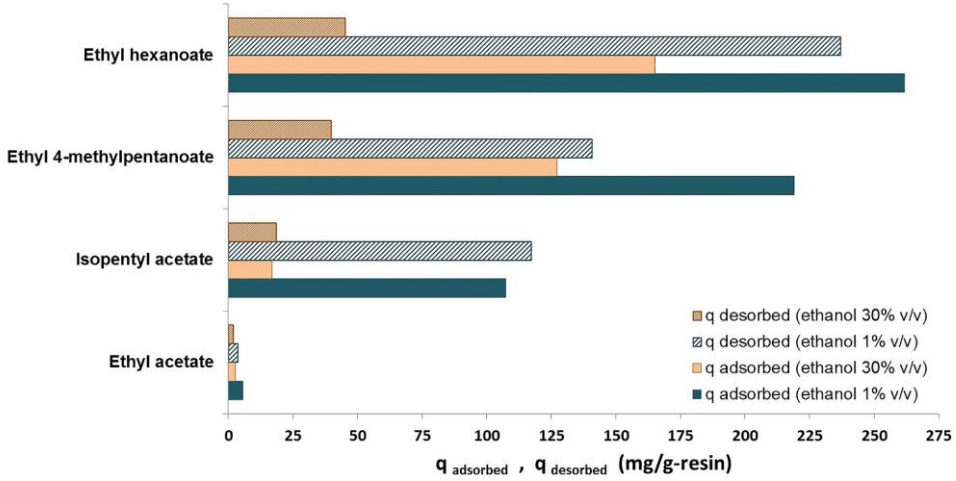

Figure 6.8. Comparison of equilibrium binding capacity and the mass of the esters eluted from the column at two tested ethanol concentrations (1% and 30% v/v); Adsorption on a 1cm Sepabeads SP20SS column at T=333.15 K

It can be concluded from **Figure 6.8** that increase in ethanol concentration from 1 to 30% v/v has influence on equilibrium binding capacity of esters, as lower amount of equilibrium binding capacity is calculated for the condition when the ethanol concentration is 30% v/v in comparison to 1% v/v from integration of the breakthrough curves. Increase in the ethanol concentration in the mixture from 1 to 30% v/v lowers the activity coefficient of esters in the liquid phase, and as esters have less tendency to leave the aqueous phase, lower amount of esters is bound to the resin at higher ethanol concentrations.

6.4.4 Cyclic operation for adsorption/elution in a fixed-bed column

6.4.4.1 Adsorption/elution cycle for each tested resin

Multi-component competitive adsorption/elution behavior of the flavor-active esters, is simulated in Aspen Adsorption and breakthrough curves are obtained for one batch cycle for adsorption on both resins, (i.e. Sepabeads SP20SS and Amberlite XAD16N), for adsorption on a 1cm column, at T=333.15 K and solutions prepared in 30% (v/v) ethanol/water co-solvent mixture. In order to compare the influence of resin structure and properties on shape of the breakthrough curves and on breakthrough cycle time, the simulation results are compared for both resins , also explained by constructed breakthrough curves derived from fraction collection and offline analysis. One batch cycle is simulated through cycle organizer in Aspen Adsorption and the breakthrough time is considered the same as the time obtained from fraction collection and complete breakthrough for all the tested esters in the mixture. The comparison of the breakthrough curves together with the collected fractions is presented in **Figure 6.9,** for adsorption on Sepabeads SP20SS and Amberlite XAD16N respectively.

It can be observed from **Figure 6.9**, that the simulated breakthrough curves are able to predict the experimental breakthrough curves with higher accuracy, for Amberlite XAD16N, and the stepwise breakthrough for ethyl hexanoate and ethyl 4-methylpentanoate and the slight overshoot observed for isopentyl acetate is not well-predicted by simulation for adsorption on Sepabeads SP20SS resin. Longer breakthrough time and mass transfer zone, is achieved for separation on XAD16N in comparison to SP20SS resin, as was also observed previously for single component adsorption of the flavor-active esters, illustrated in **Figures 6.3** and **6.4** due to larger particle size of XAD16N and smaller pore volume of this resin as discussed before.

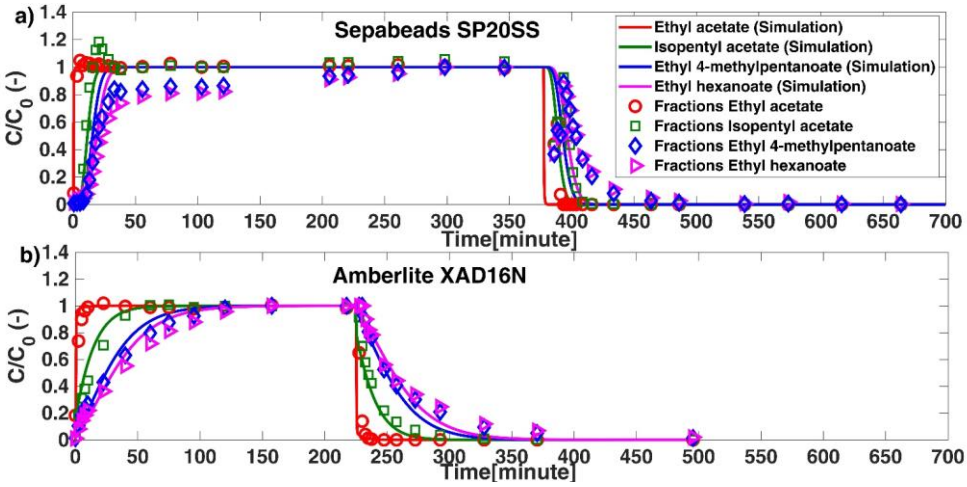

Figure 6.9. Comparison of simulated breakthrough cycle and collected fractions for adsorption of multi-component mixture of esters (prepared in 30% ethanol) on a 1cm column packed with a) Sepabeads SP20SS b)Amberlite XAD16N resin; (Adsorption at T=333.15 K)

The estimated percent standard deviation between the simulated breakthrough curves and the experimental collected fractions, and the deviation between the experimental and simulated breakthrough times are reported in **Table 6.6**.

Table 6.6. Estimated errors for breakthrough times and percent standard deviation between simulated breakthrough curves and experimental breakthrough curves obtained from fraction collection; Adsorption at 333.15 K and 30% v/v Ethanol

	Sepabeads SP20SS		**Amberlite XAD16N**	
	$E(t_b)$%	MPSD	$E(t_b)$%	MPSD
Ethyl acetate	-0.17	308.17	1.22	42.44
Isopentyl acetate		482.08		99.99
Ethyl 4-methylpentanoate		76.78		49.48
Ethyl hexanoate		87.36		48.64

From presented values in **Table 6.6**, it can be concluded that simulated breakthrough curves are able to predict the multi-component separation for XAD16N with higher accuracy in comparison to SP20SS, as lower values for MPSD are estimated for XAD16N.

6.4.4.2 Influence of temperature and ethanol concentration on adsorption/elution cycle on Sepabeads SP20SS

To investigate the influence of temperature and ethanol concentration on one adsorption/elution cycle of flavor-active esters, adsorption/elution breakthrough behavior is simulated for adsorption on 1 cm Sepabeads SP20SS column and for two tested cases a) Solution of esters prepared in 1 % v/v ethanol solution and adsorption at T=298.15 K, and b) Solution of esters prepared in 30 % v/v ethanol solution and adsorption at T=333.15 K. The simulated breakthrough cycles for the two cases are compared in **Figure 6.10**.

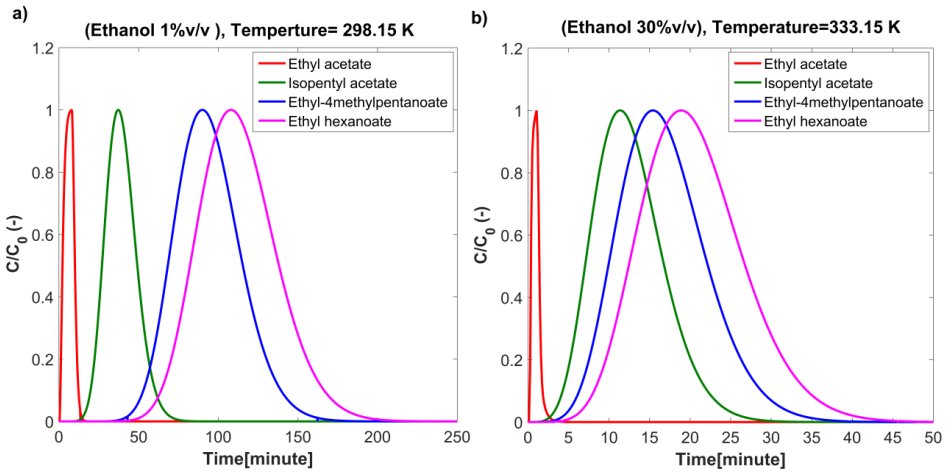

Figure 6.10. Comparison of adsorption/elution cycle for adsorption on a 1cm column packed with Sepabeads SP20SS resin and two cases;
a) Solution of esters prepared in 1% v/v Ethanol and adsorption at T=298.15 K,
b) Solution prepared in 30% v/v Ethanol and adsorption at T=333.15K

It can be detected from **Figure 6.10** that the cycle time reduces almost to one fifth, when adsorption takes place at higher temperature and adsorption/elution is performed with 30 % v/v of ethanol solution. The time for adsorption/elution cycle is also shown in **Figure 6.11,** which presents the axial concentration profiles for the ***case a*** in **Figure 6.10** (Adsorption with 30% v/v Ethanol and at T=333.15 K) as an example. The observed decrease in cycle time can be explained by influence of temperature on adsorption and elution step, which is discussed in detail in previous sections. By increasing the

temperature from 298.15 to 333.15 K, less amount of flavor-active esters will bind to the resin as was also discussed in section 6.4.3.1; due to the exothermic nature of adsorption and weaker Van der Waals forces at higher temperatures.

Also influence of increase in ethanol percentage from 1 to 30 % v/v observed as considerable on binding capacity of esters as discussed in section 6.4.3.2, and performing the experiment at both high concentration of ethanol and at high temperature, leads to less binding of ester components and enhanced elution characteristics. The reduction in adsorption/elution cycle time is observable mainly for ethyl acetate, for which breakthrough achieves the feed concentration the fastest (i.e. within 3 minutes). The cycle time for the other three esters with higher hydrophobicity takes approximately within 30 to 45 minutes, as is presented **in Figure 6.11**.

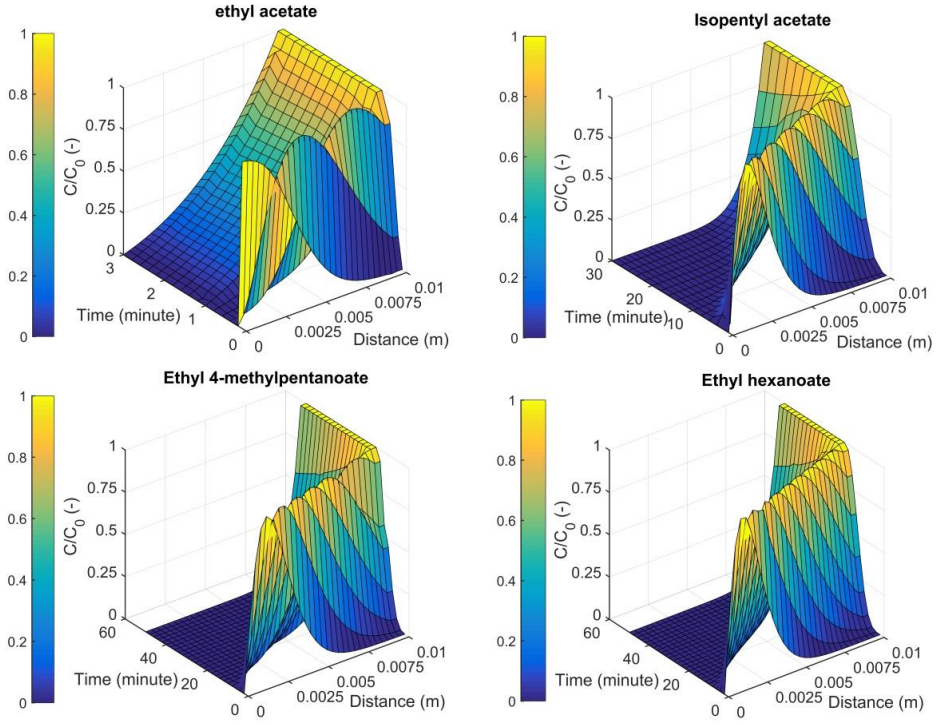

Figure 6.11. Axial concentration profiles for adsorption on 1cm column packed with Sepabeads SP20SS; Adsorption at T=333.15 K and initial solution prepared in 30% v/v Ethanol

6.4.4.3 Cyclic operation in a larger scale column

Studying the influence of temperature and ethanol concentration on adsorption/elution behavior of flavor-active esters in a lab-scale column, gives us an insight about the possibility of their separation and important parameters which are required to be considered, when tests are going to be performed in a larger scale column. With the conclusions obtained from experimental tests, a similar condition is considered for simulation of the breakthrough behavior and cyclic operation for a larger scale column. The column length of 2 m and internal column diameter of 0.08 m, are selected as typical column dimensions [33], in order to test the model based approach for prediction and approximation of breakthrough behavior for separation of flavor-active esters. Higher flow-rate, 300 L/hr is considered for each batch cycle. The simulation is performed again for the case with initial solution of esters prepared in 1% v/v ethanol/water co-solvent mixture and adsorption at T=298.15 K. Two batch cycle operations are programed using cycle organizer in Aspen Adsorption. Two different scenarios are considered for the simulation. The first scenario is simulated based on recovery and separation of ethyl acetate, the main flavor-active ester present in the beer matrix, and this ester is considered as the limiting ester in the mixture (column loading until breakthrough for ethyl acetate is achieved). The second scenario is simulated based on removal and complete adsorption of all of the flavor-active esters present in the mixture. In the initial step in each simulated cycle, the adsorption of flavor-active esters takes place at T=298.15 K, it is then followed by elution step, which is performed with 1% v/v ethanol solution and direct temperature increase from 298.15 K to 380.15 K, since according to the lab-scale tests we concluded that temperature increase will aid the elution step and release of the high hydrophobic components of the column. Temperature of 380.15 K is selected as maximum allowable temperature, due to the problem with thermo-stability of the resin and flavor-active esters at higher temperatures. After the elution step, column is washed with water at high temperature (380K) to elute the traces of ethanol for 30 minutes and cooled down during 20 minutes to the initial temperature of 298.15 K. The second cycle will start within 50 minutes with the same condition defined for the initial cycle. The result of the simulation for two batch cycles is shown in **Figure 6.12**, for the first scenario, removal of ethyl acetate, and in **Figure 6.13**, for complete removal

of all of the flavor-active esters from the initial feed stream. The considered conditions for each step are presented for one batch cyclic operation in **Figures 6.12 and 6.13.**

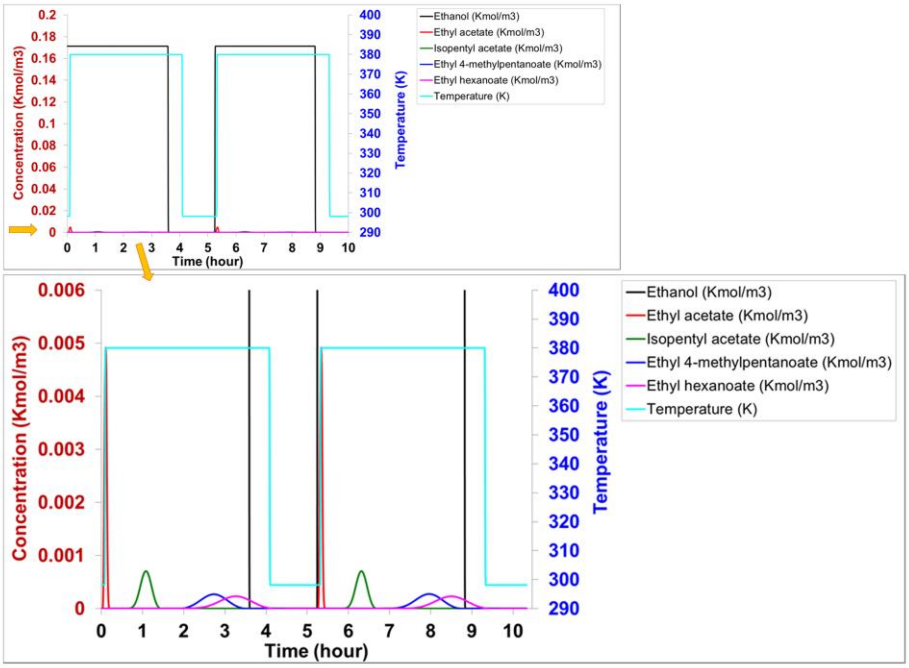

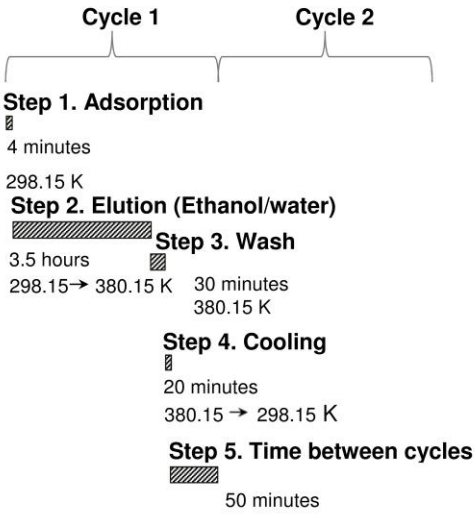

Figure 6.12. Cyclic operation for two batch cycles; Adsorption and recovery of ethyl acetate on column packed with Sepabeads SP20SS resin (L=2m, D=0.08m)

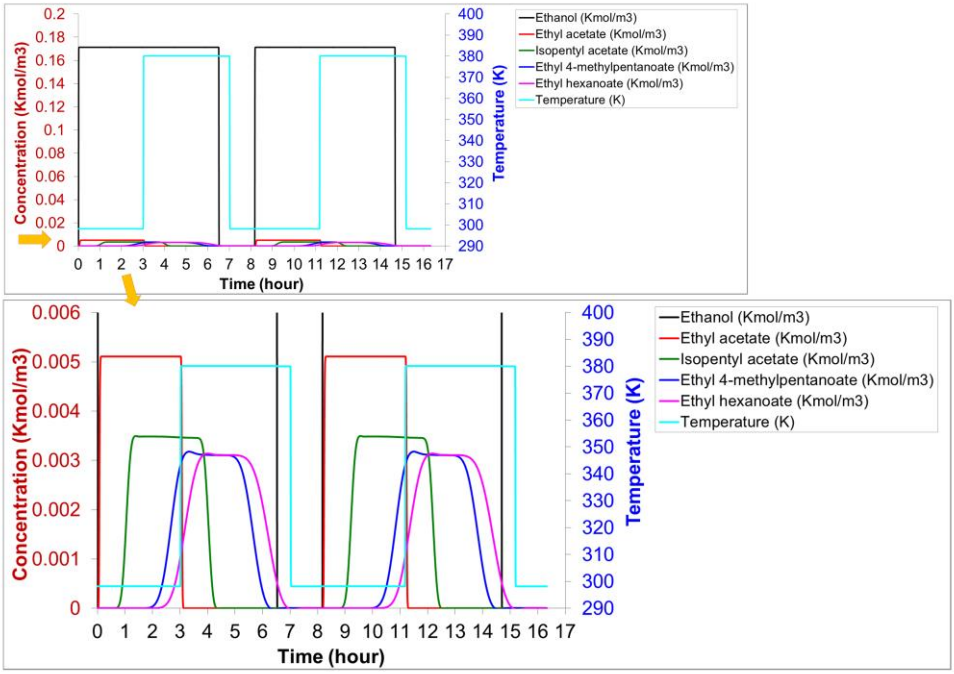

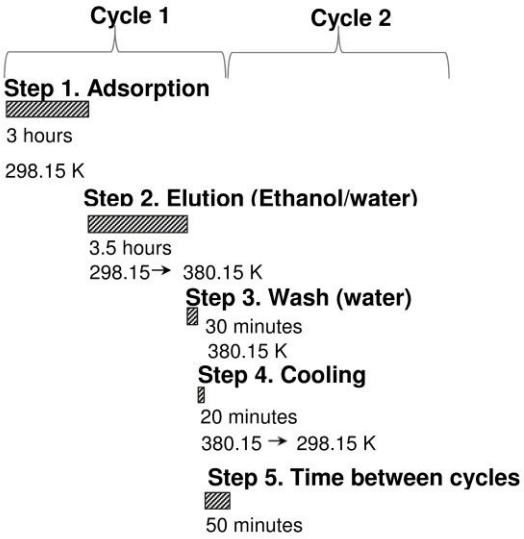

Figure 6.13. Cyclic operation for two batch cycles; Adsorption and recovery of four esters on column packed with Sepabeads SP20SS resin (L=2m, D=0.08m)

The selected operating conditions for the simulation are presented in **Table 6.7**. The number of moles loaded to the column as feeding material, is calculated, knowing the volumetric flow rate, initial concentration of each ester present in the initial feed stream and the loading time, presented in **Table 6.7** for the two simulated scenarios. In order to calculate the percentage of recovery for each ester component, the number of moles eluted after the adsorption step are calculated through integrating the area under the breakthrough curve for the similar time defined for adsorption step in the simulation, as is explained in equation (6.36).

$$Number\ of\ moles\ eluted = \int_{t_{elution,i}}^{t_{elution,i}+t_{step\ 1}} (F \times C_{i,out} \times dt) \quad (6.36)$$

Where $t_{elution,i}$, is the time that elution starts for each ester component (hr). $t_{step\ 1}$ is the loading time (hr). F is the volumetric flowrate (m^3/hr) and $C_{i,out}$ is the concentration of each ester component in the outlet stream (Kmol/m^3).

The percentage of each ester component recovered after the elution step is then calculated as the ratio of the number of moles eluted to the initial number of moles of the ester in the feed stream. The calculated percentages of recovery for each tested ester and for each simulated scenario are assembled in **Table 6.7**. The ratio of the number of moles for each ester eluted from the column to the number of moles adsorbed is calculated and reported in **Table 6.7**. The number of moles adsorbed for each tested flavor-active ester are calculated based on equation (6.37).

$$Number\ of\ moles\ adsorbed = \int_{0}^{t_{BT,i}+t_{step\ 1}} (F \times C_{i,out} \times dt) \quad (6.37)$$

Where $t_{BT,i}$ represents the breakthrough time for each ester component (hr). The productivity for each simulated scenario is reported as the volume of feed stream (m^3) that can be processed during the considered cycle time (time for loading, elution, and washing step), shown in **Table 6.7** for each scenario.

Table 6.7. Column operating condition and percentage of recovery for each ester in the product stream during each programed cycle and for each simulated scenario

Column operating condition				
Column length (m)	2			
Column diameter (m)	0.08			
F (m^3/hr)	0.3			
T (adsorption) (K)	298.15			
T (elution) (K)	298.15 , direct increase to 380.15			
	Scenario 1. Separation of ethyl acetate			
Component	*Ethyl acetate*	*Isopentyl acetate*	*Ethyl 4-methylpentanoate*	*Ethyl hexanoate*
$C_{i, Feed}$ (mol/m^3)	5.11	3.46	3.12	3.12
Moles loaded (a) (mol)	0.10	0.07	0.62	0.62
Moles adsorbed (b) (mol)	0.037	0.025	0.009	0.004
Moles eluted (c) (mol)	0.037	0.024	0.009	0.004
% c/b	100.33	94.29	100.75	100.38
% c/a	37.06	34.58	15.83	4.30
Productivity (m^3)	1.20			
	Scenario 2. Separation of all esters			
Moles loaded (a) (mol)	4.60	3.11	2.81	2.81
Moles adsorbed (b) (mol)	0.090	1.080	2.489	2.459
Moles eluted (c) (mol)	0.091	1.080	1.979	2.009
% c/b	100.67	100	79.52	81.71
% c/a	1.97	34.68	70.51	71.58
Productivity (m^3)	2.09			

For the first scenario, higher recovery of ethyl acetate can be achieved in comparison to the other tested esters, since after the breakthrough time for this ester as the limiting component, the elution step starts and specifically the two esters with the highest hydrophobicity, do not have sufficient time for adsorption. In the second scenario, the percentage of ethyl acetate which is recovered (% c/a) is less in comparison to the other esters, since some amount of this ester component is lost during the loading time until the breakthrough point for the last hydrophobic ester is achieved and higher percentage of the last hydrophobic esters, i.e. ethyl 4-methylpentanoate, and ethyl hexanoate is recovered. For the first scenario, 1.2 m^3 of the feed stream can be processed during approximately 4 hours considered for adsorption, elution, and washing steps, while in the second scenario, 2.1 m^3 of the feed stream is processed within 7 hours for the same steps as scenario 1.

The temperature profile and change in temperature of the adsorbent during each step is illustrated in **Figure 6.14** for the simulated conditions in scenario 1 and scenario 2.

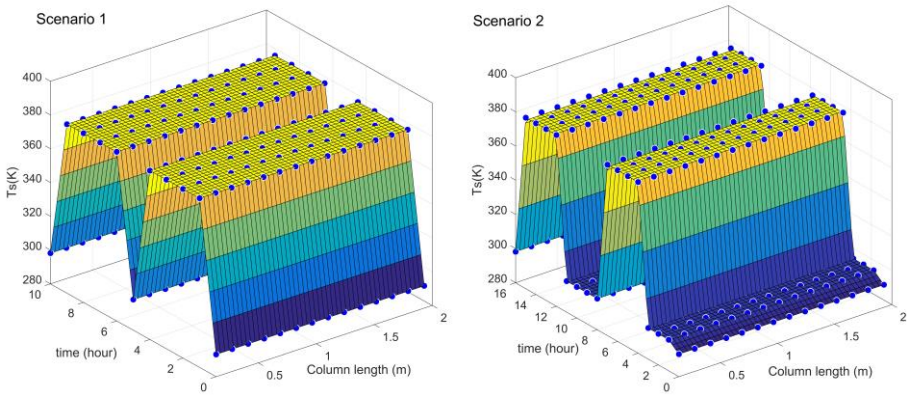

Figure 6.14. Temperature profile of adsorbent during each step for the two simulated batch cycles

The illustrated temperature profiles in **Figure 6.14**, show that the change in temperature of the solid phase during each step and for the two simulated scenarios is not significant and maximum temperature difference for the adsorbent between column inlet and column outlet, is observed as 0.002°K, for scenario 1, and 0.03°K for scenario 2, during the temperature increase for the mobile phase from 298.15 to 380.15 K in the elution step.

The condition considered for simulation here, is based on the tested condition for the lab-scale column. Similar condition is considered for adsorption and elution steps in a larger scale column to predict the breakthrough behavior, percentage of recovery, and batch operation time required for each cycle. In real process condition, the presence of other flavor and non-flavor-active components, besides CO_2 which is present in the process streams, will influence the adsorption behavior of esters, and for consideration of the adsorption step for removal of flavor-active esters or their fractionation, the influence of other components, should be considered on their competitive adsorption behaviour.

6.4.4.3.1 Column optimization and production rate

Productivity based on the considered column dimensions for scenario 1 is calculated, for the considered times for each step during one simulated cycle and the result

is compared with the optimized column dimensions, and minimum column volume for increasing the production rate. For the considered volumetric flowrate of 300 L/hr, and column dimensions with (L=2m, d_c=0.08m), for simulation in scenario 1, velocity is calculated as 99.5 cm/min and the ratio of (L/u) is approximately equal to 2. Binding capacity at 10% of the breakthrough curve, can be calculated from volume loaded to the column, according to equation (6.38), calculated as 8.5 g/L

$$BC\ 10\% \cong \frac{V_{load} \times C_F}{V_{column}} \tag{6.38}$$

The productivity for 95% recovery can then be calculated from equation (6.39), for the considered time for each step during one cyclic operation [43].

$$P = \frac{\eta_E\, BC10\%}{\frac{BC10\%}{C_F} \times \frac{L}{u} + (CV_{wash} + CV_{Elute} + CV_{Equil})\frac{L}{u} + t_{CIP}} \tag{6.39}$$

Where $CV_{wash}, CV_{Elute}, CV_{Equil}$ are column volumes considered for washing, elution, and equilibration steps. The required time for loading of the feed to the column can be calculated from equation (6.40), which is calculated approximately 4 minutes. The production rate is calculated according to equation (6.39), as 0.27 mg/(ml.min), for the considered time of 3.5 hr for the elution step, 30 minutes washing, 20 minutes for cooling step, and 50 minutes time required between two batch cyclic operations.

$$t_{load} = \frac{BC10\%}{C_F}\ \frac{L}{u} \tag{6.40}$$

To increase the production rate with the minimized column volume, the optimum ratio of 1.11 minutes is considered for (L/u) [43]. The permeability of medium is calculated according to equation (6.16) and from equation (6.14), (uL) can be calculated, knowing the pressure drop, permeability of the medium and the viscosity. For the simulated condition in scenario 1, velocity of 7.3 cm/min is calculated based on the ratio of the $(L/u)_{optimum}$. The optimum length of the column is calculated approximately 8 cm, and considering the 300 L/hr for load, dimeter of the column is calculated as 30 cm. The minimized column volume for the increased production rate is calculated as 5.6 L. The number of transfer units can be calculated according to equation (6.41) for the optimum value for Θ equal to 1/6 [33, 43]

$$N = 4\,(R_s)^2\,(\frac{\alpha+1}{\alpha-1})^2\,(1-2\theta)^{-2} \quad (6.41)$$

For R_s=1, and approximation of α as the ratio of $\bar{t}$R,A/$\bar{t}R,B$, the number of transfer units is calculated approximately equal to 10. The HETP is then calculated as 0.8 cm for the 8cm column length.

For the simulated scenario 1, for a larger volume column if we would like to pack the adsorption column with the resin Sepabeads SP20SS, and if we load the column with the adsorbent material with rate of 2 l/min, during the loading time of 4 minutes, until the breakthrough point for the desired component, ethyl acetate is achieved the associated cost for packing of the column with this resin will be approximately (18euros), considering the price of the adsorbent material 1.76 euros/g [58]. The cost for packing of the column with XAD16N resin is less in comparison if we would like to consider the same condition for the simulation in scenario 1, and it would be 2.5 euros (0.27 euros/g price of the XAD 16N adsorbent) [59] . Both tested resins show high selectivity towards tested esters, but in comparison, higher selectivity can be achieved on SP20SS resin for separation and recovery of esters with higher hydrophobicity, i.e. ethyl 4-methylpentanoate and ethyl hexanoate. As this resin represents higher selectivity towards high hydrophobic esters in comparison to XAD16N, this resin is recommended to be used, when higher recovery of these components is desired.

6.5. Conclusions

The adsorption/elution step and breakthrough curves are simulated for single and multi-compound mixture of flavour-active esters and competitive frontal analysis method is applied for prediction of breakthrough behavior and estimation of equilibrium binding capacity at various temperatures and ethanol concentrations. For the tested multi-compound mixture of esters, this method was able to predict the binding capacity for the less hydrophobic esters, i.e. ethyl acetate and isopentyl acetate with higher accuracy as separate detectable sub-plateaus were observed for these two components. The two other esters with higher hydrophobicity and similar structure, showed similar retention time in the column and both were detected in the third sub-plateau. For more accurate estimation

of binding capacity for these two esters, breakthrough curves are constructed through fraction collection and offline analysis and equilibrium binding capacity is estimated also through integration. The influence of temperature on the multi-component adsorption of esters on SP20SS resin reveals that increase in temperature is not favourable for adsorption as lower binding capacity is obtained from both methods, however temperature increase enhanced the elution of esters from the column as higher mass per gram of packed adsorbent is estimated for each ester at higher temperatures. Increase in ethanol concentration from 1 to 30% v/v , reduces the breakthrough time for adsorption to a great extent and separate breakthrough curves are not detectable in the breakthrough front, therefore the binding capacity is estimated through integration of breakthrough curves constructed through fraction collection. Almost complete recovery after adsorption is achieved in the elution step for ethyl acetate and isopentyl acetate, but complete elution of ethyl 4-methylpentanoate and ethyl hexanoate did not occur due to their higher hydrophobic nature and stronger binding to the adsorbent. The simulated breakthrough behavior both for single-component adsorption of ethyl acetate and multi-compound mixture of esters, reveal a shorter cycle time and breakthrough curves with a higher slope for SP20SS in comparison to XAD16N, which can be explained by smaller particle size and enhanced mass transfer characteristics of this resin. Simulation of adsorption/elution cycle showed a longer cycle time at lower ethanol concentration and temperature (Ethanol 1% v/v, Temperature 298.15 K) (almost five times) in comparison to tested case with (Ethanol 30% v/v, Temperature 333.15 K), as faster breakthrough is achieved at higher temperatures and also higher ethanol concentration and temperature, aids the elution step. Simulated breakthrough curves for multi-compound separation of esters in 30%v/v Ethanol and at temperature 333.15K showed higher accuracy and agreement with the experimental breakthrough curves constructed through fraction collection for XAD16N in comparison to SP20SS. Based on the results obtained from lab-scale tests, breakthrough behavior and cyclic operation simulated for a larger scale column at higher flow-rate and larger column dimensions, shows recovery for ethyl acetate and its separation from other flavor-active esters (scenario 1), and complete separation of esters (scenario 2). In order to be able to perform a more detailed simulation for prediction of breakthrough behavior, the influence of other components in the mixture

on competitive adsorption of esters and the influence of process conditions and parameters needs to be further investigated.

Nomenclature

C	Equilibrium concentration of analyte in bulk liquid (Kmol/m^3)
u	Linear velocity of mobile phase (m/s)
u_{int}	Interstitial velocity (m/s)
t	Time (s)
q	Concentration of analyte in stationary phase (Kmol/Kg $_{resin}$)
L	Column length (m)
F	Phase ratio(-)
D_{app}	Apparent dispersion coefficient (m^2/s)
D_{ax}	Axial dispersion coefficient (m^2/s)
k_{eff}	Effective mass transfer coefficient (m^2/s)
$\tilde{k}'$	Modified retention factor (-)
k'	Retention factor (-)
$t_{R,i}$	Retention time of component i (s)
t_0	Dead time of the column (for total liquid holdup) (s)
q^*	Concentration of analyte in stationary phase at equilibrium with the mobile phase (Kmol/kg $_{resin}$)
k_{ads}	Langmuir constant (m^3/Kmol)
q_{max}	Maximum load (Kmol/Kg_{resin})
T_m	Absolute temperature of mobile phase (K)
T_s	Absolute temperature stationary phase (K)
T_w	Absolute temperature column wall (K)
$C_{p,m}$	Heat capacity of mobile phase (J/Kg/K)
$C_{p,s}$	Heat capacity stationary phase(J/Kg/K)
ΔH	Heat of adsorption (KJ/mol)
h_w	Overall heat transfer coefficient at column wall (W/(m^2*K))
h	Overall heat transfer coefficient between stationary and mobile phase (W/(m^2*K))
d_c	Column diameter(m)
d_p	Average adsorbent particle diameter (m)
u_{int}	Interstitial velocity (m/s)
Q_f	Volumetric flow-rate (m^3/s)
V_{int}	Interstitial volume (ml)
V_c	Column volume (ml)
A	Cross-sectional area normal to flow direction (m^2)
K	Permeability of medium (m^2)
S_v	Surface-face-to-volume ratio (m^2/m^3)

d_{32}	Sauter mean diameter (m)
k_{ov}	Overall mass transfer coefficient (s^{-1})
k_f	External mass transfer coefficient (m/s)
V_A	Molar volume(cm^3/mol)
M_B	Molecular weight of solvent (g)
r_m	Molecular radius (m)
N	Avogadro's constant (mol^{-1})
SASA	Solvent accessible surface area (m^2)
$D_{A,B}$	Molecular diffusivity (m^2/s)
D_{eff}	Effective diffusivity (m^2/s)
V_a	Breakthrough volume for adsorption (ml)
V_h	Holdup volume (ml)
V_d	Desorbed volume (ml)
V_{init}	Initial volume (ml)
m_{resin}	Mass of resin (g)
C_0	Effluent concentration (mg/ml)
C_{out}	Concentration in outlet stream (mg/ml)
q_{EBC}	Equilibrium binding capacity (mg)
t_b	Breakthrough time (s)

Greek symbols

ε_T	Total porosity of adsorbent (-)
λ_L	Axial thermal conductivity (W/(m*K))
ν	Kinematic viscosity (m^2/s)
ε	Column void fraction (-)
ε_p	Particle porosity (-)
Φ	Sphericity of adsorbent (-)
η_B	Solvent viscosity (cP)
ψ_B	Constant for solute-solvent interaction (-)
τ_p	Tortuosity factor (-)
ψ_p	Diffusional hindrance factor (-)
λ_m	Ratio between radius of molecule and pore radius (-)

References

1. Rizvi, S.S.H., *Separation,extraction and concentration processes in the food, beverage and nutraceutical industries*. 2010: Oxford: Woodhead Pub.
2. Schoenmakers, P., *Chromatography in industry.* Annu Rev Anal Chem 2009. **2**: p. 333-357.
3. Fanali, S., et al., *Liquid Chromatography*. 2013: Elsevier Inc.
4. Olaniran, A.O., et al., *Flavor-active volatile compounds in beer: production, regulation and control.* J Inst Brew, 2016. **123**: p. 13-23.
5. Pires, E.J., et al., *Yeast: the soul of beer's aroma-a review of flavour-active esters and higher alcohols produced by the brewing yeast.* Appl Microbiol Biotechnol, 2014. **98**: p. 1937-1949.
6. Saison, D., et al., *Contribution of staling compounds to the aged flavour of lager beer by studying their flavour thresholds.* Food Chem, 2009. **114**: p. 1206-1215.
7. Hiralal, L., A.O. Olaniran, and B. Pillay, *Aroma-active ester profile of ale beer produced under different fermentation and nutritional conditions.* J Biosci Bioeng, 2014. **117**(1): p. 57-64.
8. Saffarionpour, S., et al., *The influence of ethanol concentration and temperature on adsorption of flavor-active esters on hydrophobic resins.* Sep. Purif. Technol.2019. **210**: p. 219-230.
9. Harrison, G.A.F., *The flavour of beer- a review.* J Inst Brew, 1970. **76**(5): p. 486-495.
10. Gee, D.A. and W.F. Ramirez, *A flavour model for beer fermentation.* J Inst Brew, 1994. **100**: p. 321-329.
11. Andrzejewska, A., K. Kaczmarski, and G. Guiochon, *Theoretical study of the pulse method, frontal analysis, and frontal analysis by characteristic points for the determination of single component adsorption isotherms.* J Chromatogr A, 2009. **1216**: p. 1067-1083.
12. Guiochon, G., et al., *Fundamentals of preparative and nonlinear chromatography,* second ed. 2006, San Diego, CA,USA: Elsevier Inc.
13. Kamarei, F., et al., *Accurate measurements of frontal analysis for the determination of adsorption isotherms in supercritical fluid chromatography.* J Chromatogr A, 2014. **1329**: p. 71-77.
14. Jacobson, S.C., A. Felinger, and G. Guiochon, *Optimizing the sample size and the reduced velocity to achieve maximum production rates of enantiomers.* Biotechnol Prog, 1992: p. 533-539.
15. Ma, Z. and G. Guiochon, *Comparison between the hydrograph transform method and frontal chromatography for the measurement of binary competitive adsorption isotherms.* J Chromatogr A, 1992. **603**: p. 13-25.
16. Sun, S., et al., *Determination and comparison of competitive isotherms by rectangular pulse method and frontal velocity analysis method.* J Chromatogr A, 2001. **918**: p. 13-23.
17. Saffarionpour, S., et al., *Selective adsorption of flavor-active components on hydrophobic resins.* J Chromatogr A, 2016. **1476**: p. 25-34.
18. https://www.chemaxon.com/. [cited 28 June, 2017].
19. *Sigma-Aldrich*. 2017 [cited 24 Aug 2017]; Available from: http://www.sigmaaldrich.com.
20. Lisec, O., P. Hugo, and A. Seidel-Morgenstern, *Frontal analysis method to determine competitive adsorption isotherms.* J Chromatogr A, 2001. **908**: p. 19-34.

21. Guiochon, G., *Preparative liquid chromatography.* J Chromatogr A, 2002. **965**: p. 129-161.
22. Kasten, P.R., L. Lapidus, and N.R. Amundson, *Mathematics of adsorption in beds.V.effect of intra-particle diffusion in flow systems in fixed beds.* J Phys Chem, 1952. **56**(6): p. 683-688.
23. Horvath, K., et al., *Martin-Synge algorithm for the solution of equilibrium-dispersive model of liquid chromatography.* J Chromatogr A, 2010. **1217**: p. 8127-8135.
24. Golshan-Shirazi, S. and G. Guiochon, *Modeling of preparative liquid chromatography.* J Chromatogr A, 1994. **658**: p. 149-171.
25. Nfor, B.K., et al., *Model-based rational strategy for chromatographic resin selection.* Biotechnol Prog, 2011. **27**(6): p 1629-1643.
26. Michel, M., A. Epping, and A. Jupke, *Modeling and determination of model parameters*, in *Preparative Chromatography*, H. Schmidt-Traub, Editor. 2005, WILEY-VCH Verlag GmbH &Co.: Weinheim.
27. Jungbauer, A., *Insights into the chromatography of proteins provided by mathematical modeling.* Curr Opin Biotech, 1996. **7**: p. 210-218.
28. Yanxu, L., C. Jiangyo, and S. Yinghuang, *Adsorption of multicomponent volatile organic compounds on semi-coke.* Carbon 2008. **46**: p. 858-863.
29. Storti, G., et al., *Optimal design of multicomponent countercurrent adsorption separation processes involving nonlinear equilibria.* Chem Eng Sci, 1989. **44**(6): p. 1329-1345.
30. Mazzotti, M., G. Storti, and M. Morbidelli, *Shock layer analysis in multicomponent chromatography and countercurrent adsorption.* Chem Eng Sci, 1994. **49**(9): p. 1337-1355.
31. Kaspereit, M. and A. Seidel-Morgenstern, *Process concepts in preparative chromatography*, in *Liquid Chromatography, Fundamentals and Instrumentation*, S. Fanali, et al., Editors. 2013, Elsevier Inc.
32. Qamar, S., S. Perveen, and A. Seidel-Morgenstern, *Numerical approximation of nonlinear an non-equilibrium two-dimensional model of chromatography.* Comput Chem Eng, 2016. **94**: p. 411-427.
33. Ruthven, D.M., *Principles of adsorption and adsorption processes*. 1984, USA: John Wiley & Sons Inc.
34. Carman, P.C., *Fluid flow through granular beds.* Trans Inst Chem Eng, 1937. **15**: p. 150-167.
35. Corrochano, B.R., et al., *A new methodology to estimate the steady-state permeability of roast and ground coffee in packed beds.* J Food Eng, 2015. **150**: p. 106-116.
36. Kozeny, J., *Capillary motion of water in soils, Sitzungsberichte der Akademie der Wissenschaften in Wien, Mathematisch-Naturwissenschaftliche Klasse.* Sitzb Akad Wiss, 1927. **136**: p. 271-306.
37. MacDonald, I.F., et al., *Flow through porous media-the Ergun equation revisited.* Ind Eng Chem Fundam, 1979. **18**(3): p. 199-208.
38. Scott, G.D., *Packing of spheres:Packing of Equal Spheres.* Nature, 1960. **188**: p. 908-909.
39. Lin, X., et al., *Estimation of fixed-bed column parameters and mathematical modeling of breakthrough behaviors for adsorption of levulinic acid from aqueous solution using SY-01 resin.* Sep Purif Technol, 2017. **174**: p. 222-231.
40. Wilson, E.J. and C.J. Geankoplis, *Liquid mass transfer at very low Reynolds numbers in packed beds.* Ind Eng Chem Fundam, 1966. **5**: p. 9-14.
41. Wilke, C.R. and P. Chang, *Correlation of diffusion coefficients in dilute solutions.* AICHE J, 1955. **1**: p. 264-270.
42. Mohr, C.W., et al., *An in-depth assessment into simultaneous monitoring of dissolved reactive phosphorus (DRP) and low-molecular-weight organic phosphorus (LMWOP) in*

aquatic environments using diffusive gradients in thin films (DGT). Environ Sci-Proc Imp, 2015. **17**: p. 711-727.
43. Carta, G. and A. Jungbauer, *Protein Chromatography:Process development and scale-up*. 2010, Weinheim: Wiley-VCH Verlag GmbH &Co.
44. Susanto, A., et al., *Investigation of pore diffusion hindrance of monoclonal antibody in hydrophobic interaction chromatography using confocal laser scanning microscopy.* J Chromatogr A, 2007. **1149**: p. 178-188.
45. Peighambarzadeh, M. and M. Bohlool, *Adsorption process and its simulation with ASPEN ADSIM* فرآیند جذب سطحی و شبیه سازی آن با نرم افزار Third ed. 2015, Tehran, Iran: Andishehsara.
46. Soni, V., et al., *Modeling and analysis of vacuum membrane distillation for the recovery of volatile aroma compounds from black currant juice.* J Membrane Sci, 2008. **320**(1-2): p. 442-455.
47. Quiñones, I., J.C. Ford, and G. Guiochon, *Multisolute adsorption equilibria in a reversed-phase liquid chromatography system.* Chem Eng Sci, 2000. **55**: p. 909-929.
48. Reck, J.M., et al., *Separation of antibody monomer-dimer mixtures by frontal analysis.* J Chromatogr A, 2017. **1500**: p. 96-104.9. Slaats, E.H., et al., *Distribution equilibria of solvent components in reversed-phase liquid chromatographyic columns and relationship with the mobile phase volume.* J Chromatogr 1981. **207**: p. 299-323.
50. Sun, S., et al., *Determination and comparison of competitive isotherms by rectangular pulse method and frontal velocity analysis method.* J Chromatogr A, 2001. **918**: p. 13-23.
51. Vente, J.A., et al., *Evaluation of sugar sorption isotherm measurement by frontal analysis under industrial processing conditions.* J Chromatogr A, 2005. **1066**: p. 71-79.
52. Marquardt, D.W., *An algorithm for least-squares estimation of nonlinear parameters* J.Soc.Ind.Appl.Math., 1963. **11**: p. 431-441.
53. Srivastana, V.C., et al., *Prediction of breakthrough curves for sorptive removal of phenol by bagasse fly ash packed bed.* Ind Eng Chem Res, 2008. **47**(5): p. 1603-1613.
54. Saravacos, G. and A.E. Kostaropoulos, *Handbook of Food Processing Equipment*, ed. G.V. Barbosa-Canovas. 2016: Springer International Publishing Switzerland.
55. Ferrarini, R., et al., *Variation of oxygen isotopic ratio during wine dealcoholization by membrane contactors: Experiments and modelling.* J Membrane Sci, 2016. **498**: p. 385-394.
56. Kirkham, M.B., *Structure and properties of water*, in *Principles of soil and plant water relations*. 2014, Academic Press.
57. Hahn, R., R. Schleger, and A. Jungbauer, *Comparison of protein A affinity sorbents.* J Chromatogr B-Analytical Technologies in the Biomedical and Life Sciences, 2003. **790**(1-2): p. 35-51.
58. *Sepabeads SP20SS*. [cited 30 October 2017]; Available from: http://www.sigmaaldrich.com/catalog/product/supelco/13617u?lang=en&region=NL.
59. *Amberlite XAD16N*. [cited 30 October 2017]; Available from: http://www.sigmaaldrich.com/catalog/product/sigma/xad16?lang=en&region=NL.

Concluding remarks and outlook 7

Selective removal and recovery of flavor-active components present in beer, provides an opportunity to produce products with balanced and tailored flavor profile and according to previous investigations and the techniques discussed in Chapter 2, adsorption shows potential for removal and recovery of flavor components, which can be combined with thermal processing, like distillation or stripping. Therefore, research is worthwhile to study the application of this technique for separation of small biomolecules and investigate new adsorbent materials with enhanced physical and chemical characteristics for their separation. The focus of this research is on adsorption process development and investigating the possibility for selective removal and recovery of these components, taking into account the importance of achieving high selectivity over ethanol. Selective reduction in concentration levels of these flavor-active components is possible through simple contacting the stream containing flavor components with a porous adsorbent material and subsequently reduce and adjust the level of these compounds in the initial stream. Since the desired flavor-active components, mainly esters are rather hydrophobic, hydrophobic interaction chromatography is applied to study their separation and macro and micro-porous synthetic hydrophobic adsorbents are

studied as suitable materials for their separation. The influence of adsorbents' physical and chemical structure, on achieving high selectivity for separation of these biomolecules over ethanol is discussed in Chapter 3.

7.1 Challenges in method development for selective removal of flavor components

Techniques such as Batch uptake experimentation are well-developed and widely applied for screening various adsorbent materials and performing parallel experiments in a smaller scale, tested for separation of proteins and bigger-sized biomolecules, however the main challenge for applying this technique for separation of flavor components with smaller molecular size is the volatility of these components and some amount of these components might be lost during the incubation time due to evaporation. Therefore the main aim of the study discussed in Chapter 3, was to develop an appropriate method to study the selective adsorption of the flavor components, taking into account the development of the appropriate experimental procedure to prevent the evaporation of flavor components from 96well micro-titer plates. The developed method, discussed in Chapter 3, highlights the improvements considered in the existing technique in order to prevent the evaporation effect as much as possible. Since loss of these flavor components is possible at different steps of the experimental procedure, specifically when experiments are required to be performed at higher temperature, there is a need to consider and develop a procedure with reduced steps for treating, and incubating the samples, centrifugation, and their separation from the adsorbent material. The application of a method for measuring partition coefficients for a three-phase system is discussed in Appendix A for performing batch uptake experiments, which measures the equilibrium between three phases of solid, liquid, and gas, however analysis required to be performed for this method is based on variation of the phase ratio, and requires a lot of sample preparation with long analysis time. Moreover this method works under assumption of low (close to zero) amount of analyte bound to the adsorbent material or high degree of adsorption, therefore for estimating the equilibrium binding capacity, this method might not be able to give satisfactory results for components with intermediate polarity and in case of having a mixture of compounds with different values of volatility it might not be able to estimate the equilibrium binding capacity with high accuracy. The influence of

evaporation can be reduced through applying other methods, such as the Frontal analysis technique for isotherm determination and performing the experiments in a packed column, however as the results of the tests, discussed in chapter 3 and 4 reveal, constructing the isotherms with this method is rather time-consuming, specifically for high hydrophobic compounds with longer retention time and competitive frontal analysis cannot be applied successfully for isotherm determination, when compounds with similar molecular and physical structure and properties are tested, since they can be present in one sub-plateau of the breakthrough front and for determination of the equilibrium concentration, fraction collection and offline analysis from the outlet stream is required.

7.2 Selection and development of adsorbent material

The appropriate adsorbent materials applied for selective removal of the desired flavor-active components, discussed in Chapter 3, are selected considering the criteria that the adsorbent material should be food grade, with high selectivity, surface area and available sites for binding the small biomolecules. The selected adsorbent should be feasible in terms of costs and the possibility of regeneration and using the adsorbent for different cyclic operations is an important factor that needs to be considered while selecting the adsorbent for industrial scale application. These criteria limits the selection of the adsorbent material from wide range of available materials. In the limited range for selection, the application of synthetic hydrophobic resins with the matrix structure of styrene divinylbenzene is investigated both for macro and micro-porous resin materials and the influence of particle size, pore volume, surface area, and functional groups is studied on adsorption of the flavor components. According to the studies discussed in Chapter 3, decrease in particle size of the resin for the same adsorbent material with the same structure, for the resins belong to the DIAION Sepabeads group (S version), enhances the selectivity and adsorption of the flavor-active components, mainly for hydrophobic compounds and esters, as the area per volume of the resin increases, however the higher cost of these adsorbents in comparison to their larger particle size version might be a drawback for applying them in an industrial scale. The other important factor which is required to be considered is the possibility for elution of the strongly bound compounds with high hydrophobicity from these adsorbent materials. While enhanced adsorption of flavor-active esters with high hydrophobicity was observed on the adsorbent materials

with smaller particle size, the complete elution of the high hydrophobic compounds from these adsorbents, proved to be more difficult with the requirement of consuming more eluent and energy to desorb the strongly bounded components at elevated temperatures. The estimated costs for packing of the adsorption column with these resins (e.g. Sepabeads SP20SS), discussed in Chapter 6, is higher in comparison to the resins with styrene-DVB structure with higher surface area (e.g. tested resin XAD16N), however as this resin shows higher selectivity towards high hydrophobic esters it can be applied when separation and recovery of these components is desired. Considering the limited available food grade resins, which are applicable for separation of the flavor-active components and the limited research which is conducted on the development of new adsorbent materials, further research is worthwhile to develop new materials that can have application in food industry through consideration of functional groups which increase the affinity of the adsorbent towards the desired flavor components or development of new material with mixed mode characteristics of the tested adsorbents which showed high selectivity towards the desired components.

7.3 Thermodynamic properties and isotherm models

The studies discussed in chapter 4, on the influence of temperature and ethanol concentration on adsorption of the high hydrophobic esters, and the estimation of thermodynamic properties like heat, entropy, and Gibbs energy of adsorption, gives a better insight on understanding the adsorption mechanism on each tested adsorbent and proves the strong binding of the high hydrophobic esters and the start of the chemisorption and diffusion of the molecules into the resin particles. The comparison of these properties for each component and for each tested adsorbent, provides a better understanding of the adsorption phenomena, besides the thermodynamic parameters and selectivity of each adsorbent towards each tested component which is derived from isotherm determination. The research conducted on determination of the thermodynamic properties for flavor-active components is limited and for enhanced understanding of the adsorption mechanism on each adsorbent material, estimation of these properties is recommended which provides improved knowledge on behavior of the adsorption system under the non-isothermal condition.

Expression of the equilibrium adsorption data with conventional isotherm models, i.e. Langmuir, Freundlich, and Sips models, reveal that Langmuir and Sips models are capable in predicting the adsorption behavior of the tested components with high accuracy, specifically better prediction can be obtained for adsorption of high hydrophobic components with low solubility in water through Sips model in comparison to Langmuir model. Strong binding of high hydrophobic esters, as is discussed in Chapter 4, results in low equilibrium concentrations remained in bulk liquid and high slope of the isotherm, and since these compounds are rather hydrophobic with low solubility in water, experimental determination of the maximum binding capacity for these compounds cannot be performed, therefore Langmuir model might not be able to predict the maximum binding capacity with high accuracy, with high slope of the isotherm and lack of the experimental data at high concentration region. For a more accurate determination of affinity parameter Sips model can be used instead which gives a better prediction of maximum capacity at high concentrations in comparison, or a linearized isotherm model can be applied for expression of the affinity parameter in low concentration region.

7.4 Column chromatography for separation of esters

Separation of major flavor-active esters present in beer together with prediction of their breakthrough behavior in a fixed-bed adsorption column is discussed in Chapter 6. The experimental lab-scale tests performed on packed columns for adsorption and separation of these esters, using competitive Frontal Analysis method, reveal that this method cannot be successfully applied for construction of the multicomponent adsorption isotherms, since separate breakthrough curves cannot be detected for ester components with similar molecular structure and physical properties; therefore, for more accurate determination of equilibrium binding capacity for adsorption/elution steps, fraction collection and offline analysis is required to measure the equilibrium concentration of each ester component in each sub-plateau.

The performed experiments on multicomponent separation of these esters under the influence of temperature, reveal that increase in temperature aids the elution of the highly bound components to a great extent, therefore, for designing an adsorption/elution step for separation of these esters, increase of the temperature for the eluent stream should be considered for enhanced elution of the strongly bound esters, considering the limit for

temperature increase for stability of the adsorbent material and thermo-stability of the ester components. Predicted breakthrough curves for adsorption and separation of flavor-active esters on two tested resins SP20SS and XAD16N, show enhanced mass transfer characteristics for adsorption on SP20SS, and reduced cycle time required for adsorption/elution cycle in comparison to XAD16N, due to its smaller particle size, larger pore volume and high surface area per volume of this resin, however higher pressure drop and costs associated with packing a column with this resin, can be drawbacks for applying this resin for a large-scale separation, in comparison to XAD16N. Considering the all above-mentioned factors, presence of other flavor-and non-flavor active components together with presence of ethanol at a higher concentration level can also influence the calculated selectivity of this adsorbent towards flavor-active esters, as also other components present at a higher concentration in comparison to esters, compete with esters for binding to the adsorbent. Performed simulation for prediction of the breakthrough behavior for separation of esters from a distillate stream containing mainly ester components present with higher concentration of ethanol, on a column packed with SP20SS which showed higher selectivity and reduced cycle time, in comparison to XAD16N, show that pure recovery of ethyl acetate and isoamyl acetate is possible, since they have different hydrophobicity and retention time, in comparison to two tested ester components ethyl 4-methylpentanoate and ethyl hexanoate which have similar physical structure, hydrophobicity and retention time. Pure recovery of these two components could not be achieved and the collected fractions contain both esters together or one of the esters, but not completely as a pure component. In order to enhance their separation and recovery counter-current separation can be considered or separation can be enhanced through designing the adsorption elution step in a simulated moving bed.

Appendix A.

Determination of partition coefficients for three phase equilibrium and headspace analysis

A.1 Introduction

The improvement in the well-developed Batch uptake experimentation method and its application for investigating the adsorption of volatile flavor-active components is discussed in detail in chapter three. The numerous experimental steps discussed and required for performing the experiments using 96well micro-titer plates can lead to the loss of volatile flavor-active components during sample addition, centrifugation, and transferring the samples from 96well micro-titer plates to vials for analyzing the liquid bulk samples, therefore there is a requirement to develop a method with reduced steps to perform the experiments in a closed system to prevent the effect of evaporation as much as possible. In this section the application of a method is discussed, which is developed based on three-phase equilibrium between solid adsorbent, the liquid bulk sample and the amount of volatile analyte present in the headspace and determination of partition coefficients, for performing the adsorption experiments in a closed system, which aids to prevent the influence of evaporation through eliminating the steps required for centrifugation and transferring the bulk samples. The application of headspace method for measuring the equilibrium between liquid and vapor phase is unequivocally demonstrated in many research works, however this method is not widely applied for measuring the three-phase equilibrium between the liquid phase of the bulk material, the solid adsorbent and the headspace vapor phase. In this work, the application of Phase

Ratio Variation method (PRV) is discussed for measuring the partition coefficients and equilibrium between three phases. The measurement of the partition coefficients can be performed through variation of the liquid phase (LPRV method), or variation of the amount of solid (SPRV) [1]. The application of this method for volatile flavor components showed nonlinearity between the obtained peak areas at high phase ratios, therefore modification in the already developed method is considered by applying the modified LPRV method. The developed method is tested for adsorption of ethyl acetate on the Sepabeads SP20SS adsorbent and the results obtained from both methods are compared thereafter.

A.2 Classical Phase Ratio Variation Method (PRV)

This method is based on the conservation of mass and expression of the partition coefficient K, which is described as the ratio of the equilibrium concentration of the volatile compound in the gas and liquid phase, C_G and C_L respectively, as shown in equation (A.1) [2-4].

$$n_0 = n_G + n_L \qquad (A.1)$$

$$K = \frac{C_G}{C_L} \qquad (A.2)$$

Different volumes of the prepared sample are introduced in to closed vials and the ratio between vapour volume and liquid volume is noted as β ($\beta=\frac{V_G}{V_L}$). The concentration of the volatile sample in the vapour phase (C_G) is determined by measuring its GC peak area, measuring small volume of a known concentration of the sample. The peak response factor is then calculated from equation (A.3)[5].

$$f_i = \frac{A}{C_G} \qquad (A.3)$$

A relationship between peak area and phase ratio can be derived as shown in equation (A.4) [6, 7].

$$A = f_i C_0/(1/K + \beta) \qquad (A.4)$$

Where C_0 is the initial concentration in the vial and f_i is the response factor.

Linearized form of equation 4 leads to equation (A.5).

$$\frac{1}{A} = \frac{1}{K f_i C_0} + \left(\frac{1}{f_i C_0}\right)\beta \qquad (A.5)$$

Reciprocal function of 1/A and β leads to equation (A.6)and K value is the ratio of b/a.

$$\frac{1}{A} = a + b\beta \qquad (.A.6)$$

For less volatile compounds the approximation of $C_L \approx C_0$ is verified and the linearized form, presented in equation 5 can be written as is shown in equation (A.7).

$$\frac{1}{A} = \frac{1}{f_i C_L} \times \frac{C_L}{C_G} + \left(\frac{1}{f_i C_L}\right) \times \frac{V_G}{V_L} \qquad (A.7)$$

A.2.1 Modified Phase Ratio Variation Method (M-PRV)

In case of having volatile compounds, the approximation of equality of bulk concentration and initial concentration is not valid and bulk concentration of the sample can be related to its initial concentration with the relation explained in equation (A.8) [8].

$$C_L = C_0/(1 + K\beta) \qquad (A.8)$$

By replacing C_L with its equivalent in equation (A.8), equation (A.9) can be written.

$$\frac{1}{C_G'} = \frac{1}{K C_0} + \frac{2}{C_0}\beta + \frac{K}{C_0}\beta^2 \qquad (A.9)$$

Equation (A.9) can be written in form of equation (A.10), which is the summation of classical PRV and the excess term.

$$\frac{1}{C_G} = \left(\frac{1}{K C_0} + \frac{1}{C_0}\beta\right) + \left(\frac{1}{C_0}\beta + \frac{K}{C_0}\beta^2\right) \qquad (A.10)$$

The value of partition coefficient can be calculated from a, b, and c regressed from equation (A.11) [8].

$$\frac{1}{A} = \frac{1}{f_i C_0 K} + \frac{2}{f_i C_0}\beta + \frac{K}{f_i C_0}\beta^2 \qquad (A.11)$$

Where a is equal to $\frac{1}{f_i C_0 K}$, b is equal to $\frac{2}{f_i C_0}$, c is equal to $\frac{K}{f_i C_0}$

For a dilute solution, the equilibrium distribution of a volatile compound between gas and liquid phase in a closed system is described by Henry's law, shown in equation (A.12).

$$C_G = KC_L \quad (A.12)$$

$$K = \frac{C_{G1}}{C_{L1}} = \frac{C_{G2}}{C_{L2}} \quad (A.13)$$

Numbers 1 and 2 refer to standard and unknown aqueous samples therefore the concentration of unknown sample can be calculated from equation (A.14).

$$C_{L2} = \frac{C_{G2}}{C_{G1}} C_{L1} \quad (A.14)$$

The relation of peak area with the response factor fi can be substituted in equation 14 and equation (A.15) can be written as follows.

$$\frac{A_2}{A_1} = \frac{f_i C_{G2}}{f_i C_{G1}} = \frac{C_{L2}}{C_{L1}} \quad (A.15)$$

The concentration of an unknown sample can therefore be measured by knowing the ratio of the peak areas for standard solution and the unknown sample [9].

$$C_{L2} = \frac{A_2}{A_1} C_{L1} \quad (A.16)$$

A.3 Methods for determination of three phase partition coefficients

The partition coefficient for the three phases can be determined using two various methods explained in the next sections.

A.3.1 Liquid Phase Ratio Variation method (LPRV)

The LPRV method is developed based on the HS-GC analysis for determining the partition coefficients of the volatile compound in the solid adsorbent in presence of the liquid phase. In a three-phase system the volatile component in the headspace vial distributes among three phases as is shown in **Figure A.1**, and the total mass of the species can be expressed as explained in equation (A.17).

$$m = m_G + m_L + m_S = C_G V_G + C_L V_L + C_S W_S \quad (A.17)$$

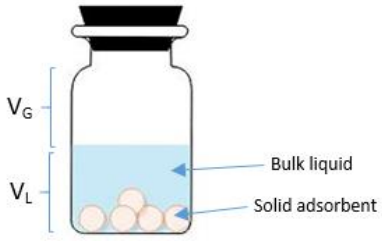

Figure A.1. Three-phase equilibrium in headspace vial

When the equilibrium is reached, the partition coefficient between the vapour and liquid phase and between the solid and the liquid phase can be obtained from equation (A.18) and equation (A.19).

$$H = \frac{C_G}{C_L} \qquad (A.18)$$

$$K = \frac{C_S}{C_L} \qquad (A.19)$$

The concentration of the volatile analyte can be obtained afterwards by combining equation (A.17), (A.18), and (A.19) as is expressed by equation (A.20).

$$C_G = \frac{m}{V_G + \left(\frac{V_L}{H}\right) + \left(\frac{W_S K}{H}\right)} \qquad (A.20)$$

And

$$\frac{1}{C_G} = \frac{1}{m}\left(V_G + \frac{V_L}{H} + \frac{W_S K}{H}\right) \qquad (A.21)$$

The mass of the analyte is proportional to the solution volume (i.e. m=$C_0 V_L$) and equation (A.21) can be expressed as equation (A.22).

$$\frac{1}{C_G} = a \times \frac{1}{V_L} + b \qquad (A.22)$$

With

$$a = \frac{1}{C_0}\left(V_T + \frac{W_S K}{H}\right) \qquad (A.23)$$

And

$$b = \frac{1}{C_0}\left(\frac{1}{H} - 1\right) \quad (A.24)$$

The slope and intercept are then obtained from linear fitting from the experimental data measured from headspace analysis.

When $H \neq 1$ the partition coefficient K can be calculated from equation A.25.

$$K = \frac{1}{W_S}\left[\frac{a}{b} \times (1 - H) - HV_T\right] \quad (A.25)$$

And if H=1, then b=0 and equation (A.25) can be written as:

$$K = \frac{1}{W_S}[aC_0 - V_T] \quad (A.26)$$

The range of H values is crucial in determining the K value in the LPRV method and when the value of H is close to one, the partition coefficient value K might be calculated with error.

For measurement of the partition coefficients for volatile flavor components, the method developed based on LPRV method might result in nonlinearity in the measurements, therefore, the developed method can be improved by considering the excess term, in the PRV method and applying the M-PRV method, which can improve the predictions of partition coefficients. The value of C_0 is replaced by C_L as explained in equation (A.27).

$$C_L = \frac{C_0}{1 + H\beta + \frac{KW_S}{V_L}} \quad (A.27)$$

Substituting equation (A.27) in equation (A.22) we can write equation (A.28) in polynomial form. Details of the calculations are explained in equations (A.29) to (A.33).

$$\frac{1}{C_G} = \frac{1}{C_0}\underbrace{\left[HV_T + V_T W_S K + KW_S V_T + \frac{(KW_S)^2}{H}\right]}_{a}\frac{1}{V_L^2} + \frac{1}{C_0}\underbrace{\left[3V_T + \frac{2W_S K}{H} - 2KW_S - H(V_T + 1)\right]}_{b}\frac{1}{V_L} + \frac{1}{C_0}\underbrace{\left[\frac{1}{H} - 2 + H\right]}_{c} \quad (A.28)$$

$$C_L = \frac{C_0}{1 + H\beta + \frac{KW_S}{V_L}} \quad (A.29)$$

$$\frac{1}{C_G} = \frac{1}{m}\left(V_G + \frac{V_L}{H} + \frac{W_S K}{H}\right) \quad (A.30)$$

$$\frac{1}{C_G} = [V_T - V_L + \frac{V_L}{H} + \frac{W_s K}{H} + H\frac{V_G}{V_L} \times V_T - H\frac{V_G}{V_L} \times V_L + H\frac{V_G}{V_L} \times \frac{V_L}{H} + H\frac{V_G}{V_L} \times \frac{W_s K}{H} + K\frac{W_s}{V_L}V_T - K\frac{W_s}{V_L}V_L + K\frac{W_s}{V_L} \times \frac{V_L}{H} + \frac{(KW_s)^2}{HV_L}]\frac{1}{C_0 V_L}$$

(A.31)

$$\frac{1}{C_G} = \frac{1}{C_0}\left[HV_G + V_G W_s K + KW_s V_T + \frac{(KW_s)^2}{H}\right]\frac{1}{(V_L)^2} + \frac{1}{C_0}\left[V_T + \frac{W_s K}{H} + V_T - HV_G + V_G - KW_s + \frac{KW_S}{H}\right]\frac{1}{V_L} + \frac{1}{C_0}[\frac{1}{H} - 2 + H]$$

(A.32)

$$\frac{1}{C_G} = \frac{1}{C_0}\left[HV_G + V_G W_s K + KW_s V_T + \frac{(KW_s)^2}{H}\right]\frac{1}{(V_L)^2} + \frac{1}{C_0}\left[3V_T + 2\frac{W_s K}{H} - HV_T - KW_s\right]\frac{1}{V_L} + \frac{1}{C_0}[\frac{1}{H} - 2 + H]$$

(A.33)

A.3.2 Solid Phase Ratio Variation Method (SPRV)

The partition coefficients for the three phases can be calculated by varying the amount of adsorbent material and keeping the phase ratio the same in all tested vials. For the analytes with low binding to the adsorbent, when the concentration in the solid phase is low in comparison to the amount remained in bulk liquid, the partition coefficients can be calculated according to the procedure explained in this section.

In this case, the total amount of analyte can be approximated according to equation (A.21) [1]. When the liquid volume is fixed, the analyte in vapour phase depends only on solid weight added in the vials, thus the equation (A.21) can be written as:

$$\frac{1}{C_G} = a \times W_S + b \quad \textit{(A.34)}$$

Where

$$a = \frac{K}{mH} \quad \textit{(A.35}$$

And

$$b = \frac{V_T - V_L + (\frac{V_L}{H})}{m} \quad \textit{(A.36)}$$

The partition coefficient can be obtained by adding different amounts of solid samples to the headspace vial. The analyte is then measured in the headspace and $\frac{1}{C_G}$ is plotted versus the Ws By obtaining the intercept and slope, the partition coefficient K can be calculated from equation (A.37) [1].

$$K = \frac{b}{a} \times [H \times (V_T - V_L) + V_L] \qquad (A.37)$$

The value of H can be obtained from LPRV method.

A.4 Experimental procedure

In order to test the application of the developed methods for measuring the partition coefficients, adsorption of ethyl acetate is studied on the synthetic hydrophobic resin Sepabeads SP20SS.

A.4.1 Measurements based on LPRV method

In order to calculate the partition coefficients by variation of the liquid sample analyte, approximately 2.7 $g.L^{-1}$ solution of ethyl acetate prepared in 4%w/v co-solvent mixture of ethanol/water by dissolving 0.14g of ethyl acetate in the co-solvent mixture. In the next step, 0.098 g of the prepared resins (Sepabeads SP20SS), washed with water and methanol 1%V/V, are added to 10ml vials for headspace measurement. Different volumes of the prepared analyte are added to the vials, (i.e.5, 4, 3, 2, 1, and 0.5 ml). The schematic view of the prepared samples is shown in **Figure A.2**.

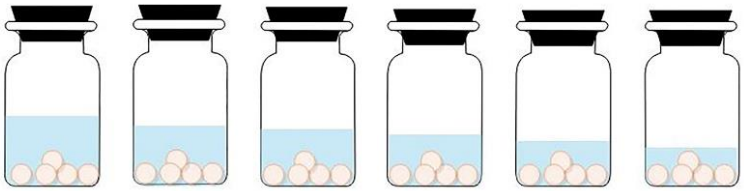

Figure A.2. Schematic view of the prepared samples for LPRV tests

For the prepared six samples, the peak areas are obtained and $1/C_G$ is plotted versus the $1/V_L$. The response factor is calculated by adding 10µl of the sample with the known concentration to the 10ml vial and measuring the maximum response for 5 minutes equilibration time at 105°C [1].

The slope and intercept are calculated afterwards by linear fitting the experimental data for ethyl acetate and ethanol respectively. **Figure A.3**, *part a* shows the relation between the concentrations change in the gas phase and variation of sample volume inside the vials.

As can be observed from Figure 3, *part a*, the linear regression is not a perfect fit for the obtained experimental data, values of R^2 0.91 for ethyl acetate and 0.92 for ethanol. In order to consider the non-linearity in the measurements for volatile compounds, as it was also explained in previous sections for modifying the PRV Method, the LPRV method is improved considering the excess term and non-linearity in equation A.22. A second order polynomial is fitted to the obtained experimental data, as is shown in **Figure A.3, *part b***.

The value of H is calculated from c in equation 28. Solving a second order equation for H, value of H is obtained as 0.01 for ethyl acetate and 0.0155 for ethanol. The values of partition coefficient H are summarized in **Table A.1** for both methods.

Table A.1. Values of partition coefficient H calculated for ethyl acetate and ethanol. LPRV and Modified-LPRV Method

	LPRV Method (First order)		**Modified-LPRV Method (Second order)**	
Compound	$H=C_G/C_L$	R^2	$H=C_G/C_L$	R^2
Ethyl acetate	0.013	0.909	0.010	0.998
Ethanol	0.0172	0.921	0.0155	0.996

The higher R^2 obtained for the second order model shows that more reliable partition coefficients can be calculated by consideration of the excess term, and non-linearity for the tested volatile compound, i.e. ethyl acetate. This method is proposed to be used for calculation of partition coefficient H, for high volatile compounds and high phase ratios.

The value of partition coefficient K will be calculated from SPRV (Solid phase ratio variation method) since the LPRV Method causes some error in the calculation of K.

a)

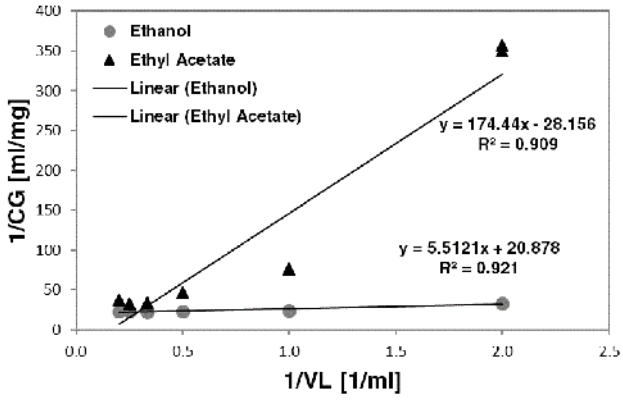

b)

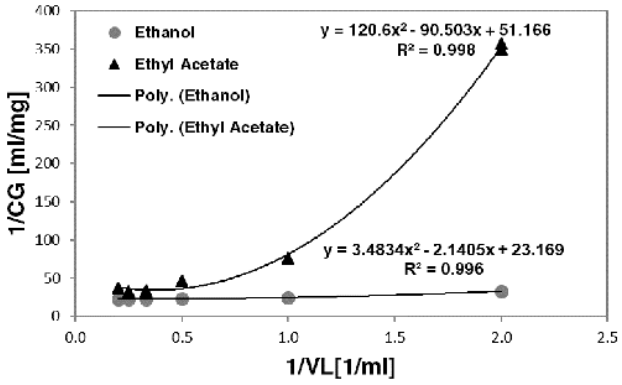

Figure A.3.Reciprocal of concentration in gas phase vs.change in volume of the liquid sample; a) LPRV method b)Modified LPRV method

A.4.2 Measurements based on SPRV method

Adsorption of ethyl acetate is studied on the same tested resin Sepabeads SP20SS and six samples are prepared by adding different weights of the resin, i.e. 0.266, 0.091, 0.083, 0.049, 0.019, and 0.003g to the headspace vials. The schematic view of the six prepared samples is shown in **Figure A.4**.

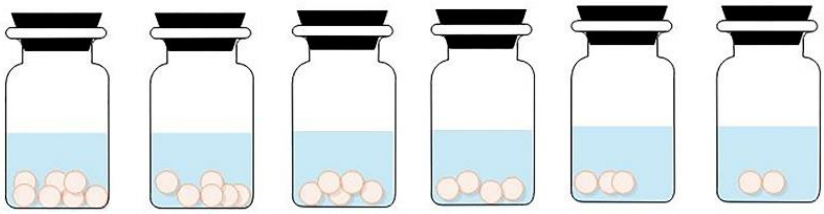

Figure A.4. Schematic view of the prepared samples for SPRV tests

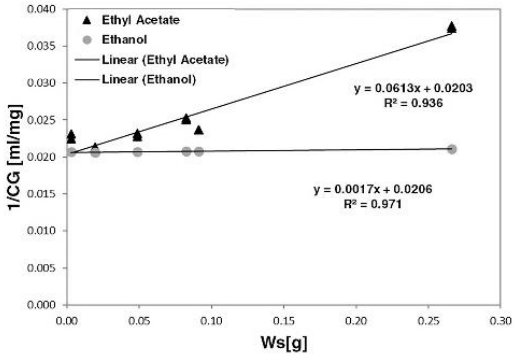

Figure A.5. Reciprocal of concentration in the gas phase vs. Mass of the resin; SPRV method

The concentrations in the gas phase are obtained for both analytes and $1/C_G$ is plotted versus the Ws, illustrated in **Figure A.5**. The obtained graphs are shown in Figures 4 and the values for peak areas and partition coefficients are sumarized in **Table A.2**.

Table A.2. Values of partition coefficients calculated for ethyl acetate and ethanol from LPRV, Modified-LPRV Method

	Ethyl acetate	**Ethanol**
LPRV method		
$H=C_G/C_L$	0.013	0.0172
R^2	0.908	0.921
$K=C_S/C_L$ $[ml.g^{-1}]$	62.71	36.92
R^2	0.936	0.971
Modified LPRV method		
$H=C_G/C_L$	0.01	0.0155
R^2	0.998	0.996
$K=C_S/C_L$ $[ml.g^{-1}]$	47.68	33.26
R^2	0.936	0.971

As the summarized values in Table A.2 reveal, higher accuracy in predicting the partition coefficient is achieved using the modified LPRV method in comparison to LPRV method. The calculated values of partition coefficient K from SPRV method are 15.3 and 1.3 for ethyl acetate and ethanol respectively.

In order to obtain the maximum capacity that can be reached from single component adsorption of ethyl acetate on Sepabeads SP20SS, the concentrations in the gas phase are calculated from the obtained peak areas and the response factor f_i. Afterwards the concentrations in the liquid phase are obtained from the calculated partition coefficient H for both methods, LPRV and Modified-LPRV.

The maximum capacity of Sepabeads SP20SS for single component adsorption of ethyl acetate is calculated as 31.6 mg.g-resin^{-1} (calculated from LPRV method) and 41.4 mg.g-resin^{-1} (calculated from Modified-LPRV method); since in the SPRV method an assumption was made that low, almost zero amount of analyte is adsorbed on the resin, the value of partition coefficient, K is calculated with error from this method.

In order to study the influence of initial concentration of the prepared ethyl acetate sample on partition coefficient H, three different concentrations are tested, i.e. 2.7, 1.6, and 1.0 mg.mL^{-1} and the partition coefficient, is calculated based on LPRV and Modified-LPRV methods. The calculated values for the partition coefficient H are shown versus the initial concentration, presented in **Figure A.6**.

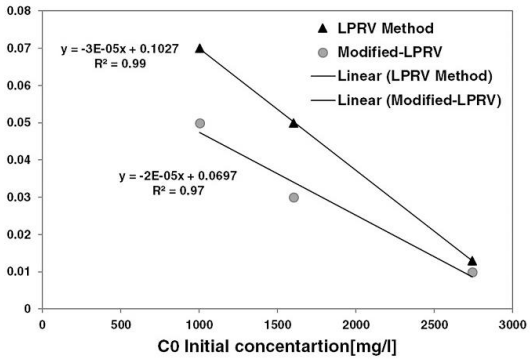

Figure A.6. Calculated partition coefficients for adsorption of ethyl acetate on Sepabeads SP20SS; Based on LPRV and Modified LPRV methods

Values of partition coefficient, calculated based on both methods, show an increasing trend with decrease in the initial concentration. According to former studies reported in the literature, no significant change in partition coefficient of ethyl acetate is observed for a two-phase system [10], for equilibrium between liquid and gas phases. In case of having a three-phase system, the bulk liquid after adsorption will not be equal to the initially tested concentration, and results in a lower value for partition coefficient.

The developed method based on variation of the liquid phase (LPRV method) with the modification considered in the PRV method by introducing the excess term, can be used for determination of partition coefficients and adsorption isotherms and this modification mainly improves the measurements for high volatile compounds. The developed method based on variation of the amount of solid (SPRV method) [1], has some drawbacks in measuring the partition coefficients, since it assumes a low amount of adsorption for the analyte, close to zero which might not be valid for all the tested components. The method developed based on variation of the liquid samples, can be further developed for determination of adsorption isotherms for a multi-compound mixture, considering the volatility of the tested components present in the mixture and selection of the suitable phase ratio, appropriate for all the tested components, however preparation of various samples necessary for this measurement can increase the time required for analysis, since the procedure would be different from conventional static headspace injection and measurement from one vial. Considering the improvement associated with this method in reducing the effect of evaporation and steps required for transferring the samples and centrifugation, it is worthwhile to apply this method for isotherm determination, considering a balance between the time required for analysis and the number of experiments which are required to be performed.

References

1. Hui-Chao, H.C., C. Xin-Sheng, and D. Barnes, *Determination of solid-liquid partition coefficient of volatile compounds by solid phase ratio variation based headspace analysis.* Fluid phase equilibr, 2014. **380**: p. 76-81.
2. Abraham, M.H., et al., *Determination of partition coefficients of refrigerants by gas liquid chromatographic headspace analysis.* Journal of Chromatography A., 2012. **1265**: p. 144-148.
3. Zhang, C.-Y., X.-S. Chai, and D.G. Barnes, *A novel solvent-assisted vapor absorption based headspace analysis technique for the determination of diffusion and solid-air partition coefficients of methanol in paper materials.* Fluid Phase Equilibria, 2015. **399**: p. 74-79.
4. Bruneel, J., et al., *Determination of the gas-to-liquid partitioning coefficients using a new dynamic absorption method (DynAb method).* Chemical Engineering Journal, 2016. **28**: p. 544-552.
5. Tipler, A., *An Introduction to headspace sampling in gas chromatography, Fundamentals and Theory*.
6. Kolb, B. and L.S. Ettre, *Static Headspace-Gas Chromatography: Theory and Prcatice, Second Edition*. 2006, New Jersey, Canada: John Wiley & Sons, Inc.
7. Rouseff, R.L. and K.R. Cadwallader, *Headspace analysis of foods and flavors, Theory and practice*. 2001, Springer Science+Business Media, LLC.
8. Tromelin, A., et al., *Proposed alternative phase ratio variation method for the calculation of liquid-vapour partition coefficients of volatiles.* J Chromatogr A, 2012. **1263**: p. 158-168.
9. Griffith, J.T. and G.A. Robbins, *A new method for field analysis of soil contaminated with aromatic hydrocarbon compounds.*
10. Jones, W.J., et al., *Determination of partition coefficients by headspace gascomatography.* J Chromatogr A, 1988. **455**: p. 45-51.

Summary

Flavor-active components are key contributors to the profile of the final produced beer product. Their preservation and control during different stages of processing is crucial, since they might be lost during processing due to their volatile nature. In order to produce a final beer product with balanced flavor profile, which is acceptable by the consumer, the level of these components in the beer matrix should be adjusted and controlled. Various techniques can be applied for flavor control and recovery, such as distillation/stripping, pervaporation, supercritical extraction, and adsorption. Chapter two of this thesis discusses the recent advances in various techniques, which are applied for flavor recovery among which adsorption is a technique, which showed potential for selective removal and recovery of flavor/non-flavor-active components. This technique can be combined with heat processing, distillation/stripping, or can be used as a standalone technique. The focus of the work presented in chapter three of this thesis is on method development for selective removal and recovery of flavor-active volatile components mainly belonging to the group of esters, higher alcohols, and diketones, through adsorption technique. In order to investigate the single and competitive adsorption behavior of flavor-active components and their synergistic effects, high throughput experimentation technique is applied, improved for volatile components and isotherms are obtained using batch uptake experimentation. The competitive adsorption behavior of flavor-active components is investigated on various food-grade hydrophobic adsorbents, in order to study the influence of physical and chemical nature of the components and adsorbent properties on selectivity for each tested adsorbate over ethanol. Based on the results obtained from thermodynamic studies through various isotherm models, the appropriate adsorbent material is selected for further studies in the design stage. In the next step, deeper study is conducted on flavor-active esters, presented in chapters four, five, and six, which contribute to beer with a fruity taste and aroma. With adjusting their level in the final beer product and their fractionation, various products can be produced with fruity taste. Further investigation is performed on their competitive adsorption behavior both through batch uptake experimentation, and dynamic breakthrough analysis tests, discussed in chapters four and six respectively. Since ester components are present at low concentration level together with ethanol, which is present

at higher concentration in comparison in various process streams, the influence of ethanol and temperature on their competitive adsorption is further investigated, discussed in chapter four. Physical properties such as isosteric heat, entropy, and Gibbs energy of adsorption, are calculated from performed thermodynamic studies, which contribute to our deeper understanding of the adsorption phenomena on the selected adsorbents. Considering the time-consuming steps, which are required to be followed for constructing the adsorption isotherms through batch uptake experimentation, the application of predictive models developed based on adsorbed solution theory, is evaluated in chapter five, for prediction of multicomponent adsorption isotherms for flavor-active esters from single-component adsorption isotherms, when experimental data for multicomponent behavior is not available. The predictive model developed based on IAST, was capable to predict the multicomponent adsorption behavior for the tested condition with accuracy and can be used as a tool for prediction of isotherms, when data on multicomponent adsorption is not available. Possibility for separation of flavor-active esters is further investigated in a fixed-bed column in lab-scale, discussed in chapter six, to study their breakthrough behavior and their separation under various process conditions (ethanol concentration and temperature). The results of the experimental tests obtained through breakthrough analysis and fractionation, are used for validation of simulations. Based on the results obtained in lab-scale, separation of flavor-active components is further investigated in a large-scale column, through simulation of various scenarios for separation. The performed experiments in the lab-scale and results of the simulations at large-scale give an insight on competitive adsorption behavior of these components, when present in a mixture. For a more detailed prediction of the adsorption behavior, future outlooks are discussed in chapter seven, to study the optimized condition considering the process conditions, and integration of the adsorption with other alternatives such as distillation/stripping.

Samenvatting

Smaak-actieve componenten dragen in belangrijke mate bij aan het profiel van het uiteindelijke geproduceerde bierproduct. Hun bewaring en controle tijdens verschillende verwerkingsstadia is cruciaal, omdat ze tijdens de verwerking verloren kunnen gaan vanwege hun vluchtige karakter. Om een uiteindelijk bierproduct te produceren met een uitgebalanceerd smaakprofiel, dat aanvaardbaar is voor de consument, moet het niveau van deze componenten in de biermatrix worden aangepast en geregeld. Verschillende technieken kunnen worden toegepast voor het regelen en terugwinnen van smaakstoffen, zoals destillatie / strippen, pervaporatie, superkritische extractie en adsorptie. Hoofdstuk twee van dit proefschrift bespreekt de recente vooruitgang in verschillende technieken, die worden toegepast voor smaakherstel, waarbij adsorptie een techniek is, die potentieel voor selectieve verwijdering en winning van smaak / niet-smaakactieve componenten liet zien. Deze techniek kan worden gecombineerd met warmtebehandeling, destillatie / strippen, of kan worden gebruikt als een standalone techniek. De focus van het werk dat in hoofdstuk drie van dit proefschrift wordt gepresenteerd, betreft de ontwikkeling van de methode voor selectieve verwijdering en terugwinning van aroma-actieve vluchtige componenten die voornamelijk tot de groep van esters, hogere alcoholen en diketonen behoren, via adsorptietechniek. Om het enkele en competitieve adsorptiegedrag van smaakactieve componenten en hun synergistische effecten te onderzoeken, wordt een high-throughput-experimentatietechniek toegepast, verbeterd voor vluchtige componenten en isothermen verkregen met behulp van batch-opname-experimenten. Het competitieve adsorptiegedrag van aroma-actieve componenten wordt onderzocht op verschillende hydrofobe adsorbentia van voedingskwaliteit, om de invloed van de fysische en chemische aard van de componenten en adsorberende eigenschappen op de selectiviteit voor elk getest adsorbaat ten opzichte van ethanol te bestuderen. Gebaseerd op de resultaten verkregen uit thermodynamische studies door verschillende isothermmodellen, wordt het geschikte adsorbensmateriaal geselecteerd voor verdere onderzoeken in de ontwerpfase. In de volgende stap wordt dieper onderzoek gedaan naar smaakactieve esters, gepresenteerd in de hoofdstukken vier, vijf en zes, die bijdragen aan bier met een fruitige smaak en aroma. Met het aanpassen van hun niveau in het uiteindelijke

bierproduct en hun fractionering, kunnen verschillende producten met een fruitige smaak worden geproduceerd. Nader onderzoek naar hun competitieve adsorptiegedrag, zowel door middel van batch-opname-experimenten, als dynamische doorbraakanalysetests, besproken in hoofdstuk vier respectievelijk zes. Aangezien estercomponenten aanwezig zijn op een laag concentratieniveau samen met ethanol, dat in vergelijking met verschillende processtromen in hogere concentraties aanwezig is, wordt de invloed van ethanol en temperatuur op hun competitieve adsorptie verder onderzocht, besproken in hoofdstuk vier. Fysieke eigenschappen zoals isosterische warmte, entropie en Gibbs-energie van adsorptie worden berekend uit uitgevoerde thermodynamische onderzoeken, die bijdragen tot ons dieper inzicht in de adsorptieverschijnselen op de geselecteerde adsorbentia. Gezien de tijdrovende stappen, die moeten worden gevolgd voor het construeren van de adsorptie-isothermen door batch-opname-experimenten, wordt de toepassing van voorspellende modellen ontwikkeld op basis van geadsorbeerde oplossingsleer, geëvalueerd in hoofdstuk vijf, voor voorspelling van adsorptie-isothermen met meerdere componenten voor smaak- actieve esters van adsorptie-isothermen met één component, wanneer experimentele gegevens voor gedrag met meerdere componenten niet beschikbaar zijn. Het voorspellende model dat is ontwikkeld op basis van IAST, was in staat om het multicomponentadsorptiegedrag voor de geteste toestand nauwkeurig te voorspellen en kan worden gebruikt als een hulpmiddel voor voorspelling van isothermen, wanneer gegevens over adsorptie van meerdere componenten niet beschikbaar zijn. Mogelijkheid tot scheiding van smaakactieve esters wordt verder onderzocht in een kolom met een vast bed op labschaal, besproken in hoofdstuk zes, om hun doorbraakgedrag en hun scheiding onder verschillende procesomstandigheden (ethanolconcentratie en temperatuur) te bestuderen. De resultaten van de experimentele testen verkregen door middel van baanbrekende analyse en fractionering, worden gebruikt voor de validatie van simulaties. Op basis van de resultaten op laboratoriumschaal wordt de scheiding van smaakactieve componenten verder onderzocht in een grootschalige kolom, door simulatie van verschillende scenario's voor scheiding. De uitgevoerde experimenten op labschaal en de resultaten van de simulaties op grote schaal geven inzicht in het competitieve adsorptiegedrag van deze componenten, indien aanwezig in een mengsel. Voor een meer gedetailleerde voorspelling van het adsorptiegedrag worden toekomstige vooruitzichten besproken in

hoofdstuk zeven, om de geoptimaliseerde toestand te bestuderen, rekening houdend met de procesomstandigheden, en integratie van de adsorptie met andere alternatieven zoals destillatie / strippen.

List of Publications

Patents

Ottens,M, Saffarionpour,S, Noordman, T.R., " Method for producing beer having a tailored flavor profile", Application date: 26 July 2017, Application number EP3193632A1

Scientific articles and journal publications

S. Saffarionpour, T.F. de Jong, L. A. M. Van der Wielen, E. Brouwer, M. Ottens, Column chromatography for separation of flavor-active esters on hydrophobic resins and simulation of breakthrough behavior, Sep. Purif. Technol., 2019**. 210**: p: 304-319 https://doi.org/10.1016/j.seppur.2018.05.008

S. Saffarionpour, S-Y S. Tam, L. A. M. Van der Wielen, E. Brouwer, M. Ottens, Influence of ethanol and temperature on adsorption of flavor-active esters on hydrophobic resins, Sep. purif. Technol., 2019. 210: p: 219-230 https://doi.org/10.1016/j.seppur.2018.05.026

S. Saffarionpour, M. Ottens, Recent advances in techniques for flavor recovery in liquid food processing, Food Eng. Rev., 2018. **10** (2): p:81-94 https://doi.org/10.1007/s12393-017-9172-8

S. Saffarionpour, D. Mendez Sevillano, L. A. M. Van der Wielen, T.R. Noordman, E. Brouwer, M. Ottens, Selective adsorption of flavor-active components on hydrophobic resins , J Chromatogr A, 2016. **1476**: p: 25-34 https://doi.org/10.1016/j.chroma.2016.10.053

Scientific conference contributions

Oral presentations

Saffarionpour,S, Van der Wielen ,L.A.M., Noordman, R., Brouwer,E., Ottens,M. (16 May 2017), "Selective removal of flavor-active components in liquid food streams", Abstract and oral presentation, Nederlandse Biotechnologische vereniging, NBC-17, Wageningsche Berg

Saffarionpour,S, Van der Wielen ,L.A.M., Brouwer,E., Ottens,M. (11-14Sep. 2016), "Predictive models for competitive adsorption of flavor-active compounds", Oral

presentation, European symposium on Biochemical Engineering Sciences, (ESBES), Dublin, Ireland; Abstract selected for final oral presentation for Malcom Lilly Award

Saffarionpour,S, Van der Wielen ,L.A.M., Brouwer,E., Ottens,M. (14-16 Feb. 2016), "Method development for recovery of flavor-active compounds through adsorption process", Oral presentation, 12th PhD Seminar on Chromatographic Separation Science, Schleiden, Germany

Poster presentations

Saffarionpour,S, Van der Wielen ,L.A.M., Brouwer,E., Ottens,M. (11-14Sep. 2016), "Predictive models for competitive adsorption of flavor-active compounds", Abstract and Poster presentation, European symposium on Biochemical Engineering Sciences, (ESBES), Dublin, Ireland

Saffarionpour,S, Van der Wielen ,L.A.M., Noordman, T.R., Brouwer,E., Ottens,M. (20May-3Jun 2016), "Selective removal of flavor-active compounds through adsorption process", Abstract and Poster presentation, 12th International conference on Fundamentals of Adsorption (FOA), Friedrichshafen, Germany

Saffarionpour,S, Van der Wielen ,L.A.M., Noordman,T.R., Ottens,M. (27Sep-1Oct 2015), "Selective removal of flavor-active components in food streams", Abstract and Poster presentation, ECCE10+ECAB3+EPIC5, Nice, France

Saffarionpour,S, Van der Wielen ,L.A.M., Noordman,T.R., Ottens,M. (7-10 Sep 2014), "Selective removal of flavor-active components in food streams", Abstract and Poster presentation, 10th European Symposium on Biochemical Engineering Sciences & 6th International Forum on Industrial Bioprocesses, Lille, France

Saffarionpour,S, Van der Wielen ,L.A.M., Noordman,T.R., Ottens,M. (7Nov 2014), "Selective removal of flavor-active components in food streams", Abstract and Poster presentation, DPTI (Delft Process Technology Institute), DPTI annual conference, Rotterdam

Scientific publications and conference contributions outside the scope of this project

Scientific articles and journal publications

Saffarionpour, S., Yaghmaei, S., & Ghobadinejad, Z., "Immobilization of Alkaline protease enzyme produced from Bacillus licheniformis PTCC1331 on Ca-alginate (Its effect on enzymatic activity)". Journal of Chemical and Petroleum Engineering, 2010.43(2): p: 33-39
https://doi: 10.22059/JCHPE.2010.20972

Oral presentations

Visscher,F., Saffarionpour, S., de Croon, M.H.J.M., van der Schaaf, J. & Shouten, J.C.(2013), "Countercurrent liquid- liquid mass transfer in a high-shear high-gravity extractor", Oral presentation, 9th European Conference of Chemical Engineering (ECCE9), The Hague, Netherlands

Visscher, F., Saffarionpour, S., de Croon, M.H.J.M., van der Schaaf, J., Schouten, J.C., (2013), "Countercurrent liquid- liquid flow in a high-shear high-gravity extractor", Oral presentation, 3rd North American Symposium on Chemical Reaction Engineering (NASCRE-3), March 17-20, Houston, TX, USA

Mortaheb,M.M., Saffarionpour,S., Zarei,H., Taghi Pour,A., (2010) "On-the-job Management Education; A case study of Iranian scholars", Oral presentation, 24th IPMA World Congress, 1-3 Nov., Istanbul, Turkey

Poster presentations

Taghi Pour, A., Zarei,H., Saffarionpour,S., Shaker,M., (2011) " Risk Assessment of Subway Construction Projects in Tehran", poster presentation, 6th International Project Management Conference, 16, 17 Jan, Tehran, Iran

Saffarionpour,S., Yaghmaei,S., Ghobadinejad,Z., (2008) "Immobilization of Alkaline Protease enzyme produced from Bacillus licheniformis PTCC1331 on Ca-alginate", poster presentation, 12th Chemical Engineering Congress (ICHEC12) 20-23 Oct. 2008, Sahand University of technology, Tabriz, Iran

About the Author

Shima Saffarionpour was born on 17th of August 1982 in Tehran, Iran. After completing her education at Aboureihan high-school in the year 2000, she started her undergraduate studies in the area of Chemical Engineering at University of Tehran. Upon receiving the degree B.Sc., she continued her master studies in the area of Chemical Engineering, Food Science at Sharif University of Technology. As her final thesis she collaborated on a research project at Biochemical and Bioenvironmental Research Center (BBRC), conducted research on *immobilization of protease enzyme produced from Bacillus Licheniformis on natural polymeric supports.* The result of this research was published as a scientific article, presented at related conference. After completion of her master studies in the area of Chemical Engineering, in order to gain more insight and practical experience on managing projects and becoming more familiar with organizations active in the field, she joined a two-year master program in Project Management Specialization offered by Schulich School of Engineering, University of Calgary with collaboration of Sharif University of Technology. During this program she not only gained valuable knowledge on principles and fundamentals of project management, project planning and execution, but also on group dynamics, principles of teamwork and the importance of managing workforce and valuing diversity within an organization. The results of successful collaboration on several group assignments and projects were presented at scientific conferences. Afterwards she moved to Netherlands to join a program in Process and Product Design (PPD) at Eindhoven University of Technology. During the first year of this program, which is designed for bridging the gap between theoretical knowledge and practice, she was trained and collaborated in teams on several group assignments and industrial projects. As her final individual research project, which was defined at Laboratory of Chemical Reactor Engineering, under supervision of Dr. ir. J. van der Schaaf, she conducted research on separation and liquid-liquid extraction in small-scale high-shear, high-gravity rotor-rotor spinning disc extractor. The result of this research, which was in collaboration with the PhD student Dr.ir. F. Visscher, were presented at scientific conferences. Gaining experience in the area of Separation technology and having educational background in the area of Food Science, she continued her education as a PhD candidate at Delft University of Technology, Department of Biotechnology, Bioprocess Engineering group. She collaborated on a research project defined within the food sector of ISPT (Institute of Sustainable Process Technology), project FO-10-05, with collaboration of academic partners from Wageningen University and Industrial partner, Heineken Supply Chain. Under supervision of Dr.ir. Marcel Ottens and Prof. Luuk A.M. van der Wielen, she

conducted research on separation and recovery of nutraceuticals and flavor-active components by means of adsorption technique. The results of successful collaborations during this project are published as scientific articles, presented at related conferences. During her research, she gained valuable knowledge on separation techniques and flavor ingredients and Separation technology and its application in Biotechnology is the area of her interest.

Acknowledgement

"Management training while being on the job", an unforgettable experience I had since I started working on this project. Of course the role of ISPT (Institute of Sustainable Process Technology) on providing this opportunity and training for me is undeniable. A great acknowledgement goes to contributors from ISPT who not only had major role in providing the opportunity for collaboration and satisfaction of different partners and collaborators, but also had major impact and role on the success of this project. The outcome of this training and collaboration was building positive, constructive relationships, which increased the group cohesion, impacted the work through focused collaboration and leadership.

Now that this journey is coming to an end, I would like to acknowledge the ones who made this journey memorable for me. First my family, my parents, who always supported and encouraged me throughout my academic career. I should acknowledge the project team, my supervisor Marcel Ottens, for his presence and patience throughout this collaboration project, and for his constructive comments and feedback. My promotor Luuk van der Wielen, for his presence and for the critical, invaluable comments I received from him. Our former project leader from Heineken Supply Chain, Reinoud Noordman for his guidance and support when I started the project, and all the other research team at Heineken Supply Chain from whom I received instructions, support, and guidance. Our current project leader Eric Brouwer for his feedbacks and for his great involvement in integration of project partners. Our partners from Wageningen University, Ali, with whom I was closely collaborating during the project. Karin Schroen and Remko Boom from whom I received invaluable comments. Frans van den Akker, Anne van der Zwaan and Peter de Jong from ISPT for their presence and kind support during the project. Marieke for her contribution to the project while she was continuing her internship at Heineken and Deborah for her significant role in process integration. My master students Suk-Ying and Tessa for their contribution to the work and for the memorable and great experience I had with them during our collaboration. I would like to acknowledge the secretary of BPE group, Kawieta, for her friendly welcome when I joined the group and

for her kind support throughout the project. My colleagues David, and Alex for their warm welcome, when I started my work in the group and for their kind support. Robin and Katelijne for their kind welcome and also other colleagues with whom I shared memories and offices, Marcelo, Susana, Chema, Carla, and Ainhoa. All other colleagues from BPE group with whom I had the opportunity to collaborate and share memories, Camilo, Arian, Eric, Carlos, Victor, Silvia, Joana, Thomas, Diego, Pillar, Carla, Monica, Bianca, Rita, and Meissa and other PhDs, PDEngs and staff members. Laboratory technicians of the BPE group, Max Zomerdijk, Stef van Hateren, and Yi Song, for their kind support throughout the project. Patricia van Dam for her kind assistance when guidance was required and other technicians for their kind support.

Without this collaboration, completion of this project was not possible. Thank you all for your invaluable support.

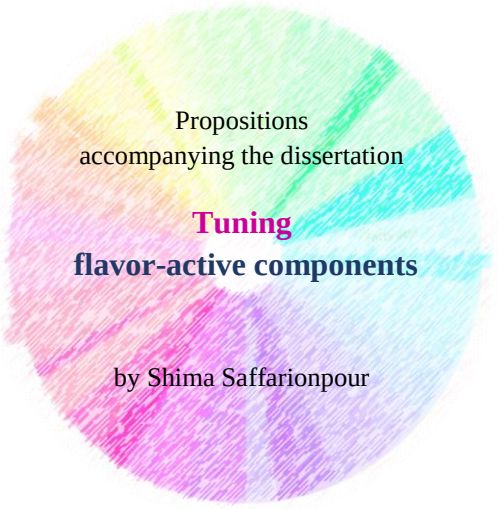

Propositions
accompanying the dissertation

Tuning
flavor-active components

by Shima Saffarionpour

1. To promote the culture of thinking, we need to understand how students think about thinking.

2. Modelling competitive adsorption gives a better understanding about single compound behavior (Chapters 3, 4, 5, and 6 of this thesis).

3. The value of knowledge increases when shared.

4. “Innovation is what agile is all about.” (Harvard Business Review)

5. When analysing volatile flavor components, one should not underestimate their evaporation (Chapters 3, 4, and 6 of this thesis).

6. New ideas come from new views.

7. Collaboration will fail in an environment designed for competition.

8. Effective leadership demands being responsive.

9. It is the flavor which describes beer’s evolution.

10. Miniaturized experimentation is relative (Chapters 3, and 4 of this thesis).

These propositions are regarded as opposable and defendable, and have been approved as such by promotors Prof. Dr. ir. L.A.M. Van der Wielen, and Dr.ir.

Stellingen
behorde bij het proefschrift

Tuning
flavor-active components

door Shima Saffarionpour

1. Om de denkcultuur te bevorderen, moeten we begrijpen hoe studenten denken over denken.

2. Het modelleren van competitieve adsorptie geeft een beter begrip van de afzonderlijke verbinding
   gedrag (hoofdstuk 3, 4, 5 en 6 van dit proefschrift).

3. De waarde van kennis neemt toe wanneer deze wordt gedeeld.

4. "Innovatie is waar het bij Agile om draait." (Harvard Business Review)

5. Bij het analyseren van vluchtige smaakcomponenten moet men hun verdamping niet onderschatten (Hoofdstukken 3, 4 en 6 van dit proefschrift).

6. Nieuwe ideeën komen van nieuwe inzichten.

7. Samenwerking mislukt in een omgeving die is ontworpen voor concurrentie.

8. Effectief leiderschap vereist responsiviteit.

9. Het is de smaak die de evolutie van bier beschrijft.

10. Geminiaturiseerde experimenten zijn relatief (Hoofdstukken 3 en 4 van dit proefschrift).

Deze stellingen worden opponeerbaar en verdedigbaar geacht en zijn als zodanig goedgekeurd door de promotoren, Prof. Dr. ir. L.A.M. Van der Wielen, en Dr. ir. M. Ottens.